ABSTRACT

WINSTON, RYAN JOSEPH. Resilience of Green Infrastructure under Extreme Conditions. (Under the direction of Dr. William F. Hunt III).

Green infrastructure improves urban runoff quality and controls runoff volume by maximizing exfiltration, evapotranspiration (ET), storage, and water harvesting. To determine their resilience to various factors (e.g., clay soils which restrict exfiltration, climate change, and application of de-icing salts), three bioretention cells and four permeable pavements were intensively monitored in northern Ohio. To ensure resilience over the long-term, permeable pavements were evaluated to determine (1) when maintenance is needed and (2) how to best maintain the pavement surface infiltration rate (SIR).

Volume reduction for bioretention cells constructed over low permeability soils varied from 36-59% and improved with higher drawdown (i.e., the sum of exfiltration and ET) rates and deeper internal water storage (IWS) zone depths. Post-construction measured drawdown rates were non-linear and greater than vertical saturated hydraulic conductivity (K_{sat}) measured on the underlying soil during construction. Collectively, this suggested (1) lateral exfiltration played a substantial role in volume reduction, and (2) ET provided a minor amount of volume reduction.

Field-collected bioretention hydrologic data were used to calibrate and validate DRAINMOD, a long-term agricultural drainage model. Nash-Sutcliffe efficiencies for runoff, drainage, overflow, and exfiltration/ET exceeded 0.7, suggesting the model was well calibrated. Analyses of bioretention design alternatives were conducted using the calibrated models and a long-term climatic record. Volume reduction was most dependent on loading ratio, IWS zone depth, and underlying soil K_{sat}.

A current and two predicted mid-21st century climate scenarios (RCP 4.5 and RCP 8.5) were input into the three calibrated DRAINMOD models. Future climate scenarios predicted decreases in annual precipitation, longer dry periods, and hotter temperatures for Northeast Ohio. Bioretention volume reduction was predicted to either modestly increase (by 4-6%) or decrease (by 5-9%) under future climate scenarios. In all modeled cases, overflow and ET increased as a percentage of the water balance. To mitigate future increases in overflow, bowl volume would need to be increased by up to 51%.

Field-monitored permeable pavements situated over low permeability soils, employing 15-cm IWS zones, and minimum loading ratios of 4:1 reduced runoff volume by16 to 53%. In comparison, volume reduction for a permeable pavement treating only direct rainfall was 99%. Post-construction drawdown rates were linear and similar to vertical K_{sat} of the underlying soil measured during construction, suggesting evaporation and lateral exfiltration were minor contributors to volume reduction.

The water quality performance of two permeable pavements was assessed in northeast Ohio. While observed nutrient load reductions were similar to past studies, TSS loads increased by 300-500%. Loss of silt and clay-sized particles from the permeable pavement subgrade was seasonal, and appeared to be related to dispersion of particulate matter caused by sodium in de-icing salts.

Eight maintenance techniques were tested for improvement of permeable pavement SIR in North Carolina, Ohio, and Sweden. Milling and pressure washing were the most successful in recovering porous asphalt SIR, while street sweepers employing suction were preferable for permeable interlocking concrete pavements.

A simple infiltration test (SIT) to determine permeable pavement maintenance needs was developed because American Society for Testing and Materials (ASTM) tests can take hours to complete and require infiltrometers not readily available to maintenance contractors. Results showed: (1) a segmented linear relationship related SIT and ASTM-measured SIRs, (2) the SIT and ASTM tests predicted approximately the same IR up to 250 mm/min, and (3) the larger surface area of the SIT reduced measurement variability by 40% compared to the ASTM method.

Bioretention cells and permeable pavements are resilient stormwater controls only when properly designed, installed, and maintained. Generally, bioretention cells are more resilient to anthropogenic and natural stressors due to their plant- and soil-based treatment processes.

Resilience of Green Infrastructure under Extreme Conditions

by
Ryan Joseph Winston

A dissertation submitted to the Graduate Faculty of
North Carolina State University
in partial fulfillment of the
requirements for the degree of
Doctor of Philosophy

Biological and Agricultural Engineering

Raleigh, North Carolina

2015

APPROVED BY:

_____	_____
Dr. William F. Hunt III Chair of Advisory Committee	Dr. Michael R. Burchell
_____	_____
Dr. Barbara A. Doll	Dr. Richard A. McLaughlin

_____
Dr. Elizabeth A. Fassman-Beck
Stevens Institute of Technology

DEDICATION

This work is dedicated to my family for all of your love, support, and guidance. I am grateful for everything that you have taught me over the years, and appreciate the investments that each of you have made in this dissertation.

BIOGRAPHY

Ryan Joseph Winston was born on November 14, 1984 in St. Petersburg, Florida to Drs. William and Norma Winston. He lived along the west coast of Florida for the majority of his formative years, except for periods where the family resided in Budapest, Hungary and London, United Kingdom. Growing up in Parrish, Florida, Ryan enjoyed the outdoors and had a love for being in or around the water. Following his high school graduation in 2003, he enrolled at the University of Florida, where he subsequently cheered the Gators on in two basketball and one football national championship over his four years in Gainesville (Go Gators!). Ryan met his wonderful wife of 6 years, Jenessa, two weeks into undergrad in a dormitory adjoining his. After following many potential career paths during his undergraduate years (Mechanical Engineering, Pharmacy, etc.), he majored in water resources and biological engineering within the Agricultural and Biological Engineering Department. During this time, he interned at HSW Engineering for two years.

While deciding on potential graduate schools, he was particularly influenced by Drs. Dukes and Bean to visit North Carolina State University (NCSU). It was there he met Dr. Bill Hunt, professor in Biological and Agricultural Engineering. Over the past 8.5 years, Ryan has worked for Bill in various capacities, including as a Master of Science student studying vegetated filter strip stormwater controls (completed in 2009), an Extension Associate (where he earned his Professional Engineering licensure, worked with many M.S. and PhD students, and continued to publish his own research work), and finally as a PhD student. I am extremely lucky to have worked on some amazing stormwater engineering projects during this time. Apart from the work (which I loved), Ryan was lucky enough to

travel extensively both in the USA and internationally while at NCSU, which is one of his true passions. And, while the sports teams were not as successful as they were in Gainesville, he still has a soft spot in his heart for the Wolfpack (Go Pack!).

While Ryan was housed in the Biological and Agricultural Engineering department at North Carolina State University during his PhD work, the work itself was all in northern Ohio. He loved working on the project and appreciated the family atmosphere that evolved as the multi-faceted work was completed under a team effort. This type of collaborative effort was inspiring, and he hopes that it will be a model for many of the projects in his future academic career. Following completion of his PhD, Ryan will continue his work in the Buckeye state as he begins a new position as a Research Scientist at (the) Ohio State University.

ACKNOWLEDGMENTS

There are many people and groups that I would like to thank for their aid during the work that supported this dissertation. Without funding, research is simply an idea and cannot be carried out. Funding provided by the following sources supported and helped me to grow as a scientist and a person: the National Oceanic and Atmospheric Administration (NOAA), the University of New Hampshire, the Old Woman Creek National Estuarine Research Reserve (OWC NERR), Ohio Department of Natural Resources (Division of Wildlife), the Interlocking Concrete Pavement Institute, and Swedish grantors VINNOVA and Norrbottens forskningsråd. We also appreciate the tremendous in-kind contributions provided by the Northeast Ohio Regional Sewer District and OWC NERR (who analyzed the water quality samples *pro bono*) and Amy and Dan Brennan (who provided lodging in Ohio *pro bono*).

First, I would like to thank Dr. Bill Hunt, my mentor for both this dissertation and my M.S. work. Your guidance over these past 8.5 years has helped me to grow as a person, researcher, speaker, and mentor. You have taught how to effectively run a research program, which will be extremely helpful in the future. While I came to NCSU's graduate recruitment weekend with an interest in groundwater modeling, you were able to convince me that stormwater research was interesting. And let me tell you, there were very few dull moments (if any?) working for you. I especially enjoyed the stormwater team trips where we integrated new team members into the fold. I will miss the camaraderie and laughter that the team atmosphere promoted. I greatly appreciate all of the time you have spent to hone my skills and knowledge related to water resources and sincerely thank you for your friendship

over nearly the past decade. I know that we will continue to work together on the massive challenge that is stormwater management.

I would like to thank my committee members, Drs. Michael Burchell, Barbara Doll, Elizabeth Fassman-Beck, Richard McLaughlin for your advice and input along the way and for your review of this dissertation, which is not particularly lightweight. I have had the pleasure of working with each of you on various research projects, manuscripts, workshops, and extension work during my time at NCSU, and greatly enjoyed the experience. I have become a more well-rounded scientist and engineer because of your respective focus areas, and for that I am truly appreciative. I hope that our paths will cross in the future.

I have had the pleasure of working with many others that have enhanced the quality of the research presented herein, both as an Extension Associate and during my one-year stint as a PhD student. Drs. Godecke Blecken and Maria Viklander were kind enough to host me at Luleå University of Technology, Luleå, Sweden for three weeks in August 2015. Ahmed Al-Rubaei, PhD student in the Urban Water Group, was invaluable in working with me to collect field data. I treasured this experience both in collecting data for chapters 7 and 8 of this dissertation and also in meeting new people, transfer of ideas and collaboration, and getting to experience the Swedish culture. Ms. Alessa Smolek (soon to be Doctor!) worked with me on the modeling portion of this project, completing similar work to chapters 3 and 4 (except focused on permeable pavements) herein as part of her PhD project. We were able to troubleshoot a number of issues in DRAINMOD together, as well as enhance the quality of each other's work. I also appreciate her time spent reviewing chapters 3, 4, and 5 of this dissertation.

Dr. Jay Dorsey, water resources engineer at Ohio Department of Natural Resources, was the science lead on the NERRS grant which was mostly responsible for funding this work. While I had never met Jay before starting the project in 2012, he quickly became a friend and mentor. He spent countless hours reviewing my work, editing all of both the monitoring and modeling reports for NOAA that became the backbone for this dissertation. He worked concurrently to Alessa and me on Storm Water Management Model (SWMM) simulations on both bioretention and permeable pavement calibrated off of the field data presented in chapters 2 and 5 herein. Therefore, he was instrumental in fact checking the data, suggesting tweaks to methods to improve analyses, and aiding with hydrograph separation analyses for the bioretention data sets. Jay also helped to collect a plurality of the data which supported chapters 7 and 8 of this work. Finally, Jay has been instrumental in helping to "bridge the gap" and convince the Ohio State University that a researcher is needed in urban water issues; for all of this, I am truly grateful.

Along with Jay, a number of people based in Ohio helped me immensely with this work. To the entire staff of the Chagrin River Watershed Partners – Amy Brennan (formerly), Heather Elmer, Keely Davidson-Bennett, Kristen Buccier, Christina Znidarsic, and Linda Moran – thank you very much for coordinating the project, helping to do permeable pavement infiltration testing, taking pictures during SCM construction, taking on water quality sampling at Willoughby Hills and Ursuline College, and countless other things. Apart from work, you all made the process fun and enjoyable, including trips to Willoughby Brewing, Cleveland Indians games, and a group trip to see LeBron play. To Frank Lopez of Old Woman Creek (OWC) NERR – thank you for providing guidance to our project, hosting

a research site at OWC, and providing housing at OWC during my visits to the "west side" of the project extents. Thanks to Will Brown and Rebecca Jacobson of the University of New Hampshire for their help documenting the project, collecting data, and taking pictures during SCM construction. Thanks are due to Kevin Grieser of Biohabitats, Inc. for downloading the data throughout the monitoring period. Thanks to Bre Hohmann, Eric Dodrill, and Crystal Dymond of Erie County Soil and Water Conservation District for their help with the Perkins Township site. Thanks to everyone in Ohio that participated in the Collaborative Learning Group as part of the NERRS project. It helped immensely to shape the direction of the project and our meetings were thought provoking and full of lively discussion. To the Project Team – this research would not have been half of what it is without your support, dedication, and guidance. I truly appreciate all that you have done for me.

To the members of the NCSU stormwater team, thank you for all of the memories! I have now been at NCSU for 8.5 years, and have had the pleasure of overlapping with perhaps 30 or more team members, all of whom I consider good friends and colleagues. Particularly, I appreciate Gabrielle Skipper, who was somewhat instrumental in getting Bill to hire me as a graduate student. She's also one of the most quick-witted people I know, and therefore fun. Dr. Rob Brown, the other half of the "grand tetons," started graduate school with me in 2007, and is a fantastic and fun person. Dr. Jon Hathaway, a good friend and guy, was always willing to be the butt of my jokes, and still is. Thanks to Stacy Luell for being my first "mentee" (M.S. student under my tutelage), and for being a fantastic person. Thanks to the M.S. and PhD students that I had the pleasure of working with during my time as an Extension Associate (Stacy Luell, Erica Petre, Natalie Bouchard, Brad Wardynski, Corinne

Dumonceau, Joshua Baird, Jon Page, Dr. Adrienne Cizek, Jacob Powell, and Alessa Smolek) – you put up with my type A, nit-picky personality and taught me more than you know. Thanks to everyone else that has been a part of the stormwater team during my time at NCSU – Hayes Lenhart, Kelly Collins, Dr. Matthew "smarty" Jones, Jason "tank" Wright, Jackie McNett (I will never forget your gullibility), Erica Tillinghast, Dr. Trisha Moore, Dr. Kathy DeBusk, Jessie Fears, Natalie Carmen, Dr. Laura Merriman, Sarah Wiackowski, Kevin Koryto, Charlie Stillwell, Rebecca Purvis, Katy Conroy, Jeffrey Johnson, Nora Onstad, and Bre Tillett. You all have contributed to the last 8.5 years of my life in various ways, and have all improved the "fun" part of work for me. I especially enjoyed our yearly team trips (though I missed the last one sadly thanks to my work in Sweden) and our time spent around conferences. My favorites were New Mexico (breaking the Jeep), Brazil (Bill's email about Porto Alegre; traveling to see Foz do Iguaçu, Rio de Janeiro, and the Amazon with Fez, Dr. KDBG, and Kyle), Singapore/Malaysia (minus the food poisoning - with Alessa and Laura), San Francisco (Golden Gate, Alcatraz, etc. with Rob and KDBG), China with Bill (eating all sorts of strange things; the cultural experience of Yixing juxtaposed with the bullet train and Shanghai), and Portland (Mount St. Helens, Mount Rainier, and the Oregon coast with Andrew, Cassie, KDBG, Joshua, and Ruthanne). These were really fantastic life memories, and I appreciate each and every one of you enhancing my experience while at NCSU.

While Shawn Kennedy was also a member of the stormwater team during my entire 8.5 year stint, he gets his own paragraph due to his sheer level of importance to everything that Bill's team does. Shawn, thanks for all that you have taught me over these past years. You understand the practical side of engineering, and have helped me to grow immensely. I have

always appreciated your wit and sense of humor, especially on the long drives between Raleigh and Cleveland. As I move on to the next chapter of my work life, I will miss having your insane construction skills and ability to "MacGyver" something out of nothing. Your skill in monitoring site installation is such a great asset to this team, and so I greatly appreciate your help not only on this project but on all the countless projects we have worked on together.

I appreciate the three people with which I have shared an office in either Weaver Admin or Weaver Labs building over the last 6.5 years. First off is Dr. Kathy DeBusk Gee, who was a fantastic officemate for about 3 years – quick with a joke and ready to laugh. As I have a GIGANTIC sweet tooth, I appreciated the plethora of delicious candy that she bestowed upon our office (and hence me). I worked alongside Kathy during my first years as an engineer, and she helped me to learn CAD, GIS, and the skills necessary to pass the P.E. exam. My second officemate was Mr. Andrew Anderson, with whom I shared Weaver 214 for 2.5 years. Andrew is both an awesome person and engineer – it was fun helping him to grow as an engineer and to learn from him. Thanks in part to both Kathy and Andrew, I have been able to learn R, and code some pretty awesome graphics for this document. Andrew is a lover of college football, and therefore a man after my own heart. I have appreciated his friendship through the past few years. Finally, to Yu Liu, with whom I shared an office as a PhD student, thank you for being so kind. From writing me a note wishing me luck on the date of my oral prelims to sharing stories about research and life, you were an excellent officemate.

To my parents, Drs. Bill and Norma Winston, thank you very much for your love and support over these past 31 years. I appreciate you taking the extra time to guide me during my formative years, ensuring that I found a career I was passionate about. Thanks for being willing to take care of our brood (the bulldogs and the cats) while we took a much needed vacation in Europe this past summer. I really appreciate all of the "little things" that you have done over the years to mold me into the person I am today. To my other set of parents, Bruce and Debbie, thanks for the awesome holiday memories in Florida – laughter is never too far away when you're around.

Last, but certainly not least, thanks to my lovely wife Jenessa, who has supported me more than I can put on paper over the past 13 years together. Perhaps the best part of this PhD was unrelated to it – the day that you finished your residency and ended 8 years of veterinary school, internship, and residency. It has been so excellent to reconnect after years of 80-hour weeks! I am excited for what lies ahead, and trust in the fact that you will be there to support me during the good times and bad. I appreciate all that you have done, do, and will do for me.

TABLE OF CONTENTS

LIST OF TABLES

LIST OF FIGURES

ABBREVIATIONS AND ACRONYMS

ADP – antecedent dry period
Al – aluminum
ARI – average recurrence interval
ASTM – American Society for Testing and Materials
Ca - calcium
Cl – chloride
CN – curve number
Cu – copper
ESP – exchangeable sodium percentage
ET - evapotranspiration
Fe – iron
GI – green infrastructure
HA – Holden Arboretum
HLR – hydrologic loading ratio
IWS – internal water storage
K_{sat} – saturated hydraulic conductivity
LID – Low Impact Development
MDL – method detection limit
Mg – magnesium
Mn - manganese
LR – loading ratio
NCSU – North Carolina State University
NO_{2-3} – nitrate and nitrite nitrogen
ON – organic nitrogen
OP – orthophosphate
OV – Orange Village, Ohio
Pb - lead
PBP – particulate bound phosphorus
PC – pervious concrete
PICP – permeable interlocking concrete pavement
PQL – practical quantification limit
PT – Perkins Township, Ohio
SAR – sodium adsorption ratio
SCM – stormwater control measure
SIR – surface infiltration rate
SIT – simple infiltration test
SWMM – USEPA Storm Water Management Model
TAN – total ammoniacal nitrogen
TKN – total Kjeldahl nitrogen
TMDL – total maximum daily load

TN – total nitrogen
TP – total phosphorus
TSS – total suspended solids
UC – Ursuline College
US EPA – United States Environmental Protection Agency
USGS – United States Geological Survey
WH – Willoughby Hills, Ohio
Zn - zinc

CHAPTER 1: **INTRODUCTION AND PROJECT OVERVIEW**

1.1 Impacts of Urban Stormwater Runoff

Across the world, population has and will continue to shift from a rural, agrarian-based society to highly urbanized centers (United Nations 2014). A consequence of urbanization is the construction of rooftops, roadways, and parking lots – impervious surfaces that have deleterious impacts on surface waters and groundwater (Wolman 1967; Arnold and Gibbons 1996; Pitt et al. 1999). Canopy interception and infiltration into the soil are reduced or eliminated by hardened surfaces, causing major shifts in the water balance (Berland and Hopton 2014; Bean and Dukes 2015). Lack of vegetation and soil compaction lead to substantial decreases in evapotranspiration (ET) and infiltration (and therefore groundwater recharge), with concomitant increases in runoff (Line and White, 2007). Increased rate and volume of stormwater runoff cause flooding, stream bank and bed erosion, and ultimately loss of aquatic habitat (Morse et al. 2003; Konrad et al. 2005; Schueler et al. 2009; Davis et al. 2012;).

Stormwater collects pollutants as it passes over impervious surfaces; they are derived from many sources, including vehicles (Barrett et al. 1998), atmospheric deposition (Wu et al. 1998; Line et al. 2002), fertilizer application (Bannerman et al. 1993), and animal waste, among others. Typical pollutants of concern in urban stormwater include: nutrients, heavy metals, sediment, salts, gross solids, pathogenic bacteria, and organic compounds. Sources of nutrients include fertilizer, atmospheric deposition, and animal waste (Passeport and Hunt 2009). Heavy metals in stormwater may result from leaching from copper flashing or galvanized materials, wearing of tires and brake pads, and atmospheric deposition (Sabin et

al. 2005; Wicke et al. 2012). As a method of preventing ice formation on roadways, salt applications are common during winter weather (Scott 1976). Indicator bacteria of pathogens most often result from pet and wild animal excrement (Hathaway et al. 2010), while organic compounds are mainly a result of industrial processes (Pitt et al. 2002).

Stormwater management thus has two goals: (1) the mitigation of urban hydrology, termed the "urban stream syndrome," (Walsh et al. 2005) and (2) the mitigation of increases in pollutant loads spurred by imperviousness. Stormwater control measures (SCMs) are often designed with both of these goals in mind. However, additional data are needed to quantify performance as a function of design and determine their resilience to the many stressors that may impact performance negatively or cause failure.

1.2 Stormwater Management and Resilience

Stormwater control measures (SCMs) were formerly designed solely to prevent flooding, primarily through the management of peak flow rates (USEPA 1999; Burns et al. 2012; Winston et al. 2013). This resulted in the construction of many wet and dry ponds, which discharge elevated (often above erosion-inducing) flow rates over elongated durations, often a detriment to urban stream health (Bledsoe 2002; Booth 2005; Tillinghast et al. 2011). More recently, Low Impact Development (LID) strategies have been devised to attempt to mimic the pre-development volume, rate, and duration of flow of a site (Page et al. 2015; Wilson et al. 2015).

The term green infrastructure (GI) was pioneered as an urban design methodology to maximize the use and benefits of green spaces, including their ecosystem services (Fletcher et al. 2014). Green infrastructure is now used interchangeably with LID (Struck et al. 2010)

and generally refers to (in a stormwater management context) vegetation and soil-based SCMs. The aims of these GI practices are to (1) reduce runoff volume by promoting beneficial use, exfiltration, and evapotranspiration (ET) of stormwater, (2) ameliorate elevated flow rates from urban catchments, and (3) improve water quality by employing treatment processes such as sedimentation, filtration, and biological and chemical processes (U.S EPA 2012). Examples of GI practices include: vegetated filter strips, bioswales, green roofs, rainwater harvesting, infiltration facilities, urban tree filters, green streets, downspout disconnection, bioretention, and permeable pavement (Winston et al. 2011; Page et al. 2015a; Page et al. 2015b). The latter two practices are the focus of this dissertation.

Bioretention cells and permeable pavements are widely used due to their versatility and established excellent treatment performance if designed, constructed, and maintained properly (Brattebo and Booth 2003; Hunt et al. 2006; Bean et al. 2007; Bratieres et al. 2008; Collins et al. 2008; Davis 2008; Hunt et al. 2008; Hatt et al. 2009; Fassman and Blackbourn 2010; Brown and Hunt 2011a; Brown and Hunt 2011b; Luell et al. 2011; Brown and Hunt 2012; Davis et al. 2012; Roseen et al. 2012; Wardynski et al. 2012; Drake et al. 2013; Olszewski and Davis 2013; Drake et al. 2014a; Drake et al. 2014b; LeFevre et al. 2014). However, bioretention cells and permeable pavement systems have not been sufficiently evaluated in the northern Ohio snow-belt and when situated over poorly drained, low permeability soils. In Ohio, these practices are designed to capture and treat the runoff from the 80^{th} percentile rainfall depth, or the 19-mm event (ODNR 2006).

Bioretention cells are engineered planted media filters designed to reduce the hydrologic and water quality impacts of imperviousness (Figure 1-1; Davis et al. 2012). They capture

the runoff from the water quality design event in their surface storage (i.e., bowl), filter stormwater as it passes through the media, exfiltrate stormwater to the underling soils, and provide ET (Davis 2008). When constructed in low permeability soils, an underdrain is often present to provide inter-event drainage. In Ohio, the standard bioretention design includes either a 15-cm or 60-cm (in soils with hydraulic conductivity <0.13 cm/hr and >1.25 cm/hr, respectively) internal water storage (IWS). This design feature uses an upturned elbow in the underdrain to force ponding within the gravel and media (Figure 1-1; ODNR 2006). If media is properly selected for target pollutants of concern (Winston et al. 2015), bioretention is one of the most effective water quality treatment SCMs, providing unit processes such as filtration, sedimentation, biological treatment (denitrification), chemical sorption of pollutants, and plant uptake (Hunt et al. 2006; Bratieres et al. 2008; Brown and Hunt 2012). Bioretention cells also provide aesthetic benefits, as they can blend into the urban landscape.

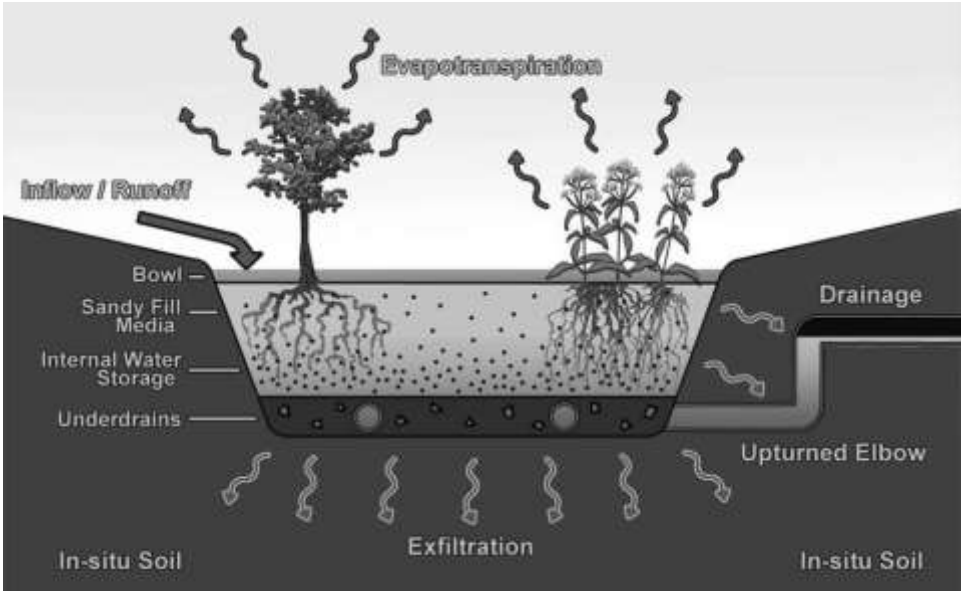

Figure 1-1. Schematic of a bioretention cell (courtesy Shawn Kennedy, NCSU)

Permeable pavement is a substitute for conventional impervious asphalt or concrete, and includes a surface course typically of permeable interlocking concrete pavers, concrete grid pavers, porous asphalt, or pervious concrete that provides void space for infiltration of stormwater (Figure 1-2; Bean et al. 2007; Eisenberg et al. 2015). The surface course is underlain with layers of aggregate, which function to both structurally support the pavement and provide void space to store and exfiltrate stormwater. Similar to bioretention, permeable pavements built in clay soils employ an underdrain. Exfiltration is the main volume reduction mechanism, since plants are not present in the system to transpire stormwater (Collins et al. 2008). Filtration in the surface course (which is the cause for clogging), sedimentation in the aggregate layers, and some chemical and biological treatment has been observed for permeable pavements (Roseen et al. 2012; Drake et al. 2014b). Due to the absence of plants, they lack some of the pollutant removal processes of bioretention. However, they have become popular in ultra-urban and high land value areas, because the parking lot can serve a dual purpose as an SCM, resulting in more developable land (Pezzaniti et al. 2009).

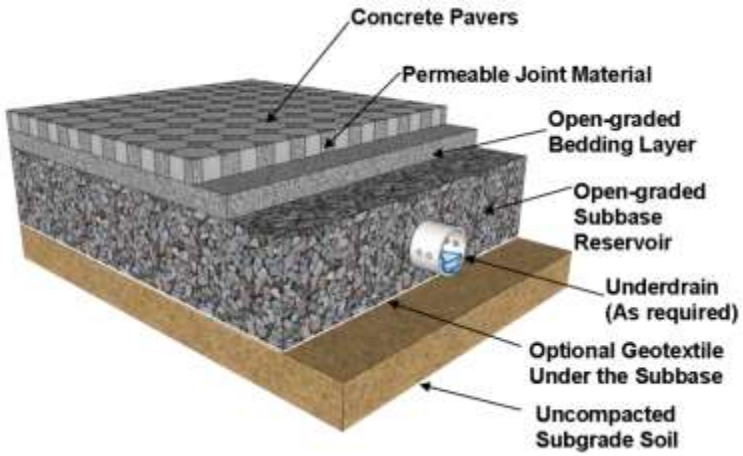

Figure 1-2. Cross-section of a permeable pavement system.

Resilience has been defined as the ability of a system to absorb shock and still maintain function, continuing to thrive as stimuli evolve (Adger 2006). Resilience is not simply about how robust a system is to disturbance, but how the system reacts to and creates opportunities from the disruption (Folke 2006). In the context of stormwater management, if an SCM is designed, constructed, and maintained properly, we expect it to function as intended. However, does its initial performance continue for the foreseeable future (Merriman and Hunt 2014; Lucke and Nichols 2015)? Do natural and anthropogenic stressors cause performance to suffer over time or, worse, system failure to occur (Hunt et al. 2011; Wardynski and Hunt 2012)? One of the purported benefits of green infrastructure is its resilience in comparison to conventional urban water management approaches (Wong and Brown 2008). Resilience to uncertainties in design, maintenance, construction, and climate are critical to ensuring return on investment in GI. This dissertation will explore questions related to resilience of GI under these stressors.

Infiltration-based SCMs, such as bioretention and permeable pavement, rely on the underlying soils (through exfiltration) as the backbone of their hydrologic performance (Figure 1-1). Is system performance resilient to underlying soils that are not highly transmissive? Sediment accumulates in a bioretention facility when maintenance is lacking. Is the system resilient to a reduction in bowl storage? Due to increases in carbon dioxide and other greenhouse gases in the atmosphere, warmer global temperatures are predicted. Will bioretention facilities be resilient to potential climate change? Winter de-icers are frequently applied in urban areas in cold climates. Do permeable pavements still provide optimal water quality benefits during and after de-icing salt application? Infiltration-based stormwater practices require maintenance to prevent hydraulic failure. How often and what type of maintenance is needed for a permeable pavement to remain resilient to the stresses it endures? This dissertation will address some of the natural and anthropogenic sources of stress (poor soils, climate, clogging, under-sizing, lack of maintenance, de-icing salt application, poor construction practices, and climate change) that test the resilience of bioretention and permeable pavement systems.

1.3 Project Overview

The *Rainwater and Land Development Manual* (ODNR 2006) provides design guidance for SCMs constructed in Ohio. It is largely based on research and design guidance from other states (J. Dorsey, personal communication, November, 2012). Through a partnership between the Chagrin River Watershed Partners, Ohio Department of Natural Resources, and Old Woman Creek National Estuarine Research Reserve, funding was obtained to evaluate, through monitoring and modeling, the performance of bioretention cells and permeable

pavement systems in northern Ohio, which is known for its low permeability glacial till soils and harsh winters. Prior to this project, few field-based evaluations of urban stormwater practices had been completed in Ohio (with the notable exception of Sansalone and Teng 2004). This project sought to determine hydrologic performance of these two SCMs when constructed in poorly drained soils to inform crediting policy for volume reduction for new development and redevelopment. The project also aimed to provide better guidance for peak flow mitigation from GI practices, so the size of detention basins within the same development could (potentially) be reduced. Finally, the resilience of permeable pavements was evaluated by quantifying the effects of de-icing salt on their water quality performance and through determination of maintenance needs and best maintenance practices.

This dissertation is divided into nine chapters. Chapters 2-4 describe the bioretention research results, including field monitoring in Kirtland and Pepper Pike, Ohio, and modeling using DRAINMOD and SWMM. Chapters 5-8 focus on permeable pavement field monitoring in northern Ohio (Willoughby Hills, Orange Village, and Perkins Township), including its hydrologic and water quality performance, a study focused on maintenance of permeable pavement, and the development of a novel infiltrometer for permeable pavement surface infiltration rate (SIR) testing.

More specifically, chapter 2 focuses on the performance of bioretention cells designed with IWS zones, constructed in low permeability soils, and under the influence of the northeast Ohio climate. The three cells were built in varying degrees of low permeability soils, specifically silt loam and silty clay loam soil types. The water balance was quantified

for each cell to determine its effects on volume reduction, peak flow mitigation, and flow duration.

Chapter 3 addresses bioretention hydrologic modeling using the agricultural drainage model DRAINMOD. There are many similarities between bioretention systems and tile-drained agricultural fields, including soil, plants, surface storage, drains, etc. Field-monitoring is an expensive undertaking, and the many design components (media depth, surface storage volume, bowl depth, catchment area to bioretention surface area ratio, media characteristics, drainage configuration, etc.), climatic variability, and underlying soil type mean it is impractical to attempt to monitor every possible bioretention configuration. Therefore, the field-collected bioretention hydrology data discussed in chapter 2 were used to calibrate and validate a separate DRAINMOD model for each of the three bioretention cells. Once the models were calibrated, a bioretention design analysis was conducted to quantify long-term hydrology under hundreds of potential design configurations to potentially effect change to Ohio's bioretention design guidance and crediting system.

Because variability in climate due to carbon emissions may cause substantial changes to temperature and rainfall patterns, the impact of climate change in this region was evaluated in Chapter 4 using the calibrated DRAINMOD models. A current and two mid-21st century precipitation and temperature data sets (dynamically downscaled from a regional climate model) for northeast Ohio were utilized to evaluate impacts of climate change on bioretention hydrology. Specific focus was given to volume reduction and overflow (i.e., untreated bypass), as these parameters most affect pollutant loading to surface waters.

In chapter 5, field-monitoring of four permeable pavements is presented to quantify improvement to urban hydrology. Many published studies report data on permeable pavements constructed over sandy soils, treating only direct rainfall, and employing an underdrain at the bottom of the cross-section (e.g., Collins et al 2008; Drake et al. 2014a). In this study, all permeable pavements were situated over silt loam or silty clay loam soils, most treated run-on from impermeable pavements, and all employed a 15-cm IWS zone. Volume reduction, peak flow mitigation, and flow duration are highlighted.

Chapter 6 focuses on water quality monitoring of the permeable pavements at Willoughby Hills, Ohio. This was some of the first water quality data to be collected for permeable pavements treating run-on, increasing the loading ratio for the SCM vis-à-vis permeable pavements treating only direct rainfall. Nutrient, sediment, chloride, and heavy metals were the focus of the analysis. Influent and effluent pollutant concentrations and loads were determined for each permeable pavement. Of particular interest were factors impacting pollutant removal, such as the winter application of de-icing salt and the underlying low permeability soils.

The aim of chapter 7 was to build on the current knowledge base regarding maintenance of permeable pavements. Various maintenance techniques have been suggested, including mechanical street sweeping, street sweeping with suction, vacuuming, pressure washing, and a combination of pressure washing and vacuuming (Bean et al. 2007; Drake and Bradford 2013). This work evaluated the effects of three different types of truck-based street sweeping, industrial hand vacuuming, pressure washing, a combination of industrial vacuuming and pressure washing, and manual removal of the upper 2 cm of clogging

material. Additionally, milling of a 21-yr old porous asphalt was attempted to rejuvenate pavement SIR. Maintenance techniques were evaluated through pre- and post-maintenance measurement of pavement surface infiltration rate (SIR). This work included permeable pavements located in the U.S. and Sweden and in three Köppen-Geiger climatic zones: humid subtropical, humid continental, and subarctic.

In Chapter 8, a novel infiltrometer, the Simple Infiltration Test (SIT), was compared against the American Society for Testing and Materials (ASTM) standard test for SIR measurement. When a permeable pavement is clogged, the duration of the ASTM test can be multiple hours, reducing its usefulness as a method to rapidly determine permeable pavement maintenance needs. The ASTM and newly-developed SIT test were evaluated in parallel via testing in North Carolina, Ohio, and Sweden in an attempt to devise a more repeatable and quicker surface infiltration testing methodology.

1.4 References

Adger, W.N. (2006). "Vulnerability." *Global Environ. Change,* 16(3), 268–281.

Arnold Jr, C.L., and Gibbons, C.J. (1996). "Impervious surface coverage: the emergence of a key environmental indicator." *J. Am. Plann. Assoc*., 62(2), 243-258.

Bannerman, R.T., Owens, D.W., Dodds, R.B., and Hornewer, N.J. (1993). "Sources of pollutants in Wisconsin stormwater." *Water Sci. Tech.*, 28(3), 241-259.

Barrett, M.E., Irish, L.B., Malina, J.F., and Charbeneau, R.J. (1998). "Characterization of highway runoff in Austin, Texas, area." *J. Environ. Eng.*, 124(2), 131-137.

Bean, E.Z., Hunt, W.F., and Bidelspach, D.A. (2007). "Evaluation of four permeable pavement sites in eastern North Carolina for runoff reduction and water quality impacts.*" J. Irrig. Drain. Eng.*, 133(6), 583-592.

Bean, E.Z., and Dukes, M.D. (2014). "Effect of Amendment Type and Incorporation Depth on Runoff from Compacted Sandy Soils." *J. Irrig. Drain. Eng*., 141(6), 04014074.

Berland, A., and Hopton, M.E. (2014). "Comparing street tree assemblages and associated stormwater benefits among communities in metropolitan Cincinnati, Ohio, USA." *Urban For. Urban Greening*, *13*(4), 734-741.

Bledsoe, B.P. (2002). "Stream erosion potential and stormwater management strategies." *J. Water Resour. Plann. Manage*. 128(6), 451-455.

Booth, D.B. (2005). "Challenges and prospects for restoring urban streams: A perspective from the pacific northwest of North America." *J. North Am. Benthological Soc.*, 24(3), 724-737.

Bratieres, K., Fletcher, T.D., Deletic, A., and Zinger, Y. (2008). "Nutrient and sediment removal by stormwater biofilters: A large-scale design optimisation study." *Water Res*., 42(14), 3930-3940.

Brattebo, B.O., and Booth, D.B. (2003). "Long-term stormwater quantity and quality performance of permeable pavement systems." *Water Res*., 37(18), 4369-4376.

Brown, R.A., and Hunt III, W F. (2011a). "Impacts of media depth on effluent water quality and hydrologic performance of undersized bioretention cells." *J. Irrig. Drain. Eng*., 137(3), 132-143.

Brown, R.A. and Hunt, W.F. (2011b). "Underdrain configuration to enhance bioretention exfiltration to reduce pollutant loads." *J. Environ. Eng*., 137(11), 1082-1091.

Brown, R.A., and Hunt, W.F. (2012). “Improving bioretention/biofiltration performance with restorative maintenance.” *Water Sci. Technol*., 65(2), 361-367.

Burns, M.J., Fletcher, T.D., Walsh, C.J., Ladson, A.R., and Hatt, B.E. (2012). “Hydrologic shortcomings of conventional urban stormwater management and opportunities for reform.” *Landscape Urban Plann*., 105(3), 230-240.

Collins, K.A., Hunt, W.F., and Hathaway, J.M. (2008). “Hydrologic comparison of four types of permeable pavement and standard asphalt in eastern North Carolina.” *J. Hydrol. Eng*., 13(12), 1146-1157.

Davis, A.P. (2008). “Field performance of bioretention: Hydrology impacts.” *J. Hydrol. Eng*., 13(2), 90-95.

Davis, A.P., Traver, R.G., Hunt, W.F., Lee, R., Brown, R.A., and Olszewski, J.M. (2012). “Hydrologic performance of bioretention storm-water control measures.” *J. Hydrol. Eng*., 17(5), 604-614.

Davis, A.P., Stagge, J.H., Jamil, E., and Kim, H. (2012). “Hydraulic performance of grass swales for managing highway runoff.” *Water Res*., 46(20), 6775-6786.

Drake, J., and Bradford, A. (2013). “Assessing the potential for restoration of surface permeability for permeable pavements through maintenance.” *Water Sci. Technol*., 68(8), 1950-1958.

Drake, J., Bradford, A., and Marsalek, J. (2013). “Review of environmental performance of permeable pavement systems: state of the knowledge.” *Water Qual. Res. J. Canada*, 48(3), 203-222.

Drake, J., Bradford, A., and Van Seters, T. (2014a). “Hydrologic performance of three partial-infiltration permeable pavements in a cold climate over low permeability soil.” *J. Hydrol. Eng.*, 19(9), 04014016.

Drake, J., Bradford, A., and Van Seters, T. (2014b). “Stormwater quality of spring–summer-fall effluent from three partial-infiltration permeable pavement systems and conventional asphalt pavement.” *J. Environ. Manage.*, 139, 69-79.

Eisenberg, B.E., Lindow, K.C., and Smith, D.R. (2015). *Permeable pavements*. 1st Ed., American Society of Civil Engineers, Reston, VA.

Fassman, E.A., and Blackbourn, S. (2010). “Urban runoff mitigation by a permeable pavement system over impermeable soils.” *J. Hydrol. Eng.*, 15(6), 475-485.

Fletcher, T.D., Shuster, W., Hunt, W.F., Ashley, R., Butler, D., Arthur, S., et al. (2014). "SUDS, LID, BMPs, WSUD and more–The evolution and application of terminology surrounding urban drainage." *Urban Water J.*, 12(7), 525-542.

Folke, C. (2006). "Resilience: The emergence of a perspective for social-ecological systems analysis." *Global Environ. Change*, 16(3): 253-267.

Hathaway, J.M., Hunt, W.F., and Simmons III, O.D. (2010). "Statistical evaluation of factors affecting indicator bacteria in urban storm-water runoff." *J. Environ. Eng.*, 136(12), 1360-1368.

Hatt, B.E., Fletcher, T.D., and Deletic, A. (2009). "Hydrologic and pollutant removal performance of stormwater biofiltration systems at the field scale." *J. Hydrol*., 365(3), 310-321.

Hunt, W.F., Jarrett, A.R., Smith, J.T., and Sharkey, L.J. (2006). "Evaluating bioretention hydrology and nutrient removal at three field sites in North Carolina." *J. Irrig. Drain. Eng*., 132(6), 600–608.

Hunt, W.F., Smith, J.T., Jadlocki, S.J., Hathaway, J.M., and Eubanks, P.R. (2008). "Pollutant removal and peak flow mitigation by a bioretention cell in urban Charlotte, NC." *J. Environ. Eng*., 134(5), 403-408.

Hunt, W.F., Greenway, M., Moore, T.C., Brown, R.A., Kennedy, S.G., Line, D.E., and Lord, W.G. (2011). "Constructed storm-water wetland installation and maintenance: Are we getting it right?" *J. Irrig. Drain. Eng.*, 137(8), 469-474.

Konrad, C., Booth, D., and Burges, S. (2005). "Effects of urban development in the Puget lowland, Washington, on interannual streamflow patterns: Consequences for channel form and streambed disturbance." *Water Resour. Res.*, 41(7), W07009.

LeFevre, G.H., Paus, K.H., Natarajan, P., Gulliver, J.S., Novak, P.J., and Hozalski, R.M. (2014). "Review of dissolved pollutants in urban storm water and their removal and fate in bioretention cells." *J. Environ. Eng*., 141(1), 04014050.

Line, D.E., White, N.M., Osmond, D.L., Jennings, G.D., and Mojonnier, C.B. (2002). "Pollutant export from various land uses in the Upper Neuse River Basin." *Water Environ. Res.*, 74(1), 100-108.

Line, D.E., and White, N.M. (2007). "Effects of development on runoff and pollutant export." *Water Environ. Res.*, 79(2), 185-190.

Lucke, T., and Nichols, P.W. (2015). "The pollution removal and stormwater reduction performance of street-side bioretention basins after ten years in operation." *Sci. Total Environ.*, 536, 784-792.

Luell, S.K., Hunt, W.F., and Winston, R.J. (2011). "Evaluation of undersized bioretention stormwater control measures for treatment of highway bridge deck runoff." *Water Sci. Technol*., 64(4), 974-979.

Merriman, L.S., and Hunt, W. F. (2014). "Maintenance versus maturation: constructed storm-water wetland's fifth-year water quality and hydrologic assessment." *J. Environ. Eng*., 140(10), 05014003.

Morse, C.C., Huryn, A.D., and Cronan, C. (2003). "Impervious surface area as a predictor of the effects of urbanization on stream insect communities in Maine, USA." *Environ. Monit. Assess.*, 89(1), 95-127.

Ohio Department of Natural Resources (ODNR), Division of Soil and Water Conservation. (2006). *Rainwater and land development: Ohio's standards for stormwater management, low impact development, and urban stream protection*. 3rd edition. Ed: John Mathews.

Olszewski, J.M., and Davis, A.P. (2013). "Comparing the hydrologic performance of a bioretention cell with predevelopment values." *J. Irrig. Drain. Eng*., 139(2), 124-130.

Page, J.L., Winston, R.J., Mayes, D.B., Perrin, C., Hunt, W.F. (2015). "Hydrologic mitigation of impervious cover in the municipal right-of-way through innovative stormwater control measures." *J. Hydrol.*, 527, 923-932.

Page, J.L., Winston, R.J., and Hunt, W.F. (2015). "Soils beneath suspended pavements: An opportunity for stormwater control and treatment." *Ecol. Eng.*, 82, 40-48.

Passeport, E., and Hunt, W.F. (2009). "Asphalt parking lot runoff nutrient characterization for eight sites in North Carolina, USA." *J. Hydrol. Eng.*, 14(4), 352-361.

Pezzaniti, D., Beecham, S., and Kandasamy, J. (2009). "Influence of clogging on the effective life of permeable pavements." *Proceedings of the ICE-Water Manage.*, 162(3), 211-220.

Pitt, R., Field, R., Lalor, M., and Brown, M. (1995). "Urban stormwater toxic pollutants: assessment, sources, and treatability." *Water Environ. Res*., 67(3), 260-275.

Pitt, R., Clark, S., and Field, R. (1999). "Groundwater contamination potential from stormwater infiltration practices." *Urban Water*, 1(3), 217-236.

Roseen, R.M., Ballestero, T.P., Houle, J.J., Briggs, J.F., and Houle, K.M. (2012). "Water quality and hydrologic performance of a porous asphalt pavement as a storm-water treatment strategy in a cold climate." *J. Environ. Eng.*, 138(1), 81-89.

Sabin, L.D., Lim, J.H., Stolzenbach, K.D., and Schiff, K.C. (2005). "Contribution of trace metals from atmospheric deposition to stormwater runoff in a small impervious urban catchment." *Water Res.*, 39(16), 3929-3937.

Sansalone, J.J., and Teng, Z. (2004). "In situ partial exfiltration of rainfall runoff. I: Quality and quantity attenuation." *J. Environ. Eng.*, 130(9), 990–1007.

Schueler, T.R., Fraley-McNeal, L., and Cappiella, K. (2009). "Is impervious cover still important? Review of recent research." *J. Hydrol. Eng.*, 14(4), 309-315.

Scott, W.S. (1976). "The effect of road deicing salts on sodium concentration in an urban water-course." *Environ Poll.*, 10(2), 141-153.

Struck, S.D., Field, R., and Pitt, R., 2010. "Green infrastructure for CSO control in Kansas City, Missouri." In *Proceedings of Conference on Low Impact Development 2010: Redefining Water in the City*. Reston, VA: American Society of Civil Engineers.

Tillinghast, E.D., Hunt, W.F., and Jennings, G.D. (2011). "Stormwater control measure (SCM) design standards to limit stream erosion for Piedmont North Carolina." *J. Hydrol.*, 411(3), 185-196.

US EPA (2012). *Green infrastructure*. Available: http://water.epa.gov/infrastructure/greeninfrastructure/index.cfm

Walsh, C.J., Roy, A.H., Feminella, J.W., Cottingham, P.D., Groffman, P.M., and Morgan, R.P. (2005). "The urban stream syndrome: current knowledge and the search for a cure." *J. North Am. Benthological Soc.*, 24(3), 706-723.

Wardynski, B.J., and Hunt, W.F. (2012). "Are bioretention cells being installed per design standards in North Carolina? A field study." *J. Environ. Eng.*, 138(12), 1210-1217.

Wardynski, B.J., Winston, R.J., and Hunt, W.F. (2012). "Internal water storage enhances exfiltration and thermal load reduction from permeable pavement in the North Carolina mountains." *J. Environ. Eng.*, 139(2), 187-195.

Wicke, D., Cochrane, T.A., and O'Sullivan, A.D. (2012). "Atmospheric deposition and storm induced runoff of heavy metals from different impermeable urban surfaces." *J. Environ. Monit., 14*(1), 209-216.

Wilson, C.E., Hunt, W.F., Winston, R.J., and Smith, P. (2015). "Comparison of runoff quality and quantity from a commercial low-impact and conventional development in Raleigh, North Carolina." *J. Environ. Eng.*, 141(2), 05014005.

Winston, R.J., Hunt, W.F., Kennedy, S.G., Wright, J.D., and Lauffer, M. S. (2011). "Field evaluation of storm-water control measures for highway runoff treatment." *J. Environ. Eng.*, 138(1), 101-111.

Winston, R.J., Hunt, W.F., Kennedy, S.G., Merriman, L.S., Chandler, J., and Brown, D. (2013). "Evaluation of floating treatment wetlands as retrofits to existing stormwater retention ponds." *Ecol. Eng.*, 54, 254-265.

Winston, R.J., Lauffer, M.S., Narayanaswamy, K., McDaniel, A.H., Lipscomb, B.S., Nice, A.J., and Hunt, W.F. (2014). "Comparing Bridge Deck Runoff and Stormwater Control Measure Quality in North Carolina." *J. Environ. Eng*., 141(1), 04014045.

Wolman, M.G. (1967). "A cycle of sedimentation and erosion in urban river channels." *Geografiska Annaler. Series A. Physical Geography*. 385-395.

Wong, T., and Brown, R. (2008). "Transitioning to water sensitive cities: ensuring resilience through a new hydro-social contract." In *11th International Conference on Urban Drainage.* Edinburgh, Scotland.

Wu, J.S., Allan, C.J., Saunders, W.L., and Evett, J.B. (1998). "Characterization and pollutant loading estimation for highway runoff." *J. Environ. Eng.*, 124(7), 584-592.

United States Environmental Protection Agency (USEPA). (1999). *Storm Water Technology Fact Sheet: Wet Detention Ponds*. EPA 832-F-99-048, Office of Water, Washington, D.C.

United Nations, Department of Economic and Social Affairs, Population Division. (2014). *World urbanization prospects: The 2014 revision, highlights*. ST/ESA/SER.A/352.

CHAPTER 2: **QUANTIFYING VOLUME REDUCTION AND PEAK FLOW MITIGATION FOR THREE BIORETENTION CELLS IN CLAY SOILS IN NORTHEAST OHIO**

2.1 Abstract

Green stormwater infrastructure aims to restore watershed hydrologic function by more closely mimicking pre-development groundwater recharge and evapotranspiration (ET). Bioretention has become a popular stormwater control due to its ability to reduce runoff volume through these pathways. Three bioretention cells constructed in low permeability soils in northeast Ohio were monitored for non-winter quantification of inflow, drainage, ET, and exfiltration. The inclusion of an internal water storage (IWS) zone allowed the three cells to reduce runoff 59%, 42%, and 36% over the monitoring period, in spite of the tight underlying soils. The exfiltration rate and the IWS zone thickness were the primary determinants of volume reduction performance. Post-construction measured drawdown rates were *higher* than pre-construction soil vertical hydraulic conductivity tests in all cases, due to lateral exfiltration from the IWS zones and ET, which are not typically accounted for in pre-construction soil testing. The minimum rainfall depths required to produce outflow for the three cells were 5.5, 7.4, and 13.8 mm. During events with 1-year design rainfall intensities, peak flow reduction varied from 24 to 96%, with the best mitigation during events where peak rainfall rate occurred before the centroid of the rainfall volume, when adequate bowl storage was available to limit overflow.

2.2 Literature Review

Urban development generates impervious surfaces and modifies the hydrological cycle by reducing infiltration and evapotranspiration (ET) while increasing surface runoff

(Bledsoe and Watson 2001; Booth et al. 2002; Walsh et al. 2012). Watershed imperviousness of 10% or more has been shown to negatively impact stream ecology, habitat, and water quality (Wang et al. 2001; Schueler et al. 2009). Incision and bank erosion caused cross-sectional area of urban streams to be 3.8 times larger than rural streams in Piedmont Pennsylvania (Hammer 1972; Booth 1990). Recent studies have shown detention basins may amplify the duration of critical erosion-causing discharges, furthering stream degradation (Palhegyi 2009; Tillinghast et al. 2011). In contrast, DeBusk et al. (2011) found drainage from bioretention cells was released at rates similar to shallow interflow in rural reference watersheds, suggesting watershed scale implementation of bioretention could benefit stream health through disconnection of imperviousness (Walsh et al. 2009; Burns et al. 2012). Low Impact Development (LID) technologies, such as bioretention (also termed biofilters), are purported to more closely mimic pre-development hydrology, including duration, rate, and volume of flow (USEPA 2007; Cizek and Hunt 2013; Page et al. 2015).

Bioretention cells are biologically-based media filters designed to temporarily store and treat a prescribed water quality volume (e.g., runoff from a 19-mm wet weather event in Ohio) from highly impervious catchments (ODNR 2006). Typically, bioretention cells pond 22-30 cm of stormwater in their surface storage (i.e., bowl), have 60-120 cm of engineered media and, when underlying soils are poorly drained, have an underdrain surrounded by a gravel layer to allow for inter-event drainage (Davis 2008; Li et al. 2009; Davis et al. 2009; Figure 2-1). Once the bowl fills, a bypass or overflow structure conveys flow to the storm or combined sewer network.

Bioretention media is a mixture of sand (usually the vast majority of the media), fines (silt and clay), and organic matter, with 5-10 cm/hr typically targeted as a design infiltration rate (Dietz and Clausen 2005; Emerson and Traver 2008; Hunt et al. 2012). The media supports the growth of plants, typically trees, shrubs, forbs, and/or grasses chosen for their ability to withstand primarily droughty but also temporarily inundated conditions (Bratieres et al. 2008). Vegetation promotes ET and maintains the soil infiltration rate over time, with root macropores appearing to offset the negative effects of media compaction and sediment deposition (Jenkins et al. 2010).

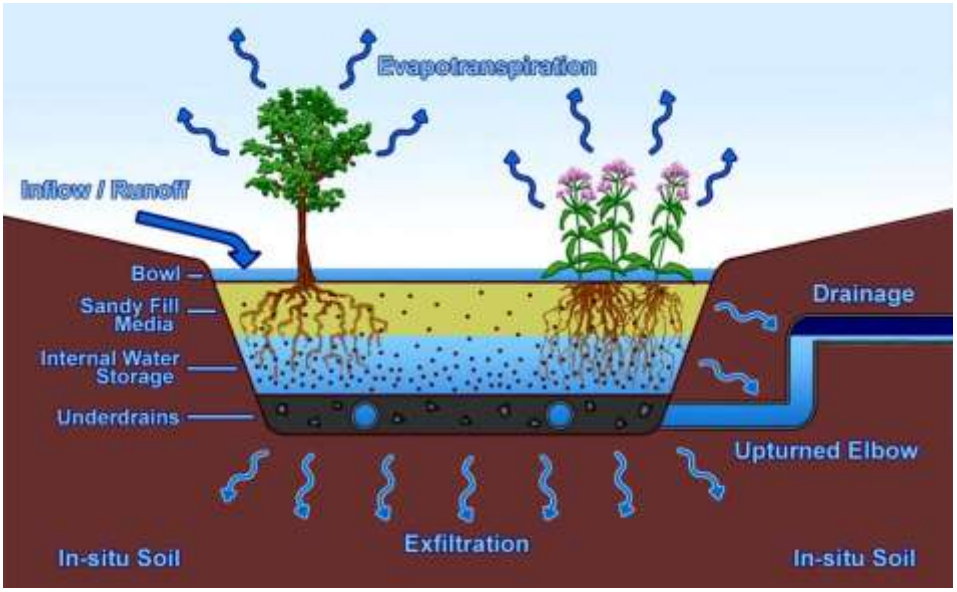

Figure 2-1. Schematic of a bioretention cell with an internal water storage (IWS) zone (courtesy Shawn Kennedy, NCSU)

Four pathways exist for outflow from bioretention cells: exfiltration to the underlying soil, ET, drainage through the underdrain, and overflow/bypass. Bioretention cells often capture in their entirety (and do not release runoff from) storms smaller than the water

quality design storm (Davis 2008; Hunt et al. 2008; Li et al. 2009; Jones and Hunt 2009), which translates into substantial abstraction of long-term runoff volume (Davis, Traver et al. 2012). For instance, 18% of events monitored at two bioretention facilities in Maryland which were lined with an impermeable membrane had no outflow (Davis 2008). Thirty-three percent of the inflow volume was retained in lined biofilters in Australia, with retention proportional to rainfall depth (Hatt et al. 2009). Luell (2011) studied two bioretention cells built in compacted sandy clay loam soils, one sized to treat the 25-mm event and one to treat the 12.5-mm event. The cells reduced runoff volume by 30% and 20%, respectively. Deeper media depths promoted additional exfiltration (Brown and Hunt 2011a). Exfiltration and ET resulted in 50-90% volume reduction from bioretention facilities (Heasom et al. 2006; Hunt et al. 2006), and was dependent on the underlying soil type. Li et al. (2009) showed ET was 15-20% of inflow for a bioretention cell in Louisburg, N.C.

Peak flow mitigation in a bioretention cell was directly associated with its surface area, surface storage volume, the infiltration rate of the media, and the exfiltration rate (Davis et al. 2009; Davis, Traver et al. 2012). Peak flow mitigation was 65% in Connecticut (Dietz and Clausen 2005), 80% in Australia (Hatt et al. 2009), and seasonally variable but lower in winter (Muthanna et al. 2008). To maximize peak flow mitigation, proportionally large bioretention surface area and deeper media depth are desired (Li et al. 2009; Davis, Traver et al. 2012).

The underdrain configuration in a bioretention cell substantially impacts volume reduction (Brown and Hunt 2011b); a bioretention cell may lack an underdrain when underlying soils are highly transmissive, employ an underdrain at the bottom of the cross-

section, have an underdrain with a valve or orifice to control outflow rate (City of Omaha 2014; MPCA 2015; Guo and Luu 2015), or utilize an internal water storage zone (IWS). An IWS zone is created by an upturned elbow in the underdrain, forcing internal ponding within the media (Figure 2-1). The IWS zone is typically 0.3 to 0.75-m deep (Hunt et al., 2006; Passeport et al., 2009). With low permeability underlying soils, the IWS zone will dewater slowly. In these conditions, a zone of aerobic media should be maintained above the IWS zone for plant growth and to prevent leaching of heavy metals (Blecken et al. 2009). The IWS zone was originally recommended to promote denitrification (Hunt et al. 2006; Dietz and Clausen 2006; Davis 2008; Passeport et al. 2009), but has been shown to substantially improve volume reduction (Dietz and Clausen 2006; Brown and Hunt 2011b; Chapter 3). Li et al. (2009) reported a bioretention cell with an IWS zone produced outflow during 37% of observed storms, while a neighboring, otherwise identical, cell with no IWS zone had outflow for 65% of storms. The mechanism for augmented volume reduction was the additional storage provided by inter-event exfiltration, which otherwise is limited in bioretention cells.

While bioretention design has been informed through synthesized research studies (e.g., Hunt et al. 2012), the hydrology of bioretention systems over poorly drained soils has not been thoroughly documented in the field to-date. These infiltration-based stormwater control measures (SCMs) are often specified in Hydrologic Soil Group (HSG) A and B soils, with some entities discouraging their use in poorly drained soils (IDNR 2010). The goal of this study was to quantify bioretention hydrologic performance with an IWS zone and when built in HSG D soils. Three bioretention cells in northeastern Ohio were examined.

2.3 Site Descriptions

The water balance was determined on a storm-by-storm basis for two bioretention cells at Holden Arboretum (HA) and one at Ursuline College (UC; Figure 2-2). Design guidance in the *Ohio Rainwater and Land Development Manual* (ODNR 2006) requires a bioretention cell to capture the 19-mm water quality volume in its bowl and have a filter bed surface area of 5% of the impervious contributing catchment. All three bioretention cells were located in areas with mapped HSG D soils according to the Ohio soil survey [Platea and Pierpont silty clay loam (HA) and Mahoning silt loam (UC), Soil Survey Staff (2015)].

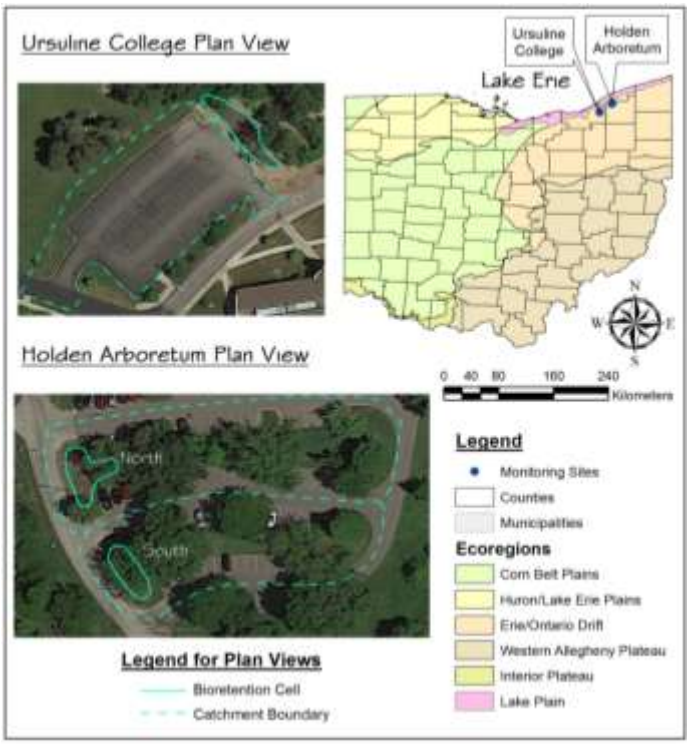

Figure 2-2. Location of bioretention facilities in northeast Ohio.

A bioretention cell was constructed during April-May of 2014 on the campus of UC to treat a 0.36 ha, 77.1% impervious catchment consisting of a parking lot and peripheral pervious areas (Table 2-1 and Figure 2-3). The filter bed surface area was 182 m^2 (6.5% of the contributing impervious catchment). The surveyed bowl depth was 30 cm, and water ponding above this level overflowed through the catch basin (Figure 2-3). Surface (i.e., bowl) storage volume was 60 m^3, compared to the water quality volume of 39 m^3; therefore, this bioretention cell was oversized and stored the runoff from a 29.5-mm storm event in its bowl (Table 2-1).

Figure 2-3. The UC (top left) bioretention cell six months post-construction and the HA South (top right) and North (bottom) bioretention cells 13 months post-construction.

Table 2-1. Summary of bioretention cell and catchment characteristics.

Characteristics	UC	HA South	HA North
Catchment area (m^2)	3600	1900	2700
Catchment percent imperviousness	77	58	58
Bioretention surface area (m^2)	182	57	79
Surface storage volume (m^3)	60	35	48
As-built design event (mm)	29.5	45.2	44.7
Average bowl storage depth (m)	0.30	0.39	0.40
Mulch layer thickness (m)	0.08	0.08	0.08
Fill media depth (m)	0.60	0.84	0.90
Gravel layer thickness (m)	0.30	0.30	0.30
Choking stone + sand layer thickness (m)	0.15	0.15	0.15
IWS zone thickness (m)	0.60	0.38	0.45
Underdrain diameter (cm)	15	10	10
Media characteristics[1]	87% sand, 4% silt, 9% clay	88% sand, 2% silt, 10% clay	88% sand, 2% silt, 10% clay
Media percent organic matter (by weight)[2]	4.3%	1.4%	1.0%
Media textural classification	Loamy sand	Loamy sand	Loamy sand
Media saturated hydraulic conductivity	17 cm/hr	10 cm/hr	10 cm/hr
Vegetation	Forbs and perennial grasses	Forbs and perennial grasses	Shrubs/trees

[1]determined using sieve methods (ASTM 2007)
[2]determined using loss-on-ignition methods (ASTM 2014)

The bioretention media was 87% sand, 4% silt, and 9% clay, resulting in a loamy sand soil texture (Table 2-1). Organic matter was 4.3% of the media by mass. The media was 0.6-m deep and was underlain by 7.5 cm of medium coarse sand, 7.5 cm of pea gravel (1.2-12.7 mm nominal diameter), and 30 cm of #57 aggregate (2.4-37 mm nominal diameter). A single 15-cm diameter underdrain drained the cell, and a 60-cm deep IWS zone extended through the gravel and sand layers and 15 cm into the bioretention media. Forty-five cm of media was located above the underdrain invert. The bioretention cell was

planted with 1450 plugs [see Winston et al. (2015) for plant list], and a 7.5-cm layer of coarse-shredded hardwood mulch was spread over the media. During the monitoring period, the plants were juvenile and developed shoots less than 30 cm tall; therefore, plant processes were not expected to play a major role in the hydrologic results of this study at UC.

Two bioretention cells were constructed at HA in September 2013 (Table 2-1 and Figure 2-3). HA South and North had catchment areas of 0.19 and 0.27 ha, respectively (Figure 2-1). Forty-two percent of each catchment was pervious and well vegetated with turfgrass and mature trees. Filter bed surface areas for HA South and North were 57 and 79 m^2, respectively; these values represented 5% of their respective impervious catchment areas. The HA South and North cells were built with 39 and 40-cm (instead of the intended 30 cm) ponding depths due to a miscommunication during construction (Table 2-1). The resulting surface storage volume of HA South was 35 m^3, compared with the water quality volume of 14.6 m^3; therefore, the bioretention cell was actually sized for the 45.2-mm storm event. For HA North, as-built surface storage was 48 m^3, considerably more than the 20.4 m^3 water quality volume. It was sized to capture the 44.7-mm event without overflow.

Media depths were 84 cm for HA South and 90 cm for HA North. The media was 88% sand, 2% silt, and 10% clay and contained 1.4% and 1.0% organic matter by weight for HA South and North, respectively. The media was underlain by 7.5 cm of coarse sand, 7.5 cm of pea gravel, and 30 cm of #57 aggregate. Coarse-shredded hardwood mulch (7.5 cm depth) was spread over the media. Underdrains were 10 cm in diameter and were tied into existing catch basins located within each cell. IWS zones of 38- and 45-cm were incorporated into the HA South and North cells, respectively. The HA cells were planted

with a mixture of 26 shrubs and one tree (woody plants) in the North cell and 172 forb and perennial grass varieties (herbaceous species) in the South cell (Winston et al. 2015).

2.4 Materials and Methods

Data Collection

A weather station (Hobo, Onset Computer Corporation, Bourne, MA) was deployed at each site to measure wind speed, wind direction, air temperature, relative humidity, and solar radiation. Rainfall was measured at each site using a 0.254-mm resolution tipping-bucket rain gauge (Davis Instruments, Hayward, California). Rainfall data were stored in the data logger in the adjacent weather station. Rain gauges and weather stations were located in areas free from obstructions. All climatic parameters were recorded on a 1-minute interval.

Combined overflow and drainage from each bioretention cell was monitored using a sharp crested, v-notch weir and a Hobo U20 pressure transducer (Onset Computer Corporation, Bourne, MA). The pressure transducer was placed immediately downstream of an internal baffle, as far upstream from the weir as possible. Forty-five degree (HA North) or 60˚ (UC and HA South) v-notch weirs were employed depending on the expected flow rates from the bioretention cells. Internal water level (stage) in the bioretention media was measured using a Hobo U20 pressure transducer within a perforated PVC well. Since the pressure transducers were non-vented, an additional U20 pressure transducer was placed in the rain gauge housing at each site to measure (and later correct for) local barometric pressure using a pressure correction algorithm built into the Hoboware software. Pressure transducers recorded data on a 2-minute interval and were downloaded every 3 weeks.

Data Analysis

Summary statistics were developed for rainfall depth (mm), average rainfall intensity (mm/hr), peak 5-minute rainfall intensity (mm/hr), and antecedent dry period (ADP, days). Discrete storm events were identified by a minimum ADP of 6 hours and rainfall depth of 2.5 mm.

The use of a weir or flume to measure inflow was precluded by diffuse inflow to each bioretention cell. Inflow was determined using a rainfall-runoff model, the NRCS curve number method (USDA-NRCS 1986):

$$Q = \frac{(P-0.2S)^2}{(P+0.8S)} \times \frac{A}{1000} \quad (2\text{-}1)$$

where Q is runoff volume (m^3), P is precipitation depth (mm), S is potential maximum soil moisture retention (mm) and is equal to $(\frac{1000}{CN} - 10) \times 25.4$, CN = curve number for the catchment, and A is the surface area of the catchment (m^2).

Inflow volumes were calculated for each runoff producing event (i.e., $P > 0.2 \times S$). Impervious areas within each catchment were assigned the standard CN of 98 (i.e., almost all rainfall becomes runoff), while pervious areas were assigned a CN of 80 for open space in good condition (>75% grass cover) on an HSG D soil (Fangmeier et al. 2006). Discrete runoff volumes for permeable and impermeable catchment areas were calculated separately and summed, as suggested in Chin (2006). Corrections were applied to the CN for dry and wet antecedent moisture conditions (USDA-NRCS 2004). Antecedent dry periods less than 2 and greater than 5 days were considered wet and dry, respectively.

Peak inflow rates were calculated using the Rational Method (Chin 2006), which relates rainfall intensity to flow rate:

$$Q_p = 2.78 \times C \times i \times A \quad (2\text{-}2)$$

where Q_p is the peak flow rate (L/s), C is the Rational runoff coefficient, i is the peak 5-minute rainfall intensity (mm/hr), and A is the catchment area (ha). The Rational coefficient is customarily 0.9 for impervious areas, while pervious areas were assigned a rational coefficient of 0.2, representative of lawns on average slope and low permeability soil (Chin 2006).

Weir equations related outflow to depth of flow above each weir crest (Grant and Dawson 2001):

$$Q = 571.4 \times H^{2.5}, 45^{\circ} \text{ v-notch weir} \quad (2\text{-}3)$$

$$Q = 796.7 \times H^{2.5}, 60^{\circ} \text{ v-notch weir} \quad (2\text{-}4)$$

where Q is flow rate (L/s) and H is head (m) above the weir crest. Outflow rates were calculated on a 2-minute interval, and the area under the hydrograph integrated over time to calculate outflow volume on a storm-by-storm basis. Cumulative inflow and outflow volumes were the sum of individual storm volumes. The peak outflow rate for each storm event was the maximum instantaneous 2-minute value.

Hydrograph separation was used at HA to separate drainage from overflow following methods proposed in Brown and Hunt (2011a). Modeling in USEPA's Storm Water Management Model (SWMM) v5.1.007 was performed to separate drainage from overflow at UC (USEPA 2015). A rating curve was developed in SWMM to predict drainage based on measured internal water level data. Assumptions were made that (1) all water stored in the

media and aggregate layers was hydraulically connected, and (2) the hydraulic conductivity was sufficient enough that the internal water level measured in observation wells reflected a true water surface elevation. Measured internal water levels then represented the driving head for drainage.

To develop the rating curve, the bioretention cell was modeled as a storage unit in SWMM with a conduit controlling discharge (i.e., pressurized pipe flow). The outlet was modeled as a 10-m length of PVC pipe (Manning's roughness of 0.011) to account for friction losses from the underdrain and fittings. A resulting internal water level-discharge relationship was used to generate a drainage hydrograph for each monitored storm event.

To determine the combined volume of exfiltration and evaporation, internal water level measurements within the bioretention media were utilized to calculate the drawdown rate. Following each storm, the water level and date/time of the end of drainage (i.e., when the water level reached the invert of the underdrain) were recorded. Immediately preceding the commencement of the following rain event, the water level and date/time were also recorded. A total drawdown time and depth could then be calculated; the drawdown rate (mm/hr) is defined as the quotient of these values. The total volume of exfiltration and ET was calculated using:

$$V_{EE} = \frac{\sum_{i=1}^{n}(Q_{DD,i} \times t_{DD,i} \times \phi) \times f_{drain} \times A_{IS}}{1000} \quad (2\text{-}5)$$

where V_{EE} is the total volume exfiltrated and evapotranspired over the monitoring period (m^3), n is the total number of inter-event periods, Q_{DD} is the drawdown rate (mm/hr), t_{DD} is the inter-event period duration (hr), ϕ is the porosity of the aggregate and/or bioretention media (measured during determination of soil-water characteristic curves, Chapter 3), f_{drain} is

the ratio of the total monitoring period duration to the total dry period duration, and A_{IS} is the area of the infiltrative surface (m^2). The f_{drain} parameter accounted for drawdown during periods of drainage.

2.5 Results and Discussion

Rainfall

Over the monitoring period at UC (May to November 2014), fifty storm events were observed. The monitoring period at HA was from October 2013 through November 2014, during which 90 separate storms were reliably monitored. Data collected during the winter (December 2013 through March 2014) at HA were not included in this analysis due to sub-freezing temperatures.

Total rainfall depths during the monitoring periods at UC and HA were 742 and 1175 mm, respectively. Over the 30-yr period from 1981-2010, Cleveland Hopkins International Airport (the nearest long-term rainfall record) received an annual average of 994 mm of precipitation (NOAA 2015); precipitation depth during the monitoring periods was greater than the long-term average at both sites. Median and mean rainfall depths were 7-8 mm and 13-14 mm, respectively (Table 2-2). Maximum event depth was 89 mm at UC and 71 mm at HA. Median and mean ADP ranged from 2 to 4 days. A frequency analysis of observed rainfall events at UC and HA is presented in Appendix A.

At UC and HA, respectively, the 79^{th} and 80^{th} percentile observed events corresponded to the 19-mm water quality design event for Ohio. Since they were oversized, the UC, HA South, and HA North treated without overflow the 86^{th}, 96^{th}, and 96^{th} percentile observed

rainfall depths, respectively. Therefore, the hydrologic performance of these bioretention cells was expected to exceed that of the typical bioretention design in northeast Ohio.

Table 2-2. Characteristics of rainfall events at UC and HA.

Site	Statistic	Depth (mm)	Average intensity (mm/hr)	Peak 5-minute intensity (mm/hr)	Antecedent dry period (days)
UC	Minimum	2.5	0.3	3	0.3
	Median	8.1	1.4	16.8	2.2
	Mean	14.4	2.3	29.2	3.5
	90th percentile	39.3	4.9	74.7	7.9
	Maximum	89.2	12.9	152.4	20
HA	Minimum	2.5	0.3	3	0.3
	Median	7.1	1.2	9.1	2.6
	Mean	12.7	2.8	22.6	4
	90th percentile	31	5.6	56.1	8.6
	Maximum	70.9	49.5	103.6	19.7

Drawdown Rate

The underlying soil properties are important to bioretention cell hydrology (Brown and Hunt 2010). If compaction of underlying soils is prevented during construction, pre-construction field-measured saturated hydraulic conductivity (K_{sat}) tests can help predict long-term hydrologic performance (Pitt et al. 2008; Tyner et al. 2009; Wardynski et al. 2012).

Construction was temporarily suspended at UC as excavation reached the final subgrade elevation to undertake soil testing (Figure 2-4). Prior to construction at HA, test pits were excavated at the locations of proposed bioretention cells for the same purpose. Two single-

ring, constant head K_{sat} tests were completed in the subsoils beneath each of the HA cells (Reynolds et al. 2002); three such tests were undertaken at UC. A hoe was used to remove loose soil and create a level test surface of uncompacted subsoil. A Mariotte bottle kept a constant head of 15 cm, and mathematical corrections were used to account for lateral water flow (Reynolds et al. 2002). The tests estimated vertical K_{sat} through the bottom of the bioretention cell. Measured K_{sat} of the underlying soils were low and representative of HSG D soils (Table 2-3; USDA-NRCS 2007): 0.5 and 0.5 mm/hr at HA North, 0.5 and 2 mm/hr at HA South, and 0.5, 0.5, and 0.75 mm/hr at UC. While these vertical K_{sat} measurements do not measure all of the processes that determine the post-construction drawdown rate (for reasons discussed below), they are likely the most useful predictor of drawdown rate.

Figure 2-4. Single ring infiltrometer with Mariotte bottle used for pre-construction infiltration testing (left) and monitoring well used for post-construction drawdown rate measurement (right).

Following construction, internal water level measurements were used to calculate drawdown rates for each bioretention cell. Drawdown rates for the bioretention cells were non-linear, but average values shown in Table 2-3 typically are used in hydrologic modeling

(Smolek et al. 2015). Post-construction drawdown rates were up to 6 to 8 (at UC) and 3 to 4-fold (at HA) *higher* than the K_{sat} measured during construction (Table 2-3).

Table 2-3. Comparison of saturated hydraulic conductivity (K_{sat}) measured during construction to post-construction drawdown rate.

Site	K_{sat} measured during construction (mm/hr)	Drawdown Rate (average ± standard deviation, mm/hr)
UC	0.5, 0.5, 0.75	4.3 ± 4.3
HA North	0.5, 0.5	1.7 ± 1.2
HA South	0.5, 2.0	2.0 ± 3.5

There are a number of potential reasons for this disparity between the two measurements. During construction, the teeth of the excavator bucket were drawn across through the subsoil to break up compaction before backfilling with aggregate and media, as recommended by Brown and Hunt (2010). Measurement of K_{sat} occurred after this de-compaction at UC. The small number of pre-construction K_{sat} tests (2-3) may not provide a representative average K_{sat}, as flow favors (potentially unmeasured) higher permeability areas. Soil K_{sat} may vary over two orders of magnitude within a given SCM (Asleson et al. 2009; Wardynski and Hunt 2012; Olson et al. 2013). Therefore, 2-3 tests may not wholly characterize the potential for exfiltration.

Because the bioretention cells were either irregularly shaped (HA) or long and thin (UC), the proportion of side-walls was relatively high, encouraging lateral exfiltration, which was not captured in vertical K_{sat} measurements during construction. When the IWS zones were completely full, the side-wall surface area represented 27%, 20%, and 22% of the total (i.e.,

side-wall plus subgrade) exfiltrative surface area at UC, HA South, and HA North, respectively. Lateral exfiltration, not accounted for in the vertical K_{sat} tests, occurs at a rate proportional to the lateral K_{sat}. The ratio of vertical to lateral K_{sat} varies spatially and as a function of soil horizon and texture (Bathke and Cassel 1991), but lateral K_{sat} is generally higher than vertical K_{sat} in clay soils, often by factors of 10 to 25 (Bathke and Cassel 1991). Modeling of exfiltration from urban SCMs has shown lateral exfiltration is often the dominant pathway for volume reduction (Browne et al. 2008; Lee et al. 2015). Additionally, ET will be responsible for a modest portion of the drawdown, especially during summer months. For these reasons, drawdown post-construction was higher than vertical K_{sat} measurements obtained during construction; a similar result was not found for permeable pavements in this region of Ohio (Chapter 5).

A subset of the internal water level data for UC is shown in Figure 2-5; 0-m depth represents the interface between the gravel drainage layer and the subsoil. Water levels above the IWS zone (0.6-m thick) corresponded to periods of drainage. The near-vertical water level recession curve between 0.6 and 0.38 m is likely due to very high lateral K_{sat} in this soil horizon (Bathke and Cassel 1991) and, to a lesser degree to greater driving head for vertical exfiltration. A slope break in the drawdown curve was present at 0.38 m; below this point exfiltration occurred at a lower rate approximated by an exponential decay, similar to Schlea et al. (2014). Drawdown below the 0.03-m internal water level represented the transition from head driven exfiltration to capillary flow.

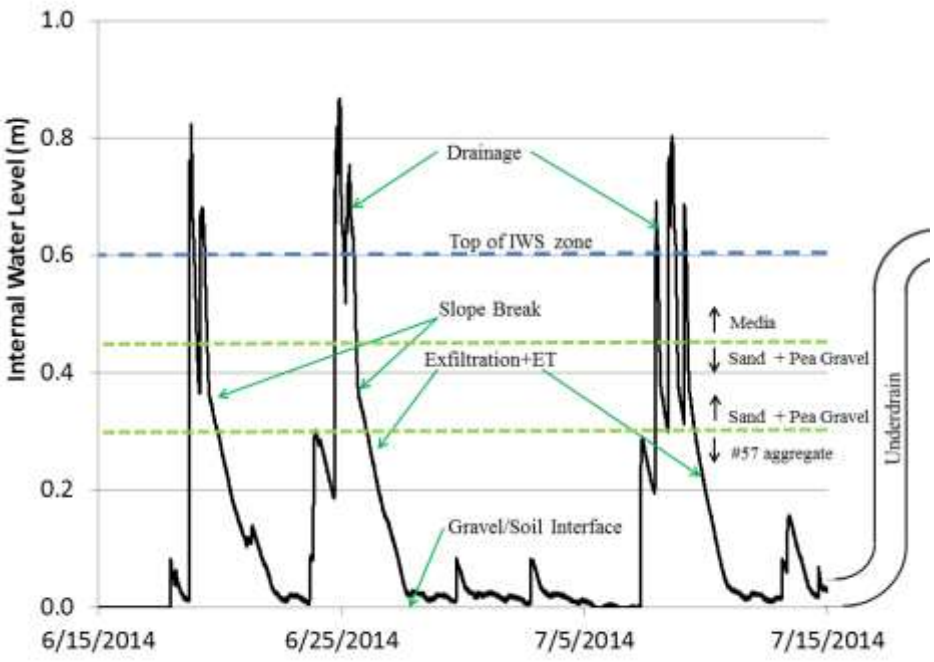

Figure 2-5. Excerpt of UC internal water level profile during June-July 2014.

The HA South and North cells had IWS zone thicknesses of 0.38 and 0.45 m (Figure 2-6). Drawdown rates again were non-linear and modeled using an exponential decay; Lee et al. (2015) suggested nonlinear drawdown curves were representative of SCMs dominated by lateral exfiltration. This is primarily due to the changes in wetted side wall surface area and decreased driving head with drawdown. Drawdown rates were, on average, about 25% higher for HA South than HA North (Figure 2-6), demonstrating the spatial variability of soils (the cells were located 20 m apart) and resulting in the South cell's better volume reduction (discussed later). Both HA cells tended to shift from head driven exfiltration to capillary flow at a 0.1-m internal water level.

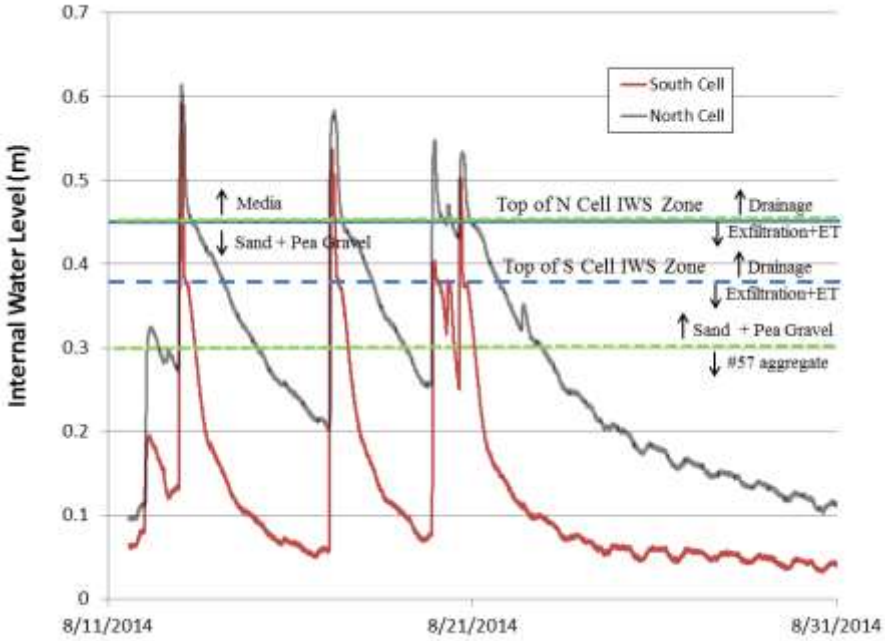

Figure 2-6. HA North and South bioretention cell internal water level profiles during August 2014.

The original intent of the HA study was to observe bioretention performance under two different plant palettes: shrubs and trees versus forbs and perennial grasses. However, differences in exfiltration rates discussed above confounded this effort. Because plants were juvenile during the monitoring period, differences in hydrologic performance between the two HA cells likely resulted from the differences in exfiltration rates.

Hydrograph Separation using SWMM

All outflow from each bioretention cell passed over a single weir; therefore, hydrograph analysis was employed to separate drainage from overflow. A depth-discharge rating curve (Appendix A) was used to generate storm event drainage hydrographs at UC based on a calibrated USEPA SWMM V5.1 model (Figure 2-7). The difference between the measured

outflow hydrograph and the modeled drainage hydrograph was the amount of overflow that occurred. This provided a more representative estimate of overflow than visual hydrograph separation, since drain flow under pressurized conditions should be dependent on internal water level. This type of hydrologic modeling can help inform field-collected data and improve the understanding of unit processes within an SCM (Smolek et al. 2015).

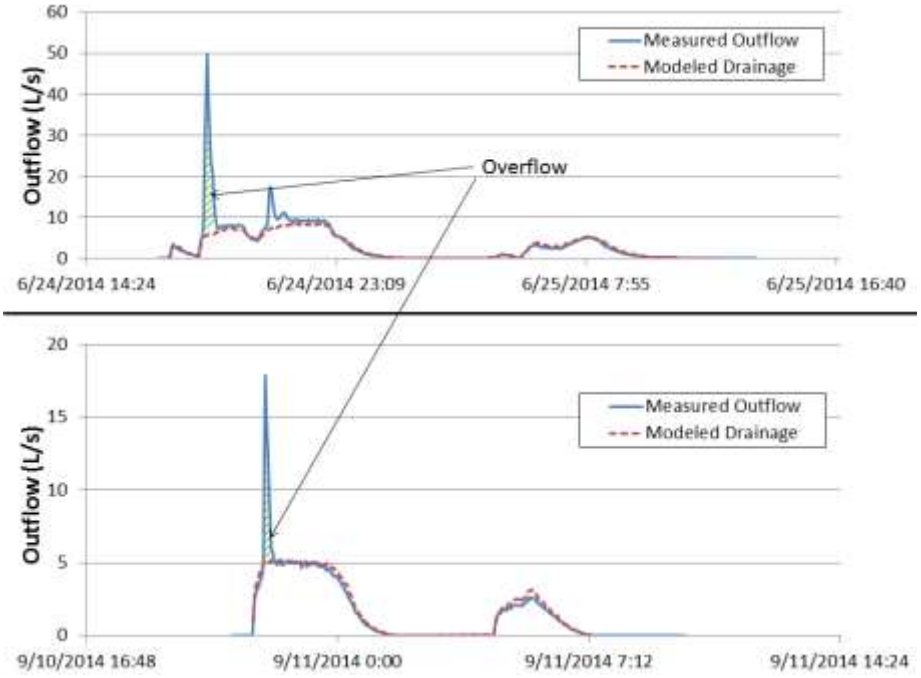

Figure 2-7. Measured outflow and modeled drainage hydrographs for UC. Modeling was completed in US EPA SWMM model V5.1.

Volume Reduction

Over the monitoring periods, the three monitored bioretention cells reduced runoff volume (i.e., the sum of exfiltration and ET) by 59% (UC), 42% (HA South), and 36% (HA North, Table 2-4). The greatest volume reduction was achieved by the cell with the largest

drawdown rate and thickest IWS zone. Additional information regarding the hydrologic performance of the bioretention cells can be found in Appendix A. While few studies of bioretention cells over similarly poor soils have been published, Sansalone and Teng (2004) found 55-70% exfiltration from an infiltration-based SCM (termed a partial exfiltration reactor) located in low permeability glacial till soils in Cincinnati, OH. Two bioretention cells built in compacted, low permeability soils and incorporating 0.6-m IWS zones reduced runoff volume by 20% and 30% when designed to capture the 12.5 and 25-mm events, respectively (Luell 2011). Cells employing IWS and built in conductive soils provided more volume reduction (e.g., 75-87% in sandy clay loam and 96-100% in sand; Brown and Hunt 2011b). Additional analysis of volume reduction as a function of rainfall depth can be found in Appendix A.

Table 2-4. Summary statistics for volume (in catchment mm) and percentage of inflow, drainage, overflow, and exfiltration/ET over the monitoring periods.

Cell Name	Total Inflow (mm)	Drainage (mm)	Overflow (mm)	Exfiltration + ET (mm)	Drainage (%)	Overflow (%)	Exfiltration/ET (%)
UC	570	189	43	338	33.2	7.6	59.2
HA South	511	261	35	215	51.1	6.8	42.1
HA North	525	300	36	189	57.2	6.9	36.0

Drainage represented 33-57% of the overall water balance, depending on the bioretention cell. Generally, drainage should have lower pollutant concentrations when compared to those of untreated runoff (provided proper media is selected, Hunt et al. 2012). Debusk et al.

(2011) suggested drainage from bioretention cells was released at rates similar to post-storm event shallow interflow in rural reference streams, mimicking pre-development hydrology. Since drainage is controlled outflow, it should not cause erosion to the same extent as overflow or uncontrolled runoff.

Overflow represented about 7% of the water balance at HA. These bioretention cells were sized to capture the 44.7 and 45.2-mm events, more than two-fold larger than the water quality event in Ohio. Peak flows at HA were probably also dampened by the impervious area disconnection in the catchments (Figure 2-2). Overflow was 7.6% of the water balance at UC. In this study, overflow represented less of the water balance than in past studies on bioretention cells, which ranged from 11 to 23% (Li et al. 2009; Brown and Hunt 2012). A bioretention cell sized for the 19-mm water quality event in Ohio would experience more overflow under similar conditions.

DRAINMOD modeling results suggested ET represented between 4.5-5.5% of the overall water balance for each of the bioretention cells (Chapter 3), similar to the 3% ET observed for cells in North Carolina (Brown and Hunt 2012). Evapotranspiration was 19% of inflow for a lined bioretention cell in Louisburg, N.C. (Li et al. 2009). Modeling of bioretention with RECARGA suggested ET was about 1% of the overall water balance (Hoskins and Peterein 2013). Based on lysimeter data, Wadzuk et al. (2014) indicate bioretention employing IWS and sized to treat 5% of its impervious catchment would evapotranspire 4% of the overall water balance.

Low Impact Development strategies focus on abstraction of small storm events to reduce stormwater volume (Davis 2008). In this study, between 31-68% of observed rainfall events

were completely captured (i.e., no drainage or overflow) by the bioretention cells (Table 2-5). For comparison, no outflow occurred during 27-63% of events at four bioretention cells in N.C. and M.D. (Li et al. 2009). Thirty-three percent of events were completely captured in a lined (to prevent exfiltration) bioretention cell in Australia (Hatt et al. 2009). Events up to 14-mm depth were completely captured, albeit different ADP were required (9 days at HA and 1.5 days at UC). Higher exfiltration rates at UC allowed faster dewatering of the IWS zone and consequently greater storage when ADP was short. Up to 25 and 121 mm events, respectively, were completely captured for two cells employing 0.6-m IWS zones and situated over sandy clay loam and sand soil types (Brown and Hunt 2011b).

Table 2-5. Summary of completely captured storm events (i.e., no outflow).

Cell name	Events completely captured (#)	Range of rainfall depths of completely captured events (mm)	Percentage of events completely captured
UC	34/50	2.5-14	68
HA South	44/90	2.5-13	49
HA North	28/90	2.5-13	31

The Bioretention Abstraction Volume (BAV) was defined by Davis, Traver et al. (2012) as the volume of water captured by the bioretention cell and either exfiltrated or evapotranspired. Soil storage availability is affected by soil moisture conditions: saturation (SAT, all pores filled), field capacity (FC, water drained under gravity), and wilting point

(WP, the water content where plants can no longer extract water for ET). As defined in Davis, Traver et al. (2012), theoretical BAV is calculated using:

$$\text{Low BAV} = \text{RZMS} \times (\text{SAT-WP}) \quad (2\text{-}6)$$

$$\text{Avg. BAV} = \text{RZMS} \times (\text{SAT-WP}) + \text{LMS} \times (\text{SAT-FC}) \quad (2\text{-}7)$$

$$\text{High BAV} = \text{Surface Storage Volume} + \text{RZMS} \times (\text{SAT-WP}) + \text{LMS} \times (\text{SAT-FC}) \quad (2\text{-}8)$$

where RZMS is the volume of the media (m^3) in the root zone and LMS is the volume of media below the root zone but above the IWS zone (m^3). In this study, the root zone was assumed to be 30 cm since plants were juvenile during the study.

Average BAV was determined by regressing outflow volume against inflow volume for each bioretention cell and using segmented linear regression to determine the slope and intercept of the bioretention response following abstraction (Table 2-6). The field-derived BAV for the three cells differed substantially, from 3.4±1.3 m^3 (BAV±95% confidence interval [CI]) for HA North, 4.5±1.8 for HA South, and 28.2±15.9 for UC. The wider CI at UC is indicative of the lower number of outflow-producing events (Table 2-5).

The HA cells had lower drawdown rates and smaller IWS zone thicknesses and were therefore able to abstract much less volume than UC. Field-derived BAVs for the HA cells were similar to the theoretical low BAV and well below the surface storage volume, suggesting outflow began well before the surface storage zone was full. The IWS zones at the HA cells often were near-full at the commencement of rainfall, limiting their abstraction capacity. The lower end of the field-derived 95% CI for BAV at UC was near the calculated low BAV (Table 2-6). Average BAV (21.1 m^3) was lower than field-derived BAV (28.2 m^3), suggesting this method may need to be modified to account for IWS zone storage

(given typical ADPs). Once the bioretention cells entered the outflow production phase, the slope of the outflow trendline at UC was lower (0.76) than at HA (0.87-0.88), suggesting greater volume reduction at UC during large events, perhaps related to intra-event drawdown.

A few modifications to the BAV calculation presented by Davis, Traver et al. (2012) are suggested for cells incorporating IWS. The IWS zone provides additional storage below the underdrain invert:

$$\text{Avg. BAV} = \text{RZMS} \times (\text{SAT-WP}) + \text{LMS} \times (\text{SAT-FC}) + Q_{DD,Avg} \times \boldsymbol{\phi} \times ADP_{Avg} \times SA \quad (2\text{-}9)$$

where $Q_{DD,Avg}$ is the average drawdown rate (mm/hr), $\boldsymbol{\phi}$ is the porosity of the aggregate or media (unitless), ADP_{Avg} is the average ADP (hours) calculated over a long-term period of record, and SA is the surface area of the cell. Storage in the IWS zone is limited by its thickness, of course. For cells with considerable exfiltration rates, this can amount to a substantial amount of additional storage. Furthermore, the results from the HA cells suggest the surface storage volume should not be included in the calculation of the high BAV for cells over poorly drained soils. When the bowl is full, the soil will be saturated or nearly saturated, meaning that at the cessation of rainfall, most of the water stored in the bowl will filter through the media and drain from the underdrain. Some of the bowl volume will also exfiltrate depending on the drawdown rate and underdrain configuration.

Table 2-6. Statistics for bioretention abstraction volume for the three bioretention facilities.

Characteristics	UC	HA South	HA North
Field-derived			
Ave. BAV (m^3)	28.2	4.5	3.4
95 CI on BAV (m^3)	15.9	1.8	1.3
Slope of best-fit line	0.76	0.88	0.87
Theoretical BAV			
Low BAC (m^3)	16.6	5.5	5.9
Ave. BAV (m^3)	21.1	7.8	8.4
High BAV (m^3)	81.1	42.8	56.4

The runoff threshold, originally proposed by Hood et al. (2007), is the minimum rainfall depth generating discharge from an urban catchment. Herein, the discharge threshold (D_T) is defined as the minimum rainfall depth producing outflow from a bioretention facility. There are two phases of bioretention hydrology: (1) abstraction and (2) outflow production. During abstraction, practically all events below a threshold rainfall depth, the D_T, have no outflow. Using segmented linear regression, the D_T was 13.8, 7.4, and 5.5 mm for UC, HA South, and HA North, respectively; bootstrapping was performed to determine the 95% confidence interval around the D_T (Figure 2-8). While UC was built to capture a smaller rainfall depth (Table 2-1), the thicker IWS zone and 2-2.5 times greater exfiltration rate resulted in greater abstraction. Once outflow began, the steeper slope of the outflow volume best-fit line for UC was indicative of the larger catchment area, higher percentage imperviousness, and directly connected impervious area (Figure 2-8Figure 2-8). Discharge thresholds in this study were similar to (HA cells) or higher (UC) than those reported for LID developments in Connecticut (Hood et al. (2007) and North Carolina (Page et al. 2015), which were 3-6 mm.

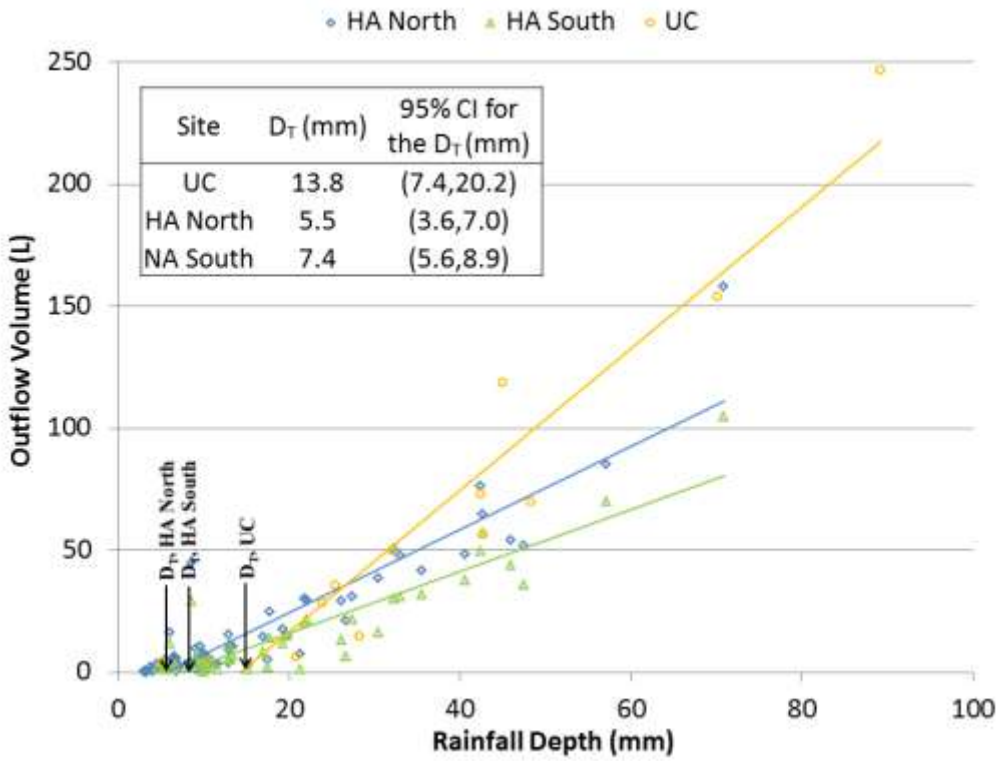

Figure 2-8. Determination of the discharge threshold for the bioretention facilities. Events with zero outflow were omitted for clarity.

Figure 2-9 depicts the volume discharge ratio (VDR), defined by the event-by-event ratio of outflow to inflow volume, for all three bioretention cells. Data were plotted as ranked probability distributions, as suggested in Piechota et al. (2001). Zero-outflow events were plotted at 0.001 VDR for inclusion on the log-scale plot.

Twenty-six percent of events at UC had substantial outflow (VDR>0.1), 6% of events with minor outflow (0<VDR<0.1), and 68% were completely captured. The HA South and North cells (both with lower underlying soil K_{sat}) produced substantial outflow during 44% and 54% of events and minor outflow during 5% and 10% of events, respectively, highlighting the importance of underlying soil K_{sat} to volume reduction (Table 2-3). Volume

reduction occurred in all monitored storms, with the bioretention cells abstracting at minimum 14% of the inflow volume.

Davis (2008) suggested a VDR less than or equal to 0.33 as a target for LID efficacy. Two bioretention cells in Maryland met this target for 54% and 61% of observed events (Davis 2008). The HA North, HA South, and UC cells had VDR<0.33 for 51%, 67%, and 82% of events. The two cells in Maryland incorporated impermeable liners for research purposes, eliminating exfiltration, and explaining why UC, with a moderate drawdown rate of 4.3 mm/hr, had better performance. Undersized bioretention cells in North Carolina met this criterion for 44% of events (Brown and Hunt 2011a).

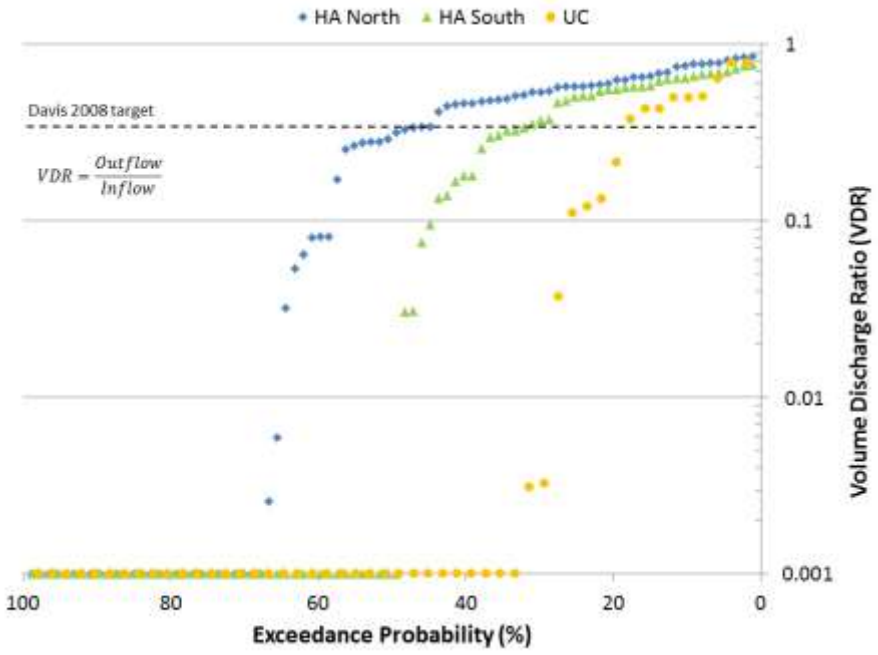

Figure 2-9. Exceedance probability for volume discharge ratio.

Peak Flow Mitigation and Flow Duration

Peak flow mitigation was greatest for the smallest rainfall intensities and depths, as the bowl completely stored the event, eliminating overflow, and limiting outflow rates to the drainage capacity of the underdrain (Table 2-7; Appendix A). Similar results have been found in other bioretention studies (Davis 2008; Hatt et al. 2009; Brown and Hunt 2012). Generally, as rainfall intensity increased, peak flow mitigation decreased, especially for storms with overflow. For the three bioretention cells, peak flow mitigation was a minimum of 29% (except for one storm at HA North with no peak flow mitigation). Additional analysis of peak flow mitigation as a function of rainfall depth can be found in Appendix A.

Oversized bioretention systems decrease the number of overflow producing events by providing greater bowl storage volume; for instance, only 10, 12, and 12 events at UC, HA South, and HA North, respectively, exceeded the design storage capacity of the bowl. Had the cells been sized to capture only the runoff volume from the 19-mm water quality event, the number of events with overflow would have increased to 11, 19, and 19. Oversizing a bioretention cell with respect to its catchment area caused the most marked changes in long-term fraction of overflow during bioretention hydrologic simulations in DRAINMOD (Chapter 3). Deeper bowl depths are one method to accomplish this.

Table 2-7. Statistics for peak flow mitigation at the UC and HA bioretention cells.

Site Name	Location	Median Peak Flow Rate (L/s)	75th Percentile Peak Flow Rate (L/s)	90th Percentile Peak Flow Rate (L/s)	Maximum Peak Flow Rate (L/s)	Median Peak Flow Reduction (%)	Range of Peak Flow Reduction (%)
UC	Inflow	10.5	25.2	45.2	105.0	100	50-100
	Outflow	0.0	0.2	8.0	49.9		
HA South	Inflow	3.9	8.7	23.2	32.7	98.9	29-100
	Outflow	0.1	0.6	1.8	23.3		
HA North	Inflow	6.1	13.7	36.8	51.9	96.6	0-100
	Outflow	0.2	0.7	2.7	36.6		

Stormwater controls are often designed to mitigate flood risk for storms greater than the 1 year event. Design rainfall event intensities were obtained for Cleveland Hopkins International airport, the nearest reliable source of long term data (located approximately 39 km from UC and 60 km from HA) (NOAA 2015). Because the times of concentration from the catchments of interest were small (i.e., less than 5 minutes), a 5-minute rainfall duration was used for this analysis. During the monitoring period, five events occurred at HA with peak rainfall intensities that exceeded the 1-yr, 5-minute rainfall intensity (99 mm/hr); four such events occurred at UC – of those, one event exceeded the 5-yr, 5-minute (141 mm/hr) rainfall intensity. While all four such events at UC exceeded the bowl storage capacity of 29.5 mm, peak outflow rates were still reduced by 53-88%. In all cases, the peak rainfall intensity occurred within the first few hours of the hyetograph, before the bowl volume filled. Outflow rates were then restricted by the K_{sat} of the media and the capacity of the underdrain. The K_{sat} of the media at UC (168 mm/hr) allowed a substantial amount of runoff to be routed into the media during the event. At HA, only 3 of the 5 intense

events produced overflow. Peak flow reductions for these three events ranged from 24-96%. Even during events with overflow, substantial peak flow mitigation was provided by the UC (worst case 53%) and HA (worst case 24%) bioretention cells. These results suggest that center-weighted design hyetographs (wherein the majority of the rainfall arrives over a 3 hour period) may not represent observed rainfall patterns, resulting in conservative SCM designs for peak flow mitigation.

Flow duration curves are used to summarize the hydraulic response of bioretention cells by amalgamating outflow rates measured on a 2-minute interval across all observed storm events into a single distribution (Figure 2-10; Davis, Stagge et al. 2012). The monitoring period duration was 209 days at UC and 304 days at HA. Outflow from the UC bioretention cell occurred for 82 hours, or 1.6% of the monitoring period. For the HA South and North cells, outflow duration was 464 and 1099 hours, respectively, representing 6.4 and 15.1% of the monitoring periods. The total duration of rainfall during the monitoring periods was 452 and 821 hours at UC and HA, respectively. For bioretention facilities providing considerable exfiltration (UC), the duration of outflow will be substantially reduced, while lower drawdown rates (e.g., HA North) result in periods of drainage extending beyond rainfall duration. Similar elongated outflow durations were observed by Davis (2008) for two lined bioretention cells and for retention basins by Roesner et al. (2001) and Tillinghast et al. (2011). Stormwater control measures promoting volume reduction have been shown to reduce duration of outflow from urban impervious surfaces by up to 50% (Davis, Stagge et al. 2012).

The duration of outflow from a bioretention cell is related primarily to the IWS zone thickness, exfiltration rate, and bowl storage volume. Regardless of underlying soil type, the reduced outflow volume from bioretention facilities will reduce bed load transport and/or potential bank erosion (Pomeroy et al. 2008).

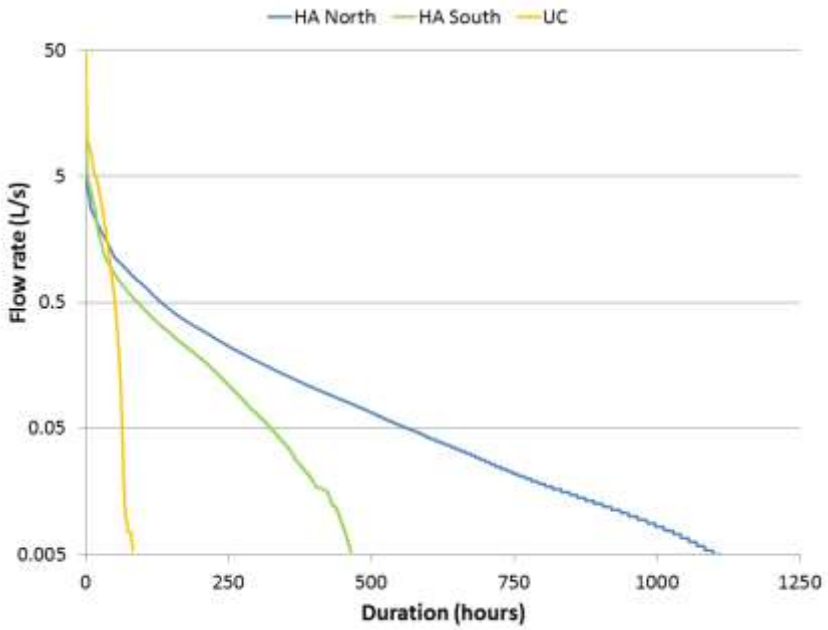

Figure 2-10. Flow duration curves for outflow from the bioretention cells.

2.6 Summary and Conclusions

Three bioretention cells were evaluated for hydrologic performance in northeast Ohio. The water balance was quantified at each site, and volume reduction and peak flow mitigation were related to design characteristics. The following conclusions may be drawn from this study:

1) Vertical K_{sat} is an intensive property of the soil underlying the bioretention cell, whereas drawdown rate in the IWS zone is dependent on other factors, including driving head, IWS zone depth, and lateral soil K_{sat}. Measured post-construction drawdown rates for all three bioretention cells exceeded the measured vertical K_{sat} of the soils underlying the bioretention cells. This was likely due to lateral exfiltration through the side walls of the bioretention cells, increased head (compared to the infiltration testing) from the 0.38 to 0.60-m IWS zones, and relatively minor amounts of ET. While the soils were mapped as HSG D, measured post-construction drawdown rates in the cells were in the range of HSG C soils (1.7-4.3 mm/hr). These results support the installation of a greater number of smaller, distributed bioretention systems, as opposed to one large SCM, to drive additional exfiltration by augmenting the side-wall surface area. The incorporation of an IWS zone is also critical to stimulating lateral exfiltration.

2) Runoff reduction for the UC, HA South, and HA North cells was 59%, 42%, and 36%, primarily related to the drawdown rates of the underlying soils. These SCMs were oversized and could store the 29.5, 45.2, and 44.7-mm events without overflow, contributing to improved performance. Substantial volume reduction can occur when bioretention cells are situated over poorly drained soils, especially with the inclusion of an IWS zone that exfiltrates stormwater during inter-event periods.

3) Discharge thresholds were 13.8, 7.4, and 5.5 mm for the UC, HA South, and HA North cells, respectively, showing that bioretention cells eliminate outflow from small events even when situated over low permeability soils. The maximum rainfall depth that could be abstracted without outflow was a result of storage capacity in the IWS and media. No

outflow occurred from the cells during 31-68% of the observed events at the three bioretention cells.

4) Median peak flow reduction for the three cells was 96% or greater. The smallest storms were either completely captured with no outflow or outflow rates were throttled by the media and the underdrain. During events exceeding the 1-yr, 5-minute rainfall intensity, the UC and HA cells provided 53-88% and 24-96% peak flow mitigation, respectively. The peak rainfall rate often occurred well before the centroid of the rainfall volume, meaning there was adequate bowl storage to mitigate peak inflow rates without producing overflow. These results support over-sizing bioretention cells to aid in peak flow mitigation goals.

5) The duration of outflow represented 1.6%, 6.4%, and 15.1% of the monitoring period at UC, HA South, and HA North bioretention cells, respectively. The UC, HA South, and HA North cells produced outflow during 18%, 56%, and 134% of the total rainfall duration; outflow duration was elongated as underlying soil K_{sat} decreased. The duration of outflow from SCMs will be critical as the profession moves from single-storm peak flow based designs to pre- and post-development hydrograph matching.

2.7 References

American Society for Testing and Materials (ASTM). (2007). *Standard test method for particle-size analysis of soils.* ASTM D422-63.

American Society for Testing and Materials (ASTM). (2014). *Standard test methods for moisture, ash, and organic matter of peat and other organic soils*. ASTM D2974-14.

Asleson, B.C., Nestingen, R.S., Gulliver, J.S., Hozalski, R.M., and Nieber, J.L. (2009). "Assessment of rain gardens by visual inspection and controlled testing." *J. Am. Water Resour. Assoc.*, 45, 1019–1031.

Bathke, G.R., and Cassel, D.K. (1991). "Anisotropic variation of profile characteristics and saturated hydraulic conductivity in an Ultisol landscape." *Soil Sci. Soc. Am. J.*, 55(2), 333-339.

Blecken, G.T., Zinger, Y., Deletić, A., Fletcher, T.D., and Viklander, M. (2009). "Impact of a submerged zone and a carbon source on heavy metal removal in stormwater biofilters." *Ecol. Eng*., 35(5), 769-778.

Bledsoe, B., and Watson, C. (2001). "Effects of urbanization on channel instability." *J. Am. Water Resour. Assoc*., 37(2), 255–270.

Booth, D.B. (1990). "Stream-channel incision following drainage-basin urbanization." *J. Am. Water Resour. Assoc*., 26(3), 407-417.

Booth, D., Hartley, D., and Jackson, R. (2002). "Forest cover, impervious surface area, and the mitigation of storm-water impacts." *J. Am. Water Resour. Assoc*., 38(3), 835–845.

Bratieres, K., Fletcher, T.D., Deletic, A., and Zinger, Y. (2008). "Nutrient and sediment removal by stormwater biofilters: A large-scale design optimisation study." *Water Res*., 42(14), 3930-3940.

Brown, R.A., and Hunt, W.F. (2010). "Impacts of construction activity on bioretention performance." *J. Hydrol. Eng*.,15(6), 386-394.

Brown, R.A. and Hunt, W.F. (2011a). "Impacts of media depth on effluent water quality and hydrologic performance of under-sized bioretention cells." *J. Irrig. Drain. Eng.*, 137(3), 132-143.

Brown, R.A. and Hunt, W.F. (2011b). "Underdrain configuration to enhance bioretention exfiltration to reduce pollutant loads." *J. Environ. Eng.*, 137(11), 1082-1091.

Brown, R.A., and Hunt, W.F. (2012). "Improving bioretention/biofiltration performance with restorative maintenance." *Water Sci. Technol*., 65(2), 361-367.

Browne, D., Deletic, A., Mudd, G.M., and Fletcher, T.D. (2008). "A new saturated/unsaturated model for stormwater infiltration systems." *Hydrol. Processes*, 22(25), 4838–4849.

Burns, M.J., Fletcher, T.D., Walsh, C.J., Ladson, A.R., and Hatt, B.E. (2012). "Hydrologic shortcomings of conventional urban stormwater management and opportunities for reform." *Landscape Urban Plann*., 105(3), 230-240.

Chin, D.A. (2006). *Water resources engineering*. 2nd edition. Pearson Prentice Hall, Upper Saddle River, NJ.

City of Omaha. (2014). *Omaha regional stormwater design manual*. Chapter 8: Stormwater best management practices. City of Omaha environmental quality control division. Available: http://www.omahastormwater.org/download/chapter-8-stormwater-best-management-practices/

Cizek, A.R., and Hunt, W.F. (2013). "Defining predevelopment hydrology to mimic predevelopment water quality in stormwater control measures (SCMs)." *Ecol. Eng.*. 57, 40-45.

Davis, A.P. (2008). "Field performance of bioretention: hydrology impacts." *J. Hydrol. Eng*., 13(2), 90-95.

Davis, A.P., Hunt, W.F., Traver, R.G., and Clar, M. (2009). "Bioretention technology: Overview of current practice and future needs." *J. Environ. Eng., 135*(3), 109-117.

Davis, A.P., Stagge, J.H., Jamil, E., and Kim, H. (2012). "Hydraulic performance of grass swales for managing highway runoff." *Water Res*., 46(20), 6775-6786.

Davis, A.P., Traver, R.G., Hunt, W.F., Lee, R., Brown, R.A., and Olszewski, J.M. (2012). "Hydrologic performance of bioretention storm-water control measures." *J. Hydrol. Eng*., 17(5), 604-614.

DeBusk, K.M., Hunt, W.F., and Line, D.E. (2011). "Bioretention outflow: Does it mimic nonurban watershed shallow interflow?" *J. Hydrol. Eng*.,16(3), 274-279.

Dietz, M.E. and Clausen, J.C. (2005). "A field evaluation of rain garden flow and pollutant treatment." *Water Air Soil Poll*., 167(1-4), 123-138.

Dietz, M.E. and Clausen, J.C. (2006). "Saturation to improve pollutant retention in a rain garden." *Environ. Sci. Technol*., 40(4), 1335-1340.

Emerson, C. and Traver, R. (2008). "Multiyear and seasonal variation of infiltration from storm-water best management practices." *J. Irrig. Drain. Eng.*, 134(5), 598-605.

Fangmeier, D.D., Elliot, W.J., Workman, S.R., Huffman, R.L., Schwab, G.O. (2006). *Soil and water conservation engineering*. 5th edition. Thomson Delmar learning, Clifton Park, NY.

Grant, D.M. and Dawson, B.D. (2001). *Isco open channel flow measurement handbook*. 5th edition. Isco, Inc., Lincoln, NE.

Guo, J.C., and Luu, T.M. (2015). "Operation of Cap Orifice in a Rain Garden." *J. Hydrol. Eng.*, 20(10), 1-6. 06015002

Hammer, T.R. (1972). *Stream channel enlargement due to urbanization*. Regional Science Research Institute Discussion Paper Series, No. 55. Philadelphia, PA, 41 pp.

Hatt, B.E., Fletcher, T.D., and Deletic, A. (2009). "Hydrologic and pollutant removal performance of stormwater biofiltration systems at the field scale." *J. Hydrol.*, 365(3), 310-321.

Heasom, W., Traver, R.G., and Welker, A. (2006). "Hydrologic modeling of a bioinfiltration best management practice." *J. Am. Water Resour. Assoc.*, 42(5), 1329-1347.

Hood, M.J., Clausen, J.C., and Warner, G.S. (2007). "Comparison of stormwater lag times for low impact and traditional residential development." *J. Am. Water Resour. Assoc.*, 43(4), 1036-1046.

Hoskins, J., and Peterein, J. (2013). "Case study of St. Louis, Missouri: Comparison of bioretention performance to the runoff component of a restored water balance." *J. Environ. Eng.*, 139(4), 516-521.

Hunt, W.F., Jarrett, A.R., Smith, J.T., and Sharkey, L.J. (2006). "Evaluating bioretention hydrology and nutrient removal at three field sites in North Carolina." *J. Irrig. Drain. Eng.*, 132(6), 600–608.

Hunt, W.F., Smith, J.T., Jadlocki, S.J., Hathaway, J.M., and Eubanks, P.R. (2008). "Pollutant removal and peak flow mitigation by a bioretention cell in urban Charlotte, NC." *J. Environ. Eng.*, 134(5), 403-408.

Hunt, W.F., Davis, A.P., and Traver, R.G. (2012). "Meeting hydrologic and water quality goals through targeted bioretention design." *J. Environ. Eng.*, 138(6), 698-707.

Iowa Department of Natural Resources (IDNR). (2010). *Iowa stormwater management manual*. Chapter 2E: Infiltration practices. Available: http://www.iowadnr.gov/Environmental-Protection/Water-Quality/NPDES-Storm-Water/Storm-Water-Manual

Jenkins, J.K.G., Wadzuk, B.M., and Welker, A.L. (2010). "Fines accumulation and distribution in a storm-water rain garden nine years postconstruction." *J. Irrig. Drain. Eng.*, 136(12), 862-869.

Jones, M.P. and Hunt, W.F. (2009). "Bioretention impact on runoff temperature in trout sensitive waters." *J. Environ. Eng.*, 135(8), 577-585.

Lee, J.G., Borst, M., Brown, R.A., Rossman, L., and Simon, M.A. (2015). "Modeling the hydrologic processes of a permeable pavement system." *J. Hydrol. Eng*., 20(5), 1-9.

Li, H., Sharkey, L.J., Hunt, W.F., and Davis, A.P. (2009). "Mitigation of impervious surface hydrology using bioretention in North Carolina and Maryland." *J. Hydrol. Eng*., 14(4), 407–415.

Luell, S.K. (2011). *Evaluating the impact of bioretention cell size and swale design in treating highway bridge deck runoff.* M.S. thesis, Department of Biological and Agricultural Engineering, North Carolina State University.

Minnesota Pollution Control Agency (MPCA). (2015). *Minnesota stormwater manual*. Design criteria for bioretention. Available: http://stormwater.pca.state.mn.us/index.php/Design_criteria_for_bioretention

Muthanna, T.M., Viklander, M., and Thorolfsson, S.T. (2008). "Seasonal climatic effects on the hydrology of a rain garden." *Hydrol. Processes*, 22(11), 1640-1649.

National Oceanic and Atmospheric Administration (NOAA). (2015). *NOAA Atlas 14 point precipitation frequency estimates, Ohio.* Hydrometeorological Design Studies Center, Precipitation Frequency Data Server. Available: http://dipper.nws.noaa.gov/hdsc/pfds/pfds_map_cont.html?bkmrk=oh

Ohio Department of Natural Resources (ODNR), Division of Soil and Water Conservation. (2006). *Rainwater and land development: Ohio's standards for stormwater management, low impact development, and urban stream protection*. 3rd edition. Ed: John Mathews.

Olson, N.C., Gulliver, J.S., Nieber, J.L., and M. Kayhanian. (2013). "Remediation to improve infiltration into compact soils." *J. Environ. Manage.*, 117,85–95.

Page, J.L., Winston, R.J., Mayes, D.B., Perrin, C., Hunt, W.F. (2015). "Hydrologic mitigation of impervious cover in the municipal right-of-way through innovative stormwater control measures." *J. Hydrol.*, 527, 923-932.

Palhegyi, G. E. (2009). "Designing storm-water controls to promote sustainable ecosystems: science and application." *J. Hydrol. Eng*., 15(6), 504-511.

Passeport, E., Hunt, W.F., Line, D.E., Smith, R.A., and Brown, R.A. (2009). "Field study of the ability of two grassed bioretention basins to reduce storm-water runoff pollution." *J. Irrig. Drain. Eng.*, 135(4), 505-510.

Piechota, T.C., Chiew, F.H., Dracup, J.A., and McMahon, T.A. (2001). "Development of exceedance probability streamflow forecast." *J. Hydrol. Eng*., 6(1), 20-28.

Pitt, R., Chen, S.E., Clark, S.E., Swenson, J., and Ong, C.K. (2008). "Compaction's impacts on urban storm-water infiltration." *J. Irrig. Drain. Eng.*, 134(5), 652-658.

Pomeroy, C.A., Postel, N.A., O'Neill, P.A., and Roesner, L.A. (2008). "Development of storm-water management design criteria to maintain geomorphic stability in Kansas City metropolitan area streams." *J. Irrig. Drain. Eng.*, 134(5), 562-566.

Reynolds, W.D., Elrick, D.E., Youngs, E.G., and Amoozegar, A. (2002). "Ring or cylinder infiltrometers (vadose zone)." *Methods of Soil Analysis - Part 4: Physical Methods*, J.H. Dane and G.C. Topp, eds., Soil Science Society of America. Madison, WI.

Roesner, L.A., Bledsoe, B.P., and Brashear, R.W. (2001). "Are best-management-practice criteria really environmentally friendly?" *J. Water Res. Plann. Manage.*, 127(3), 150-154.

Sansalone, J.J., and Teng, Z. (2004). "In situ partial exfiltration of rainfall runoff. I: Quality and quantity attenuation." *J. Environ. Eng.*, 130(9), 990–1007.

Schlea, D., Martin, J.F., Ward, A.D., Brown, L.C., and Suter, S.A. (2014). "Performance and Water Table Responses of Retrofit Rain Gardens." *J. Hydrol. Eng*., 19(8), 05014002.

Schueler, T.R., Fraley-McNeal, L., and Cappiella, K. (2009). "Is impervious cover still important? Review of recent research." *J. Hydrol. Eng*., 14(4), 309–315.

Smolek, A.P.*, Winston, R.J.*, Dorsey, J.D., and Hunt, W.F. (2015). *Modeling the hydrologic performance of bioretention and permeable pavement stormwater controls in northern Ohio using DRAINMOD: Calibration, validation, sensitivity analysis, and future climate scenarios.* Final report submitted to the University of New Hampshire and the Chagrin River Watershed Partners. In fulfilment of NOAA Award number NA09NOS4190153. *These authors contributed equally to this work.

Soil Survey Staff, Natural Resources Conservation Service, United States Department of Agriculture. (2015). Web Soil Survey. http://websoilsurvey.nrcs.usda.gov/. Accessed 28 January 2015.

Tillinghast, E.D., Hunt, W.F., and Jennings, G.D. (2011). "Stormwater control measure (SCM) design standards to limit stream erosion for Piedmont North Carolina." *J. Hydrol.*, 411(3), 185-196.

Tyner, J.S., Wright, W.C., and Dobbs, P.A. (2009). "Increasing exfiltration from pervious concrete and temperature monitoring." *J. Environ. Manage.*, 90(8), 2636-2641.

United States Department of Agriculture, Natural Resources Conservation Service (USDA-NRCS). (1986). *Urban hydrology for small watersheds*. Technical Release 55 (TR-55). 2nd edition. United States Department of Agriculture (USDA), Natural Resources Conservation Service, Conservation Engineering Division.

United States Department of Agriculture, Natural Resources Conservation Service (USDA-NRCS). (2007a). *Estimation of Direct Runoff from Storm Rainfall*. Part 630, Chapter 10, National Engineering Handbook. Natural Resources Conservation Service.

United States Department of Agriculture, Natural Resources Conservation Service (USDA-NRCS). (2007b). *Hydrologic Soil Groups*. Part 630, Chapter 7, National Engineering Handbook. Natural Resources Conservation Service.

United States Environmental Protection Agency (USEPA). (2007). "Reducing storm-water costs through low impact development strategies and practices." *Rep. No. EPA 841-F-07-006*, EPA, Washington, D.C. www.epa.gov/nps/lid. Accessed Feb 2012.

United States Environmental Protection Agency (USEPA). (2015). *Storm water management model reference manual: Volume 1 – Hydrology.* Office of Research and Development, Water Supply and Water Resources Division. EPA/600/R-15/162.

Wadzuk, B.M., Hickman Jr, J.M., and Traver, R.G. (2014). "Understanding the role of evapotranspiration in bioretention: Mesocosm study." *J. Sustainable Water Built Environ.*, 1(2), 04014002.

Walsh, C.J., Fletcher, T.D., and Ladson, A.R. (2009). "Retention capacity: a metric to link stream ecology and storm-water management." *J. Hydrol. Eng.*, 14(4), 399-406.

Walsh, C.J., Fletcher, T.D., and Burns, M.J. (2012). "Urban Stormwater Runoff: A New Class of Environmental Flow Problem." *PLoS ONE*. 7(9): e45814. doi:10.1371/journal.pone.0045814.

Wang, L., Lyons, J., Kanehl, P., and Bannerman, R. (2001). "Impacts of urbanization on stream habitat and fish across multiple spatial scales." *J. Environ. Plann. Manage.*, 28(2), 255–266.

Wardynski, B.J., and Hunt, W.F. (2012). "Are bioretention cells being installed per design standards in North Carolina? A field study." *J. Environ. Eng.*, 138(12), 1210-1217.

Wardynski, B.J., Winston, R.J., and Hunt, W.F. (2012). "Internal water storage enhances exfiltration and thermal load reduction from permeable pavement in the North Carolina mountains." *J. Environ. Eng.*, 139(2), 187-195.

Winston, R.J., Dorsey, J.D. and Hunt, W.F. (2015). *Monitoring the performance of bioretention and permeable pavement stormwater controls in Northern Ohio: Hydrology, water quality, and maintenance needs*. Final Report Submitted to the University of New Hampshire and the Chagrin River Watershed Partners. In Fulfilment of NOAA Award number NA09NOS4190153. Available: http://www.crwp.org/files/OH_StormwaterControls_MonitoringReport2015.pdf

CHAPTER 3: **MODELING THE HYDROLOGIC PERFORMANCE OF BIORETENTION STORMWATER CONTROLS IN NORTHERN OHIO USING DRAINMOD: CALIBRATION, VALIDATION, AND ANALYSIS OF BIORETENTION DESIGN ALTERNATIVES**

3.1 Abstract

Factors such as underlying soil type, media depth, media characteristics, bowl storage depth, climatic conditions, internal water storage (IWS) zone depth, presence or absence of flow restriction on the underdrain, and loading ratio (LR, ratio of catchment to bioretention surface area) have been shown to affect the hydrologic performance of a bioretention cell. Long-term models are needed to simulate bioretention hydrology under varying design parameters to quantify fractions of treated drainage, untreated overflow, and volume removed through exfiltration and evapotranspiration (ET). Commonly-used bioretention models lack at least one of the following: (1) accurate simulation of soil-water movement to a drain, (2) ability to model the IWS zone drainage configuration, (3) consideration of soil-water content using the soil water characteristic curve, and/or (4) ability to perform long-term simulations to account for inter- and intra-event variability in soil moisture. As a solution to many of these shortfalls, the widely-accepted agricultural drainage model, DRAINMOD, was adapted to model bioretention cells.

Separate DRAINMOD models were calibrated with and validated against field-collected hydrologic data from three bioretention cells in northeast Ohio. The models were parameterized using as-built characteristics and laboratory-measured soil parameters. One-half of the hydrologic data were used to calibrate and the other half to validate the model. Nash-Sutcliffe efficiencies for each portion of the water balance (runoff, drainage, overflow

and exfiltration/ET) commonly exceeded 0.8 during the calibration and validation periods. At most, a 2% difference existed between the total modeled and measured volumes of each portion of the water balance for all three bioretention cells, suggesting DRAINMOD could be applied as a tool for analysis of long-term bioretention hydrology.

Analyses of bioretention design alternatives were conducted using the calibrated DRAINMOD models by singularly modifying design parameters including: LR, IWS zone depth, bowl storage depth, media depth, underlying soil hydraulic conductivity (K_{sat}), and rooting depth. Bioretention hydrology was most sensitive to LR, IWS zone depth, and underlying soil K_{sat}; media depth and bowl storage depth mainly impacted overflow, and the model was least sensitive to rooting depth. Because it impacted the runoff depth entering the bioretention cell, LR was the only design parameter that substantially affected the percentage of ET. When LR was 10:1 and 50:1, respectively, the ET fraction of the water balance decreased from 6.2% to 1.7% and the overflow fraction increased from approximately 1% to 20-25%. The inclusion of an optimally-designed IWS zone increased exfiltration by 20-30% regardless of underlying soil K_{sat}; IWS zone depth of 0.38-0.45 meters were optimal for the low permeability soils studied herein. Modeling showed 70-80% and 15-30% long-term exfiltration for underlying soil K_{sat} of 1.27 and 0.05 cm/hr, respectively, suggesting bioretention cells should be located over the most permeable soils on a development site. Results from the analysis of bioretention design alternatives could be used to create a "sliding scale" crediting system for bioretention cells based on the fractions of treated drainage and volume reduction through exfiltration and ET.

3.2 Literature Review

Urbanization amplifies the rate and volume of stormwater runoff during wet-weather events, causing impairment of surface waters, stream channel incision, loss of habitat and real estate, and increased pollutant transport (USEPA, 2009; Wang et al., 2001; Dietz and Clausen, 2008). To mitigate these negative consequences, engineers and regulators are increasingly attempting to mimic pre-development rate, volume, and duration of stormwater flows using Low Impact Development (LID) approaches (Page et al. 2015; Wilson et al. 2015). These strategies employ infiltration-based stormwater control measures (SCMs) which recharge groundwater and enhance evapotranspiration (ET) (DeBusk et al., 2010; Denich and Bradford, 2010). Bioretention, arguably the most popular green infrastructure stormwater control, partially restores the natural site hydrology and improves runoff water quality from urbanized watersheds (Brown and Hunt, 2011a; Davis et al., 2012; Hunt et al., 2012).

Bioretention cells are planted media filters designed to capture and treat the water quality volume of stormwater runoff (Hathaway and Hunt, 2011; Figure 3-1). A number of field and laboratory-based research studies have focused on their hydraulics and pollutant removal processes (Hatt et al., 2009; Lucas and Greenway, 2011; Paus et al., 2014). These studies have informed bioretention design recommendations (e.g., Davis et al., 2009; Hunt et al., 2012). Bioretention hydrologic performance varies widely based on its design characteristics, the underlying soils, the local climate, maintenance practices, interaction with the groundwater table, and the vegetation present in the bioretention cell (Dietz and Clausen, 2005; Hunt et al., 2006; Bratieres et al., 2008; Hunt et al., 2008; Davis, 2008; Muthanna et

al., 2008; Passeport et al., 2009; Hatt et al., 2009; Li et al., 2009; Line and Hunt 2009; Brown and Hunt, 2011a; Luell, 2011; Brown and Hunt, 2012; Olszewski and Davis, 2013; Hathaway et al., 2014; Géhéniau et al., 2014). Deeper media depth (Li et al., 2009; Brown and Hunt, 2011a), decreasing the catchment to bioretention cell surface area ratio (Hatt et al., 2009; Jones and Hunt, 2009), and constructing the SCM over sandy underlying soils as opposed to clayey (Brown and Hunt, 2011a, 2011b; Passeport et al., 2009) provide increased exfiltration and reduced outflow volume and frequency. The internal water storage (IWS) design feature retains stormwater within the bioretention media, promoting denitrification and providing greater pollutant load mitigation through enhanced exfiltration in both sandy and clayey soils (Figure 3-1; Dietz and Clausen, 2006; Hunt et al., 2006; Brown and Hunt, 2011b; Li et al., 2009; Passeport et al., 2009; Zinger et al., 2013; Chapter 2). Despite the depth and breadth of research, it is difficult to determine the expected water balance (e.g., the fraction of drainage, overflow, exfiltration, and ET) from a bioretention cell under varying site conditions and design configurations. Benefits of enumerating the water balance include (1) estimating pollutant load reduction, (2) determining the long-term fraction of untreated overflow, (3) meeting LID goals through targeted groundwater recharge and ET, and (4) determining whether a design matches pre-development runoff volume.

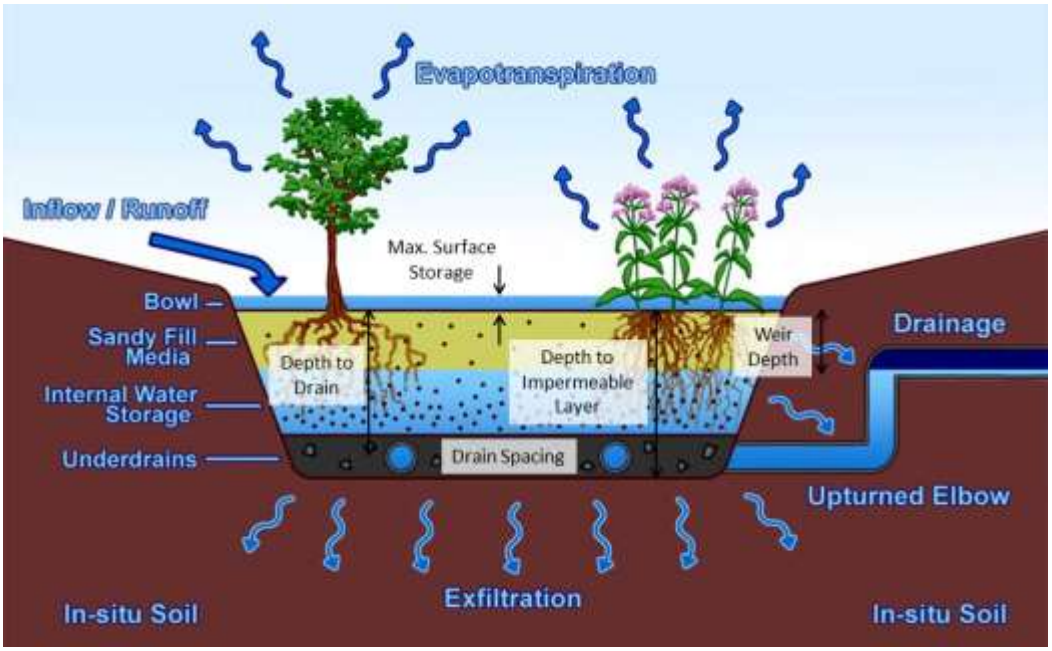

Figure 3-1. Bioretention cell design parameters with DRAINMOD model inputs.

To characterize bioretention performance under a multitude of design scenarios, an effective model is needed to determine its hydrologic and hydraulic functionality. No widely accepted long-term model exists for bioretention. Currently available bioretention models either: (1) are single-storm models, (2) use unsubstantiated estimation methodologies to calculate drainage, (3) do not account for the variations in the volumetric water content in the media, and/or (4) cannot model the IWS configuration. For example, Brander et al., (2004), Heasom et al., (2006), Lucas, (2010), He and Davis (2011), and Christianson et al. (2012) used single-event models to predict bioretention hydrology. Single-event models assume the bioretention cell is dry prior to the onset of rainfall; long-term models are better able to predict the variability in performance under alternating saturated and unsaturated conditions. Dussaillant et al. (2004) and Dussaillant et al. (2005) developed two long-term, continuous

simulation numerical models (RECHARGE and RECARGA) which have been used to simulate bioretention hydrology but cannot simulate IWS (Hoskins and Peterein, 2013). SWMM 5.1, WinSLAMM 10.2, and MUSIC 6 are continuous, long-term simulations which can simulate IWS. However, these models use rudimentary calculation methods (e.g., the orifice equation) to determine water movement to the drains and soil-water content changes as a function of water table depth.

An alternative to these models is DRAINMOD, a long term, continuous simulation drainage model typically used to simulate water movement in parallel tile drained or ditch-drained agricultural fields. It has been used to model controlled drainage, wetland and forest hydrology, soil salinity and nitrogen dynamics in drained soils, crop yield, agricultural field trafficability, and on-site wastewater treatment, among other applications (Skaggs, 1978, 1982, 1999; Youssef et al., 2005). Bioretention and permeable pavement modeling are two of its latest applications (Brown et al., 2013; Smolek et al., 2015). DRAINMOD calculates drainage rates as a function of soil properties (using the soil water characteristic curve) and drainage configuration (IWS, conventional, orifice, or valve restrictions) based on field-verified agricultural drainage concepts. The previously described bioretention models (not DRAINMOD) either calculate water storage capacity as the difference between total porosity and field capacity or use a void ratio of the media. In reality, water table depth affects the water storage in the media profile, for reasons explained in detail in Brown et al. (2013).

A mechanistic model such as DRAINMOD is perhaps most useful as a tool for determining bioretention function under various design scenarios. Instead of the current "one-size-fits-all" design technique (i.e., meeting minimum design criteria and receiving

static credit toward pollution mitigation goals) used in most U.S. states (e.g. NC, OH, and TX), a more flexible crediting system incorporating hundreds of different bioretention designs could be underpinned by an analysis of design alternatives performed using calibrated models. Three drivers for developing flexible design and crediting mechanisms are: (1) bioretention hydrologic performance varies widely, (2) bioretention retrofits often must be undersized due to spatial constraints, and (3) accurately projecting bioretention hydrology may encourage wider application where site conditions favor use or expansion of the practice.

DRAINMOD was calibrated with and validated against hydrologic data sets from three field-monitored bioretention cells located in Northeast Ohio. Analyses of bioretention design alternatives were conducted using 30 years of historical climatic records. These models were used to predict performance of myriad bioretention design configurations and optimize fill media depth, bowl storage (i.e., ponding) depth, and underdrain configuration over various underlying soil types (Davis et al., 2009; Hunt et al., 2012). Through this modeling, a better understanding of critical design parameters to bioretention hydrologic performance will be developed.

3.3 Model Background

Description of DRAINMOD

As presented by Skaggs (1978, 1982, 1999), the governing equations for DRAINMOD are based on two water balances: (1) in the soil profile (Equation 3.1) and (2) at the soil surface (Equation 3.2). The first water balance is determined for a unit surface area of soil, located

midway between drains, and extending from the impermeable layer (i.e., the interface between the bottom of the bioretention cells and the underlying soil) to the soil surface:

$$\Delta V_a = D + ET + DS - F \quad (3\text{-}1)$$

where ΔV_a = change in the air volume, D = lateral drainage from the section, ET = evapotranspiration, DS = deep seepage, and F = infiltration entering the section in Δt (time increment). The Green and Ampt method is used to calculate the surface infiltration rate in DRAINMOD (Green and Ampt 1911). The water balance at the surface is computed per unit surface area:

$$P = F + \Delta S + RO \quad (3\text{-}2)$$

where P = precipitation, F = infiltration, ΔS = change in depth of water stored on the surface, and RO = runoff during time period Δt.

The model computes the water balance for a time increment Δt (usually 1 hour), with all units expressed in terms of depth (cm). When the rainfall rate exceeds the infiltration capacity, Δt decreases to 3 minutes or less. When drainage and ET rates are low, Δt is increases to a maximum of 24-hours (daily) to reduce computational time.

Hooghoudt's equation (Equation 3.3) is used to compute drainage flux when the water table is below the soil surface (Hooghoudt 1940). The flux is determined based on the water table at the midway point between the drains and the hydraulic head in the drains:

$$q = \frac{8Kd_e m + 4Km^2}{L^2} \quad (3\text{-}3)$$

where q = drainage flux, K = effective lateral hydraulic conductivity, L = drain spacing, m = water table height above the drains at the midpoint, and d_e = equivalent drain depth. An

equivalent depth is determined using equations in Moody (1967) to correct for convergence near the drain.

When the surface is ponded and the profile is saturated, the drainage rate is calculated with the Kirkham equation (Kirkham 1957):

$$q = \frac{4\pi K(t+d-r)}{GL} \tag{3-4}$$

where t = ponding depth, r = drain radius, and G = Kirkham's coefficient. It is dependent on drain depth, drain spacing, and depth of the profile:

$$G = 2\ln\left[\frac{\tan(\frac{\pi(2d-r)}{4h})}{\tan(\frac{\pi r}{4h})}\right] + 2\sum_{m=1}^{\infty}\ln\left[\frac{\cosh(\frac{\pi mL}{2h})+\cos(\frac{\pi r}{2h})}{\cosh(\frac{\pi mL}{2h})-\cos(\frac{\pi r}{2h})}\cdot\frac{\cosh(\frac{\pi mL}{2h})-\cos(\pi(2d-r)/2h}{\cosh(\frac{\pi mL}{2h})+\cos(\pi(2d-r)/2h}\right] \tag{3-5}$$

where h = depth of profile. The maximum drainage flux may be limited using a user-specified drainage coefficient when drainage rate is limited by pipe size, valves or other structural features.

There are multiple ways to calculate potential evapotranspiration (PET) in DRAINMOD, including user input of daily PET or use of common calculation methods, with some requiring more meteorological data than others. Under the most basic application, DRAINMOD uses the Thornthwaite method (with monthly correction factors) to calculate daily PET (Thornthwaite 1948). PET is distributed daily between 6:00 a.m. and 6:00 p.m, and PET is set equal to zero when rainfall occurs. ET is calculated based on the soil water conditions; if water is available in the root zone, ET is set equal to PET. If not, ET is equivalent to the upward flux from the water table.

Additional details about DRAINMOD's governing equations, model components, how various model utilities function, and ways to measure model input parameters are provided in Skaggs (1999) and in the DRAINMOD Reference Report (Skaggs 1980).

Bioretention Modeling in DRAINMOD

Water movement through underdrained bioretention media is analogous to that in agricultural fields drained by drain tiles, which is what DRAINMOD was originally designed to model. Bioretention cells are planted (similar to agricultural crop inputs in DRAINMOD), temporarily store water both on the surface and in the media (modeled with surface storage and water flow to drains in DRAINMOD), have drains of a given diameter, depth, and spacing, and can incorporate varying control structures throughout the year to restrict outflow (such as IWS, similar to controlled drainage in DRAINMOD). Many DRAINMOD inputs correspond directly to bioretention cell design parameters (Figure 3-1). Further description of these inputs may be found in Brown et al. (2013). DRAINMOD outputs the total volume of drainage (cognate to underdrain flow; volume treated), deep seepage (cognate to exfiltration; volume eliminated), runoff (cognate to overflow or bypass flow; untreated volume), and ET (volume eliminated).

While DRAINMOD can be utilized to effectively predict the long-term water balance from bioretention cells, there are some drawbacks to using DRAINMOD as a model for urban stormwater management: (1) to model runoff from a highly impervious watershed, the Green-Ampt infiltration parameters for the watershed must be modified to limit infliltration, (2) it only predicts total volume of drainage, exfiltration, ET, and overflow, and does not predict peak flow rates, (3) the highest resolution DRAINMOD will accept for weather files

(temperature and rainfall) is hourly, (4) DRAINMOD will only provide outputs in daily, monthly, or yearly format, (5) the model does not provide hydrographs as an output, so dynamic responses in the hydrograph due to bioretention cell implementation are not provided, and (6) except drainage configuration, all inputs are held constant for the entire period of the simulation. Emerson and Traver (2008), Muthanna et al. (2008), and Braga et al. (2007) have shown seasonality in hydrologic performance of bioretention; this cannot be effectively simulated in DRAINMOD.

A general description of bioretention modeling using DRAINMOD follows; the detailed step-by-step process is found in Brown (2011). First, runoff from the catchment is simulated by varying model input parameters to match surface conditions and runoff from an urban catchment: wide drain spacing, shallow surface storage, and low soil infiltration rate. From this initial simulation, the contributing area runoff file was created and included in the overall bioretention model simulation. DRAINMOD was then parameterized based on as-built conditions, underlying soil parameters, and watershed characteristics for the bioretention cell of interest.

3.4 Materials and Methods

Site Descriptions and Monitoring Methods

DRAINMOD was calibrated and validated using data sets collected at three bioretention cells in northeast Ohio: two at Holden Arboretum (HA) and one on the campus of Ursuline College (UC; Table 3-1). The monitoring sites and the methods utilized to obtain field data are described in detail in Winston et al. (2015) and Chapter 2 herein. Approximately one year of data was collected at each site, with the exception of the winter months, when sub-

freezing temperatures precluded stormwater monitoring. The bioretention cells provided a diversity of design characteristics. The surface area of the bioretention cells at HA was sized to be 5% of the impervious drainage area, while that at the UC cell was slightly over-sized at 6.5% of the impervious drainage area (ODNR, 2006). The media depth for the HA cells was 0.84-0.9 m while the UC cell had 0.6 m of media. All three cells employed IWS zones of varying depth: 0.38 m (HA South), 0.45 m (HA North), and 0.6 m (UC). Each cell had a total of 0.45 m of aggregate and sand layers underlying the media. The average bowl storage depth at UC was 30 cm, within range of standard bioretention cell design, while HA South and North cells had 39 and 40-cm average bowl storage depths, respectively. The UC, HA South, and HA North cells captured (without overflow) the 29.4, 45.2, and 44.7-mm rainfall events, respectively.

Table 3-1. Characteristics of the bioretention cells and their catchments.

Characteristics	UC	HA South	HA North
Location	Pepper Pike, OH	Kirtland, OH	Kirtland, OH
Catchment area (ha)	0.36	0.19	0.27
Catchment imperviousness (%)	77	58	58
Bioretention surface area (m^2)	182	57	79
Loading ratio (LR)[1]	19.8	33.3	34.1
As-built design event (mm)	29.5	45.2	44.7
Bowl storage depth (m)	0.30	0.39	0.40
Fill media depth (m)	0.60	0.84	0.90
Aggregate and sand depth (m)	0.45	0.45	0.45
Drainage configuration	IWS	IWS	IWS
IWS zone depth (m)	0.60	0.38	0.45
Fill media characteristics	87% sand, 4% silt, 9% clay	88% sand, 2% silt, 10% clay	
Fill media K_{sat} (mm/hr)	168	102	
Underlying Soil Type	Mahoning silt loam and fill	Pierpont silty clay loam	Platea silty clay loam
Drawdown Rate (mm/hr)	4.3	2.0	1.7
Vegetation	Forbs and perennial grasses	Forbs and perennial grasses	Shrubs and trees
Length of calibration (months)	3	5	5
Length of validation (months)	4	5	5

[1]defined as the ratio of catchment area to bioretention surface area.

Runoff, drainage, and overflow volumes were measured or estimated for each bioretention monitoring site, as described in Chapter 2. Because runoff entered each bioretention cell in a diffuse manner, runoff was estimated using the Curve Number (CN) method offset by an antecedent moisture correction (USDA, 1986; USDA 2004). At each bioretention cell, sharp crested, v-notch weirs were utilized to measure combined drainage and overflow. Drainage was separated from overflow using either hydrograph separation (HA) or by modeling drainage in USEPA SWMM 5.1 (UC, Chapter 2).

The sum of exfiltration and ET (i.e., drawdown) was measured for each bioretention cell using a Hobo U20 pressure transducer (corrected for barometric pressure measured on site) housed inside a shallow monitoring well installed in each bioretention cell (Chapter 2). Drawdown was only considered between the top and bottom of the IWS zone and calculated during inter-event periods. The rate at which water was lost through combined exfiltration and ET was calculated as:

$$Avg\ DD_{rate} = \frac{\sum_{j=1}^{n}(\frac{WL_{i,j}-WL_{f,j}}{T_{ie,i}})}{n} \times \phi \quad (3\text{-}6)$$

where Avg DD_{rate} is the average drawdown rate (mm/hr), n is the number of inter-event periods, WL_i and WL_f are the initial and final water levels in the IWS zone for event j (mm), T_{ie} is the inter-event period duration (hr), and $\boldsymbol{\phi}$ is the media (0.32) or aggregate (0.40) effective drainable porosity. Drawdown rates were non-linear, and varied as a function of water depth in the IWS zone. This was presumably due to lateral exfiltration and hydraulic head (Browne et al., 2008; Chapter 2). Because DRAINMOD uses a single constant seepage rate, the average measured exfiltration rates of 2.0 mm/hr, 1.7 mm/hr, and 4.3 mm/hr were used as inputs to the HA South, HA North, and UC DRAINMOD models, respectively (Winston et al., 2015).

Drainage Coefficient

The drainage coefficient sets a maximum hydraulic limit on the amount of drainage that can occur in a day (cm/day). This is typically limited by the diameter and slope of the drain, the number and type of perforations, the drainage configuration, and/or any restrictions to flow in the drain (e.g., orifice plate or valve). The flux to the drain can be calculated using

the Kirkham equation (equation 3-4) when the surface storage is fully ponded and the media is saturated. The maximum drainage rate predicted by the Kirkham equation is limited to the drainage coefficient. The drainage coefficients were set to 50 cm/day and 45 cm/day for the South and North cells, respectively, which were the maximum observed drainage rates during the largest events from the cells at HA. Similarly, the drainage coefficient at UC was set to 120 cm/day.

Soil Inputs

To model soil water movement in DRAINMOD, two input parameters are required: (1) the saturated hydraulic conductivity and (2) the soil water characteristic curve of the media. To determine these inputs, three 7.5-cm diameter by 7.6-cm long soil core samples were obtained from the upper 30 cm of the bioretention media at the UC, HA South, and HA North bioretention cells. The soil water characteristic curve was measured using a pressure plate apparatus to determine the volume of water drained from an initially saturated soil core under various suction pressures (Table 3-2; Klute, 1986). The soil parameterization program within DRAINMOD uses this curve to relate the water table depth to volume drained, accounting for variability in soil-water content as the water level fluctuates within the bioretention media. Saturated hydraulic conductivity was measured using the constant head permeability test, as described in Klute and Dirksen (1986). The saturated hydraulic conductivity of the sand and gravel layers underlying the bioretention media were estimated at 15 cm/hr and 200 cm/hr, respectively (Rawls et al., 1998; Domenico and Schwartz, 1990).

Table 3-2. Soil water characteristics for UC, HA South, and HA North bioretention cells.

Pressure head		Volumetric Water Content (m^3/m^3)		
(m)	(kPa)	UC	HA South	HA North
0	0	0.331	0.387	0.312
-0.04	-0.39	0.331	0.380	0.290
-0.1	-0.98	0.331	0.375	0.290
-0.3	-2.94	0.258	0.271	0.206
-0.6	-5.88	0.217	0.156	0.112
-1	-9.81	0.201	0.135	0.096
-2	-19.6	0.190	0.123	0.090
-3	-29.4	0.179	0.113	0.093
-4	-39.2	0.174	0.110	0.082
-6	-58.8	0.150	0.105	0.075

Specifications for bioretention media in Ohio include a minimum of 80% sand and maximum 10% clay in the mineral fraction, and 3-5% organic matter by weight (ODNR, 2006). The HA North and South media (88% sand, 2% silt, 10% clay) and the UC media (87% sand, 4% silt, and 9% clay) were classified as loamy sands using sieve analysis (ASTM, 2007). Organic matter was 1.4%, 1.0%, and 4.3% of the media by weight [determined using loss-on-ignition methods (ASTM 2014)] at HA South, HA North, and UC, respectively.

Climatic Inputs

Temperature

Minimum and maximum daily air temperatures are required to estimate daily potential evapotranspiration (PET) in DRAINMOD. Air temperature was measured at UC and HA using Onset U-30 weather stations. Each weather station was located at most 150 m from the bioretention cells and measured air temperature on a 1-minute interval. Daily minimum and

maximum temperatures were determined using a script in R statistical software (R Core Team, 2015).

Precipitation

Rainfall was measured at UC and HA using an automated tipping bucket rain gauge with 0.25-mm resolution (Davis Instruments). The data logger recorded total rainfall depth over each 1-minute interval. For input into DRAINMOD, rainfall data were aggregated to hourly totals using R statistical software (R Core Team, 2015).

Potential Evapotranspiration (PET)

The Thornthwaite method was used in DRAINMOD to model PET. It is not as precise as other methods, such as Penman-Monteith, as it requires only the mean monthly temperature to calculate PET (Amatya et al., 1995). DRAINMOD has an option to include PET correction factors, which were utilized but were not specific to northern Ohio, as these data were not available.

Calibration and Validation

To calibrate and validate DRAINMOD, the measured/estimated water table depths, runoff, drainage, overflow, and exfiltration/ET data were split in two. To account for seasonality in bioretention performance (Emerson and Traver, 2008; Muthanna et al., 2008), storm events occurring during even-numbered months of the year (April, June, etc.) were used for model calibration. Data collected during odd-numbered months of the year (May, July, etc.) were extracted for model validation. Field monitoring methods were consistent during calibration and validation periods. A separate model was created for each bioretention cell, and the models were parameterized with measured or estimated

bioretention cell characteristics, catchment characteristics, and other inputs which remained constant during the calibration and validation periods. Model parameters that could not be measured, such as piezometric head of the contributing aquifer and thickness of the restricting layer, were used as calibration parameters to maximize the values of goodness of fit tests.

The quality of model fit to the calibration and validation data sets was quantified using the numerical difference and percent difference between measured and modeled runoff (inflow to the bioretention cell), drainage, overflow, and combined exfiltration and ET (in cm per bioretention surface area). Nash-Sutcliffe efficiency (NSE) and coefficients of determination (R^2) were calculated for each modeled and measured portion of the water balance. Nash-Sutcliffe efficiencies were calculated on an event-basis using:

$$NSE = 1 - \frac{\sum_{i=1}^{N}(Q_{measured,i} - Q_{modeled,i})^2}{\sum_{i=1}^{N}(Q_{measured,i} - Q_{average})^2} \quad (3\text{-}7)$$

where, $Q_{measured,i}$ = measured volume for event i, $Q_{modeled,i}$ = modeled volume for event i, $Q_{average}$ = average measured volume for N events, N = total number of events for the monitoring period, and NSE = Nash-Sutcliffe efficiency coefficient (Nash and Sutcliffe, 1970).

Analysis of Bioretention Design Alternatives

Once each DRAINMOD model was calibrated and validated, the baseline models from UC and HA South (i.e., employing all as-built characteristics) were used as the basis for an analysis of how bioretention design affects hydrologic performance. Long-term climatic data sets were obtained from the National Oceanic and Atmospheric Administration (NOAA,

2015). These included hourly temperature and rainfall data measured during 1983-2012 at the Cleveland Hopkins Airport. Four base models were created to represent varying exfiltration rates for Hydrologic Soil Groups (HSG) B, C, and D: 1.27, 0.51, 0.13, and 0.05 cm/hr; these rates were chosen to (1) bound the low-permeability soils that are common in Ohio, and (2) since past research has shown greater than 80% volume reduction for bioretention cells constructed in HSG A soils (Brown and Hunt 2011b). From these base models, design variables were modified one-at-a-time to determine the sensitivity of bioretention hydrologic performance to: media depth, IWS zone depth, bowl storage depth, and LR. A matrix of modeled design characteristics is presented in Table 3-3; a total of 256 modeling runs were undertaken for each bioretention cell. Modeled design characteristics were chosen to match typical bioretention designs in Ohio or to observe how extreme changes to typical designs would affect hydrologic performance.

For each model run, total volume of runoff, drainage, overflow, exfiltration, and ET (all reported in cm per bioretention surface area) was each summed over the 30-year simulations. The percentage of each portion of the water balance was then calculated for these long-term simulations. Performance comparisons were made among varying underlying soil types and design scenarios.

Table 3-3. Matrix of input values modeled in the analysis of bioretention design alternatives.

Design Characteristics	Baseline UC	Baseline HA South	Other Model Runs				
Media depth (m)	0.60	0.84	0.60	0.90	1.2		
IWS zone depth (m)	0.60	0.38	0	0.15	0.30	0.45	0.60
Loading ratio	15:1	20:1	10:1	20:1	35:1	50:1	
Rooting depth (m)	0.30	0.30	0.60				
Bowl depth (m)	0.27	0.38	0.23	0.30	0.45	0.60	

3.5 Results and Discussion

Contributing Area Runoff

The contributing runoff to each bioretention cell was the first parameter to be calibrated. Methods for estimating runoff were modified from those in Brown et al. (2013). Runoff calibration was improved by modeling impervious and pervious fractions as separate sub-catchments, parameterizing each with measured values, and then varying Green-Ampt infiltration characteristics and drain spacing to modify the amount of surface runoff (i.e., inflow to the bioretention cell). The runoff from each sub-catchment was summed to determine total runoff. Coefficients of determination between CN estimated and DRAINMOD modeled runoff (NRCS, 1986) at each site were 0.98-0.99, suggesting the runoff was well-calibrated. Nash-Sutcliffe efficiencies during the calibration period for runoff were 0.99 for all catchments. During the validation period, the model fit the estimated runoff very well, with NSE of 0.99, 0.96, and 0.96 for UC, HA South, and HA North, respectively. The slightly lower NSEs for the HA watersheds likely were due to the greater pervious fractions in these watersheds. Modeling runoff processes from soils using the CN

method is more tenuous than from an impervious surface due to variations in predicted runoff as a function of soil permeability, soil moisture and vegetative cover type.

DRAINMOD Calibration and Validation

Ursuline College

At UC, DRAINMOD was calibrated to the field collected data over the 7 month monitoring period (Figure 3-2). Percent difference between modeled and measured portions of the water balance (i.e., runoff, exfiltration/ET, drainage, and overflow) was within 6% during the calibration period (Table 3-4). During the calibration period, Nash-Sutcliffe efficiencies for drainage, overflow, and exfiltration/ET were 0.94, 0.97, and 0.95, respectively; R^2 were all greater than 0.95, suggesting DRAINMOD was well-calibrated against the hydrologic data from June, August, and October. Nash-Sutcliffe efficiencies were 0.98 and 0.95 and R^2 was greater than 0.96 for drainage and exfiltration/ET for the validation period. However, the NSE for overflow was 0.73 (R^2 of 0.89), with a 35% difference between modeled and measured overflow volume. This was likely due to the small number of overflow-producing events (4) during the validation period (McCuen et al., 2006). While percent difference between measured and modeled overflow during the validation period was relatively large, the percent difference for overflow was only 1% when considering the entire monitoring period. Overall model performance during the validation period was robust, with measured drainage, overflow, and exfiltration/ET representing 33.1%, 8.9%, and 57.9% of estimated runoff, while DRAINMOD modelled these parameters to be 30.6%, 11.9%, and 57.4%, respectively.

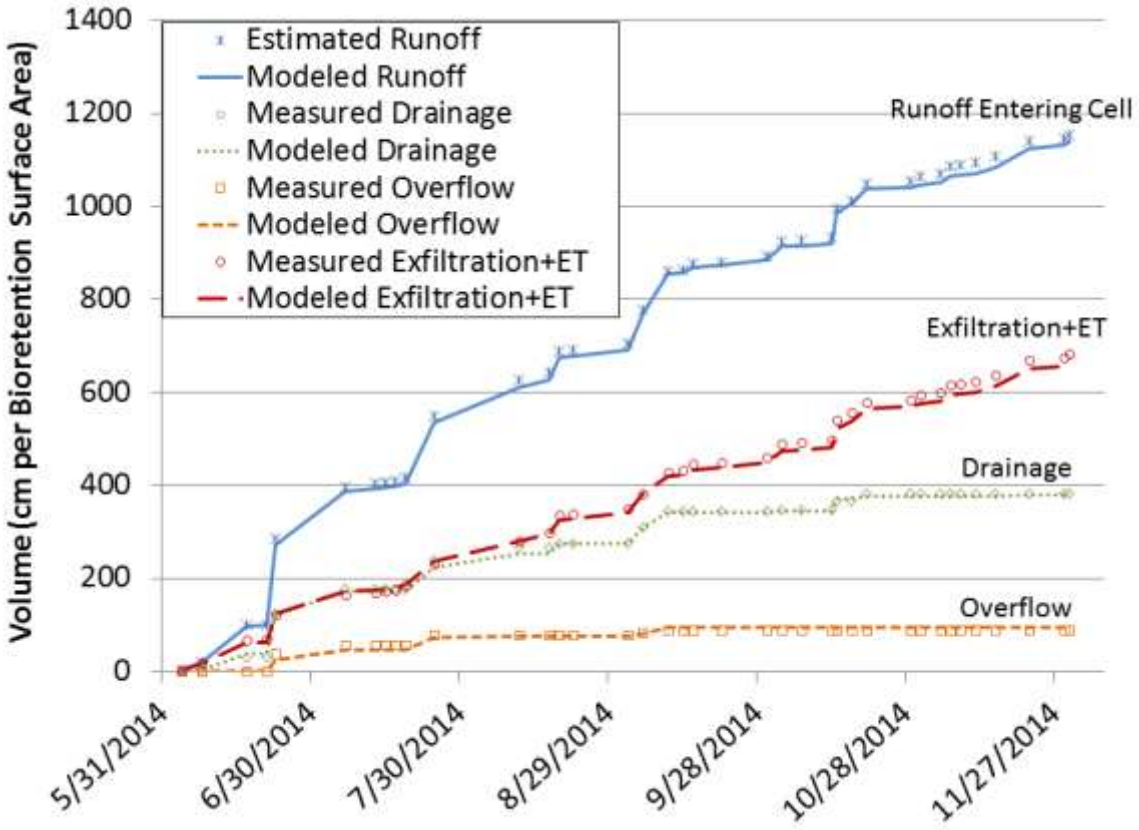

Figure 3-2. Cumulative fate of runoff for the UC bioretention cell with field-measured depths represented by symbols and modeled depth displayed as lines.

Table 3-4. Comparison of measured/estimated and modeled results for the UC bioretention cell.

Monitoring Period	Method of Comparison	**Fate of runoff from catchment**: (cm per bioretention surface area over the monitoring period [percent of annual runoff])			
		Runoff	**Drainage**	**Overflow**	**Exfiltration/ET**
Calibration (June, August, October 2014)	Measured/estimated volume	600	209	29.3	362
			[34.8]	[4.9]	[60.4]
	Modeled volume	577	207	28.9	342
			[35.8]	[5.0]	[59.2]
	Difference between modeled and measured	-23	-2	-0.4	-20
	Nash-Sutcliffe Efficiency	0.99	0.94	0.97	0.95
	Coefficient of Determination (R^2)	0.99	0.95	0.99	0.95
Monitoring Period	**Method of Comparison**	**Fate of runoff from catchment**: (cm per bioretention surface area over the monitoring period [percent of annual runoff])			
		Runoff	**Drainage**	**Overflow**	**Exfiltration/ET**
Validation (May, July, September, November 2014)	Measured/estimated volume	554	183	49.5	321
			[33.1]	[8.9]	[57.9]
	Modeled volume	562	172	66.7	323
			[30.6]	[11.9]	[57.4]
	Difference between modeled and measured	8	-11	17	2
	Nash-Sutcliffe Efficiency	0.99	0.98	0.73	0.95
	Coefficient of Determination (R^2)	1.00	0.99	0.89	0.96

Holden Arboretum

The duration of the HA monitoring period was 10 months; even months were used for calibration, and odd for validation (Tables 3-5 and 3-6). Rainfall was more frequent (47 events) and precipitation depth larger (average 15.2 mm) during the calibration period than in the validation period (39 events with average depth of 10.9 mm) and, as a result, approximately two-thirds of the runoff occurred during the calibration period. Both the HA South and North DRAINMOD models accurately predicted the fractions of drainage, overflow, and exfiltration/ET (Figures 3-3 and 3-4).

For HA South, the model was well-calibrated against the field measured data, with NSEs of 0.95, 0.87, and 0.76 for drainage, overflow, and exfiltration/ET, respectively; corresponding R^2 values were 0.96, 1.0, and 0.80. Nash-Sutcliffe efficiencies during the validation period were 0.95, 0.71, and 0.75 for drainage, overflow, and exfiltration/ET volume. Only 3 overflow events occurred during the monitoring period (2 during the calibration period and 1 during validation), resulting in divergence of modeled and measured overflow depths (McCuen et al., 2006; Jain and Sudheer, 2008). However, as a percentage of the overall water balance, overflow was predicted to within 3.3% and 1.5% of the measured values during the calibration and validation periods, respectively. Coefficient of determination tended to be higher than NSE for overflow, since the calculation of R^2 accounts for storm events with zero overflow, while these events only marginally affect the NSE. Modeled drainage and exfiltration/ET volumes were within 2% of the corresponding measured values during both the calibration and validation periods, suggesting DRAINMOD again provided reliable long-term water balance predictions.

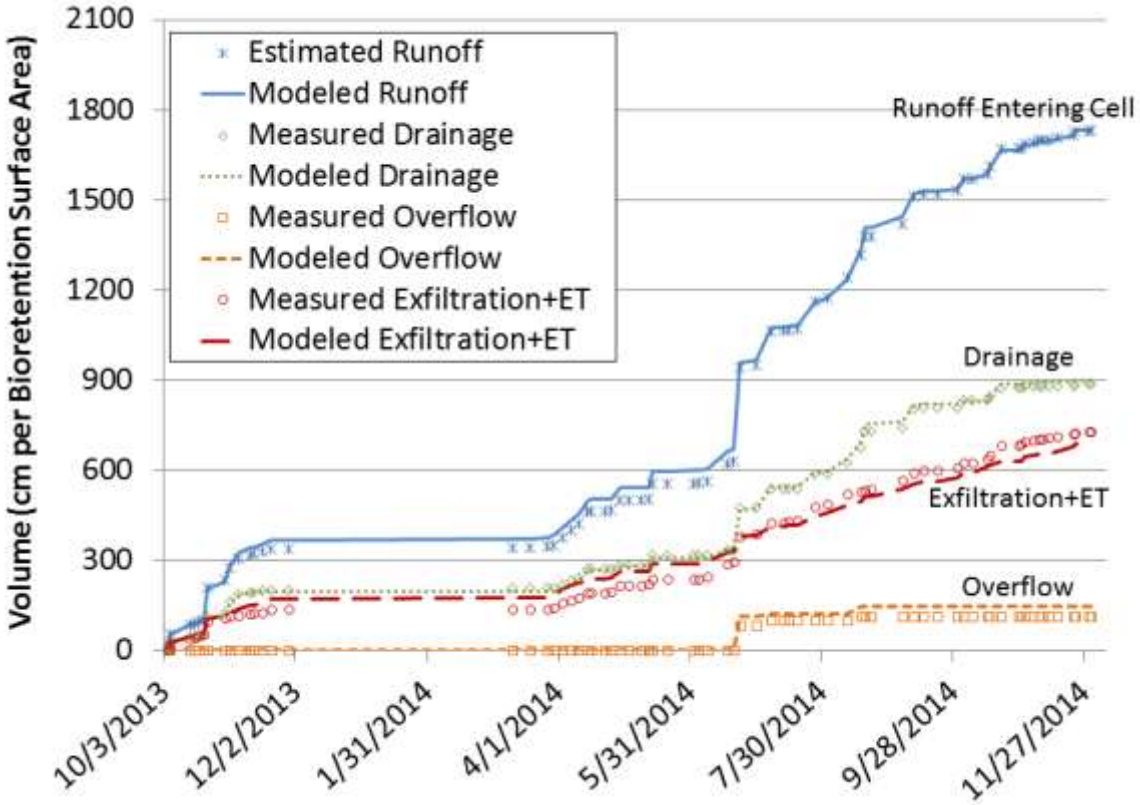

Figure 3-3. Cumulative fate of runoff for the HA South bioretention cell with field-measured depths represented by symbols and modeled depth displayed as lines.

Table 3-5. Comparison of measured/estimated and modeled results for the HA South bioretention cell.

Monitoring Period	Method of Comparison	Fate of runoff from catchment: (cm per bioretention surface area over the monitoring period [percent of annual runoff])			
		Runoff	**Drainage**	**Overflow**	**Exfiltration/ET**
Calibration (Oct 2013, Apr, Jun, Aug, Oct 2014)	Measured/estimated volume	1149	573	99	477
			[49.9]	[8.6]	[41.5]
	Modeled volume	1150	589	137	424
			[51.2]	[11.9]	[36.9]
	Difference between modeled and measured	2	16	39	-53
	Nash-Sutcliffe Efficiency	0.99	0.96	0.87	0.76
	Coefficient of Determination (R^2)	0.99	0.96	1.00	0.80
Monitoring Period	**Method of Comparison**	**Fate of runoff from catchment**: (cm per bioretention surface area over the monitoring period [percent of annual runoff])			
		Runoff	**Drainage**	**Overflow**	**Exfiltration/ET**
Validation (Nov 2013, May, Jul, Sep, Nov 2014)	Measured/estimated volume	570	306	15.9	247
			[53.8]	[2.8]	[43.4]
	Modeled volume	569	311	7.5	251
			[54.6]	[1.3]	[44.1]
	Difference between modeled and measured	0	4	-8	4
	Nash-Sutcliffe Efficiency	0.96	0.95	0.71	0.75
	Coefficient of Determination (R^2)	0.97	0.96	1.00	0.76

The predicted and measured water balance at the HA North cell were also in good agreement (Figure 3-4). Nash-Sutcliffe efficiencies during the calibration period were 0.97, 0.87, and 0.81 for drainage, overflow, and exfiltration/ET volumes; corresponding R^2 values

were all greater than 0.82 (Table 3-6). During the calibration period, measured and monitored volumes of drainage and exfiltration/ET were within 4%. Overflow was over-predicted by about 50% during the calibration period and under-predicted by approximately the same amount during the validation period. This was again likely due to the small number of overflow events (2 apiece during each modeling period) (Jain and Sudheer, 2008). Nash-Sutcliffe efficiencies during the validation period for HA North were similar to those at HA South: 0.98, 0.74, and 0.76 for drainage, overflow, and exfiltration/ET, respectively.

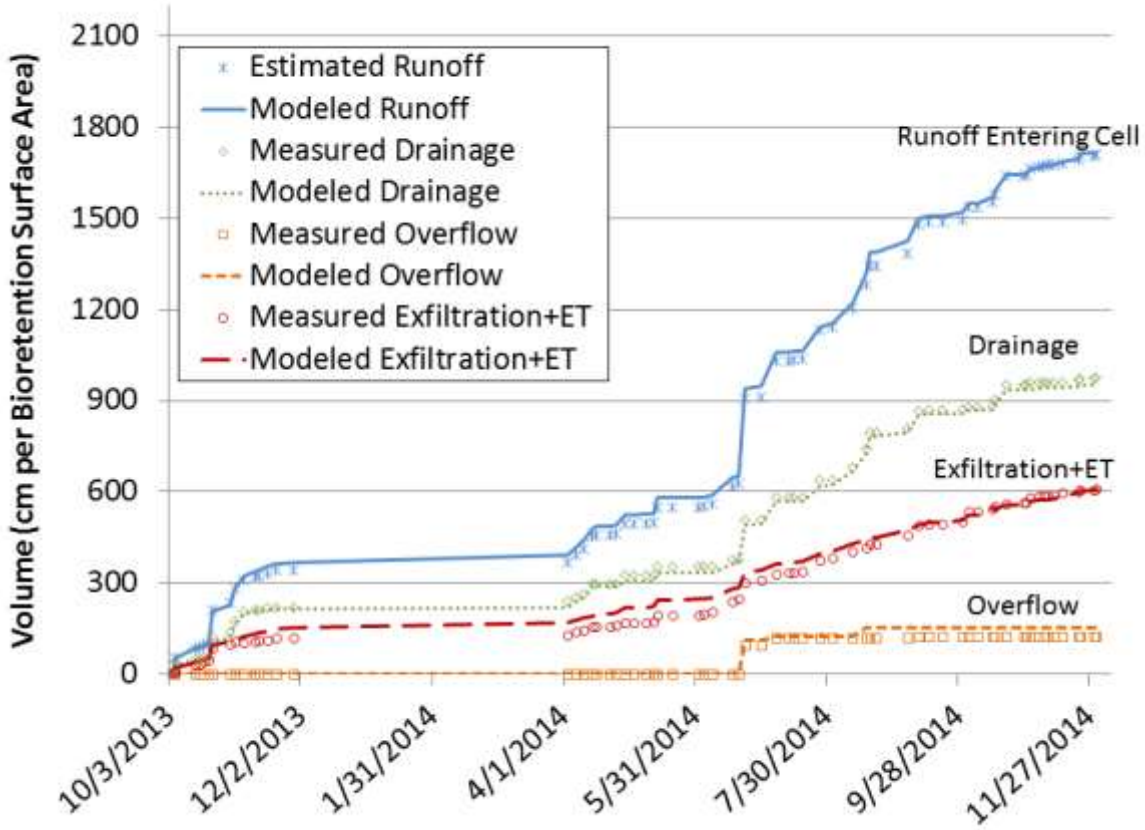

Figure 3-4. Cumulative fate of runoff for the HA North bioretention cell with field-measured depths represented by symbols and modeled depth displayed as lines.

Table 3-6. Comparison of measured/estimated and modeled results for the HA North bioretention cell.

Monitoring Period	Method of Comparison	Fate of runoff from catchment: (cm per bioretention surface area over the monitoring period [percent of annual runoff])			
		Runoff	**Drainage**	**Overflow**	**Exfiltration/ET**
Calibration (Oct 2013, Apr, Jun, Aug, Oct 2014)	Measured/estimated volume	1130	644	94.7	391
			[57]	[8.4]	[34.6]
	Modeled volume	1147	618	141.5	387
			[53.9]	[12.3]	[33.8]
	Difference between modeled and measured	17	-26	47	-4
	Nash-Sutcliffe Efficiency	0.99	0.97	0.87	0.81
	Coefficient of Determination (R^2)	0.99	0.97	0.94	0.82
Monitoring Period	**Method of Comparison**	**Fate of runoff from catchment**: (cm per bioretention surface area over the monitoring period [percent of annual runoff])			
		Runoff	**Drainage**	**Overflow**	**Exfiltration/ET**
Validation (Nov 2013, May, Jul, Sep, Nov 2014)	Measured/estimated volume	592	329	29.1	234
			[55.5]	[4.9]	[39.5]
	Modeled volume	567	336	12.9	219
			[59.1]	[2.3]	[38.6]
	Difference between modeled and measured	-25	7	-16	-15
	Nash-Sutcliffe Efficiency	0.96	0.98	0.74	0.76
	Coefficient of Determination (R^2)	0.97	0.98	0.96	0.77

Measured vs. Modeled: Overall Water Balance

Over the entire monitoring period, the monitored versus modeled percentage of the water balance pathways were in excellent agreement (Table 3-7), with at most 2% difference between monitored and modeled drainage, overflow, or exfiltration/ET. Supplementing the work of Brown et al. (2013), these results illustrate that DRAINMOD was an excellent long-term, mechanistic model for prediction of bioretention performance. While percent differences between measured and modeled overflow were quite high during calibration and validation periods (Tables 3-4, 3-5, and 3-6), modeled results were in reasonable agreement with measured over the entire monitoring period. This meant defensible conclusions could be drawn from analyses of bioretention design alternatives conducted using these models.

Due to the monitoring design, the HA North bioretention cell had the most inherent error in measurement of outflow hydrology (Chapter 2). Because design configurations and catchment characteristics were similar for the HA South and North cells, the North cell DRAINMOD model was not used for the analysis of bioretention design alternatives that follows.

Table 3-7. Monitored versus modeled percentage of the water balance over the entire monitoring period for each of the bioretention cells in northeast Ohio.

Type of Data	Hydrologic Fate	UC	HA South	HA North
Monitored	Drainage	33	51	57
Modeled		33	52	56
Monitored	Overflow	8	7	7
Modeled		9	8	9
Monitored	Exfiltration/ET	59	42	36
Modeled		58	40	35

Analysis of Bioretention Design Alternatives

Calibrated models for UC and HA South were used as the basis for an analysis of bioretention design alternatives. Base models were not modified from the design parameters determined from as-built surveys and laboratory measurements (Table 3-3). The one exception was the underlying soil K_{sat}, which was set at four rates (1.27, 0.51, 0.13, and 0.05 cm/hr) to create four base models for each site. This factor was varied in order to characterize the effects of the underlying soils on bioretention hydrology; K_{sat} representative of low permeability soils were chosen, since hydrologic performance over high K_{sat} soils has been proven excellent (Brown and Hunt 2011b). One design variable in each base model was modified at a time and all other design variables held constant at their base values to reduce modeling error (Saltelli, 2002). For each modeled case, the total volume and percentage of runoff, drainage, overflow, exfiltration, and ET over the 30-yr weather record were quantified.

Baseline model runs were utilized to develop benchmark long-term water balances for each of the underlying soil K_{sat} values for both UC and HA South (Figure 3-5). Because the two cells had different design cross-sections, soil water characteristic curves, and exfiltration rates (Tables 3-1 and 3-2), the models yielded modestly divergent results for the long-term water balance; the fraction of drainage was within 10-20% and exfiltration within 5-20% for each base scenario. Because UC had higher media K_{sat} and a higher drawdown rate than HA South (Chapter 2), this cell filtered and exfiltrated a greater fraction of the water balance, resulting in less overflow. In both base models, overflow decreased with increasing

underlying soil infiltration rate, with a maximum 5-7% overflow for the 0.05 cm/hr underlying K_{sat} case. Modeled percentage of ET was not impacted by underlying soil K_{sat} and represented approximately 5% of the water balance. For all base scenarios, a minimum of 93% of the stormwater infiltrated the filter media, meaning these bioretention cells treated the vast majority of the stormwater over the long-term.

For the sake of brevity, the primary focus of the remainder of this discussion will be on UC, since it was better calibrated to the field data than HA South. Trends in the data were similar in both model outputs, and results for HA South can be found in Smolek et al. (2015).

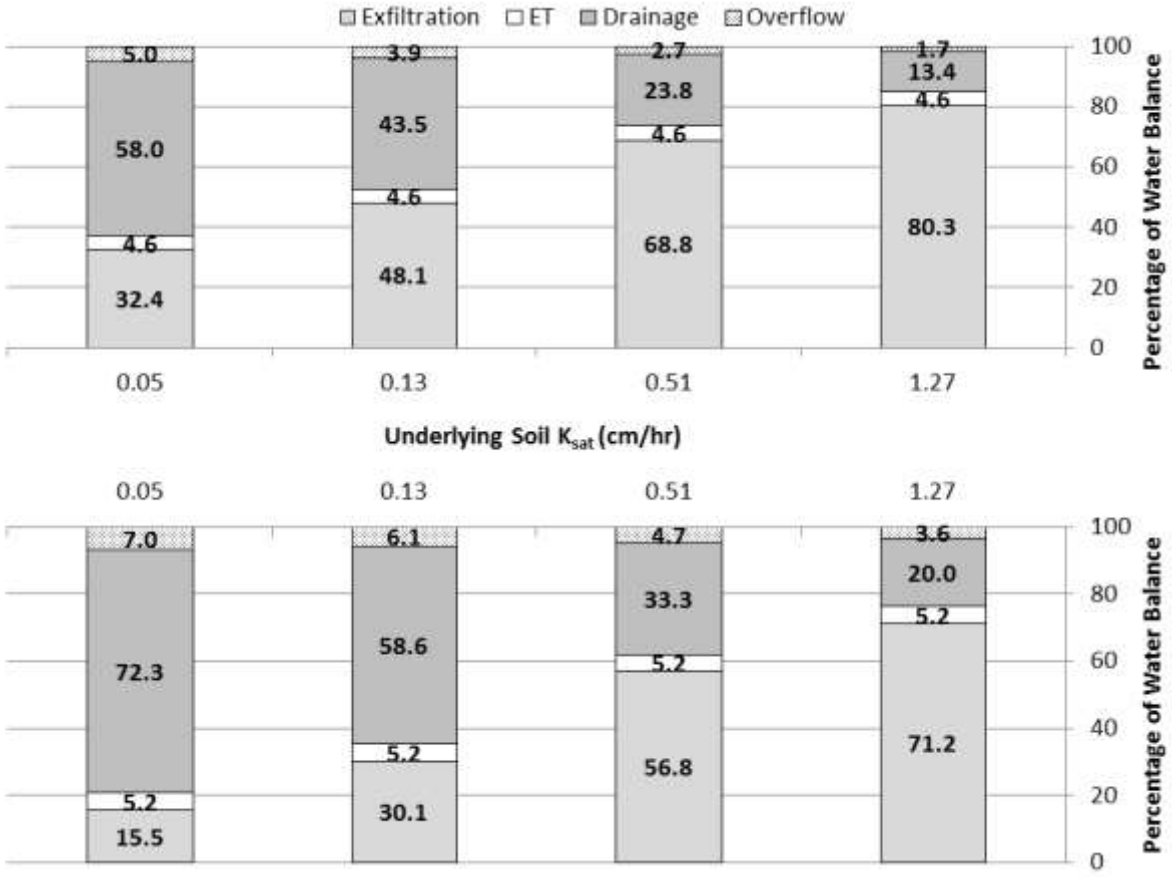

Figure 3-5. Base case model results for UC (top) and HA South (bottom).

Media Depth

Media depth was varied within the DRAINMOD soil file among commonly-used media depths of 0.6, 0.9, and 1.2 m (Hunt et al., 2012). The depth to the underdrain and the depth to the top of the IWS zone also were modified in the model to keep a consistent IWS zone depth of 0.6 m (Table 3-3). Results of each of the modeling runs as a function of media depth and underlying soil K_{sat} are presented in Figure 3-6.

With each 0.3-m increase in media depth, drainage and overflow decreased while exfiltration increased, albeit modestly (<3%) in all cases; the second 0.3-m increase in media depth resulted in little change to long-term hydrology. Media depth had similar impacts on the drainage, exfiltration, and ET for each underlying soil K_{sat}. Media depth had the greatest impact on the volume of overflow; for each additional 0.3 meters of media depth, the overflow fraction decreased very modestly (by 0.2-1.5%) for a given underlying soil infiltration rate. This effect was most pronounced when underlying soils had low permeability. Increasing media depth did not measurably impact the ET fraction of the water balance; concomitant increases in rooting depth, which might have augmented the ET from the bioretention cells, were not modeled. While the modeled effects of media depth on long-term hydrology were modest, greater media depths provide additional hydraulic retention time for treatment of nutrients (LeFevre et al. 2014) and dissipation of thermal load (Jones and Hunt, 2009). Modeled results showing little appreciable hydrologic benefit to increasing media depth are in contrast to past field monitoring results (Brown and Hunt, 2011a; Davis et al., 2012) and recommendations for bioretention design published in the literature (Hunt et al., 2012), which claim media depth is a critical factor in bioretention hydrologic

functionality. Since increases in media depth substantially add to construction costs, additional research focusing on this design factor is merited.

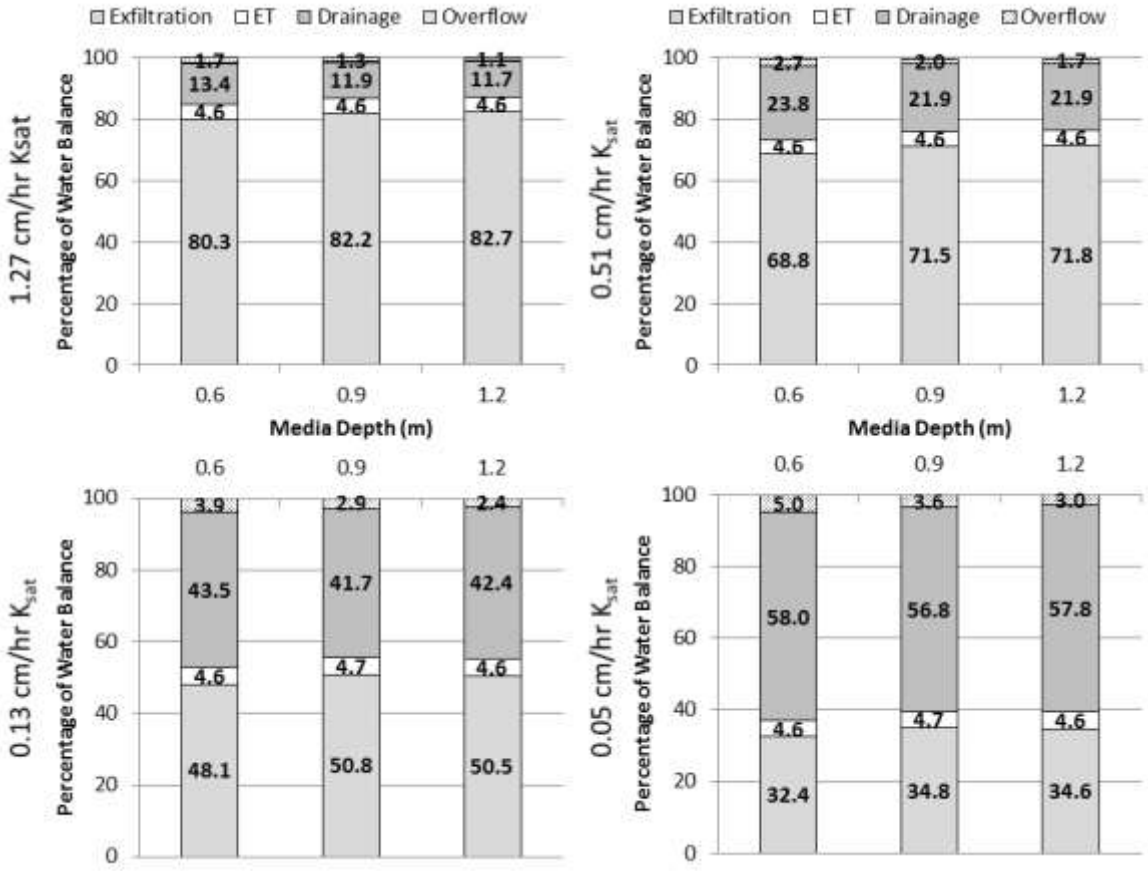

Figure 3-6. Effects of media depth on the long-term water balance.

Internal Water Storage Zone Depth

For the base models, the IWS zone depth varied from: 0 cm (i.e., drainage configuration with underdrain at the bottom of the cell), 15 cm, 30 cm, 38 cm, 45 cm, and 60 cm (Figure 3-7).

The inclusion of an IWS zone improved volume reduction substantially for each underlying soil K_{sat} by increasing the fraction of exfiltration. The inclusion of a 15-cm IWS zone, a simple retrofit or design modification, increased the exfiltration fraction (and therefore volume reduction) by 7-13% over the no IWS configuration. A deeper 60-cm IWS zone increased the exfiltration fraction by 20-30% compared to the no IWS configuration. While modeling results support the inclusion of an IWS zone across soil types, the greatest impact on overall volume reduction was observed for the moderate underlying soil K_{sat} cases (0.13 and 0.51 cm/hr). These results confirm those from field and lab-scale testing of the effects of IWS zones on bioretention hydrology and support the recommended 60-cm IWS zone in Ohio's design standards (ODNR, 2006; Li et al., 2009; Brown and Hunt, 2011b; Brown 2011; Lucas and Greenway, 2011).

Results from the UC model suggested the optimal IWS zone depth was 0.38-m, maximizing exfiltration and minimizing drainage. In the poorest underlying soil conditions (0.05 and 0.13 cm/hr infiltration rates), increasing the IWS zone marginally increased the long-term fraction of overflow. Substantial increases in overflow were not observed with the inclusion of an IWS zone, regardless of underlying soil K_{sat}. The long-term fraction of ET was not impacted by the inclusion of an IWS zone, and was between 4.5-5% of the annual runoff volume for UC.

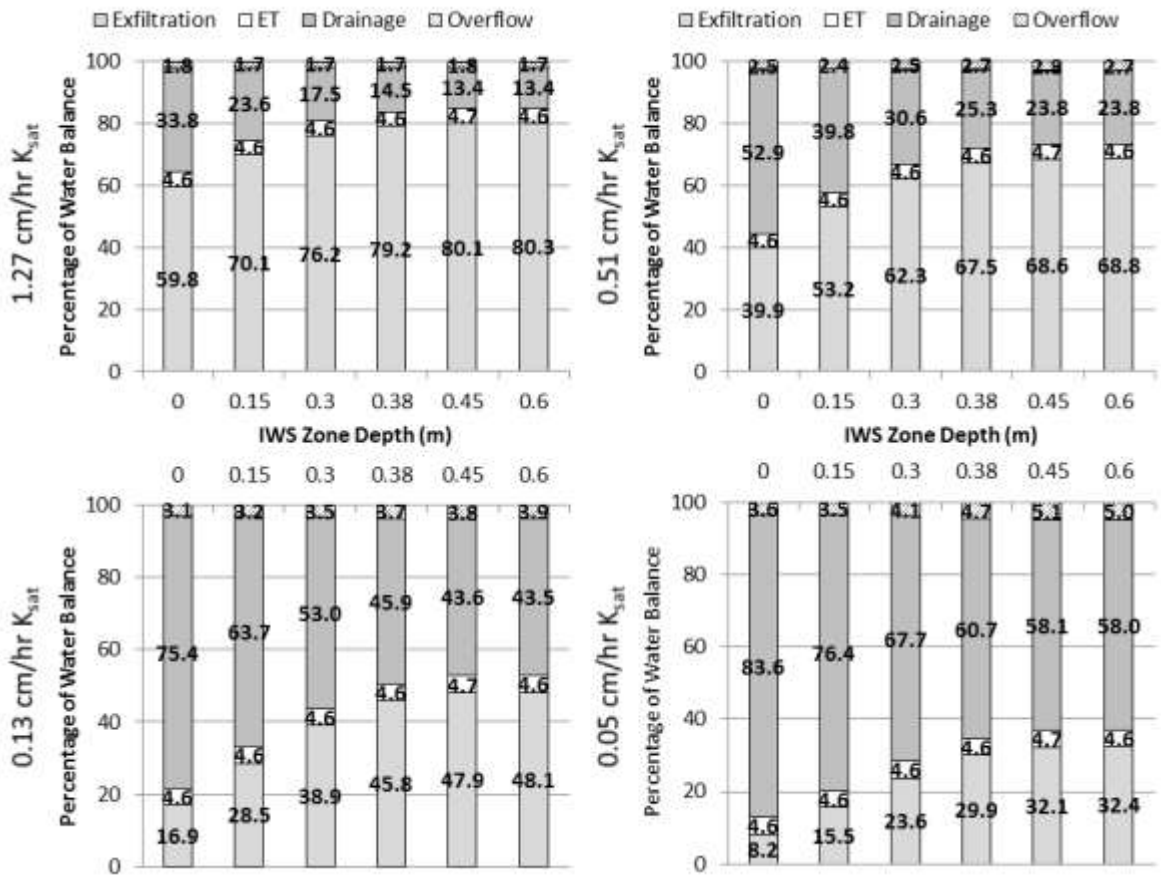

Figure 3-7. Effect of IWS zone depth on the water balance.

Rooting Depth

The base models assumed a 0.3-m rooting depth, since plants were juvenile during the monitoring periods. The rooting depth was increased to 0.6 meters to simulate mature plants. Concomitant increases in media K_{sat}, which might be spurred by the development of root macropores (Jenkins et al., 2010), were not modeled.

Of the parameters simulated in the analysis of bioretention designs, rooting depth had the least effect on long-term bioretention hydrology. The inclusion of a deeper rooting depth provided essentially no change in the fraction of ET (0.1% increase) at UC. The UC model

also essentially no change in drainage (0-0.1% increase), overflow (0-0.1% increase), and exfiltration (0.2-0.3% decrease) with deeper rooting depth.

Bowl Storage Depth

Bowl storage depth was varied within the model to determine its effects on long-term volume capture. For each base model, bowl storage depth was set to the following values: 22 cm, 30 cm, 38 cm, 45 cm, and 60 cm. Contributing watershed area was not modified, so the increase or decrease in ponding depth modified the volume captured and treated.

Increasing the bowl storage depth augmented the fraction of water treated by the media by reducing the fraction of overflow (Figure 3-8). This was most prevalent in the least transmissive soils, with a 4-5% increase in the drainage fraction as bowl storage depth increased from 0.22-m to the 0.6-m ponding depth; the drainage fraction increased by 1-2% when K_{sat} was greater than 0.5 cm/hr. Corresponding decreases in overflow occurred, and were of similar magnitude. For instance, for the 0.05 cm/hr underlying soil case, the fraction of the annual runoff volume that bypassed treatment decreased from 6.3% to 1.5% when ponding depth increased from 0.22 to 0.6 meters. Bowl storage depth had no appreciable influence on exfiltration and ET.

While the fraction of treated outflow modestly increased with deeper bowl storage depth, the intended benefit is peak flow mitigation (which DRAINMOD does not model; Hunt et al., 2012). A greater bowl volume increases the likelihood the runoff conveyed during the period of peak rainfall intensity will be entirely captured (i.e., no overflow) by the bioretention cell (Heasom et al., 2006; Davis et al., 2012). It should be noted, however, deeper ponding depths could have detrimental effects on plant health, jeopardizing

bioretention cell functionality (Hunt et al., 2012). For instance, if deep ponding depths caused plant mortality, the fraction of long-term ET certainly would decline. Due to clogging, long-term media K_{sat} could be jeopardized without plants since the benefits of root macropores and soil loosening by plant roots would not be assured (Pitt et al., 2008; Jenkins et al., 2010).

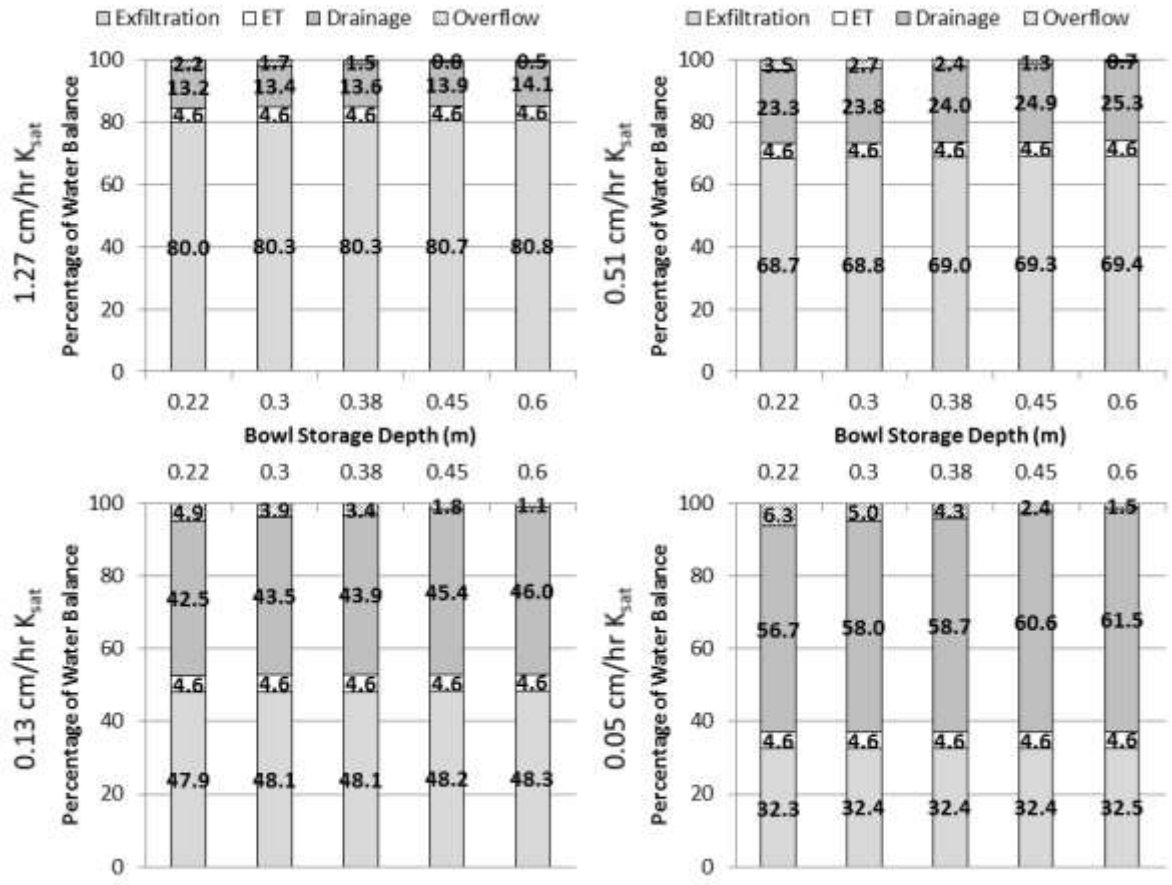

Figure 3-8. Effect of bowl storage depth on the water balance.

Watershed Area to Bioretention Surface Area Ratio

The field ratio in DRAINMOD was varied to simulate changes in loading ratio (LR), or the ratio of catchment area to bioretention surface area. The imperviousness of the catchments was not modified, nor was the surface area of the bioretention cell.

The volume of runoff to the bioretention cell increased with increasing LR due to the change in catchment surface area. Substantial differences in drainage, overflow, exfiltration, and ET existed across LRs and underlying soil K_{sat} (Figure 3-9). For the standard 20:1 LR designated for bioretention designs in Ohio, overflow represented between 3-8% of the water balance, with greater overflow in poorly drained underlying soils. The most undersized bioretention cells (50:1 LR) increased the overflow fraction by up to 20% compared to the standard 20:1 design. When LR was greater than 20:1, the fraction of overflow increased substantially. Moving from the most-oversized (10:1 LR) to the most-undersized case (50:1 LR), the fraction of exfiltration decreased by as much as 30% of the annual runoff budget. LR was the only factor to substantially affect the long-term percentage of ET, with bioretention cells sized for 10% and 2% of their drainage areas producing 6% and 2% ET, respectively. Since the bioretention cell surface area was static, the modeled volume of ET remained constant, but the percentage varied based on the runoff volume.

Results suggested undersized systems might function proportionally better (per dollar spent on construction) than systems designed to be 5% of the contributing impervious drainage area, which is supported by field research on undersized bioretention cells (Luell et al., 2011; Wardynski and Hunt, 2012). The long-term fraction of overflow declines in undersized systems as the underlying soil infiltration rate increases; thus, undersized systems

situated over sandy soils might be particularly good retrofits. However, the potential for surface clogging and reduced hydraulic functionality will increase as the bioretention cell becomes increasingly undersized, simultaneously increasing maintenance frequency and strain on pre-treatment devices (Luell et al. 2011; Brown and Hunt 2011a).

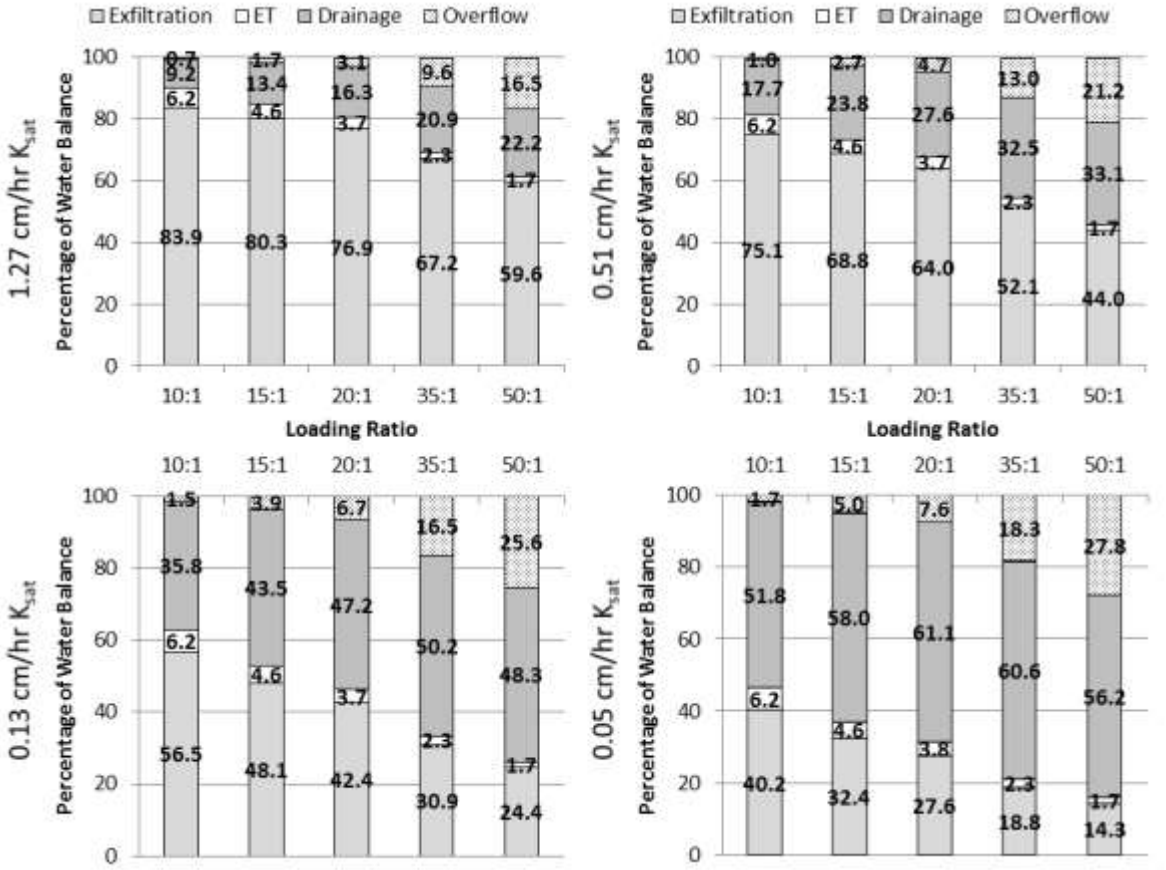

Figure 3-9. Effect of loading ratio on the water balance.

Summary of Volume Reduction and Overflow

The intent of this work was to optimize bioretention design when constructed on lower permeability soils (underlying soil Ksat 0.05-0.5 cm/hr). Separate from an overall annual

water balance, design modifications were identified that, in particular, led to substantial reductions in runoff volume on the positive side or substantial increases in untreated bypass flow on the negative side. A couple of the more meaningful results are highlighted here.

Of bioretention design factors, volume reduction was most affected by IWS depth and LR. As an example, Figure 3-10 shows exfiltration for a bioretention cell constructed in a soil with K_{sat} of 0.13 cm/hr. Each incremental 15-cm increase in IWS depth increased exfiltration, with correlative runoff volume reduction. From the no IWS configuration (i.e., drain at the bottom of the excavated cell), increasing the IWS depth to 15 cm, 30 cm and 45 cm resulted in 69%, 130% and 183% increases in exfiltration. Increasing the IWS depth further to 60 cm provided no meaningful increase in volume reduction. However, there may be other reasons, such as enhancement of denitrification and provision of water for plants during droughts (Hunt et al. 2006; Davis 2008; Chapter 4), to consider increasing the IWS zone depth.

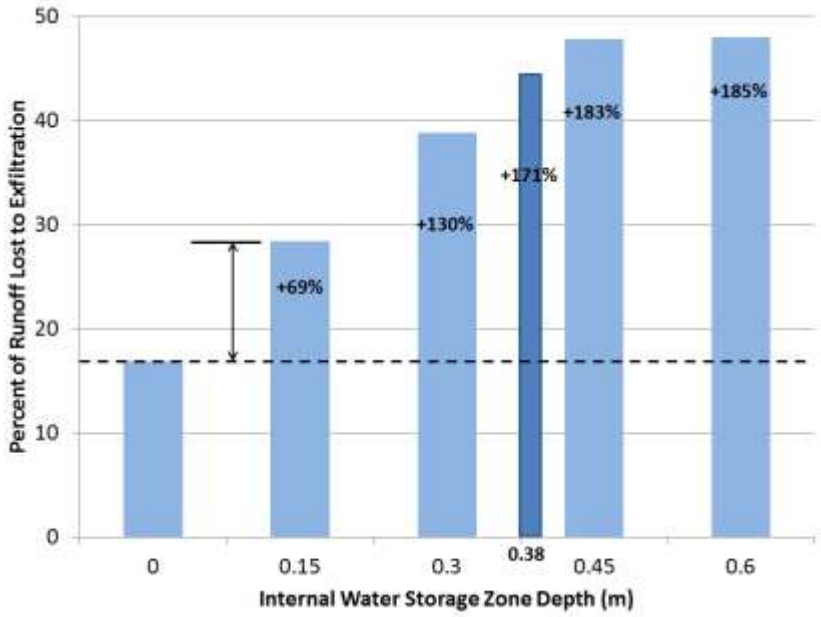

Figure 3-10. Percent increase in exfiltration as a function of IWS zone depth for an underlying soil K_{sat} of 0.13 cm/hr.

As might be expected, the amount of overflow was most affected by the HLR and bowl depth. As an example, from the monitored condition at UC (HLR of 15:1), increasing the HLR to 20:1, 35:1 and 50:1 resulted in 72%, 323% and 556% more overflow bypassing treatment through the filter media (Figure 3-11). When a bioretention cell is sized to be 10% of its contributing catchment, overflow is nearly eliminated. Sizing the bioretention cell becomes a balance amongst economics, water quality goals, and maintenance realities, as decreasing the bioretention surface area increases the rate of surface clogging (Wardynski and Hunt 2012).

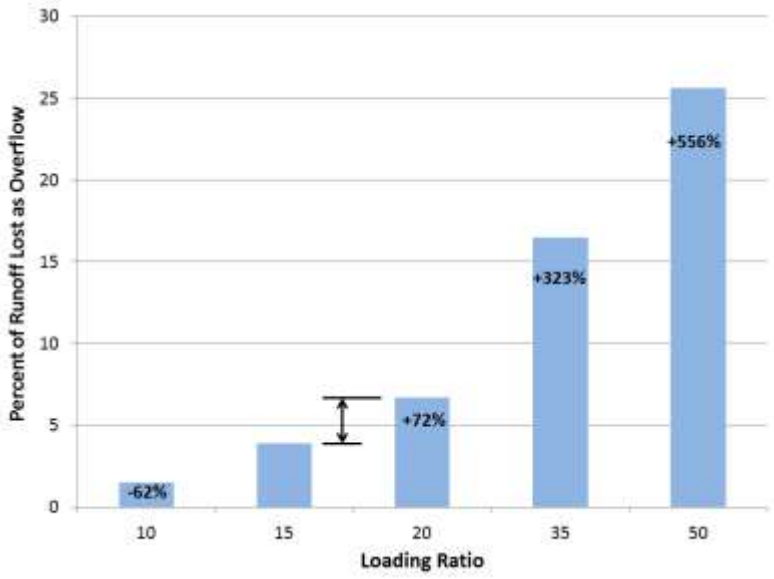

Figure 3-11. Percent increase or decrease in overflow as a function of loading ratio for an underlying soil K_{sat} of 0.13 cm/hr relative to the UC condition (15:1).

3.6 Summary and Conclusions

Design engineers and regulators currently work within a rigid framework for design and crediting of bioretention cells. Designs must meet technical specifications outlined in a jurisdiction's stormwater manual. There are many situations where these specifications may not produce the best results or may even preclude the use of bioretention cells, such as in design of retrofits. A more flexible design and crediting mechanism is needed for bioretention. To create said mechanisms, long-term models are needed to simulate the hydrologic performance of bioretention cells; field-monitoring of every design scenario is not economically feasible.

In this study, DRAINMOD models calibrated with field-measured data were utilized to conduct bioretention design alternative analyses on six parameters: media depth, IWS zone

depth, rooting depth, bowl storage depth, loading ratio, and underlying soil saturated hydraulic conductivity. The following conclusions can be derived from this work:

1. DRAINMOD accurately predicted runoff volume from drainage areas with a mixture of pervious and impervious surfaces. Green-Ampt infiltration parameters were separately varied in sub-watershed models for impervious and pervious areas, which improved runoff predictions. The goodness-of-fit of modeled runoff was inversely related to the percentage of pervious area in the catchment.

2. DRAINMOD provided accurate predictions of long-term bioretention hydrology. Model fit was excellent for all three sites modelled (UC, HA South, and HA North). Over the entire monitoring period, the monitored and modeled drainage, overflow, and exfiltration/ET fractions at each site never diverged by more than 2%. Nash-Sutcliffe efficiencies for drainage were greater than 0.94 and those for exfiltration/ET were greater than 0.71. Overflow was the most difficult parameter to predict in DRAINMOD, with validation period NSE of 0.73, 0.74, and 0.71 for UC, HA South, and HA North, respectively. This was due to the relatively small number of overflow events.

3. An analysis of bioretention design alternatives was performed using calibrated DRAINMOD models to determine bioretention cell performance over a range of underlying soil K_{sat}. The models were most sensitive to LR and IWS zone depth, which modified the fraction of drainage and exfiltration by at least 20%, regardless of underlying soil type. The simple inclusion of a 0.15-m IWS zone increased the fraction of exfiltration by 7-13% over the no IWS configuration. IWS zone depths were optimized at 0.38 and 0.45 meters for the two modeled bioretention cells. Optimal IWS zone depth should decrease with increasing

underlying soil K_{sat}. The models were also highly sensitive to underlying soil K_{sat}, suggesting bioretention cells should be placed where underlying soils have higher permeability. Modeled data were moderately sensitive to bowl storage and media depths, especially with respect to overflow. Modeled bioretention hydrology was least sensitive to rooting depth.

4. Undersized bioretention cells, common in retrofit situations, may still serve to ameliorate urban watershed hydrology as long as they are appropriately maintained. In underlying soils with K_{sat} greater than 0.51 cm/hr, a 35:1 LR overflow was 13% or less of the water balance, in the range of prior studies on bioretention cells. With lower underlying soil K_{sat}, overflow was up to 20% of the water balance. At a 50:1 LR, overflow was greater than 15% in all underlying soils, suggesting these bioretention cells are too undersized and should be avoided in practice. However, undersized bioretention cells in moderate or high conductivity underlying soils might be particularly good retrofits.

3.7 References

Amatya, D.M., Skaggs, R.W., and Gregory, J.D. (1995). "Comparison of methods for estimating REF-ET." *J. Irrig. Drain. Eng*., 121(6), 427-435.

American Society for Testing and Materials (ASTM). (2007). *Standard test method for particle-size analysis of soils.* ASTM D422-63.

American Society for Testing and Materials (ASTM). (2014). *Standard test methods for moisture, ash, and organic matter of peat and other organic soils*. ASTM D2974-14.

Braga, A., Horst, M., and Traver, R.G. (2007). "Temperature effects on the infiltration rate through an infiltration basin BMP." *J. Irrig. Drain. Eng*., 133(6), 593-601.

Brander, K.E., Owen, K.E., and Potter, K.W. (2004). "Modeled impacts of development type on runoff volume and infiltration performance." *J. Am. Water Res. Assoc*., 40(4), 961-969.

Bratieres, K., Fletcher, T.D., Deletic, A., and Zinger, Y. (2008). "Nutrient and sediment removal by stormwater biofilters: A large-scale design optimisation study." *Water Res*., 42(14), 3930-3940.

Brown, R.A. (2011). "Evaluation of bioretention hydrology and pollutant removal in the upper coastal plain of North Carolina with development of a bioretention modeling application in DRAINMOD." Ph.D. Dissertation, North Carolina State University, Raleigh, NC. Avaialable: http:// repository.lib.ncsu.edu/ir/bitstream/1840.16/6783/1/etd.pdf.

Brown, R.A., and Hunt III, W F. (2011a). "Impacts of media depth on effluent water quality and hydrologic performance of undersized bioretention cells." *J. Irrig. Drain. Eng*., 137(3), 132-143.

Brown, R.A. and Hunt, W.F. (2011b). "Underdrain configuration to enhance bioretention exfiltration to reduce pollutant loads." *J. Environ. Eng*., 137(11), 1082-1091.

Brown, R.A., and Hunt, W.F. (2012). "Improving bioretention/biofiltration performance with restorative maintenance." *Water Sci. Technol*., 65(2), 361-367.

Brown, R.A., R.W. Skaggs, and W.F. Hunt. (2013). "Calibration and validation of DRAINMOD to model bioretention hydrology." *J. Hydrol*., 486, 430-442.

Browne, D., Deletic, A., Mudd, G.M., and Fletcher, T.D. (2008). "A new saturated/unsaturated model for stormwater infiltration systems." *Hydrol. Processes*, 22(25), 4838-4849.

Christianson, R.D., Brown, G.O., Chavez, R.A., and Storm, D E. (2012). "Modeling field-scale bioretention cells with heterogeneous infiltration media." *Trans. ASABE*, 55(4), 1193-1201.

Davis, A.P. (2008). "Field performance of bioretention: Hydrology impacts." *J. Hydrol. Eng*., 13(2), 90-95.

Davis, A.P., Hunt, W. F., Traver, R.G., and Clar, M. (2009). "Bioretention technology: Overview of current practice and future needs." *J. Environ. Eng*., 135(3), 109-117.

Davis, A.P., Traver, R.G., Hunt, W.F., Lee, R., Brown, R.A., and Olszewski, J.M. (2012). "Hydrologic performance of bioretention storm-water control measures." *J. Hydrol. Eng*., 17(5), 604-614.

DeBusk, K.M., Hunt, W.F., and Line, D.E. (2010). "Bioretention outflow: Does it mimic nonurban watershed shallow interflow?" *J. Hydrol. Eng*., 16(3), 274-279.

Denich, C., and Bradford, A. (2010). "Estimation of evapotranspiration from bioretention areas using weighing lysimeters." *J. Hydrol. Eng*., 15(6), 522-530.

Dietz, M.E., and Clausen, J.C., (2005). "A field evaluation of rain garden flow and pollutant treatment." *Water, Air, and Soil Poll*., 167(1-4), 123-138.

Dietz, M.E. and Clausen, J.C. (2006). "Saturation to improve pollutant retention in a rain garden." *Environ. Sci. Tech.*, 40(4), 1335-1340.

Dietz, M.E., and Clausen, J.C. (2008). "Stormwater runoff and export changes with development in a traditional and low impact subdivision." *J. Environ. Man*., 87(4), 560-566.

Domenico, P.A., and Schwartz, F.W. (1990). *Physical and chemical hydrogeology*. John Wiley and Sons, New York, pp. 1–824.

Dussaillant, A.R., Wu, C.H., and Potter, K.W. (2004). "Richards equation model of a rain garden." *J. Hydrol. Eng*., 9(3), 219-225.

Dussaillant, A.R., Cuevas, A., and Potter, K.W. (2005). "Raingardens for stormwater infiltration and focused groundwater recharge: Simulations for different world climates." *Water Sci. Tech.: Water Sup*., 5(3-4), 173-179.

Emerson, C.H., and Traver, R.G. (2008). "Multiyear and seasonal variation of infiltration from storm-water best management practices." *J. Irrig. Drain. Eng*., 134(5), 598-605.

Géhéniau, N., Fuamba, M., Mahaut, V., Gendron, M.R., and Dugué, M. (2014). Monitoring of a Rain Garden in Cold Climate: Case Study of a Parking Lot near Montréal. *J. Irrig. Drain. Eng.*, 141(6), 04014073.

Green, W.H., and Ampt, G.A. (1911). "Studies on soil physics. I. The flow of air and water through soil." *J. Agric. Sci*., 4(01), 1–24.

Hathaway, J.M., and Hunt, W.F. (2011). "Evaluation of first flush for indicator bacteria and total suspended solids in urban stormwater runoff." *Water, Air, and Soil Poll*., 217(1-4), 135-147.

Hathaway, J.M., Brown, R.A., Fu, J.S., and Hunt, W.F. (2014). "Bioretention function under climate change scenarios in North Carolina, USA." *J. Hydrol*., 519, 503-511.

Hatt, B.E., Fletcher, T.D., and Deletic, A. (2009). "Hydrologic and pollutant removal performance of stormwater biofiltration systems at the field scale." *J. Hydrol*., 365(3), 310-321.

He, Z., and Davis, A.P. (2011). "Process modeling of stormwater flow in a bioretention cell." *J. Irrig. Drain. Eng*., 137(3), 121-131.

Heasom, W., Traver, R.G., and Welker, A. (2006). "Hydrologic modeling of a bioinfiltration best management practice." *J. Am. Water Res. Assoc*., 42(5), 1329-1347.

Hooghoudt, S.B. (1940). "General consideration of the problem of field drainage by parallel drains, ditches, watercourses, and channels." Publ. No.7 in the series: *Contribution to the knowledge of some physical parameters of the soil* (titles translated from Dutch). Bodemkundig Instituut, Groningen, The Netherlands.

Hoskins, J., and Peterein, J. (2013). "Case Study of St. Louis, Missouri: Comparison of Bioretention Performance to the Runoff Component of a Restored Water Balance." *J. Environ. Eng*., 139(4), 516-521.

Hunt, W.F., Jarrett, A.R., Smith, J.T., and Sharkey, L.J. (2006). "Evaluating bioretention hydrology and nutrient removal at three field sites in North Carolina." *J. Irrig. Drain. Eng*., 132(6), 600–608.

Hunt, W.F., Smith, J.T., Jadlocki, S.J., Hathaway, J.M., and Eubanks, P.R. (2008). "Pollutant removal and peak flow mitigation by a bioretention cell in urban Charlotte, NC." *J. Environ. Eng*., 134(5), 403-408.

Hunt, W.F., Davis, A.P., and Traver, R.G. (2012). "Meeting hydrologic and water quality goals through targeted bioretention design." *J. Environ. Eng*., 138(6), 698-707.

Jain, S.K., and Sudheer, K.P. (2008). “Fitting of hydrologic models: a close look at the Nash–Sutcliffe index.” *J. Hydrol. Eng*., 13(10), 981-986.

Jenkins, J.K.G., Wadzuk, B.M., and Welker, A.L. (2010). “Fines accumulation and distribution in a storm-water rain garden nine years postconstruction.” *J. Irrig. Drain. Eng*., 136(12), 862-869.

Jones, M.P., and Hunt, W.F. (2009). “Bioretention impact on runoff temperature in trout sensitive waters.” *J. Environ. Eng*., 135(8), 577-585.

Kirkham, D. (1957). “Theory of land drainage.” *Drainage of Agricultural Lands: Agronomy Monograph No. 7*, J. N. Luthin, ed., American Society of Agronomy, Madison, Wisc., 139-181.

Klute, A. (1986). “Water retention: Laboratory methods.” *Methods of soil analysis. Part 1: Physical and mineralogical methods*, A. Klute, ed., Soil Science Society of America, Madison, Wis., 635–662.

Klute, A., and Dirksen, C. (1986). “Hydraulic conductivity and diffusivity: Laboratory methods.” *Methods of soil analysis. Part 1: Physical and mineralogical methods*, A. Klute, ed., Soil Science Society of America, Madison, Wis. 697-732

LeFevre, G.H., Paus, K.H., Natarajan, P., Gulliver, J.S., Novak, P.J., and Hozalski, R.M. (2014). “Review of dissolved pollutants in urban storm water and their removal and fate in bioretention cells.” *J. Environ. Eng*., 141(1), 04014050.

Li, H., Sharkey, L.J., Hunt, W.F., and Davis, A.P. (2009). “Mitigation of impervious surface hydrology using bioretention in North Carolina and Maryland.” *J. Hydrol. Eng*., 14(4), 407-415.

Line, D.E., and Hunt, W.F. (2009). “Performance of a bioretention area and a level spreader-grass filter strip at two highway sites in North Carolina.” *J. Irrig. Drain. Eng*., 135(2), 217-224.

Lucas, W.C. (2010). “Design of integrated biofiltration-detention urban retrofits with design storm and continuous simulation methods.” *J. Hydrol. Eng*., 15(6), 486-498.

Lucas, W.C., and Greenway, M. (2011). “Hydraulic response and nitrogen retention in bioretention mesocosms with regulated outlets: Part I—hydraulic response.” *Water Environ. Res*., 83(8), 692-702.

Luell, S.K. (2011). “Evaluating the impact of bioretention cell size and swale design in treating highway bridge deck runoff.” M.S. thesis, North Carolina State University.

Luell, S.K., Hunt, W.F., and Winston, R.J. (2011). "Evaluation of undersized bioretention stormwater control measures for treatment of highway bridge deck runoff." *Water Sci. Technol*., 64(4), 974-979.

McCuen, R.H., Knight, Z., and Cutter, A.G. (2006). "Evaluation of the Nash–Sutcliffe efficiency index." *J. Hydrol. Eng*., 11(6), 597-602.

Moody, W.T. (1967). "Nonlinear differential equation of drain spacing." *J. Irrig. Drain. Div. ASCE*, 92(IR2), 1-9.

Muthanna, T.M., Viklander, M., and Thorolfsson, S.T. (2008). "Seasonal climatic effects on the hydrology of a rain garden." *Hydrol. Processes*, 22(11), 1640-1649.

Nash, J.E., and Sutcliffe, J.V. (1970). "River flow forecasting through conceptual models part 1 – A discussion of principles." *J. Hydrol*., 10(3), 282-290.

National Oceanic and Atmospheric Administration (NOAA) (2015). National climatic data center, U.S. local climatological data. Cleveland, OH airport. Available: http://www.ncdc.noaa.gov/

Ohio Department of Natural Resources (ODNR), Division of Soil and Water Conservation, (2006). *Rainwater and land development: Ohio's standards for stormwater management, low impact development, and urban stream protection*. 3rd edition. Ed: John Mathews.

Olszewski, J.M., and Davis, A.P. (2013). "Comparing the hydrologic performance of a bioretention cell with predevelopment values." *J. Irrig. Drain. Eng*., 139(2), 124-130.

Page, J.L., Winston, R.J., Mayes, D.B., Perrin, C., and Hunt, W.F. (2015). "Hydrologic mitigation of impervious cover in the municipal right-of-way through innovative stormwater control measures." *J. Hydrol*., 527, 923-932.

Passeport, E., Hunt, W.F., Line, D.E., Smith, R.A., and Brown, R.A. (2009). "Field study of the ability of two grassed bioretention basins to reduce storm-water runoff pollution." *J. Irrig. Drain. Eng*., 135(4), 505-510.

Paus, K.H., Morgan, J., Gulliver, J.S., Leiknes, T., and Hozalski, R.M. (2014). "Assessment of the hydraulic and toxic metal removal capacities of Bioretention cells after 2 to 8 years of service." *Water, Air, and Soil Poll*., 225(1), 1-12.

Pitt, R., Chen, S.E., Clark, S.E., Swenson, J., and Ong, C.K. (2008). "Compaction's impacts on urban storm-water infiltration." *J. Irrig. Drain. Eng*., 134(5), 652-658.

Rawls, W.J., Gimenez, G., and Grossman, R. (1998). "Use of soil texture, bulk density, and slope of the water retention curve to predict saturated hydraulic conductivity." *Trans. ASAE*, 41(4), 983–988.

R Core Team, 2015. *A language and environment for statistical computing*. R Foundation for Statistical Computing. Vienna, Austria.

Saltelli, A. (2002). "Sensitivity analysis for importance assessment." *Risk Anal*., 22(3), 579-590.

Skaggs, R.W. (1978). *A water management model for shallow water table soils*. Technical Report No. 134, Water Resources Research Institute of the University of North Carolina, N.C. State University, Raleigh, N.C., 1-128.

Skaggs, R.W. (1980). *DRAINMOD: Reference report - Methods for design and evaluation of drainage-water management systems for soils with high water tables*. U.S. Department of Agriculture – Soil Conservation Service, Fort Worth, TX.

Skaggs, R.W. (1982). "Field evaluation of a water management simulation model." *Trans. ASAE*, 25(3), 666-674.

Skaggs, R.W. (1999). *Drainage simulation models*. Agricultural drainage: Monograph No. 38, R. W. Skaggs and J. van Schilfgaarde, eds., American Society of Agronomy, Madison, Wisc., 469-500.

Smolek, A.P.*, Winston, R.J.*, Dorsey, J.D., and Hunt, W.F. (2015). *Modeling the hydrologic performance of bioretention and permeable pavement stormwater controls in northern Ohio using DRAINMOD: Calibration, validation, sensitivity analysis, and future climate scenarios*. Final report submitted to the University of New Hampshire and the Chagrin River Watershed Partners. In fulfilment of NOAA Award number NA09NOS4190153. *These authors contributed equally to this work. Available: http://crwp.org/files/DRAINMOD_OH_ModelingReport2015.pdf

Thornthwaite, C.W. (1948). "An approach toward a rational classification of climate." *Geog. Rev*., 38(1), 55-94.

United States Department of Agriculture (USDA) (1986). *Urban hydrology for small watersheds*. Technical Release 55 (TR-55). 2nd edition. Natural Resources Conservation Service, Conservation Engineering Division.

United States Department of Agriculture (USDA) (2004). *Estimation of direct runoff from storm rainfall*. Chapter 10, Part 630 Hydrology, National Engineering Handbook. Natural Resources Conservation Service.

United States Environmental Protection Agency (USEPA) (2009). *Technical guidance on implementing the stormwater runoff requirements for federal projects under Section 438 of the Energy Independence and Security Act*. Rep. No. EPA 841-B-09-001, Washington, D.C.

Wang, L., Lyons, J., Kanehl, P., and Bannerman, R. (2001). "Impacts of urbanization on stream habitat and fish across multiple spatial scales." *J. Environ. Plan. Manage*., 28(2), 255–266.

Wardynski, B.J., and Hunt III, W.F. (2012). "Are bioretention cells being installed per design standards in North Carolina? A field study." *J. Environ. Eng*., 138(12), 1210-1217.

Wilson, C.E., Hunt, W.F., Winston, R.J., and Smith, P. (2015). "Comparison of runoff quality and quantity from a commercial low-impact and conventional development in Raleigh, North Carolina." *J. Environ. Eng*., 141(2), 05014005.

Winston, R.J., Dorsey, J.D. and Hunt, W.F. (2015). *Monitoring the performance of bioretention and permeable pavement stormwater controls in Northern Ohio: Hydrology, water quality, and maintenance needs*. Final Report Submitted to the University of New Hampshire and the Chagrin River Watershed Partners. In Fulfilment of NOAA Award number NA09NOS4190153. Available: http://crwp.org/files/OH_StormwaterControls_MonitoringReport2015.pdf

Youssef, M.A., Skaggs, R.W., Chescheir, G.M., and Gilliam, J.W. (2005). "The nitrogen simulation model, DRAINMOD-N II." *Trans. ASAE,* 48(2), 611-626.

Zinger, Y., Blecken, G.T., Fletcher, T.D., Viklander, M., and Deletić, A. (2013). "Optimising nitrogen removal in existing stormwater biofilters: Benefits and tradeoffs of a retrofitted saturated zone." *Ecol. Eng*., 51, 75-82.

CHAPTER 4: **MODELING THE HYDROLOGIC PERFORMANCE OF BIORETENTION STORMWATER CONTROLS UNDER CLIMATE CHANGE SCENARIOS IN OHIO, USA**

4.1 Abstract

The impacts of climate change on urban water systems, especially green infrastructure, have been largely unexplored. Quantifying the effects of changing precipitation and temperature patterns on stormwater controls is critical to building resilience into urban drainage networks. Three bioretention hydrology data sets collected in Northeast Ohio were used to calibrate the continuous simulation model DRAINMOD. Precipitation and temperature data derived from dynamically downscaled climate predictions for the mid-21st century (2055-2059) under two climate scenarios (RCP 4.5 and RCP 8.5) were used to assess changes in the bioretention water balance (drainage, overflow, exfiltration, and evapotranspiration) compared to current climate conditions (2001-2004). Future climate scenarios suggested lower annual average rainfall depths, longer dry periods, and hotter temperatures for Northeast Ohio, leading to relatively modest changes to the overall water balance. Volume reduction provided by the bioretention cells was predicted to either increase by 4-6% or decrease by 5-9% under future climate. In all modeled cases, overflow and ET increased as a percentage of the water balance. To maintain current volumes of overflow in future climate scenarios, the bowl storage volume needed to be increased up to 51%. Results from this analysis suggest current bioretention designs may need modification to be resilient to climate change in this region; proper design, installation, and long-term maintenance are perhaps just as important in bioretention functionality as planning for

climate change. However, similar analyses should be conducted in other regions where predicted changes to precipitation patterns are more pronounced.

4.2 Introduction

Climate change has the potential to alter the frequency and severity of rainfall and droughts [Mailhot and Duchesne 2010; Trenberth 2011; Intergovernmental Panel on Climate Change (IPCC) 2012; Berggren et al. 2012]. Due to anthropogenic greenhouse gas emissions, mean global air temperature is predicted to increase (Wernstedt and Carlet 2014; Voskamp and Van de Ven 2015). Global and regional-scale models indicate this will cause extreme precipitation events to become more frequent and severe over many regions of the globe (Grum et al. 2006; Kharin et al. 2007; Fowler et al. 2007; May 2008; Gao et al. 2012, Kharin et al. 2013). For instance, the 10-yr design rainfall intensity in Belgium is projected to increase by about 50% by the end of this century (Willems 2013). However, standards for urban drainage design are based on statistical analysis of historical rainfall records which are assumed stationary (Rosenberg et al. 2010), and therefore do not include resilience needed for a changing climate (Mailhot and Duchesne 2010). Current levels of service provided by stormwater treatment systems will not be maintained under climate change unless additional infrastructure investments are made (Willems 2013; Mamo 2015). Changes in seasonal and annual precipitation will also impact nutrient and TSS loading pathways (Borris et al. 2014; Wu and Malmström 2015).

Decentralized water systems, including green infrastructure, increase drainage network resiliency and adaptability to a changing climate (Norton 2009; Grant et al. 2013). Voskamp and Van de Ven (2015) suggest measures promoting evapotranspiration (ET), peak discharge

attenuation, groundwater recharge, and seasonal water storage should be implemented within watersheds to synergistically reap multiple benefits. Stormwater control measures (SCMs), such as bioretention, have been shown to mitigate some of the stressors on streams and rivers present under a changing climate, such as the increased volume and rate of runoff (Semadeni-Davies et al. 2008; Zahmatkesh et al. 2014). Downspout disconnection, additional street detention storage, and increased depressional storage were three effective methods to combat increased peak discharge due to climate change (Waters et al. 2003).

Bioretention cells are planted media filters which promote ET, exfiltration (infiltration of stormwater into the underlying soil), and filtration (Hunt et al. 2012). They improve stormwater quality (Blecken et al. 2009; Luell et al. 2011) and mitigate impervious surface hydrology (Olszewski and Davis 2013; LeFevre et al. 2014; Chapter 2). Bioretention can delay and dampen peak flow rates (Li et al. 2009; Line and Hunt 2009) while reducing runoff volume from urban catchments. Long-term runoff reduction by bioretention cells varies greatly (13-100%) based on their design characteristics, the ability of the underlying soil to transmit water, and the climate (Li et al. 2009; Brown and Hunt 2011a; Brown and Hunt 2011b; Chapter 2). However, these benefits are not assured under augmented precipitation depth and intensity, and elongated dry periods predicted under climate change. Fine temporal and spatial resolution future climate data may be used as inputs to long-term, mechanistic models to predict bioretention performance under climate change scenarios (Lucas 2010; Brown et al. 2013; Hathaway et al. 2014). Examining the ability of individual SCMs, such as bioretention, to combat climate change effects on urban hydrology is critical to understanding resiliency of water resources infrastructure.

The analysis of single SCM performance under climate change scenarios has not been researched extensively (Sharma et al. 2011; Vanuytrecht et al. 2014). While one previous study has modeled bioretention hydrology under climate change in North Carolina (Hathaway et al. 2014), this study aims to build on this work by observing bioretention function: (1) constructed in low permeability soils, (2) in a cold climate, and (3) under two future climate scenarios. The purpose of this study was to couple dynamically downscaled future climate predictions with long-term, continuous simulation modeling to determine how future climate might impact bioretention hydrologic performance. Future climate data for the mid-twenty-first century were used to model bioretention performance in DRAINMOD. Simple retrofits or improvements to bioretention design will be suggested to improve bioretention cell resilience to climate change.

4.3 Materials and Methods

Site Descriptions

Three bioretention cells located in Kirtland and Pepper Pike, Ohio, USA, were intensively monitored to quantify the water balance (Figure 4.1). Characteristics of the three cells - Ursuline College (UC), Holden Arboretum South (HA South) and Holden Arboretum North (HA North) - are presented in Table 4.1 and described in detail in Chapter 2. All three bioretention cells employed internal water storage (IWS), a design feature created using an upturned elbow in the underdrain, promoting both denitrification and exfiltration (Brown and Hunt 2011b). A variety of IWS zone depths, media types, drawdown rates, surface storage depths, saturated hydraulic conductivities (K_{sat}), vegetation types, as well as catchment compositions characterized the three cells (Table 4.1). As discussed in Chapter 2, the

bioretention cells were oversized compared to the 19-mm water quality volume used for design in Ohio. Detailed analysis of the hydrologic performance of these bioretention cells was presented in Chapter 2.

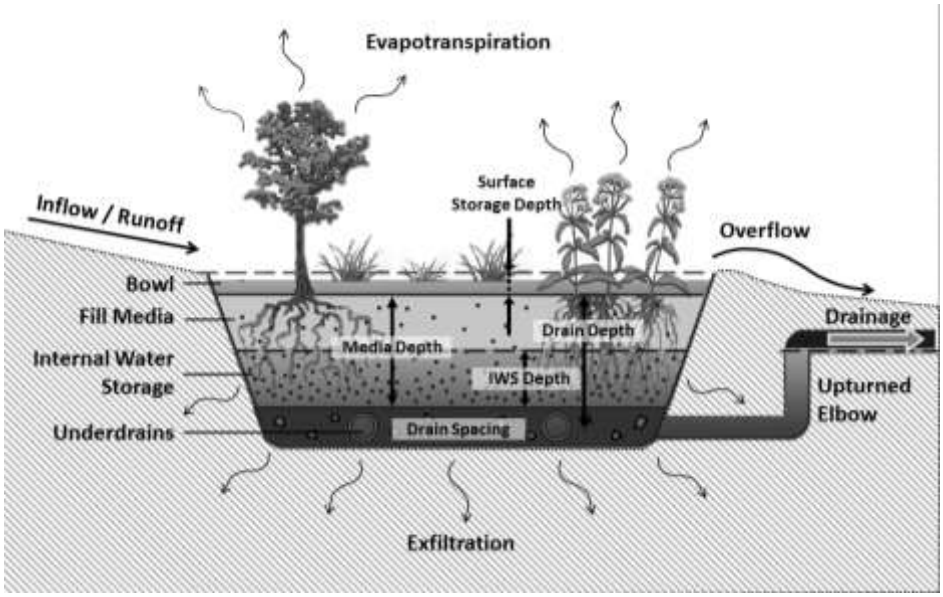

Figure 4-1. Bioretention cell cross-section with stormwater fates and system components identified. Modified from Brown et al. (2009).

Each bioretention cell was monitored to quantify the water balance on an event-by-event basis, including runoff (inflow), drainage (treated outflow), overflow (untreated bypass flow), exfiltration (volume eliminated), and ET (volume eliminated). Because runoff entered each bioretention cell in a diffuse manner that precluded direct measurement, runoff was estimated using the discrete curve number method offset by an antecedent moisture correction (USDA, 1986), as conducted by Pandit and Heck (2009). Similar methodologies have been employed in studies such as Brown and Hunt (2011a) and Brown and Hunt (2011b). Weirs and pressure transducers were utilized concurrently to measure drainage and

overflow. Overflow (bypass) was determined either using hydrograph separation (HA cells) or by modeling drainage in USEPA SWMM 5.1 (UC) (Chapter 2). The sum of exfiltration and ET (i.e., the drawdown rate) was measured using a pressure transducer housed inside a shallow monitoring well in each bioretention cell. A weather station was installed at each site to record ambient temperature and rainfall. For more information on monitoring methods, see Chapter 2.

DRAINMOD was used to simulate bioretention hydrologic performance. It was parameterized using as-built survey data and construction notes on the drainage area, bioretention cell surface area, average bowl storage depth, media depth, drain depth, and depth to drain outlet (for the IWS zones). Laboratory measurements of the media soil-water characteristic curves and soil saturated hydraulic conductivities were also used as inputs to the model (Table 4.1).

Table 4-1. Characteristics of the bioretention cells and their catchments.

Characteristics	UC	HA South	HA North
Location	Pepper Pike, OH	Kirtland, OH	Kirtland, OH
Fill media depth (m)	0.60	0.84	0.90
Fill media composition	87% sand, 4% silt, 9% clay	88% sand, 2% silt, 10% clay	88% sand, 2% silt, 10% clay
Bowl storage depth (m)	0.30	0.39	0.40
Catchment area (ha)	0.36	0.19	0.27
Catchment imperviousness (%)	77	58	58
Bioretention to catchment area ratio (%)	5.1	3.0	2.9
Drainage configuration	IWS	IWS	IWS
IWS zone depth (m)	0.60	0.38	0.45
Fill media K_{sat} (mm/hr)	168	102	102
Underlying Soil Type	Mahoning silt loam and fill	Pierpont silty clay loam	Platea silty clay loam
Drawdown Rate (mm/hr)	4.3	2.0	1.7
Vegetation	Forbs and perennial grasses	Forbs and perennial grasses	Shrubs and trees
Length of field monitoring (months)	7	14	14
Length of calibration (months)	3	5	5
Length of validation (months)	4	5	5

Description of DRAINMOD models and Modeling Methods

As described in Brown et al. (2013), the agricultural drainage model DRAINMOD was adapted to model bioretention hydrology. DRAINMOD uses the Hooghoudt and Kirkham equations to explicitly determine drainage when the water table is below and above the soil surface, respectively (Hooghoudt 1940; van Schilfgaarde 1957; Kirkham 1957). It is able to simulate an IWS zone, which is analogous to controlled drainage in agricultural fields. Drainage characteristics and soil attributes, such as K_{sat}, the soil water characteristic curve,

and exfiltration rate are input into DRAINMOD to simulate water movement through drained soil profiles and model changes in water content with water table depth.

The governing equations for DRAINMOD are based on water balances (1) in the soil profile and (2) at the soil surface. In the soil profile, the water balance is determined midway between the drains as:

$$\Delta V_a = D + ET + DS - F \quad (4\text{-}1)$$

where ΔV_a = change in the air volume, D = lateral drainage from the section, ET = evapotranspiration, DS = deep seepage, and F = infiltration entering the section in Δt (time increment). DRAINMOD uses the Green and Ampt method to calculate infiltration rate (Green and Ampt 1911). The water balance at the surface is computed using:

$$P = F + \Delta S + RO \quad (4\text{-}2)$$

where P = precipitation, F = infiltration, ΔS = change in depth of water stored on the surface, and RO = runoff during time period Δt. The Thornthwaite method (with monthly correction factors) was used to determine daily potential evapotranspiration (PET; Thornthwaite 1948). ET is calculated based on the soil water conditions. Detailed descriptions of DRAINMOD can be found in Skaggs (1980).

A separate DRAINMOD model was calibrated with and validated against the measured or estimated runoff, drainage, overflow, and exfiltration+ET from each bioretention cell. Since bioretention hydrologic performance is seasonal in nature (Emerson and Traver 2008; Muthanna et al. 2008), storm events occurring during even-numbered months (April, June, etc.) were used for model calibration. Data collected during odd-numbered months (May,

July, etc.) were extracted for model validation. Field monitoring methods were consistent over the calibration and validation periods.

Using DRAINMOD, the water balance [i.e. inflow (runoff), drainage, overflow, exfiltration (seepage), and ET] was quantified over the monitoring periods. Since the sum of exfiltration and ET were measured together (as drawdown rate), these DRAINMOD outputs were similarly lumped for comparison. DRAINMOD outputs were compared to field-collected data using Nash-Sutcliffe efficiencies and coefficients of determination (R^2). Nash-Sutcliffe efficiencies were calculated using:

$$NSE = 1 - \frac{\sum_{i=1}^{N}(Q_{i,measured} - Q_{i,predicted})^2}{\sum_{i=1}^{N}(Q_{i,measured} - Q_{average})^2} \quad (4\text{-}3)$$

where, $Q_{i,measured}$ = measured volume for event *i*, $Q_{i,predicted}$ = predicted volume for event *i*, $Q_{average}$ = average measured volume for N events, N = total number of events for the monitoring period, and NSE = Nash-Sutcliffe efficiency (Nash and Sutcliffe 1970). Tabulated NSE and R^2 values for the calibration and validation periods indicated the DRAINMOD models were well calibrated to the field observations (Table 4-2).

Table 4-2. Nash-Sutcliffe efficiency and coefficient of determination between measured and modeled data during calibration and validation periods.

Nash-Sutcliffe efficiency					
Site	**Period**	**Runoff**	**Drainage**	**Overflow**	**Exfiltration/ET**
UC	Calibration (June, August, October 2014)	0.99	0.94	0.97	0.95
	Validation (May, July, September 2014)	0.99	0.98	0.73	0.95
HA South	Calibration (October 2013, April, June, August, October 2014)	0.99	0.96	0.87	0.76
	Validation (November 2013, May, July, September, November 2014)	0.96	0.95	0.71	0.75
HA North	Calibration (October 2013, April, June, August, October 2014)	0.99	0.97	0.87	0.81
	Validation (November 2013, May, July, September, November 2014)	0.96	0.98	0.74	0.76
Coefficient of determination (R^2)					
Site	**Period**	**Runoff**	**Drainage**	**Overflow**	**Exfiltration/ET**
UC	Calibration (June, August, October 2014)	0.99	0.95	0.99	0.95
	Validation (May, July, September 2014)	1.00	0.99	0.89	0.96
HA South	Calibration (October 2013, April, June, August, October 2014)	0.99	0.96	1.00	0.80
	Validation (November 2013, May, July, September, November 2014)	0.97	0.96	1.00	0.76
HA North	Calibration (October 2013, April, June, August, October 2014)	0.99	0.97	0.94	0.82
	Validation (November 2013, May, July, September, November 2014)	0.97	0.98	0.96	0.77

Current and Future Climatic Data

Site specific climate change predictions were gleaned from Gao et al. (2012), who generated high resolution projected future climate data for the eastern United States. A 4 km

by 4 km spatial resolution was modeled in the Community Earth System Model version 1.0 (CESM v1.0), which established boundary conditions for the Weather Research and Forecasting (WRF) model used for dynamic downscaling. Surface and three-dimensional variables needed for dynamic downscaling were extracted from Community Atmosphere Component Version 4 (CAM4) and Community Land Model (CLM4) output from CESM v1.0 [discussed in detail in Gao et al. (2012)]. Horizontal interpolation of surface variables from CESM v1.0 output to the WRF domains was performed in the WRF pre-processing system. Dynamic downscaling provided high spatial resolution, allowing analysis of changes in precipitation and temperature at two different locations (UC and HA) within the Chagrin River Watershed.

Three modeled climate scenarios were utilized, one (current) base and two future climate data sets, each containing 4 or 5 years of data. These scenarios were derived as the average of nine grid cells within the climate model (i.e., the cell containing the site and the eight surrounding it) to provide representative data. The base model was created for 2001-2004 climate data. To ensure the downscaled data were reasonable, modeled precipitation from 2001-2004 was compared against measured data from Cleveland Hopkins International Airport (CHIA; NOAA 2015), similar to the approach taken in Gao et al. (2012). This location, approximately 60 and 39 km from HA and UC, respectively, was the nearest, long-term, reliable precipitation data set to both sites. The distance from the monitoring sites to CHIA adds some level of uncertainty to this analysis. The modeled average annual rainfall for 2001-2004 was 1005 mm (range 854-1272 mm) at Ursuline and 1009 mm (range 885-1117 mm) at Holden. During the same time period, CHIA experienced on average

970 mm (range 874-1080 mm) of rainfall per year (NOAA 2015). Over the 30-yr period from 1981-2010, CHIA received an annual average of 994 mm of precipitation (NOAA 2015), very similar to the modeled base scenarios during 2001-2004. The modeled precipitation and dry period data had comparable median and 90th percentile rainfall depth, respectively, to those measured at CHIA.

Modeled and measured 2001-2004 precipitation data were further analyzed by separating individual rainfall events, defined as greater than 2.5-mm depth with an antecedent dry period greater than 6 hours. UC and HA data were compared against measured CHIA data on a seasonal basis to determine any bias present in the model (Table 4-3). Bias was defined as:

$$Bias = \frac{(RF_{Mod,i} - RF_{Meas,i})}{RF_{Meas,i}} \times 100 \quad (4\text{-}4)$$

where RF_{Mod} is modeled rainfall depth (mm), RF_{Meas} is measured rainfall depth at CHIA (mm), and i is the season of interest. While bias during any given season was up to 114%, the model was, on average, quite effective at predicting precipitation patterns at UC and HA during the fall, winter, and spring seasons. During the summer, the model over-predicted rainfall by approximately 25% on average, with particularly high error during 2004. Substantial seasonal bias has been observed in other regional climate models (Jacob et al. 2007). Overall bias over the 4-yr period was 1.6% at UC and 2.2% at HA.

Table 4-3. Seasonal bias (%) in modeled data for UC and HA.

Site & year	Percent bias			
	Dec.-Jan.-Feb.	Mar.-Apr.-May	Jun.-Jul.-Aug.	Sep.-Oct.-Nov.
Ursuline 2001	16.8	46.4	20.7	-29.0
Ursuline 2002	26.2	-21.4	3.1	-19.5
Ursuline 2003	-32.4	-20.5	-42.4	-8.3
Ursuline 2004	44.8	1.2	114.0	29.0
Average	**13.8**	**1.4**	**23.9**	**-7.0**
Holden 2001	10.8	53.1	35.3	-28.4
Holden 2002	39.7	-25.1	13.4	-27.9
Holden 2003	-39.3	-14.1	-14.3	7.1
Holden 2004	43.9	-9.2	59.6	36.5
Average	**13.8**	**1.2**	**23.5**	**-3.2**

For future climate scenarios, data from the IPCC Representative Concentration Pathways (RCP) were the basis of this study. Bioretention performance was analyzed under two greenhouse gas scenarios, one where emissions moderate by 2100 (RCP 4.5) and another where emissions continue to rise on the current trajectory (RCP 8.5). Modeled precipitation and temperature data from 2055 to 2059 (5 years) were used for both climate change scenarios. Uncertainty is quite high for projections of climate under varying future greenhouse gas emissions (Berggren 2012; Wernstedt and Carlet 2014); therefore conclusions were constrained to differences between the base and each future climate scenario. Comparisons between results from RCP 4.5 and RCP 8.5 were not made, but the different scenarios were important in establishing the range of possibilities for impacts of climate change on bioretention.

Modeling Current and Future Climate Scenarios

Calibrated and validated DRAINMOD models described in Chapter 3 were utilized as the basis of this study. Hourly precipitation and daily temperature data derived from the dynamically downscaled climate model over a 4- or 5-yr period were used as inputs to DRAINMOD in all climate scenarios. Outputs from DRAINMOD were analyzed on a daily basis. Given the flashiness of the small urban watersheds modeled (Table 4-1), an hourly time step for the inputs might limit model accuracy, especially for prediction of overflow. However, DRAINMOD models total overflow volume (rather than overflow rate); given the finite bowl storage volume and consistent K_{sat} of the media, the volume of overflow is likely predicted adequately. As downscaling techniques develop, climate data with finer temporal resolution will allow engineers and scientists to better interpret expected impacts of climate change, in this case related to overflow (Willems et al. 2012).

4.4 Results and Discussion

Summary of Climatic Data

To frame the hydrologic modeling, temperature and rainfall data were summarized for the UC and HA sites under both current (2001-2004, base) and mid-century (2055-2059, RCP4.5 and RCP8.5) scenarios (Table 4-4). Average annual precipitation was greatest in the current climate (2001-2004) data, and mean and median event depth tended to decrease under RCP 4.5 and RCP 8.5. At HA, extreme rainfall event (represented by the 90^{th} percentile and maximum) depth, tended to moderate in the future; however, extreme precipitation intensity increased for RCP 4.5. At UC, maximum rainfall depths increased in both future climate scenarios and extreme precipitation intensity increased under RCP 8.5; these differences in

extreme rainfall illustrate how spatially-varied future climate predictions are, as the two sites were located only 25 km apart. Rainfall is highly spatially variable even under current climate conditions, especially in areas affected by lake-effect precipitation, such as northern Ohio (Laird et al. 2009).

A dry period, or the number of days without a qualifying rainfall event, also tended to increase in future climate scenarios for measures of central tendency and extreme cases at UC and HA. Longer dry periods and moderating rainfall depths are consistent with some future climate data presented for this region (Gao et al. 2012; Giorgi et al. 1994). However, due to the variability inherent in future climate projections, future work should evaluate multiple data sets from differing regional climate models and downscaling techniques. Mean and median daily temperatures were predicted to increase by 2-3˚C for this region, and maximum and minimum average daily temperatures were exacerbated under future climate scenarios, warming by 2-6˚C. In combination with decreased annual precipitation depths, these data suggest a hotter, drier, and more drought-prone climate for Northeast Ohio.

Table 4-4. Precipitation and temperature summary statistics for UC and HA under all climate scenarios.

Parameter	Statistic	UC			HA		
		Base	RCP 4.5	RCP 8.5	Base	RCP 4.5	RCP 8.5
Dry Period (Days)	Maximum	35.7	43.3	31.8	36.3	51.3	39.8
	90th percentile	9.5	11.3	11.4	10.0	11.6	11.9
	Mean	4.4	5.0	5.1	4.8	5.1	5.2
	Median	3.4	3.3	3.4	3.3	3.4	3.4
	St. Dev	4.3	5.3	4.9	5.3	5.7	5.6
Precipitation Depth	Annual average rainfall (mm)	961	844	930	964	804	823
	Max (mm)	80	91	135	105	95	101
	90th percentile (mm)	35	31	36	35	28	29
	Mean (mm)	14	14	15	15	14	14
	Median (mm)	10	9	8	10	9	9
	St. Dev. (mm)	13	15	17	15	14	15
Precipitation Intensity	Max (mm/hr)	43.8	43.7	57.0	53.0	61.7	43.3
	90th percentile (mm/hr)	5.8	6.0	6.3	5.6	5.8	5.6
	Mean (mm/hr)	2.6	2.5	2.7	2.8	2.5	2.6
	Median (mm/hr)	1.2	1.2	1.2	1.1	1.1	1.1
	St. Dev. (mm/hr)	4.3	4.1	4.6	5.8	5.2	4.7
Temperature	Mean (˚C)	12.2	14.0	14.6	11.0	12.8	13.4
	Median (˚C)	13.2	15.1	16.0	12.1	14.0	14.8
	St. Dev (˚C)	10.9	11.0	11.6	10.6	10.7	11.3
	Maximum daily average (˚C)	32.9	34.1	36.6	30.1	32.1	34.2
	Minimum daily average (˚C)	-19.7	-21.9	-17.7	-24.8	-23.7	-18.8

Hydrologic Balance under Climate Change Scenarios

Calibrated DRAINMOD models for UC, HA South, and HA North were utilized in the modeled climate change scenarios without modification, similar to methods in

Hathaway et al. (2014). Current, RCP 4.5, and RCP 8.5 rainfall and temperature data were input into DRAINMOD, contributing runoff files created, and the bioretention models simulated. Summary statistics of the results are presented in Table 4-5. The percent difference in depth (i.e., the quotient of stormwater volume to bioretention surface area) for each portion of the overall water balance was calculated as:

$$\%\ diff._{depth} = \frac{Depth_{RCP} - Depth_{Base}}{Depth_{Base}} * 100 \quad (4\text{-}5)$$

where $Depth_{RCP}$ (cm) and $Depth_{Base}$ (cm) are the depths of a particular portion of the water balance under a climate change projection and current climate, respectively. Differences in the water balance among the base and future climate scenarios were calculated as (with the given example for drainage):

$$\%\ diff._{water\ balance} = \%Drain_{RCP} - \%Drain_{Base} \quad (4\text{-}6)$$

where $Drain_{RCP}$ and $Drain_{Base}$ are the percentage of the water balance represented by drainage under a climate change projection and current climate, respectively.

Because of predicted decreases in future annual rainfall totals, the runoff entering the HA bioretention cells was less under the future climate scenarios than under the current climate. While average and extreme event rainfall depth tended to decrease under future climate scenarios at HA (Table 4-4), overflow depth increased in one future climate scenario and its percentage of the water balance increased by 1-3% under RCP 4.5 and RCP 8.5. This is related to either (1) the increase in antecedent dry period under RCP 8.5, creating shorter duration, higher average intensity rain events under future climate conditions (Table 4-4), or (2) moderating future annual rainfall. Drainage depth was 28-33% less in future climate scenarios, representing 5-8% less of the overall water balance. Exfiltration depth was

15-18% less under future climate scenarios, but modestly increased (by 1-2%) as a fraction of the overall water balance due to the aforementioned decrease in runoff entering the bioretention cells under future climate scenarios. Due to the warmer air temperatures and longer dry periods, coupled with low exfiltration rates that result in long-term storage of water in the IWS zone, depth of ET increased by 16-23% under future climate, resulting in a 2-3% increase in ET as a fraction of the overall water balance. For the HA bioretention cells, the percentage of runoff volume abstracted (i.e., the sum of exfiltration and ET) increased by 4-5%; however, increases in untreated overflow (1-3%) were also observed. The HA cells were expected to have improved volume reduction under future climate, but the depth of overflow was predicted to increase by up to 24%.

Because of divergent rainfall patterns at UC (Table 4-4), DRAINMOD predicted a modest decrease (RCP 4.5) or slight increase (RCP 8.5) in surface runoff. This factor combined with higher average and extreme rainfall depths under future climate scenarios resulted in a 2-6% greater drainage fraction of the water balance under future climate. Drainage depth was either unchanged (RCP 4.5) or increased by 30% (RCP 8.5) from the base scenario. Overflow depth increased by 23-66% under future climate scenarios, representing a 1-2% increase in the overall water balance under RCP 4.5 and 8.5, respectively. Exfiltration depth decreased by 11-18% from the base, representing 5-9% of the water balance; this decrease was partially offset by increases in ET, 1 and 2% of the water balance and 12-19% in depth. Overall, volume reduction as a percentage of inflow was 73% under the base climate scenario; this decreased to 68% and 64% under

RCP 4.5 and 8.5, respectively. Thus, the UC bioretention cell is expected to produce more drainage and overflow under future climate conditions.

Taken together, the future climate modeling suggests volume mitigation provided by bioretention SCMs in Northeast Ohio is mixed; HA improves slightly (by 4-5%) while UC declines (by 5-9%). Spatially disparate rainfall and temperature data under future climate scenarios caused this, and suggest the need for additional spatial and temporal resolution to effectively model small catchment hydrology. Overflow as a percentage of total inflow to the bioretention cells increased by 1-3% under all future climate scenarios. ET increased in all modeled future climate scenarios due to elevated temperatures, elongated dry periods, and available water stored in the IWS zones.

Table 4-5. Annual average water balances for each site and climate profile. Depths are in terms of cm per bioretention surface area.

Site	Climate Scenario	Runoff	Drainage				Overflow				Exfiltration				Evapotranspiration			
		Depth (cm)	Depth (cm)	% Diff.[1] Depth	% of Runoff	% Diff. WB[2]	Depth (cm)	% Diff. Depth	% of Runoff	% Diff. WB	Depth (cm)	% Diff. Depth	% of Runoff	% Diff. WB	Depth (cm)	% Diff. Depth	% of Runoff	% Diff. WB
UC	Base	1395	328	-	23	-	50	-	4	-	928	-	67	-	81	-	6	-
	RCP 4.5	1238	321	-2	26	2	61	23	5	1	758	-18	61	-5	91	12	7	2
	RCP 8.5	1439	429	31	30	6	82	66	6	2	825	-11	57	-9	96	19	7	1
HA South	Base	1368	706	-	52	-	72	-	5	-	517	-	38	-	69	-	5	-
	RCP 4.5	1070	470	-33	44	-8	90	24	8	3	424	-18	40	2	86	23	8	3
	RCP 8.5	1099	510	-28	46	-5	72	0	7	1	429	-17	39	1	84	22	8	3
HA North	Base	1366	745	-	55	-	84	-	6	-	467	-	34	-	67	-	5	-
	RCP 4.5	1070	499	-33	47	-8	98	17	9	3	391	-16	37	2	82	22	8	3
	RCP 8.5	1099	540	-28	49	-5	84	0	8	1	395	-15	36	2	77	16	7	2

[1]% diff. = % difference
[2]% diff. WB = % difference water balance

Analysis of Overflow Events

Because overflow represents the fraction of runoff that bypasses treatment in the bioretention media, the increase in overflow depth (up to 66%) under future climate scenarios is of particular interest. Daily overflow events were extracted and summary statistics for them computed (Table 4-6). The average annual overflow depth either did not change (2 cases) or increased (4 cases) under climate change. The 90th percentile and maximum overflow event depths increased in all but one case, indicating extreme overflow events are more likely under climate change. The two sites illustrated overflow predictions: (1) the frequency of overflow increased but the distribution of overflow depths remained similar (UC) or (2) the number of overflow events decreased but the magnitude of overflow was higher (HA, Figure 4-2); bioretention under future climate projections in North Carolina always exhibited an increase in the number of overflow days (Hathaway et al. 2014).

While 90th percentile and maximum rainfall depths at HA were less than those of the base (Table 4-4), overflow depths under RCP 4.5 far exceeded those of the base model. Back-to-back storm events, where the bowl storage was not able to dewater sufficiently fast to create storage for a follow-on storm, and increases in rainfall intensity were responsible for these effects (Table 4-4). Five of the overflow events for RCP 4.5 at HA were larger in magnitude than the maximum overflow depth under the base scenario. Average and extreme event overflow depths for RCP 8.5 at HA were greater than those of the base model but annual average overflow occurrences modestly decreased from 13 to 12 and 16 to 14 for HA South and North, respectively. Comparing HA to UC suggested (1) future climate scenarios may produce disparate results with respect to overflow even over a small spatial scale (the two

sites were 25 km apart) and (2) overflow will become more frequent and/or greater in magnitude under these climate change scenarios. These results are interesting because an increase in total rainfall depth was not observed under future climate projections; it appears rainfall depth is not as critical to bioretention resiliency as the distribution of the rainfall.

An analysis of bioretention design alternatives in Chapter 3 indicated controlling factors for bioretention hydrologic performance were underlying soil hydraulic conductivity, loading ratio (i.e., catchment area to bioretention surface area ratio), and bowl storage depth. While underlying soil and loading ratio are static and cannot be easily manipulated after bioretention installation, but storage may be increased. Thus, additional modeling was conducted in DRAINMOD to match the total overflow depths in the base to those under climate change scenarios by increasing the bowl storage depth of the bioretention cell. Under RCP 8.5 at both HA cells, the average annual overflow was already the same (Table 4-5), and so no increase in bioretention cell size would be needed under future climate. For the other 4 bioretention-climate scenario pairs, bowl storage volume would need to be increased 18-51% (5- to 17-cm depth) to restrict overflow depths to those of the base. In comparison, Hathaway et al. (2014) found bioretention cells in North Carolina would need an additional 9- to 31-cm bowl storage depth to observe no net increase in overflow.

Simple retrofits to a bioretention cell, such as increasing the overflow invert elevation, removing some media, or a combination, could be made to increase bowl storage depth and limit overflow. If space were available, the surface area of the bioretention cell could also be increased to achieve the same goal. For newly-constructed bioretention cells, bowl storage

volume would need to be increased by up to 50% to ensure resilience to climate change in this region.

Long-term maintenance is also a critical piece to the resilience of bioretention, since an influx of sediment from the catchment or over-mulching can reduce bowl storage depth (Asleson et al. 2009). Proper construction of these systems is also critical, since over half of bioretention cells surveyed in North Carolina were moderately or severely undersized with respect to their design storage volume (Wardynski et al. 2012). Resilience to climate change cannot be assured without proper bioretention design, construction, and long-term maintenance.

Table 4-6. Statistics for overflow from the three bioretention cells under current and future climate.

Site	Climate Projection	Days with Inflow	Days with Overflow	Overflow depth					
				Mean (cm)	Median (cm)	Standard deviation (cm)	90th percentile (cm)	Maximum (cm)	Average Yearly (cm)
UC	Base	588	9	22	24	23	42	75	50
	RCP 4.5	561	10	23	16	21	49	72	61
	RCP 8.5	543	12	27	22	26	69	80	82
HA South	Base	554	13	22	24	18	47	58	72
	RCP 4.5	541	6	64	78	46	101	130	90
	RCP 8.5	515	12	24	17	22	51	73	72
HA North	Base	554	16	21	22	20	45	65	84
	RCP 4.5	541	10	41	8	49	87	135	98
	RCP 8.5	515	14	26	22	23	54	77	84

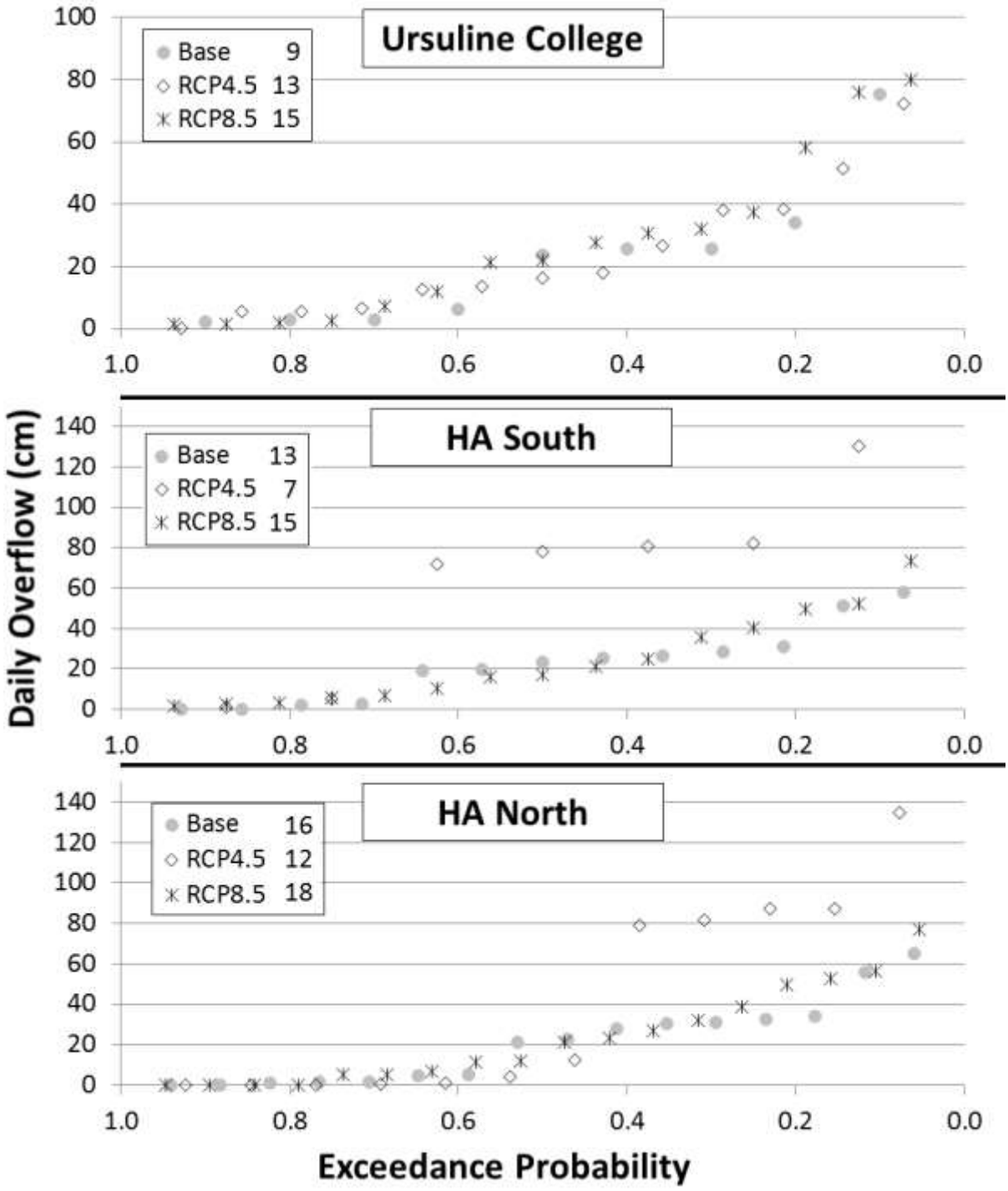

Figure 4-2. Exceedance probability plots for daily overflow depth for UC (top), HA South (middle), and HA North (bottom). The number of overflow events is also presented in each respective legend.

Analysis of Dry Days

Potential impacts of climate change include a warming trend for atmospheric temperature and increases in the frequency and depth of extreme precipitation (IPCC 2012). Through crop, drainage, and ET inputs, DRAINMOD simulates and tabulates in its outputs the number of dry days, defined as the days where soil moisture in the rooting zone is insufficient to meet PET demand. As described in Chapter 3, DRAINMOD simulations incorporated 30 cm rooting depths, since both the UC and HA bioretention cells were less than 1.5 years old during the monitoring periods.

In most cases, annual average dry days increased under future climate scenarios, in some cases by more than two-fold (Table 4-7). In planted SCMs such as bioretention, this may result in drought stress to plants and soil microbes (Flexas et al. 2006). Consecutive dry days statistics (Table 4-4) showed prolonged mean and 90th percentile dry periods for this region of Ohio under predicted mid-21st century climate. DRAINMOD was used to simulate a 60-cm rooting depth, representing a bioretention cell with a more established, extensive root system (Bratieres et al. 2008). In all cases, simulating a more developed root zone (versus 30-cm in establishing cells) resulted in vast decreases in dry days, in some cases eliminating them entirely over the 4- to 5-yr simulation periods. Bioretention cells containing plants with developed root systems may provide resilience to climate change, especially when an IWS zone is incorporated, providing a reservoir of water to buffer against long dry periods (Blecken et al. 2009). Thus, vegetation with deeper rooting depths and more developed root zones could be specified for bioretention cells. Somewhat surprisingly, DRAINMOD simulations showed the presence or absence of an IWS zone made only minor differences in

annual average dry days under a 30-cm rooting depth, and did not affect results under 60-cm rooting depth. More research is needed on the impacts of climate change on soil moisture, as extended droughts can have profound impacts on plants and soil biota.

Table 4-7. Annual average dry days predicted by DRAINMOD under varying rooting depths.

Site	Climate Projection	30 cm rooting depth	60 cm rooting depth
UC	Base	3	0
	RCP 4.5	7	0
	RCP 8.5	10	0
HA South	Base	10	1
	RCP 4.5	5	0
	RCP 8.5	13	0
HA North	Base	17	5
	RCP 4.5	12	1
	RCP 8.5	25	3

4.5 Summary and Conclusions

DRAINMOD models were calibrated using three bioretention hydrology data sets collected in Northeast Ohio. Rainfall and temperature data derived from dynamically downscaled future climate data were used to represent both existing (2001-2004) and future (2055-2059) climate scenarios for Northern Ohio. DRAINMOD models were simulated with these data to quantify changes to the overall bioretention water balance (runoff, drainage, overflow, exfiltration, and ET). The following conclusions were drawn:

1. The climate model predicted elongated dry periods under future climate scenarios for this region. Average annual rainfall decreased by 3-17% under future climate, with moderated mean and median rainfall depths. However, the largest rainfall events were either similar to current climate or up to 50% greater depth. Mean and median daily air temperatures increased by 2-3˚C in the mid-21st century climate. Generally, future climate scenarios suggested lower annual average rainfall depths, longer dry periods, and hotter temperatures for Northeast Ohio.

2. Due to decreases in annual average rainfall, runoff entering each bioretention cell moderated or did not appreciably change under predicted climate conditions. Results indicate the bioretention water balance was little changed under RCP 4.5 and RCP 8.5, with at most 10% difference in any portion of the water balance. Due to warmer temperatures and longer dry periods, ET depth increased by 12-23%, representing an increase of 1-3% with respect to the overall water balance. Because of larger and in some cases more intense extreme rainfall events, overflow increased by 1-3% of the overall water balance and increased in depth by 0-66%.

3. Volume reduction under predicted climates was variable, with the UC cell mitigating 5-9% less runoff under future climate scenarios. The HA cells reduced 4-6% more volume under future climate, mostly related to the approximately 20% decrease in runoff volume under future climate. Climate change impacts appear very divergent even over small spatial scales.

4. Evapotranspiration and overflow will represent a greater fraction of the bioretention water balance under projected future climate. Analysis of overflow events indicated bowl

storage volume would need to be increased by up to 51% to keep future climate overflow depth at current levels. Overall, existing bioretention designs may need only minor modifications to be resilient to climate change along the Northeast Ohio Lake Erie shoreline. Proper design, installation, and long-term maintenance are critical to assuring the resilience of bioretention to climate change.

5. Two RCPs from one global climate model using a single downscaling technique and at a fine time scale (hourly) were used in this analysis. While the modeled bioretention cells were located 25-km apart in the eastern suburbs of Cleveland, Ohio, substantial differences in future climate were predicted, suggesting high spatial variability. Given the uncertainty in climate modeling and predictions of future fossil fuel use, these analyses are considered representative of this portion of Northeast Ohio, not of the exact project locations. This study was specific to a region of Ohio where climate change is predicted to have limited impacts – thus the magnitude of the changes in bioretention hydrology presented herein could be vastly different in regions where climate change is projected to have a greater impact on precipitation. Despite these uncertainties, efforts to quantify the impacts of climate change on bioretention cell (and other SCM) performance are needed so resilience can be incorporated into designs.

4.6 References

Asleson, B.C., Nestingen, R.S., Gulliver, J.S., Hozalski, R.M., and Nieber, J. L. (2009). "Performance Assessment of Rain Gardens." *J. Am. Water Resour. Assoc*., 45(4), 1019-1031.

Berggren, K., Olofsson, M., Viklander, M., Svensson, G., and Gustafsson, A.M. (2012). "Hydraulic impacts on urban drainage systems due to changes in rainfall caused by climatic change." *J. Hydrol. Eng*., 17(1), 92-98.

Blecken, G.T., Zinger, Y., Deletić, A., Fletcher, T.D., and Viklander, M. (2009). "Impact of a submerged zone and a carbon source on heavy metal removal in stormwater biofilters." *Ecol. Eng.*, 35(5), 769-778.

Borris, M., Viklander, M., Gustafsson, A.M., and Marsalek, J. (2014). "Modelling the effects of changes in rainfall event characteristics on TSS loads in urban runoff." *Hydrol. Proc.*, 28(4), 1787-1796.

Bratieres, K., Fletcher, T.D., Deletic, A., and Zinger, Y. (2008). "Nutrient and sediment removal by stormwater biofilters: A large-scale design optimisation study." *Water Res*., 42(14), 3930-3940.

Brown, R.A, Hunt, W.F., and Kennedy, S.G. (2009). *Designing bioretention with an internal water storage (IWS) layer: design guidance for an innovative bioretention feature*. Urban Waterways Factsheet, North Carolina Cooperative Extension, Raleigh, N.C.

Brown, R.A., and Hunt, W.F. (2011a.) "Impacts of media depth on effluent water quality and hydrologic performance of undersized bioretention cells." *J. Irrig. Drain. Eng*., 137(3), 132-143.

Brown, R.A., and Hunt, W.F. (2011b). "Underdrain configuration to enhance bioretention exfiltration to reduce pollutant loads." *J. Environ. Eng*., 137(11), 1082-1091.

Brown, R.A., R.W. Skaggs, and Hunt, W.F. (2013). "Calibration and validation of DRAINMOD to model bioretention hydrology." *J. Hydrol*., 486, 430-442.

Emerson, C.H., and Traver, R.G. (2008). "Multiyear and seasonal variation of infiltration from storm-water best management practices." *J. Irrig. Drain. Eng*., 134(5), 598-605.

Flexas, J., Bota, J., Galmés, J., Medrano, H., and Ribas-Carbó, M. (2006). "Keeping a positive carbon balance under adverse conditions: responses of photosynthesis and respiration to water stress." *Physiol. Plant*., 127, 343–352.

Fowler, H.J., Ekström, M., Blenkinsop, S., and Smith, A.P. (2007). "Estimating change in extreme European precipitation using a multimodel ensemble." *J. Geophys. Res.: Atmos.*, 112(D18).

Gao, Y., Fu, J.S., Drake, J.B., Liu, Y., and Lamarque, J.F. (2012). "Projected changes of extreme weather events in the eastern United States based on a high resolution climate modeling system." *Environ. Res. Let*., 7(4), 044025.

Giorgi, F., Shields Brodeur, C., and Bates, G.T. (1994). "Regional climate change scenarios over the United States produced with a nested regional climate model." *J. Climate*, 7(3), 375-399.

Grant, S.B., Fletcher, T.D., Feldman, D., Saphores, J.D., and Cook, P.L., Stewardson, M., Low, K., Burry, K., Hamilton, A. J. (2013). "Adapting urban water systems to a changing climate: lessons from the millennium drought in Southeast Australia." *Environ. Sci. Technol*., 47(19), 10727-10734.

Green, W.H., and Ampt, G.A. (1911). "Studies on soil physics. I. The flow of air and water through soil." *J. Agric. Sci*., 4(01), 1–24.

Grum, M., Jorgensen, A., Johansen, R., and Linde, J. (2006). "The effect of climate change on urban drainage: an evaluation based on regional climate model simulations." *Water Sci. Technol*., 54(6-7), 9-15.

Hathaway, J.M., Brown, R.A., Fu, J.S., and Hunt, W.F. (2014). "Bioretention function under climate change scenarios in North Carolina, USA." *J. Hydrol.*, 519, 503-511.

Hooghoudt, S.B. (1940). "General consideration of the problem of field drainage by parallel drains, ditches, watercourses, and channels." Publ. No.7 in the series: *Contribution to the knowledge of some physical parameters of the soil* (titles translated from Dutch). Bodemkundig Instituut, Groningen, The Netherlands.

Hunt, W.F., Davis, A.P., and Traver, R.G. (2012). "Meeting hydrologic and water quality goals through targeted bioretention design." *J. Environ. Eng*., 138(6), 698-707.

Intergovernmental Panel on Climate Change (IPCC). (2012). "Summary for policymakers." In: Field, C.B., Barros V., Stocker T.F., Qin D., Dokken D.J., Ebi K.L., Mastrandrea M.D., Mach K.J., Plattner G.K., Allen S.K., Tignor M., Midgley P.M. (Eds.), *Managing the Risks of Extreme Events and Disasters to Advance Climate Change Adaptation. A Special Report of Working Groups I and II of the Intergovernmental Panel on Climate Change.* Cambridge University Press, Cambridge, UK, and New York, NY, USA, pp. 1–19.

Jacob, D., Bärring, L., Christensen, O.B., Christensen, J.H., de Castro, M., Deque, M., Giorgi, F., Hagemann, S., Hirschi, M., Jones, R., Kjellström, E., Lenderink, G., Rockel, B., Sánchez, E., Schär, C., Seneviratne, S., Somot, S., van Ulden, A., and van den Hurk, B. (2007). "An inter-comparison of regional climate models for Europe: model performance in present-day climate." *Clim. Change*, 81(1), 31-52.

Kharin, V.V., Zwiers, F.W., Zhang, X., and Hegerl, G.C. (2007). "Changes in temperature and precipitation extremes in the IPCC ensemble of global coupled model simulations." *J. Clim*., 20(8), 1419-1444.

Kharin, V.V., Zwiers, F.W., Zhang, X., and Wehner, M. (2013). "Changes in temperature and precipitation extremes in the CMIP5 ensemble." *Clim. Change*., 119(2), 345-357.

Kirkham, D. (1957). "Theory of land drainage." *Drainage of Agricultural Lands: Agronomy Monograph* No. 7, J. N. Luthin, ed., American Society of Agronomy, Madison, Wisc., 139-181.

Laird, N. F., Desrochers, J., and Payer, M. (2009). "Climatology of lake-effect precipitation events over Lake Champlain." *J. Appl. Meteorol. Climatol.*, 48(2), 232-250.

LeFevre, G.H., Paus, K.H., Natarajan, P., Gulliver, J.S., Novak, P.J., and Hozalski, R.M. (2014). "Review of dissolved pollutants in urban storm water and their removal and fate in bioretention cells." *J. Environ. Eng*., 141(1), 04014050.

Li, H., Sharkey, L.J., Hunt, W.F., and Davis, A.P. (2009). "Mitigation of impervious surface hydrology using bioretention in North Carolina and Maryland." *J. Hydrol. Eng*., 14(4), 407-415.

Line, D.E., and Hunt, W.F. (2009). "Performance of a bioretention area and a level spreader-grass filter strip at two highway sites in North Carolina." *J. Irrig. Drain. Eng*., 135(2), 217-224.

Lucas, W.C. (2010). "Design of integrated biofiltration-detention urban retrofits with design storm and continuous simulation methods." *J. Hydrol. Eng*., 15(6), 486-498.

Luell, S.K., Hunt, W.F., and Winston, R.J. (2011). "Evaluation of undersized bioretention stormwater control measures for treatment of highway bridge deck runoff." *Water Sci. Technol*., 64(4), 974-979.

Mailhot, A., and Duchesne, S. (2010). "Design criteria of urban drainage infrastructures under climate change." *J. Water Res. Plan. Man*., 136(2), 201-208.

Mamo, T.G. (2015). "Evaluation of the Potential Impact of Rainfall Intensity Variation due to Climate Change on Existing Drainage Infrastructure." *J. Irrig. Drain. Eng*., 141(10), 05015002.

May, W. (2008). "Potential future changes in the characteristics of daily precipitation in Europe simulated by the HIRHAM regional climate model." *Cli. Dyn*., 30(6), 581-603.

Muthanna, T.M., Viklander, M., and Thorolfsson, S.T. (2008). "Seasonal climatic effects on the hydrology of a rain garden." *Hydrol. Processes*., 22(11), 1640-1649.

Nash, J.E., and Sutcliffe, J.V. (1970). "River flow forecasting through conceptual models part 1 – A discussion of principles." *J. Hydrol*., 10(3), 282-290.

National Oceanic and Atmospheric Administration (NOAA), 2015. National climatic data center, U.S. local climatological data. Cleveland, OH airport. Available: http://www.ncdc.noaa.gov/

Norton, J.W. (2009). "Decentralized systems." *Water Environ. Res*., 81(10), 1440-1450.

Olszewski, J.M., and Davis, A.P. (2013). "Comparing the hydrologic performance of a bioretention cell with predevelopment values." *J. Irrig. Drain. Eng*., 139(2), 124-130.

Pandit, A., and Heck, H.H. (2009). "Estimations of soil conservation service curve numbers for concrete and asphalt." *J. Hydrol. Eng*., 14(4), 335-345.

Rosenberg, E.A., Keys, P.W., Booth, D B., Hartley, D., Burkey, J., Steinemann, A. C., and Lettenmaier, D.P. (2010). "Precipitation extremes and the impacts of climate change on stormwater infrastructure in Washington State." *Clim. Change*., 102(1-2), 319-349.

Semadeni-Davies, A., Hernebring, C., Svensson, G., and Gustafsson, L.G. (2008). "The impacts of climate change and urbanisation on drainage in Helsingborg, Sweden: Suburban stormwater." *J. Hydrol*., 350(1), 114-125.

Sharma, A.K., Vezzaro, L., Birch, H., Arnbjerg-Nielsen, K., and Mikkelsen, P.S. (2011). "Effect of climate change on stormwater characteristics and treatment efficiencies of stormwater retention ponds." *Proc. 12th International Conference on Urban Drainage, Porto Alegre, Brazil*.

Skaggs, R.W. (1980). *DRAINMOD: Reference report - Methods for design and evaluation of drainage-water management systems for soils with high water tables*. U.S. Department of Agriculture – Soil Conservation Service, Fort Worth, TX.

Thornthwaite, C.W. (1948). "An approach toward a rational classification of climate." *Geog. Rev*., 38(1), 55-94.

Trenberth, K.E. (2011). "Changes in precipitation with climate change." *Clim. Res*., 47(1), 123.

United States Department of Agriculture (USDA) (1986). *Urban hydrology for small watersheds*. Technical Release 55 (TR-55). 2nd edition. Natural Resources Conservation Service, Conservation Engineering Division.

van Schilfgaarde, J. (1957). "Approximate solutions to drainage flow problems." *Drainage of agricultural lands*. Agron. Monogr. 7, Ed. J.N.Luthin, p.79-112, ASA, Madison, WI, USA.

Vanuytrecht, E., Van Mechelen, C., Van Meerbeek, K., Willems, P., Hermy, M., and Raes., D. (2014). "Runoff and vegetation stress of green roofs under different climate change scenarios." *Landsc. Urban Plan*., 122, 68-77.

Voskamp, I.M., and Van de Ven, F.H.M. (2015). "Planning support system for climate adaptation: Composing effective sets of blue-green measures to reduce urban vulnerability to extreme weather events." *Building Environ*., 83, 159-167.

Wardynski, B.J., and Hunt, W.F. (2012). "Are bioretention cells being installed per design standards in North Carolina? A field study." *J. Environ. Eng*., 138(12), 1210-1217.

Waters, D., Watt, W.E., Marsalek, J., and Anderson B.C. (2003). "Adaptation of a storm drainage system to accommodate increased rainfall resulting from climate change." *J. Environ. Plan. Man*., 46(5), 755-770.

Wernstedt, K., and Carlet, F. (2014). "Climate change, urban development, and storm water: Perspectives from the field." *J. Water Res. Plan. Man*., 140(4), 543-552.

Willems, P. (2013). "Revision of urban drainage design rules after assessment of climate change impacts on precipitation extremes at Uccle, Belgium." *J. Hydrol*., 496, 166-177.

Willems, P., Arnbjerg-Nielsen, K., Olsson, J., and Nguyen, V.T.V. (2012). "Climate change impact assessment on urban rainfall extremes and urban drainage: methods and shortcomings." *Atmos. Res*., 103, 106-118.

Wu, J., and Malmström, M.E. (2015). "Nutrient loadings from urban catchments under climate change scenarios: Case studies in Stockholm, Sweden." *Sci. Total Environ*., 518, 393-406.

Zahmatkesh, Z., Burian, S.J., Karamouz, M., Tavakol-Davani, H., and Goharian, E. (2014). "Low-impact development practices to mitigate climate change effects on urban stormwater runoff: Case study of New York City." *J. Irrig. Drain. Eng*., 141(1), 04014043.

CHAPTER 5: **HYDROLOGIC PERFORMANCE OF FOUR PERMEABLE PAVEMENT SYSTEMS CONSTRUCTED IN LOW PERMEABILITY SOILS IN NORTHERN OHIO**

5.1 Abstract

Permeable pavements benefit urban hydrology through detention of stormwater in the aggregate base and subsequent exfiltration to the underlying soil. The majority of previous research has focused on permeable pavements constructed in sandy soils and/or treating only direct rainfall. Four permeable pavements employing internal water storage (IWS) zones and situated over low permeability soils were intensively monitored for their hydrologic performance in northern Ohio. Volume reduction varied from 16% to 53% for permeable pavements with low drawdown rates (<0.35 mm/hr) and loading (impermeable : permeable pavement) ratios exceeding 4:1. Post-construction drawdown rates were similar to saturated hydraulic conductivity (K_{sat}) measured during construction, suggesting lateral exfiltration and evaporation were relatively minor contributors to volume reduction. Outflow was eliminated from 4-80% of observed storm events. Average depth of abstraction ranged from 3.0 mm (site with highest LR) to 25.2 mm (site treating only direct rainfall). Substantial peak flow mitigation was observed for all rainfall events not producing surface runoff. Peak flow was diminished by more than 80% for 7 events exceeding the 1-year, 5-minute design rainfall intensity for Cleveland, Ohio. Lower loading ratios, reduced surface runoff, an IWS zone, and higher underlying soil K_{sat} directly impacted volume reduction and peak flow mitigation. Overall, permeable pavement mitigated negative hydrologic impacts of impervious surfaces even when sited over low conductivity clay soils.

5.2 Literature Review

Impervious surfaces and urban drainage networks amplify the rate and volume of stormwater runoff that reaches water bodies, resulting in stream bank erosion, degradation of aquatic health, and increased pollutant loading (Meyer et al. 2005; Walsh et al. 2005; Line and White 2007; Schueler et al. 2009). To mitigate these deleterious effects, Low Impact Development (LID) strategies have been adopted to more closely mimic pre-development rate, volume, and duration of flow in the built environment (Dietz and Clausen 2008; Page et al. 2015). Stormwater control measures (SCMs), such as permeable pavement, are utilized to achieve these goals.

Permeable pavement consists of a permeable surface course of concrete, asphalt, or interlocking concrete pavers that allows water to infiltrate and access underlying aggregate storage layers (Figure 5-1). Permeable pavements usually have an underdrain to dewater the aggregate void spaces inter-event. Stormwater leaves permeable pavement through four hydrologic pathways: evaporation, exfiltration (i.e., infiltration into the underlying soil), drainage through the underdrain, and surface runoff (i.e., bypass of treatment).

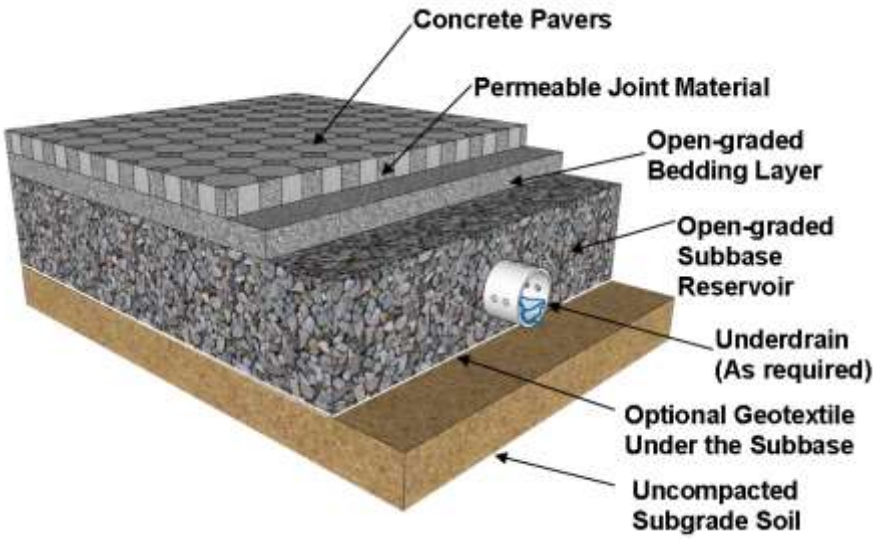

Figure 5-1. Schematic cross-section of permeable pavement.

To date, most permeable pavement studies have focused on systems located over permeable, sandy soils that were designed to treat only direct rainfall (Pratt et al. 1995; James and Thompson 1997; Rushton 2001; Brattebo and Booth 2003; Dreelin et al. 2006; Gilbert and Clausen 2006; Bean et al. 2007). Permeable pavements have been shown to substantially reduce flow volumes and peak flow rates under these conditions (Bean et al. 2007; Ball and Rankin, 2009). Mean curve numbers (CNs) for three permeable pavements located over sandy soils were 44, 77, and 80, much lower than the standard CN of 98 for impermeable pavements (Bean et al. 2007).

Relatively little research has been completed on permeable pavement systems situated over clay soils (Tyner et al. 2009; Fassman and Blackbourn, 2010; Drake et al. 2014). The median estimated volumetric runoff coefficient (the ratio of outflow volume to inflow volume) for permeable pavement in one such study was 0.49, while that for standard asphalt was 0.85 (Fassman and Blackbourn, 2010). Mean runoff reductions of greater than 98%

were observed for permeable pavements situated over sandy clay loam soils (Collins et al. 2008). Permeable pavements in Canada reduced runoff volume by 43% and were able to capture storm events less than a 7.1-mm depth (Drake et al. 2014). Runoff reduction in clay soils was enhanced when the subgrade was ripped or trenched to alleviate compaction and improve exfiltration (Tyner et al. 2009). These studies suggested permeable pavements provide hydrologic mitigation to move a site toward pre-development hydrology, even over Hydrologic Soil Group (HSG) D soils; however, all referenced permeable pavement studies treated only direct rainfall.

In poorly drained soils, drainage from permeable pavements can be quite substantial (Collins et al. 2008; Smolek, Winston, and Hunt, submitted; Smolek, Winston, Dorsey, et al. submitted). Inclusion of an internal water storage (IWS) zone within the aggregate by creating an upturned elbow in the underdrain has been suggested to increase exfiltration and reduce drainage (Collins et al. 2008; Wardynski et al. 2012). In clay soils, if the underdrain is located at the bottom of the cross-section (i.e., conventionally drained), the drainage rate will be many times greater than the exfiltration rate. By incorporating IWS, stormwater has time to drain (albeit slowly) both intra- and inter-event. Wardynski et al (2012) studied varying drainage configurations for a permeable pavement constructed over sandy loam texture, compacted urban fill. Over the year-long monitoring period, the conventionally drained permeable pavement reduced runoff by 77%. The system with a 15-cm deep IWS zone reduced runoff by 99.5%. The incorporation of a 30-cm deep IWS zone eliminated outflow. This proof-of concept study suggested an IWS zone will greatly enhance permeable pavement hydrologic performance.

The primary goals of this study were to evaluate permeable pavements constructed in clay soils (HSG D) and under high hydrologic loading ratios to assess how well this SCM functions under less than optimal conditions. This combination of factors has not been researched and published to date. Additionally, the study served as a proof-of-concept for use of the IWS drainage configuration in low permeability soils. To this end, four permeable pavements in northern Ohio were monitored for their hydrologic performance.

5.3 Site Descriptions

The water balance of four permeable pavements was quantified at three sites (Figure 5-2 and Table 5-1). All permeable pavements employed 15-cm diameter underdrains, had 15-cm thick IWS zones, and were located over mapped HSG D soils (Soil Survey Staff 2015; Table 5-1). The IWS zone extended ponding within the aggregate, allowing for both vertical and lateral exfiltration into the underlying soils. The sites were built as retrofits [Willoughby Hills (WH)] or redevelopment [Perkins Township (PT) and Orange Village (OV)], and were underlain by fill soil.

Three of the permeable pavements treated run-on from impermeable surfaces, while OV treated only direct rainfall. The loading ratio (LR) for each permeable pavement SCM was determined using:

$$LR = \frac{A_{WS}}{A_{PP}} \tag{5-1}$$

where A_{WS} is the surface area of the watershed and A_{PP} is the surface area of the permeable pavement. Two different loading ratios were calculated for each permeable pavement: (1) clogging and (2) exfiltration. The LR for clogging related the watershed area draining onto

the permeable pavement surface, representing the amount of run-on to the permeable pavement. The LR for exfiltration was based on the relationship between the watershed area and infiltrative surface area (the area where subgrade ponding occurred in the aggregate due to the IWS zone).

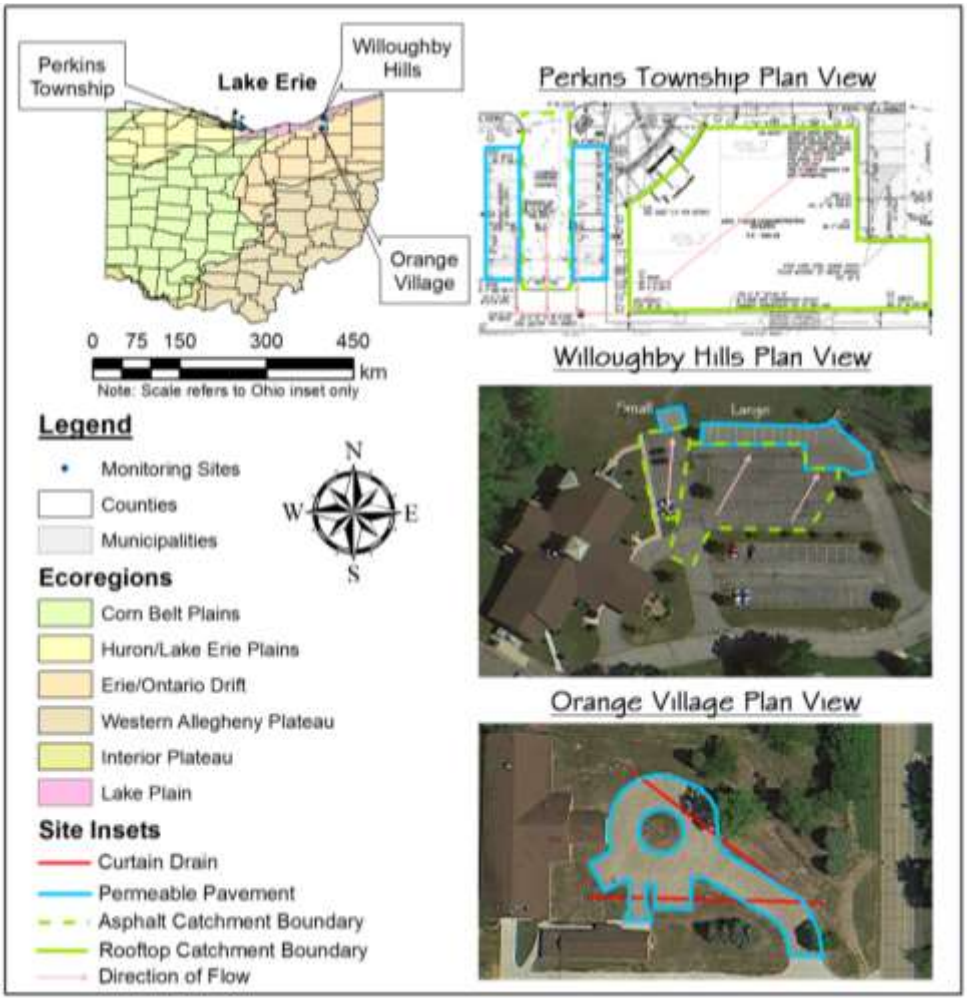

Figure 5-2. Locations and plan views of permeable pavement monitoring sites in this study.

Table 5-1. Summary of catchment and permeable pavement characteristics.

Characteristics	PT	WH Small	WH Large	OV
Permeable pavement type	PC[1]	PICP[2]	PICP	PICP
Contributing catchment area (m^2)	2140	320	890	0
Catchment imperviousness (%)	81	100	100	N/A
Permeable pavement surface area (m^2)	240	45	410	880
Infiltrative surface area (m^2)	450[3]	45	205	880
Loading ratio: clogging	0.6	7.2	2.2	0
Loading ratio: exfiltration	4.8	7.2	4.3	0
Pavement thickness (cm)	15	8	8	8
Total aggregate depth (cm)	38-45	51	51	58-74
IWS zone depth (cm)	15	15	15	15
Underdrain diameter (cm)	15	15	15	15
Mapped soil	Bennington silty clay loam	Mahoning silt loam	Mahoning silt loam	Wadsworth silt loam
Hydrologic soil group	C/D	D	D	D

[1]permeable concrete
[2]permeable interlocking concrete paver
[3]this represents the footprint of the IWS zone

The pervious concrete (PC) at PT was installed October-December 2012. Two sets of PC parking stalls, with a total surface area of 240 m^2, were separated by and received runoff from an impermeable concrete drive aisle with a surface area of 140 m^2 (Figure 5-3). The design included open-graded aggregate beneath the impermeable concrete drive aisle as well as the permeable concrete, and thus the effective infiltrative surface area was increased to 450 m^2 (Table 5-1). Runoff from the rooftop of the adjacent township administration building (1740 m^2, Figure 5-2) was routed from the downspouts into the subgrade aggregate reservoir. A small (400 m^2) pervious area also drained directly to the subgrade, resulting in a

total drainage area of 2140 m^2. Given this, the LR for exfiltration for PT was 4.8; that for clogging was only 0.6 because the rooftop and pervious area drainage entered the subgrade aggregate. Total aggregate depth varied from 38 to 45 cm, with a flat infiltrative surface over the underlying soil.

Figure 5-3. Photographs of the permeable concrete at Perkins Township, Ohio (top left), Willoughby Hills Small permeable interlocking concrete pavement (PICP) application (top right), Willoughby Hills Large PICP application (bottom left), and PICP at Orange Village (bottom right).

Two permeable interlocking concrete pavement (PICP) applications, hereafter referred to as WH Small and Large, were retrofitted into the parking lot at the WH community center during September-October 2013 (Figure 5-3). The contributing drainage areas for both the Small and Large applications were impermeable asphalt, except for parking lot islands and a small portion of concrete sidewalk in the Small application watershed. Both cells had 51-cm of aggregate. The Small application, 45 m^2 in surface area, had a flat infiltrative surface (Table 5-1). The LRs for exfiltration and clogging for the Small application were 7.2, the largest monitored in this work. The Large application (surface area of 410 m^2) had a stepped subgrade to compensate for the 1-2% surface slope, resulting in a no-IWS drainage configuration over one-half the permeable pavement surface area. Thus, the effective infiltrative surface area was reduced to 205 m^2. The LR for clogging (2.2) was near the maximum recommended value of 2.0 in the *Ohio Rainwater and Land Development Manual* (ODNR 2006). Due to the stepped subgrade, however, the LR for exfiltration was 4.3.

A newly-constructed PICP parking lot was built at the OV recycling facility during September-October 2013 (Figure 5-3). The total aggregate depth at the site varied from 58 to 74 cm. This permeable pavement treated only direct rainfall, resulting in a LR for both clogging and exfiltration of 0.0 (Table 5-1). The total surface area of the parking lot was 880 m^2. Two 15-cm diameter curtain drains were installed 84 cm below the permeable pavement cross-section (approximately 1.5 m below ground surface) to mitigate a potentially high water table at the site (Figure 5-2). These curtain drains probably increased the drainage capacity of the pavement. Because of this, caution should be applied when interpreting results from OV.

5.4 Materials and Methods

Data Collection

Instrumentation was installed at each site to monitor climatic parameters and permeable pavement hydrologic performance. A 0.254-mm resolution tipping-bucket rain gauge affixed approximately 2 m above the ground measured rainfall (Davis Instruments, Hayward, California). A Hobo U30 weather station measured wind speed, wind direction, air temperature, relative humidity, and solar radiation (Onset Computer Corporation, Bourne, MA). All climatic parameters were recorded on a 1-minute interval and measured in open areas free from interference.

Drainage was measured using a weir box and a Hobo U20 pressure transducer (Onset Computer Corporation, Bourne, MA). Weir boxes were purpose-built for each monitoring location, included a baffle to ensure laminar flow, and utilized sharp crested weirs. Either 30˚ (WH Small and OV) or 60˚ (WH Large and PT) v-notch weirs were installed depending on expected flow rates from the underdrain. At WH, surface runoff monitoring began on August 5, 2014 (because surface runoff was observed the prior week due to surface clogging). Surface runoff was diverted into existing weir boxes using metal baffles and was quantified and separated from drainage using hydrograph separation techniques, such as those used by Brown and Hunt (2011).

Hobo U20 pressure transducers housed in 2.5-cm diameter shallow wells measured internal water level within the aggregate at the PT, WH Small, and WH Large applications. To compute water level, an additional Hobo U20 pressure transducer was placed in the rain

gauge housing at each site to measure (and later correct for) local barometric pressure. All pressure transducer measurements were obtained on a 2-minute interval.

Data Analysis

Rainfall event summary statistics were calculated for depth (mm), duration (hours), average intensity (mm/hr), peak 5-minute intensity (mm/hr), and antecedent dry period (ADP, days). Discrete storm events were identified by a minimum rainfall depth of 2.5 mm and a minimum ADP of 6 hours (Driscoll 1989).

Since inflow to each permeable pavement was dispersed, direct measurement of inflow was impractical. The volume of direct rainfall was calculated as the product of rainfall depth and permeable pavement surface area. A rainfall-runoff model, the Natural Resources Conservation Service (NRCS) curve number (CN) method, was used to determine run-on to each permeable pavement (NRCS 1986):

$$Q = \frac{(P-0.2S)^2}{(P+0.8S)} \times 0.0254 \times A \quad (5\text{-}2)$$

where Q is runoff volume (m^3), P is precipitation depth (mm), S is potential maximum soil moisture retention (mm) and is equal to $(\frac{1000}{CN} - 10) \times 25.4$, CN = curve number for the catchment, and A is the surface area of the catchment (m^2).

Inflow volumes were calculated for each runoff producing event (i.e., $P > I_a$). Impervious areas within each watershed were assigned a CN of 98 (i.e., nearly all rainfall becomes runoff), while pervious areas were assigned a CN of 80, representative of open space in good condition on an HSG D soil (Fangmeier et al. 2006). Additionally, antecedent moisture

corrections were applied to the CN for wet (ADP less than 2 days) and dry (ADP greater than 5 days) antecedent moisture conditions using methods in NRCS (2004).

Peak inflow rates were estimated using the Rational Method (Chin 2006), a commonly-used engineering method relating rainfall intensity and flow rate:

$$Q_p = 2.78 \times C \times i \times A \tag{5-3}$$

where Q_p is the peak flow rate (L/s), C is the rational runoff coefficient, i is the measured rainfall intensity (mm/hr), and A is the watershed area (ha). The rational coefficient was set to 0.9 for impervious areas, while pervious areas were assigned a rational coefficient of 0.2 (lawns on heavy soil and average slope; Chin 2006).

Weir equations corresponding to the particular weir geometries were utilized to calculate discharge as a function of measured flow depth above the weir invert (Grant and Dawson 2001):

$$Q = 373.2 \times H^{2.5}, 30^{\circ} \text{ v-notch weir} \tag{5-4}$$

$$Q = 796.7 \times H^{2.5}, 60^{\circ} \text{ v-notch weir} \tag{5-5}$$

where Q is flow rate (L/s) and H is head (m) above the weir invert. Flow rates were calculated on a 2-minute interval, and the area under each hydrograph was integrated to determine total outflow volumes on a storm-by-storm basis. The peak outflow rate was the maximum measured value during each storm event. Cumulative volumes of inflow, drainage, surface runoff, and exfiltration/evaporation were calculated as the sum of storm-by-storm values.

Water level measured within the aggregate of each permeable pavement was utilized to determine the drawdown rate, a combined measure of exfiltration and evaporation. The drawdown rate (Q_{DD}, mm/hr) was calculated as:

$$Q_{DD} = \frac{(WL_{Beg} - WL_{End}) \times \phi}{t_{DD}} \quad (5\text{-}6)$$

where WL_{Beg} and WL_{End} are the water levels (mm) in the aggregate at the beginning and end of the dry period, respectively, ϕ is the porosity of the aggregate (0.4, Eisenberg et al. 2015), and t_{DD} is the inter-event period duration (hr). This calculation was made only after cessation of drainage to isolate exfiltration and evaporation. The total volume of exfiltration and evaporation was calculated using:

$$V_{EE} = \sum_{i=1}^{n} \left(\frac{Q_{DD,i} \times t_{DD,i}}{1000} \right) \times f_{drain} \times A_{IS} \quad (5\text{-}7)$$

where V_{EE} is the total volume exfiltrated and evaporated over the monitoring period (m^3), n is the total number of inter-event periods, Q_{DD} is the drawdown rate (mm/hr), f_{drain} is the quotient of the total monitoring period duration to the total dry period duration, and A_{IS} is the area of the infiltrative surface (m^2). The f_{drain} parameter accounted for drawdown during periods of drainage.

5.5 Results and Discussion

Rainfall

Over the course of the approximately two-year monitoring period (April 2013-November 2014) at PT, 87 wet-weather events were observed. The monitoring period at WH and OV lasted thirteen months (October 2013 through November 2014), during which 77 separate wet-weather events were observed. Climatic and hydrologic data were collected during the

winter months of December 2013 through March 2014, but were deemed unreliable due to sub-freezing temperatures and not analyzed. Summary statistics for rainfall depth, average intensity, peak five-minute intensity, and antecedent dry period are presented in Table 5-2. Total rainfall depths over the monitoring periods were 1285, 995, and 928 mm at PT, WH, and OV, respectively. Over the 30-yr period from 1981-2010, Cleveland Hopkins International Airport (the nearest long-term rainfall record) received an annual average of 994 mm of precipitation (NOAA 2015); precipitation depth during the monitoring periods was similar to the long-term average at WH and OV, but PT was substantially drier than the long-term average.

Median and mean rainfall depths during the monitoring periods were approximately 9 and 13 mm at all three sites. Maximum observed rainfall depths were 66 mm at PT and 87-89 mm for WH and OV. For all but the most extreme events, average and peak 5-minute rainfall intensities were lower at OV than the other two sites. Median and mean antecedent dry periods varied from 4-6 days for PT to 2.5-4 days for WH and OV. This meant the IWS zone at PT typically had, on average, more time between rain events for drawdown to occur. A frequency analysis of the rainfall events observed at PT, WH, and OV is presented in Appendix A.

Table 5-2. Summary statistics for rainfall events at Perkins Township (PT), Willoughby Hills (WH), and Orange Village (OV).

Monitoring Site	Statistic	Depth (mm)	Average Intensity (mm/hr)	Peak 5-minute Intensity (mm/hr)	Antecedent Dry Period (days)
PT	Minimum	2.5	0.3	3.0	0.3
	Median	8.9	1.5	25.9	4.2
	Mean	13.5	3.0	33.8	5.7
	90th percentile	30.2	7.4	79.5	13.4
	Maximum	66.0	22.1	128.0	24.8
WH	Minimum	2.5	0.3	3.0	0.3
	Median	8.9	1.0	12.2	2.6
	Mean	13.5	2.5	25.4	3.5
	90th percentile	29.5	4.8	65.8	7.9
	Maximum	86.9	21.8	167.6	18.6
OV	Minimum	2.5	0.2	3.0	0.3
	Median	8.5	1.2	18.3	2.9
	Mean	12.3	2.4	24.4	4.2
	90th percentile	24.9	3.4	45.7	8.4
	Maximum	89.2	30.5	152.4	24.4

Drawdown Rate

Understanding underlying soil properties, particularly saturated hydraulic conductivity (K_{sat}), is critical to predicting post-construction permeable pavement performance, as local variability in soils and site conditions greatly impact performance (Wardynski et al. 2012; Olson et al. 2013; Eisenberg et al. 2015). Underlying soil K_{sat} is the primary factor explaining the vast differences in runoff reduction from permeable pavement studies (Bean et al. 2007; Ball and Rankin 2010; Fassman and Blackbourn 2010; Drake et al. 2013; Drake et al. 2014). Various soil de-compaction methods may be used during construction to rejuvenate soil K_{sat} (Tyner et al. 2009; Wardynski et al. 2012).

As the final subgrade elevation was reached during construction, excavation was temporarily suspended to perform K_{sat} testing (Figure 5-4). Between two and six single-ring, constant head K_{sat} tests were completed in the subsoils beneath each of the permeable pavements [Gulliver et al. (2010), Table 5-3]. In some cases, the subsoils had been raked with the teeth of the excavator bucket prior to soil testing to reduce compaction; if this was the case, then a hand-held garden hoe was used to remove loose soil. A Mariotte bottle was used to keep a constant head on the soil, and mathematical corrections as described in Reynolds et al. (2002) were used to offset for lateral water flow. Thus, the vertical component of the soil K_{sat} was quantified. While vertical K_{sat} measurements are not the same as post-construction drawdown rate (for reasons discussed below), they are the most typical pre-construction soil test used for permeable pavement design.

Figure 5-4. Single ring, constant head K_{sat} test with Mariotte syphon (left). K_{sat} tests carried out at the WH Large application (right).

Table 5-3. Comparing subsoil K_{sat} measured during construction to post-construction drawdown rates for each of the permeable pavements.

Site	Mapped Soil	K_{sat} measured during construction (mm/hr)	Drawdown Rate (average ± standard deviation, mm/hr)
PT	Bennington	0.25, 0.25, 1.0, 1.25	0.33 ± 0.12
WH small	Mahoning	0.25, 1.25	0.05 ± 0.03
WH large	Mahoning	0, 0.25, 1.0, 1.5	0.05 ± 0.025 0.15 ± 0.18
OV	Wadsworth	0.25, 0.75, 1.25, 1.5, 18.3, 39.1	N/A

At PT, underlying soil K_{sat} ranged from 0.25 to 1.25 mm/hr, while those for the WH Small and Large applications were between 0.25 to 1.25 mm/hr and 0 to 1.5 mm/hr, respectively. These were within the expected range for HSG D soils. However, at OV, six measurements of K_{sat} varied from 0.25 mm/hr to 39.1 mm/hr. Lower readings at this site reflected excavation into the underlying HSG D soil, whereas the higher readings were recorded in areas excavated into coarse fill material.

The average post-construction drawdown rate was 0.33 mm/hr at PT. Post-construction drawdown rates were within the range of K_{sat} measured during construction at PT, suggesting the soil de-compaction implemented at the subgrade elevation was successful. However, the WH Small and Large applications had post-construction drawdown rates less than and on the low end, respectively, of K_{sat} measured during construction (Table 5-3). The contractor followed similar methods for soil de-compaction as at PT. One plausible explanation for this disparity was the application of salt to the catchments; salt was sparingly applied during winter weather at PT, while at WH it was applied liberally. Utilizing sodium-based deicing

salts with clayey soils augments soil sodium adsorption ratio (SAR) and exchangeable sodium percentage (ESP). These chemical soil parameters quantify the amount of sodium in relation to other cations, such as Ca^{2+}, Mg^{2+}, and K^{+}. As SAR and ESP increase, deflocculation of clay particles occurs and macroporosity decreases (Sparks 2003). Frenkel et al. (1978) found "caking" of fine textured soils under sodic conditions, reducing both infiltration rate and saturated hydraulic conductivity. This finding is supported by others (e.g., McNeal and Coleman 1966; Pupisky and Shainberg 1979; Shainberg et al. 1981); decreases in soil hydraulic conductivity were particularly pronounced for 2:1 layer silicates, such as montmorillonite and illite (McNeal and Coleman 1966). Previous studies showed the Mahoning soil type mapped at Willoughby Hills had 40% more 2:1 than 1:1 clays (McConnell et al. 1956). This is a potential cause for the apparent decreases in K_{sat} post-construction at WH.

Internal water level over a two month period at PT is presented in Figure 5-5. The cumulative drainage duration was nearly identical to the cumulative duration the internal water level was above the invert of the underdrain. The IWS zone at PT completely dewatered once during the two-year monitoring period. The IWS zones at the Small and Large applications at WH never dewatered entirely. Therefore, near-continuous (albeit slow) exfiltration occurred at all sites.

Below the invert of the underdrain, exfiltration and evaporation were the only means for drawdown of the internal water level. Unlike results for bioretention cells in Northeast Ohio (Chapter 2), drawdown rate for all three permeable pavements was linear, suggesting vertical exfiltration was the dominant pathway. There was proportionally less lateral (i.e., side wall)

surface area in the permeable pavements because they had much larger surface area to perimeter ratios and shallower IWS zones; when the IWS zone was full, the subgrade represented 97%, 95%, and 91%, respectively, of the infiltrative surface area at PT, WH Small, and WH Large. The lateral hydraulic conductivity becomes more important as the IWS zone depth increases and the footprint of the SCM decreases; the converse holds as well.

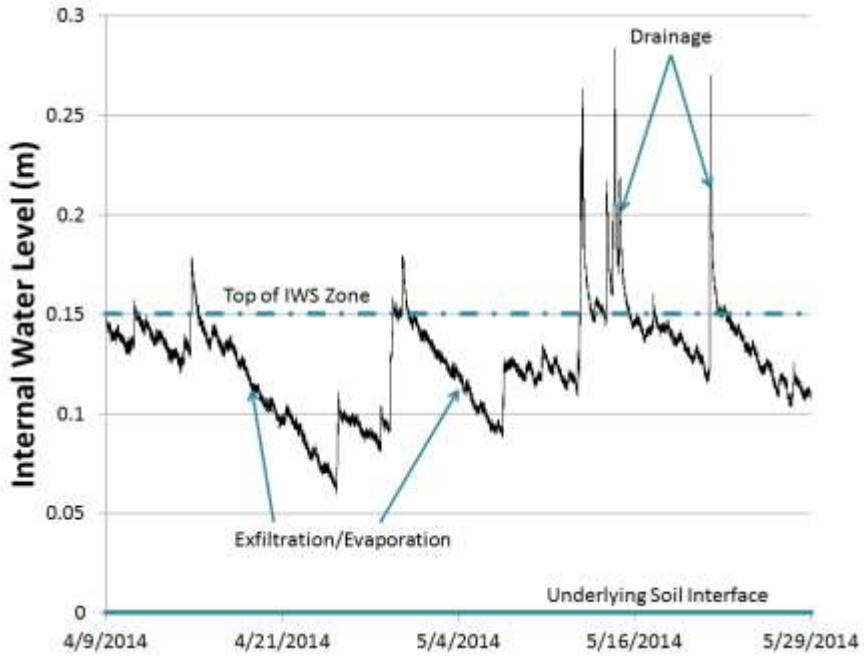

Figure 5-5. Internal water level as a function of time for the PT pervious concrete site.

Water Balance

Runoff reduction, the sum of exfiltration and evaporation, varied from 16-99% for the four permeable pavements (Table 5-4). The WH Small application, which had the highest LR for exfiltration (7.2) and lowest drawdown rate (0.05 mm/hr), reduced runoff by only

16%. WH Large, with a slightly higher average drawdown rate (0.10 in/hr) and lower LR for exfiltration (4.3), reduced runoff by 32%. PT had an even higher drawdown rate (0.33 mm/hr) and comparable LR for exfiltration (4.8), resulting in a 53% volume reduction. Permeable pavement hydrologic modeling in DRAINMOD estimated the inclusion of a 15-cm IWS zone improved runoff reduction by 10-30% over permeable pavement with no IWS (Smolek et al. 2015). Additional information regarding the hydrologic performance of these permeable pavements, including curve number analysis and volume reduction as a function of rainfall depth, can be found in Appendix A.

Orange Village, which treated only direct rainfall and had pre-construction K_{sat} values up to 39.1 mm/hr, provided by far the best volume reduction (99%); the curtain drains probably enhanced exfiltration and modified the water balance. The curtain drains discharged 1646 mm (over the permeable pavement area) of drainage (while only 928 mm of rainfall occurred during the monitoring period), suggesting they were draining parts of the site beyond the permeable pavement. Thus, it was not possible to isolate their effects on the water balance.

Table 5-4. Volume and percentage of inflow, drainage, surface runoff, and exfiltration+evaporation.

Site name	Total inflow (mm)	Drainage (mm) [% of inflow]	Surface runoff (mm) [% of inflow]	Exfiltration and evaporation (mm) [% of inflow]
PT	972	460 [47.4]	0 [0]	512 [52.6]
WH small	602	455 [75.6]	52 [8.4]	96 [15.9]
WH large	543	240 [44.2]	132 [24.2]	171 [31.6]
OV	928	11 [1.2]	0 [0]	917 [98.8]

At PT and OV, surface runoff did not occur during the monitoring period, because extremely high initial surface infiltration rates (2000-3000 mm/hr) were maintained through the monitoring period due to the low LRs for clogging (0.6 and 0.0, respectively). Therefore, runoff not reduced through exfiltration or evaporation drained through the underdrain. The elevated LR (7.2) caused clogging at the Small application at WH and resulted in 8% surface runoff. If runoff is to be prevented, a LR this high should be avoided due to concerns with surface clogging.

While WH Large appeared to have a LR for clogging near the maximum 2.0 commonly approved in Ohio, substantial clogging occurred in one portion of the parking lot (Figure 5-6). Three parking stalls drained approximately 30% of the catchment, receiving stormwater from the upper regions of the catchment as concentrated flow along the curb line of a parking lot island. This created an effective LR for clogging near 6. Because the parking lot also had substantial surface slope (4.5%) in the direction of flow, stormwater passed over the clogged pavement surface to the curb, flowed along the curb line, and then overflowed into the catch basin (Figure 5-6). At the cessation of monitoring, the water balance did not sum to 100%. Since surface runoff was not monitored for most of the monitoring period, the missing volume (24% of the water balance) was attributed to surface runoff.

Figure 5-6. Flow from Willoughby Hills large catchment passing over PICP as surface runoff (left) and surface runoff continuing along the curbline and overflowing into the catch basin (right).

To determine the fraction of surface runoff, a calibrated DRAINMOD model for the WH Small application was modified using design parameters from the WH Large application (Smolek, Winston, Dorsey, et al. submitted). To recalibrate the WH Large model to account for surface runoff, the LR in the model was adjusted until the modeled drainage best matched the measured drainage. Based on this analysis, approximately 16% of the PICP was estimated to be clogged (65 m^2), which matched visual estimates during rainfall. The clogged portion drained 300 m^2 of the 890 m^2 catchment and resulted in surface runoff equivalent to 24% of the overall water balance. Valuable insight was gained by applying DRAINMOD as a tool to verify the extent of clogged permeable pavement.

Figure 5-7. Estimated clogged PICP surface area (red) and contributing drainage area to the clogged PICP (green). Catchments are outlined using dashed lines and flow directions are annotated with arrows.

One of the tenets of an LID strategy is to apply measures to more closely mimic pre-development hydrology. An SCM must capture and infiltrate or evapotranspire a substantial fraction of the smallest events to mimic the pre-development initial abstraction provided by soil and vegetation (Ahiablame et al. 2012). The percentage of completely captured events varied widely (Table 5-5); only 4% of events had no outflow at WH Small, while the OV permeable pavement eliminated outflow for 78% of events. The maximum completely captured rainfall depths were 3.3, 10.7, 12.7, and 25.9 mm, respectively, for WH Small, WH Large, PT, and OV. Because the IWS zone depths were the same among sites, two factors impacted the number and depth of completely captured storms: (1) the LR for exfiltration and (2) the drawdown rate. The WH applications had the lowest exfiltration rates

and moderate to high LRs for exfiltration, resulting in the worst performance with respect to completely captured events. OV, with an LR of 0.0 and relatively permeable soils, had the best overall performance. This confirms: (1) effort should be made to locate permeable pavements over the most permeable soils on a development site and (2) reducing the LR as much as practicable (by increasing the permeable pavement surface area) will improve volume mitigation.

Table 5-5. Completely captured storm events (i.e., no outflow) for the permeable pavements.

Site name	Events completely captured (#)	Percentage of events completely captured	Depth of completely captured events (mm)
PT	17/87	20	2.5-12.7
WH small	3/77	4	2.8-3.3
WH large	15/77	19	2.5-10.7
OV	60/77	78	2.5-25.9

The fraction of outflow from a permeable pavement increases with rainfall depth (Fassman and Blackbourn 2010). When an IWS zone is included in the design, the available storage volume within the system increases, and exfiltration is augmented over the long-term (Smolek et al. 2015). The discharge threshold, defined as the minimum rainfall depth to produce outflow from a permeable pavement, was determined by plotting outflow volume against rainfall depth. A piecewise linear regression with an initial slope of zero was used to model the relationship; bootstrapping was performed to determine the 95% confidence interval around the D_T (Vieth 1989; Figure 5-7). Discharge thresholds were 3.0 mm at WH Small, 5.2 mm at WH Large, 8.5 mm at PT, and 25.2 mm at OV. The discharge

threshold was impacted by the LR for exfiltration, the drawdown rate, and antecedent dry period (ADP).

Because longer ADP (5-10 days) allows more drawdown, events larger than the discharge threshold were captured by each of the permeable pavements (Table 5-5). The smallest and largest discharge thresholds were an order of magnitude different, highlighting the variability of permeable pavement hydrologic performance (Bean et al. 2007; Ball and Rankin 2010; Fassman and Blackbourn 2010; Drake et al. 2013; Drake et al. 2014).

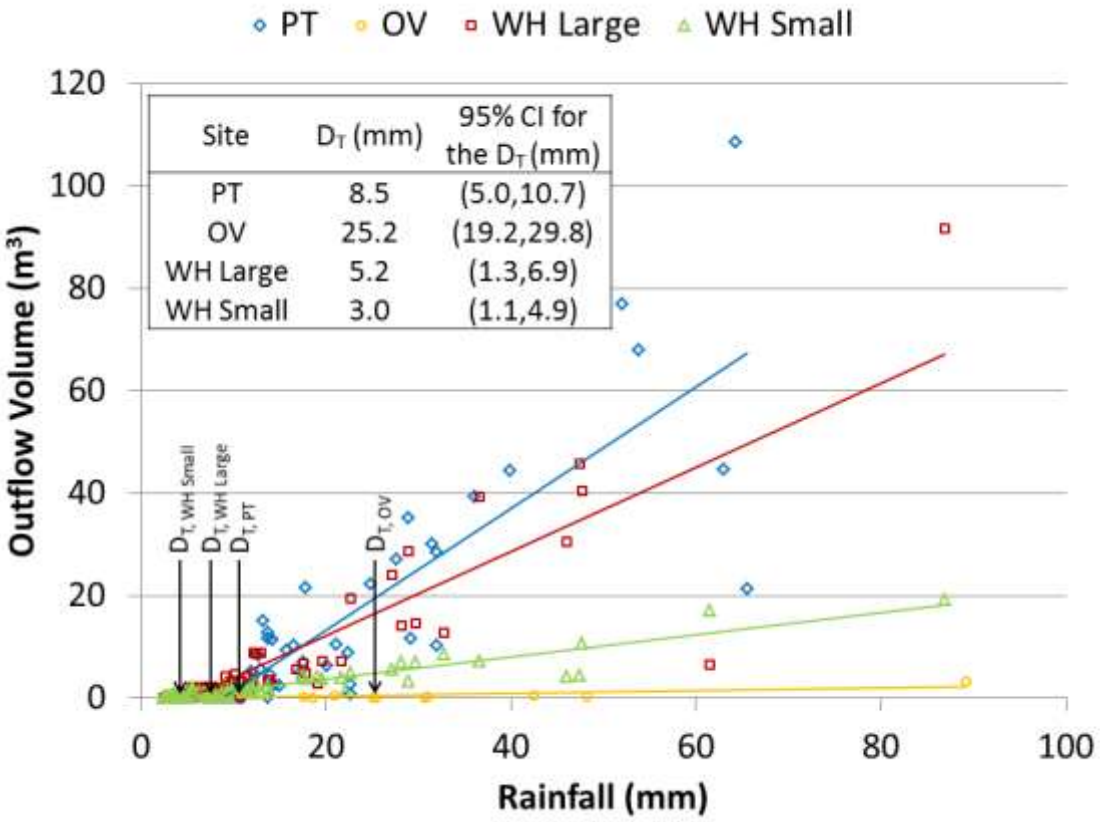

Figure 5-8. Determination of the discharge threshold (D_T) for each permeable pavement.

Figure 5-9 depicts the volume discharge ratio (VDR), the ratio of effluent to influent volume, for the four permeable pavements. Data were plotted as ranked exceedance probability. For OV, of the 17 events (or 22% of the total) that had measurable outflow, none had *substantial* outflow (defined herein as VDR>0.1). Higher exfiltration rates and a lack of run-on at OV kept VDRs low, albeit the curtain drain probably influenced these results. Minor outflow (defined herein as VDR<0.1) occurred at WH Large and PT for 0% and 36% of storms, while substantial outflow (VDR>0.1) occurred in 81% and 44% of events, respectively. Perkins Township reduced volume to a greater extent due to higher drawdown rates and the lack of surface runoff. For the WH Small application, volume reduction was relatively poor due to the high loading ratio and presence of surface bypass. Ninety-six percent of events produced substantial outflow.

Davis (2008) suggested a maximum target VDR of 0.33 for SCM efficacy based on the ratio of rational coefficients for impervious and undeveloped lands. The OV, PT, WH Large, and WH Small permeable pavements met this target for 100%, 71%, 52%, and 4% of observed rainfall events, respectively. Volume discharge ratio performance appeared to be a function of underlying soil K_{sat} and LR for exfiltration.

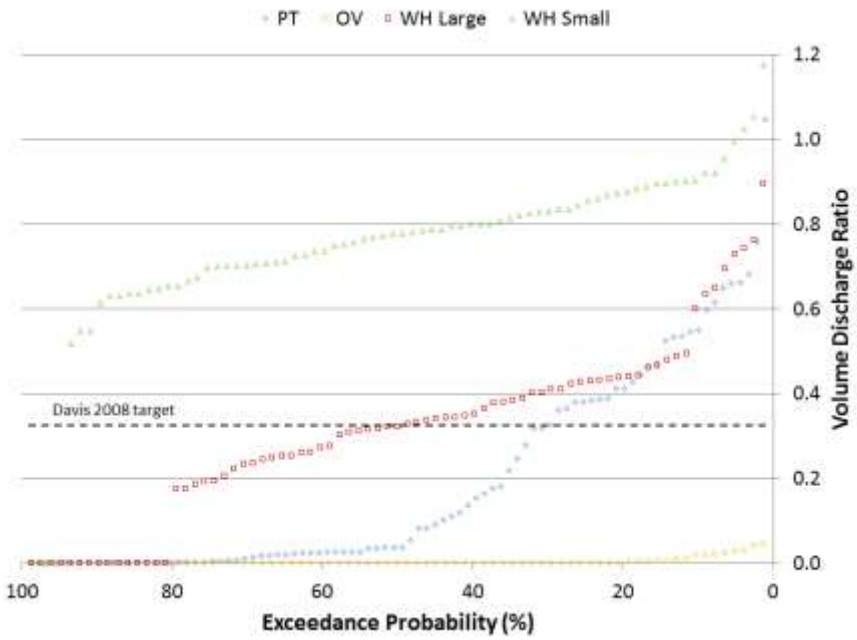

Figure 5-9. Exceedance probability for volume discharge ratio for the four permeable pavements.

Peak Flow Mitigation and Flow Duration

The peak runoff rate from a catchment is substantially increased when impervious surfaces are constructed, resulting in erosion of stream banks and loss of in-stream habitat (Finkenbine et al. 2000). There is interest in using permeable pavement to meet peak flow mitigation requirements, since the SCM frees valuable land for other beneficial uses. Summary statistics for inlet and outlet peak flow rate and peak flow percent reduction are presented in Table 5-6. Inflow rates were proportional to the size of the watershed, while outflow rates were throttled substantially by storage in the IWS, lateral flow to the drain, and flow restriction provided by the single underdrain in each permeable pavement. The 90th percentile peak outflow rate, which could be used as a surrogate for stream protection (Tillinghast et al. 2011), was mitigated by 14% (WH Large), 42% (WH Small), 85% (PT),

and 100% (UC). Clogging of a portion of the WH Large pavement elevated 90th percentile and maximum peak effluent rates. This exemplified why eliminating surface runoff either through preventative design and/or prescriptive maintenance to prevent clogging or through delivery of stormwater to the subgrade (as at PT) is critical. Additional analysis of peak flow mitigation as a function of rainfall depth can be found in Appendix A.

Provided stormwater infiltrated the pavement, some peak flow mitigation was assured through storage in the IWS zone and attenuation provided by flow to and through the underdrain. Perkins Township and OV had *minimum* peak flow reductions of 45 and 92% during the monitoring periods, which shows these systems can mitigate peak flow when (1) surface clogging does not occur, and (2) the IWS zone is able to dewater inter-event. Other studies of permeable pavement hydrology have generally observed excellent peak flow mitigation, albeit often with no run-on to the permeable pavement (Bean et al. 2007; Brattebo and Booth 2003; Roseen et al. 2009; Fassman and Blackbourn 2010; Roseen et al. 2012).

Table 5-6. Peak flow mitigation at the PT, WH, and OV permeable pavements.

Site Name	Location	Median peak flow rate (L/s)	75th percentile peak flow rate (L/s)	90th percentile peak flow rate (L/s)	Maximum peak flow rate (L/s)	Median peak flow reduction (%)	Range of peak flow reduction (%)
PT	Inlet	11.2	22.7	34.3	55.2	98.3	45-100
	Outlet	0.2	0.8	5.2	13.2		
WH small	Inlet	1.2	2.9	5.4	13.5	71.8	16-100
	Outlet	0.3	1.2	3.1	5.7		
WH large	Inlet	2.7	8.0	14.3	36.7	69.7	0-100
	Outlet	0.6	5.8	12.2	34.4		
OV	Inlet	4.0	6.7	10.0	33.3	100	92-100
	Outlet	0.0	0.0	*	2.7		

*Flow occurring but below lowest measurable value (0.3 L/s)

For compliance with flood control regulations, local regulations require matching the post-development peak flow to the pre-development peak flow for events between and including 1-yr and 100-yr storms (ODNR 2006). Design rainfall intensities (with time of concentration equal to 5 minutes for the small watersheds studied) were obtained from the National Oceanic and Atmospheric Administration (NOAA 2015) for Cleveland Hopkins International Airport, the nearest reliable source of long term data (located approximately 85 km from PT, 45 km from WH, and 35 km from OV). At each monitoring site, a minimum of two events exceeded the 1-yr, 5-minute rainfall intensity (Table 5-7). A dichotomy in peak flow mitigation performance existed for these high intensity rainfall events. For PT and OV, peak flow mitigation exceeded 84% in all cases; the aggregate subbase served as an underground storage reservoir with the outflow rate metered by the underdrain. During two design rainfall events (5 and 10 yr ARI) at a permeable pavement in Auckland, New Zealand,

peak flow rate was reduced by 40-50% from modeled *pre-development* (Fassman and Blackbourn 2010). Additionally, that site did not employ an IWS zone and had a 5% subgrade slope to direct water to the underdrain.

At WH, substantial surface runoff and low drawdown rates were likely the drivers for lower peak flow mitigation at the Small (27-61%) and Large (0-11%) applications during design rainfall intensities. The Small application had a higher LR but greater peak flow mitigation, a result of less surface clogging at the site. Across the research sites, the peak precipitation rate occurred before the centroid of the rainfall depth for approximately 80% of these more intense storm events. Consequently, storage was often available in the IWS zone, resulting in greater peak flow mitigation than if the systems received a center-weighted Type II rainfall distribution (NRCS 1986), often used for design in Ohio.

Table 5-7. Distribution of storm events greater than design rainfall intensities and peak flow mitigation during these events.

Statistic	PT	WH large	WH small	OV
No. Events >1yr storm (99 mm/hr)	6	4	4	3
No. Events >2yr storm (118 mm/hr)	1	1	1	3
No. Events >5yr storm (141 mm/hr)	0	1	1	1
No. Events >10yr storm (160 mm/hr)	0	1	1	0
Peak flow reduction (%)	84-98	0-11	27-61	92-99

Flow duration curves were used to summarize the hydraulic response of permeable pavements by combining flow rates across all observed storm events into a single distribution (Figure 5-10; after Davis et al. 2012). They describe the percentage of time specified flow rates are equaled or exceeded (Leopold 1994). The distributions can be compared against

stream health metrics such as the duration of critical erosion-inducing flow rates (Tillinghast et al. 2011) or against rainfall duration to determine how the SCM affects outflow.

Monitoring period durations were 609 days at PT and 423 days at both WH and OV. Outflow occurred from the OV permeable pavement for 269 hours, or 2.6% of the monitoring period due to the high underlying soil K_{sat}, lack of run-on to the permeable pavement, and 15-cm IWS zone. Willoughby Hills Large had a similar duration of outflow (291 hours) to OV, representing 2.9% of the monitoring period. Surface bypass at the WH Large reduced the fraction of water passing through the underdrain and subsequently reduced the total drainage time. Drainage from PT occurred during 6.6% (967 hours) of the monitoring period, perhaps due to the lack of bypass and greater LR for exfiltration at this site. Drainage or surface runoff occurred over 1283 hours at WH Small, representing 12.6% of the monitoring period. Because the LR was highest and the drawdown rate lowest of the four permeable pavements, the drainage duration was greatly extended.

The total rainfall durations at PT, WH, and OV were 732, 796, and 645 hours, respectively. The PT and WH Small applications increased the overall duration of outflow compared to rainfall duration. These two sites had the highest LRs for exfiltration (Table 5-1) and had very low drawdown rates (<0.35 mm/hr), elongating the drainage time. The sites with lower LRs, more permeable soils, and greater fractions of surface runoff decreased the duration of outflow, which is a key metric for stream health (Walsh et al. 2012). However, duration of flow is only of concern above erosion-inducing threshold flow rates. Flow duration curves from a nearby stream (Mill Creek, located in Northeast Ohio) draining an agricultural watershed were used for comparison (OEPA 2011). High flows

(i.e., greater than 90th percentile) for this creek varied from 1.7 to 21.3 L/s/ha. Outflow rates from the permeable pavements were less than this 1.7 L/s/ha threshold 87.6% (WH Small), 89.3% (PT), 94.1% (WH Large), and 99.7% (PT) and of the total flow duration. This suggested high flows were in a similar range and duration to a nearby agricultural (i.e., low imperviousness) watershed.

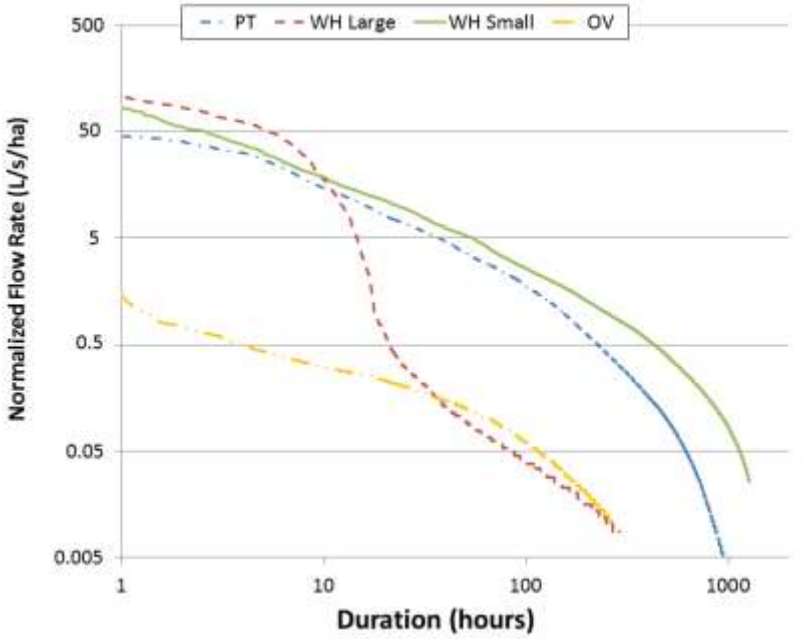

Figure 5-10. Flow duration curves for outflow for the permeable pavements.

5.6 Summary and Conclusions

Four permeable pavements in northern Ohio were monitored to quantify their water balances and hydrologic benefits. Based on analysis presented herein, the following conclusions can be drawn:

1) Underling soil vertical K_{sat} measured during construction was representative of HSG D soils at two of the research sites, but varied over 3 orders of magnitude at the third. This shows (1) the spatial variability of soils (especially fill soils) at the site-scale and (2) the need for soil K_{sat} better predict the post-construction hydrologic performance of permeable pavements.

2) Post-construction drawdown rates generally followed linear trends, suggesting vertical exfiltration was the dominant factor for volume reduction. At PT, the post-construction drawdown rates were similar to vertical K_{sat} measured during construction, suggesting soil de-compaction efforts during construction were effective. De-icing salt may have negatively impacted post-construction K_{sat} at WH. Perhaps additional lateral exfiltration could have been achieved through design of deeper IWS zones.

3) Cumulative volume reduction varied from 16% to 53% for permeable pavements with low drawdown rates (<0.35 mm/hr) and LRs for exfiltration of at least 4:1. At OV, which treated only direct rainfall, outflow volume was reduced by 98.8%, but results from this site were probably impacted by the curtain drains. Inclusion of a 15-cm IWS zone in each SCM was identified as a major contributing factor to volume reduction through exfiltration and evaporation. Given proper design and installation, permeable pavement can successfully reduce volume, even when constructed in extremely low permeability soils.

4) Four to eighty percent of observed storm events produced no outflow from the permeable pavements. Lower LRs for exfiltration, reduced surface bypass, and higher drawdown rates positively impacted the percentage of completely captured events. Discharge thresholds for each site varied from a minimum of 3.0 mm at WH Small (highest

LR for exfiltration) to 25.2 mm at OV (which treated only direct rainfall). A synthesis of these results suggests: (1) pre-construction soil infiltration testing is critical to understanding potential hydrologic performance of permeable pavements, (2) minimizing LR will improve hydrologic function while reducing surface clogging, (3) for volume reduction to occur, stormwater has to infiltrate the pavement surface (and therefore maintenance is critical), and (4) implementing an IWS zone will dramatically improve hydrologic performance, especially in low permeability soils.

5) Across all sites, substantial peak flow mitigation was observed for rainfall events when surface runoff did not occur. This included at least 80% peak flow mitigation for all 7 events at PT and OV exceeding the 1-year, 5-minute design rainfall intensity for the Cleveland, Ohio area. For sites that had surface runoff, peak flow mitigation was impacted substantially [e.g., WH Small (27-61%) and WH Large (0-11%)]. The fraction of rainfall infiltrating the pavement surface, the presence of an IWS zone, the drawdown rate, and the LR were the governing factors for peak flow mitigation.

5.7 References

Ahiablame, L.M., Engel, B.A., and Chaubey, I. (2012). "Effectiveness of low impact development practices: literature review and suggestions for future research." *Water Air Soil Poll*., 223(7), 4253-4273.

Ball, J.E., and Rankin, K. (2010). "The hydrological performance of a permeable pavement." *Urb. Water J*., 7(2), 79-90.

Bean, E.Z., Hunt, W.F., and Bidelspach, D.A. (2007). "Evaluation of four permeable pavement sites in eastern North Carolina for runoff reduction and water quality impacts.*" J. Irrig. Drain. Eng.*, 133(6), 583-592.

Brattebo, B.O., and Booth, D.B. (2003). "Long-term stormwater quantity and quality performance of permeable pavement systems." *Water Res*., 37(18), 4369-4376.

Brown, R.A., and Hunt, W.F. (2011). "Impacts of media depth on effluent water quality and hydrologic performance of undersized bioretention cells." *J. Irrig. Drain. Eng*., 137(3), 132-143.

Chin, D.A. (2006). *Water resources engineering*. 2nd edition. Pearson Prentice Hall, Upper Saddle River, NJ.

Collins, K.A., Hunt, W.F., and Hathaway, J.M. (2008). "Hydrologic comparison of four types of permeable pavement and standard asphalt in eastern North Carolina." *J. Hydrol. Eng*., 13(12), 1146-1157.

Davis, A.P. (2008). "Field performance of bioretention: hydrology impacts." *J. Hydrol. Eng*., 13(2), 90-95.

Davis, A.P., Stagge, J.H., Jamil, E., and Kim, H. (2012) "Hydraulic performance of grass swales for managing highway runoff." *Water Res*., 46(20), 6775-6786.

Dietz, M.E., and Clausen, J.C. (2008). "Stormwater runoff and export changes with development in a traditional and low impact subdivision." *J. Environ. Man.*, 87(4), 560-566.

Drake, J., Bradford, A., and Marsalek, J. (2013). "Review of environmental performance of permeable pavement systems: state of the knowledge." *Water Qual. Res. J. Canada*, 48(3), 203-222.

Drake, J., Bradford, A., and Van Seters, T. (2014). "Hydrologic performance of three partial-infiltration permeable pavements in a cold climate over low permeability soil." *J. Hydrol. Eng.*, 19(9), 04014016-1.

Dreelin, E.A., Fowler, L., and Carroll, C.R. (2006). "A test of porous pavement effectiveness on clay soils during natural storm events." *Water Res.*, 40(4), 799-805.

Driscoll, E. (1989). *Analysis of Storm Event Characteristics for Selected Rainfall Gages Throughout the United States: Draft*. US Environmental Protection Agency.

Eisenberg, B.E., Lindow, K.C., and Smith, D.R. (2015). *Permeable pavements*. 1st Ed., American Society of Civil Engineers, Reston, VA.

Fangmeier, D.D., Elliot, W.J., Workman, S.R., Huffman, R.L., and Schwab, G.O. (2006). *Soil and water conservation engineering*. 5th edition. Thomson Delmar learning, Clifton Park, NY.

Fassman, E.A., and Blackbourn, S. (2010). "Urban runoff mitigation by a permeable pavement system over impermeable soils." *J. Hydrol. Eng.*, 15(6), 475-485.

Finkenbine, J.K., Atwater, J.W., and Mavinic, D.S. (2000). "Stream health after urbanization." *J. Am. Water Res. Assoc.*, 36(5), 1149-1160.

Frenkel, H., Goertzen, J.O., and Rhoades, J.D. (1978). "Effects of clay type and content, exchangeable sodium percentage, and electrolyte concentration on clay dispersion and soil hydraulic conductivity." *Soil Sci. Soc. Am. J.*, 42(1), 32-39.

Gilbert, J.K., and Clausen, J.C. (2006). "Stormwater runoff quality and quantity from asphalt, paver, and crushed stone driveways in Connecticut." *Water Res.*, 40(4), 826-832.

Grant, D.M., and Dawson, B.D. (2001). *Isco open channel flow measurement handbook*. 5th edition. Isco, Inc., Lincoln, NE.

Gulliver, J.S., Erickson, A.J., and Weiss, P. (2010). *Stormwater treatment: Assessment and maintenance*. University of Minnesota, St. Anthony Falls Laboratory. Minneapolis, MN. http://stormwaterbook.safl.umn.edu.

James, W., and Thompson, M.K. (1997). "Contaminants from four new pervious and impervious pavements in a parking lot." In: James W (ed) *Advances in modeling and management of stormwater impacts*, CHI, Guelph, Canada, 207–222.

Line, D.E., and White, N.M. (2007). "Effects of development on runoff and pollutant export." *Water Environ. Res.*, 79(2), 185–190.

McConnell, D., Levinson, A.A., and de Pablo-Galan, L. (1956). "Study of some chemically analyzed Ohio clays by X-ray diffraction and differential thermal analysis." *Ohio J. Sci.*, 56(5), 275-284.

McNeal, B.L., and Coleman, N.T. (1966). “Effect of solution composition on soil hydraulic conductivity.” *Soil Sci. Soc. Am. J.*, 30(3), 308-312.

Meyer, J.L., Paul, M.J., and Taulbee, W.K. (2005). “Stream ecosystem function in urbanizing landscapes.” *J. North Am. Benth. Soc.*, 24(3), 602–612.

Mulvany, T.J. (1851). “On the use of self-registering rain and flood gauges in making observations of the relation of rainfall and flood discharges in a given catchment.” *Trans. Inst. Civil Eng. Ireland.*, 4, 18-33.

National Oceanic and Atmospheric Administration (NOAA) (2015) NOAA Atlas 14 point precipitation frequency estimates, Ohio. Hydrometeorological Design Studies Center, Precipitation Frequency Data Server. Available: http://dipper.nws.noaa.gov/hdsc/pfds/pfds_map_cont.html?bkmrk=oh

Natural Resources Conservation Service (NRCS) (1986) *Urban hydrology for small watersheds*. Technical Release 55 (TR-55). 2nd edition. United States Department of Agriculture (USDA), NRCS, Conservation Engineering Division.

NRCS (2004) “Estimation of direct runoff from storm rainfall.” In: *National engineering handbook*, Chapter 10: hydrology. Washington, DC, pgs. 1–22.

National Oceanic and Atmospheric Administration (NOAA). (2015). *NOAA Atlas 14 point precipitation frequency estimates, Ohio.* Hydrometeorological Design Studies Center, Precipitation Frequency Data Server. Available: http://dipper.nws.noaa.gov/hdsc/pfds/pfds_map_cont.html?bkmrk=oh

Ohio Environmental Protection Agency (OEPA). (2011). *Total maximum daily loads for the Grand River (lower) watershed*. Available: http://www.epa.ohio.gov/portals/35/tmdl/LowerGrand_PN_Report.pdf

Ohio Department of Natural Resources (ODNR), Division of Soil and Water Conservation (2006) *Rainwater and land development: Ohio’s standards for stormwater management, low impact development, and urban stream protection*. 3rd edition. Ed: John Mathews.

Olson, N.C., Gulliver, J.S., Nieber, J.L., and Kayhanian, M. (2013). “Remediation to improve infiltration into compact soils.” *J.Environ. Man.* 117, 85–95.

Page, J.L., Winston, R.J., Mayes, D.B., Perrin, C., and Hunt, W.F. (2015). “Hydrologic mitigation of impervious cover in the municipal right-of-way through innovative stormwater control measures.” *J. Hydrol.* 527, 923-932.

Pratt, C.J., Mantle, J.D.G., and Schofield, P.A. (1995). “UK research into the performance of permeable pavement, reservoir structures in controlling stormwater discharge quantity and quality.” *Water Sci. Technol.*, 32(1), 63–69.

Pupisky, H., and Shainberg, I. (1979). “Salt effects on the hydraulic conductivity of a sandy soil.” *Soil Sci. Soc. Am. J.*, 43(3), 429-433.

Reynolds, W.D., Elrick, D.E., Youngs, E.G., and Amoozegar, A. (2002) “Ring or cylinder infiltrometers (vadose zone).” In: Dane JH, Topp GC (eds) *Methods of Soil Analysis - Part 4: Physical Methods*. Soil Science Society of America. Madison, WI.

Roseen, R.M., Ballestero, T.P., Houle, J.J., Avellaneda, P., Briggs, J., Fowler, G., and Wildey, R. (2009). “Seasonal performance variations for storm-water management systems in cold climate conditions.” *J. Environ. Eng.*, 135(3), 128-137.

Roseen, R.M., Ballestero, T.P., Houle, J.J., Briggs, J.F., and Houle, K.M. (2012). “Water quality and hydrologic performance of a porous asphalt pavement as a storm-water treatment strategy in a cold climate.” *J. Environ. Eng*., 138(1), 81-89.

Rushton, B.T. (2001). “Low-impact parking lot design reduces runoff and pollutant loads.” *J. Water Res. Plan. Man.*, 127(3), 172–179.

Schueler, T.R., Fraley-McNeal, L., and Cappiella, K. (2009). “Is impervious cover still important? Review of recent research.” *J. Hydrol. Eng.*, 14(4), 309–315.

Schwartz, S.S. (2010). “Effective curve number and hydrologic design of pervious concrete storm-water systems.” *J. Hydrol. Eng.*, 15(6), 465-474.

Shainberg, I., Rhoades, J.D., and Prather, R.J. (1981). “Effect of low electrolyte concentration on clay dispersion and hydraulic conductivity of a sodic soil.” *Soil Sci. Soc. Am. J.*, 45(2), 273-277.

Smolek, A.P., Winston, R.J., Dorsey, J.D., and Hunt, W.F. (2015). *Modeling the hydrologic performance of bioretention and permeable pavement stormwater controls in northern Ohio using DRAINMOD: Calibration, validation, sensitivity analysis, and future climate scenarios.* Final report submitted to the University of New Hampshire and the Chagrin River Watershed Partners, Inc. In fulfilment of NOAA Award number NA09NOS4190153. *These authors contributed equally to this work.

Smolek, A.P., Winston, R.J., and Hunt, W.F. (2016). “Hydrologic and water quality performance of a permeable pavement with internal water storage over a Hydrologic Soil Group D soil in North Carolina.” Submitted to *J. Environ. Eng.*

Smolek, A.P., Winston, R.J., Dorsey, J.D., Youssef, M., Hunt, W.F. (2016). “Calibration and validation of DRAINMOD to predict annual permeable pavement hydrology.” Submitted to *J. Hydrol.*

Soil Survey Staff, NRCS, United States Department of Agriculture (2015) Web Soil Survey. http://websoilsurvey.nrcs.usda.gov/. Accessed 28 January 2015.

Sparks, D.L. (2003). *Environmental soil chemistry*. 2nd edition, Academic Press.

Tillinghast, E.D., Hunt, W.F., and Jennings, G.D. (2011). "Stormwater control measure (SCM) design standards to limit stream erosion for Piedmont North Carolina." *J. Hydrol*., 411(3), 185-196.

Tyner, J.S., Wright, W.C., and Dobbs, P.A. (2009). "Increasing exfiltration from pervious concrete and temperature monitoring." *J. Environ. Man.*, 90(8), 2636-2641.

Vieth, E. (1989). "Fitting piecewise linear regression functions to biological responses." *J. App. Phys.*, 67(1), 390-396.

Walsh, C.J., Roy, A.H., Feminella, J.W., Cottingham, P.D., Groffman, P.M., and Morgan, R.P. (2005). "The urban stream syndrome: current knowledge and the search for a cure." *J. North Am. Benthological Soc.*, 24(3), 706-723.

Walsh, C.J., Fletcher, T.D., and Burns, M.J. (2012). "Urban stormwater runoff: a new class of environmental flow problem." *PLOS ONE*, 7(9).

Wardynski, B.J., Winston, R.J., and Hunt, W.F. (2012). "Internal water storage enhances exfiltration and thermal load reduction from permeable pavement in the North Carolina mountains." *J. Environ. Eng.*, 139(2), 187-195.

CHAPTER 6: **SEASONAL VARIABILITY IN STORMWATER QUALITY TREATMENT FOR PERMEABLE PAVEMENTS CONSTRUCTED IN CLAY SOILS AND IN A COLD CLIMATE**

6.1 Abstract

Permeable pavements mitigate impacts of urbanization on surface waters through pollutant load reduction, both by sequestration of pollutants and stormwater volume reduction through exfiltration. This study examined the non-winter water quality performance of two side-by-side permeable pavements in the Ohio snow-belt. The permeable interlocking concrete pavements were designed to drain impervious catchments 2.2 (Large) and 6.2 (Small) times larger than their surface area, were located over clay soils, and incorporated the internal water storage design feature. Nutrient reduction was similar to past studies – organic nitrogen and particulate phosphorus were removed through filtration and settling, while dissolved constituents received little treatment. Because of 16 and 32% volume reductions in the Small and Large installations, respectively, nutrient loads were often significantly reduced, but generally by less than 50%. Heavy metals, chloride, and TSS concentrations and loads often increased after passing through the permeable pavements; TSS loads were 3- to 5-fold higher. This was apparently due to seasonal release of clay- and silt-sized particles from the permeable pavement subgrade and inversely related to elapsed time since winter. The application of de-icing salt is thought to have caused deflocculation of particulate matter, allowing solids to exist with stormwater as it discharged from the permeable pavements. By autumn, both permeable pavements were discharging metals and TSS similarly to others in the literature, suggesting the de-icing effects lasted 3-6 months post-winter. Sodium may substantially affect the performance of permeable pavements

following winter road salt application, particularly when 2:1 clays, such as vermiculites and smectites, predominate.

6.2 Introduction

Urbanization results in the construction of impervious surfaces, leading to flashier hydrology, increased runoff volume, and prolonged duration of erosive flow rates (Epsey et al. 1966; Roesner et al. 2001; Roy et al. 2005). Urbanization modifies stream channel morphology and cause stream bank erosion and channel incision, thereby reducing biotic richness in-stream (Neller 1989; Paul and Meyer 2001; Grimm et al. 2005). Collectively, these impacts have been termed the "urban stream syndrome," with total catchment imperviousness, distance between the stream and the urban land use, and hydraulic efficiency of drainage infrastructure greatly impacting the level of stream degradation (Dunne and Leopold 1978; Hirsch et al. 1990; Booth et al. 2004; Walsh et al. 2005).

To combat the deleterious effects of impervious cover, engineers have developed stormwater control measures (SCMs), such as permeable pavement, to attempt to match pre- and post-development hydrologic fates (Li et al. 2009; Fassman and Blackbourn 2010; DeBusk et al. 2010). Permeable pavements allow stormwater to infiltrate, and then stormwater is stored in an underlying aggregate reservoir. They provide the unique dual benefits of stormwater treatment and maintenance of buildable area (Pezzaniti et al. 2009). Previous research studies have shown permeable pavements attenuate runoff volume when compared to impervious parking lots, thereby reducing pollutant loading to receiving water bodies (Bean et al. 2007; Collins et al. 2008; Fassman and Blackbourn 2010; Roseen et al. 2012; Drake et al. 2014a).

Permeable pavements generally improve stormwater quality by reducing total suspended solids (Legret et al. 1996; Roseen et al. 2012; Drake et al. 2014b), metals (Legret et al. 1996; Bean et al. 2007; Roseen et al. 2012; Drake et al. 2014b), and hydrocarbon concentrations (Roseen et al. 2012; Drake et al. 2014b). The pavement layer, where sediment and grit are retained, is cited as a major sink for sediment and sediment-bound pollutants (such as the metals lead, cadmium, copper, and zinc) in permeable pavements (Roseen et al. 2012). Additionally, settling, biological degradation, and chemical mechanisms further pollutant retention within permeable pavements, typically at a geotextile layer or at the interface with the *in situ* soil (Pratt et al. 1999; Franks et al. 2014). Forty to 90% of total phosphorus has been retained by permeable pavement (Bean et al. 2007; Roseen et al. 2012; Drake et al. 2014b).

Dissolved constituents, such as chloride from road salts and nitrate and nitrite nitrogen ($NO_{2\text{-}3}$), tend to migrate through the permeable pavement cross-section with little to no treatment (Collins et al. 2010; Borst and Brown 2014). In fact, nitrification within the permeable pavement often causes export of $NO_{2\text{-}3}$ (Collins et al. 2010; Drake et al. 2014b). Buildup of chloride in the permeable pavement cross-section may cause it to be detectable year-round in drainage samples (Borst and Brown 2014). Because porous asphalt provides better skid resistance and improved drainage when compared to dense-mix asphalt, it required four times less winter salt application to achieve the same level-of-service (Roseen et al. 2014).

Given dissolved pollutants are often cited for causing water quality degradation such as eutrophication (Smith et al. 1999) and chloride toxicity (U.S. EPA 1988; Fay and Shi 2012),

novel permeable pavement designs must be developed to further reduce their discharge to surface waters. One such design, now common in bioretention, includes an internal water storage (IWS) zone, which utilizes an upturned elbow in the underdrain to create ponding within an SCM (Hunt et al. 2012). The IWS zone has been shown to promote denitrification in bioretention, thereby reducing nitrate concentrations (Kim et al. 2003) and to promote exfiltration of additional stormwater from permeable pavements (Wardynski et al. 2012, when compared to traditional drainage configurations), thereby reducing pollutant loads. Given its promising results for nutrient treatment in bioretention and initially positive hydrologic results in permeable pavement, this design feature should be studied for its impacts on pollutant concentrations and loads from permeable pavements.

Research is also needed to determine how permeable pavements function for water quality goals under higher hydrologic loading. Additionally, the vast majority of permeable pavements studied have been located over sandy soils (e.g., Rushton 2001; Brattebo and Booth 2003; Bean et al. 2007; Kwiatkowski et al. 2007; Collins et al. 2008) characterized by elevated infiltration rates. The goals of this study were to determine (1) the effects of hydrologic loading on the water quality performance of permeable pavements over poorly-drained soils and under northeast Ohio climatic conditions, (2) the impact of purposefully-designed IWS zones within permeable pavements on water quality, and (3) how a poorly-drained HSG D soil affects pollutant retention. Two side-by-side permeable pavement applications were monitored for a fourteen-month period to explore these questions.

6.3 Site Description

Two permeable interlocking concrete pavement (PICP) applications were retrofitted into the parking lot at the Willoughby Hills, Ohio, community center in September-October 2013 (Table 6-1, Figure 6-1, and Figure 6-2). PICP consists of impermeable brick pavers with interstitial void spaces filled with aggregate, allowing water to infiltrate the pavement surface. Both applications employed a 50-cm total aggregate depth: 5 cm of #89 stone (1.2-12.5 mm nominal diameter) bedding course immediately below the pavers, 15 cm of #57 aggregate (2.4-37 mm nominal diameter) beneath that, and 30 cm of #2 aggregate (19-75 mm nominal diameter) serving as a base course. Each PICP application had a 15-cm diameter PVC underdrain with a 15-cm upturned elbow, creating an IWS zone within the aggregate. Given the poor underlying soils, the IWS zone was expected to hold water. This extended ponding within the aggregate allowed for both vertical and lateral exfiltration into the underlying soils.

The Small application, 45 m^2 in surface area, was built with a flat subgrade so water could exfiltrate from the entire footprint (Table 6-1). The Large application (surface area of 460 m^2) had a stepped subgrade to account for the 1-2% surface slope; this resulted in four, 15-cm tall steps with the underdrain at the bottom of the cross-section. An IWS zone was present over only one-half the permeable pavement surface area, reducing the effective infiltrative surface area to 205 m^2. The contributing drainage areas for both the Small and Large applications were impermeable asphalt, with modest exception. The site was located over poorly drained Mahoning silt loam soils, a HSG D soil according to the soil survey

maps (Soil Survey Staff 2015). An adjacent 100% impervious asphalt catchment served as a control for this experiment (Figure 6-2).

The loading ratio (LR) for a permeable pavement affects hydrologic and water quality functionality. LR is calculated as:

$$LR = \frac{A_{CA}}{A_{PP}} \quad (6\text{-}1)$$

where A_{CA} is the surface area of the catchment and A_{PP} is the surface area of the permeable pavement. The LR for the Small application was 7.2, while that of the Large application was 2.2. One of the purposes of this study was to tax the Small application with much higher hydrologic loading than the 2.0 that is currently allowed in the *Ohio Rainwater and Land Development Manual* (ODNR 2006). Past studies of permeable pavement water quality have all been conducted on systems nominally treating only direct rainfall (i.e., LRs of 0.0, with no contributing run-on).

During winter months (typically November through April), the parking lot was salted prior to and plowed following each snowfall. Qualitatively, de-icing salt application rates were greatest in the Small application catchment due to its proximity to the community center and sidewalks.

Figure 6-1. Small (left) and Large (right) PICP applications at Willoughby Hills, Ohio community center.

Figure 6-2. Overview of Willoughby Hills site including permeable pavement and standard asphalt sampling sites. Existing slopes directed stormwater from south to north in each catchment.

Table 6-1. Characteristics of the Willoughby Hills permeable pavements.

Monitoring site	Total aggregate depth (cm)	Contributing watershed area (ha)	Permeable pavement surface area (m^2)	Infiltrative surface area (m^2)	Loading ratio (LR)
WH Small	50	0.032	45	45	7.2
WH Large		0.089	410	205	2.2

6.4 Materials and Methods

Data Collection

Water quality samples were obtained from three locations at the Willoughby Hills site: (1) a control (impervious asphalt location representative of the inflow to the permeable pavement), and the underdrain outfall for the (2) Small and (3) Large applications (Figure 6-2). Samples were collected within weir boxes used to measure hydrology: a 30˚ v-notch, a 60˚ v-notch, and a 30-cm wide, contracted rectangular weir were utilized for the Small application, the Large application, and the control monitoring sites, respectively. ISCO 730 bubbler modules were attached to ISCO 6712 samplers at each monitoring location and used to measure depth of flow over the weir on two minute intervals (Teledyne ISCO, Lincoln, NE). Flow depths were converted to flow rate within each automated sampler using standard weir equations:

$$Q = 373.2 * H^{2.5}, \text{ 30˚ v-notch weir} \quad (6\text{-}2)$$

$$Q = 796.7 * H^{2.5}, \text{ 60˚ v-notch weir} \quad (6\text{-}3)$$

$$Q = 1838 * (0.3 - 0.2H) * H^{1.5}, \text{ 0.3 m contracted rectangular weir} \quad (6\text{-}4)$$

where Q is flow rate (L/s) and H is head (m) over the weir crest. Flow rate was integrated over time to determine stormwater volume. Cumulative stormwater volume was used to trigger flow-proportional, composite samples obtained in 200 mL aliquots. A minimum of five aliquots were obtained from each storm, describing a minimum of 80% of the pollutograph (U.S. EPA 2002). Sample intake strainers were placed in each weir box where flow was well-mixed. Separate rainfall events were characterized by a minimum antecedent dry period of 6 hours and 2.5-mm rainfall depth. Rainfall data were collected at the site using both a manual and a 0.025-mm resolution tipping bucket rain gauge.

Internal water level within both permeable pavement cross-sections was measured on a 2-minute interval using a Hobo U20 pressure transducer within a 2.5-cm diameter well (Onset Computer Corporation, Bourne, MA). Since the pressure transducers were non-vented, an additional U20 pressure transducer was placed in the rain gauge housing at each site to measure (and later offset by) local barometric pressure. From these measurements, drawdown rate and total exfiltrated volume were determined.

The monitoring period spanned April 2014 to June 2015; stormwater samples were not obtained during December through March due to sub-freezing temperatures and frequent snowfall. During these months, the average daily temperature was -5.7˚C with a total of 1.2 meters of snowfall at Cleveland-Hopkins international airport, located approximately 50 km from Willoughby Hills (NOAA 2015).

To characterize the soils, a soil auger was used to obtain soil samples from the subgrade elevation (60 cm below grade). Eight soil samples were collected from four boring locations adjacent to the PICP installations. The two samples from each boring were composited, oven

dried, and particle size analysis tests were performed using the hydrometer method (Gee and Bauder 1986).

Laboratory Methods

Aqueous water quality samples were obtained from automated sampling equipment within 24 hours of the cessation of rainfall. They were shaken vigorously in the composite 10 L jar to re-suspend solids, and were then subsampled into laboratory sample bottles. Composite samples were divided among two 1L plastic jars for total suspended solids (TSS) analysis, one 500 mL pre-acidified bottle for nutrient analysis, and one 500 mL pre-acidified bottle for metals analysis. Orthophosphate (OP) and chloride (Cl^-) analysis was completed in the lab by subsampling from the TSS bottle and prior to filtering solids using a 0.45 μm filter.

Samples were placed immediately on ice and chilled to less than 4˚C and were delivered to the Northeast Ohio Regional Sewer District Laboratory within 18 hours of sample collection. Samples were analyzed using U.S. EPA (1983) or American Public Health Association (APHA et al. 2012) methods to determine event mean concentrations (EMCs) for: total Kjeldahl nitrogen (TKN), $NO_{2\text{-}3}$, total ammoniacal nitrogen (TAN), OP, total phosphorus (TP), TSS, chloride, and the metals aluminum, calcium, copper, iron, magnesium, manganese, sodium, lead, and zinc (Table 6-2). Total nitrogen (TN), organic nitrogen (ON), and particle-bound phosphorus (PBP) EMCs were calculated using equations in Table 6-2.

Water quality samples from a single storm event on June 10, 2015, were evaluated in the laboratory for particle size distribution (PSD) using a Beckman-Coulter 13-320 Laser Diffraction Particle Size Analyzer equipped with a Universal Liquid Module. It measured volumetric fraction of particles in the range of 0.04 – 2000 μm in 117 separate bins of particle size. This allowed for a glimpse of particle sizes which were trapped within or leached from the permeable pavement cross-section.

Table 6-2. Laboratory testing and preservation methods as well as method detection limits (MDL) and practical quantification limits (PQL) for pollutants of concern.

Parameter	Laboratory method	Preservation	MDL (mg/L)	PQL (mg/L)
TKN	EPA method 351.2[1]	H_2SO_4 (<2 pH), <4˚C	0.122	0.5
NO_{2-3}	EPA method 353.2	H_2SO_4 (<2 pH), <4˚C	0.003	0.02
TN	Calculated as TKN + NO_{2-3}	N/A	N/A	N/A
TAN	EPA method 350.1	H_2SO_4 (<2 pH), <4˚C	0.003	0.02
ON	Calculated as TKN-TAN	N/A	N/A	N/A
OP	EPA method 300.0	<4˚C	0.03	0.082
PBP	Calculated as TP-OP	N/A	N/A	N/A
TP	EPA method 365.1	H_2SO_4 (<2 pH), <4˚C	0.001	0.01
Chloride	EPA method 300.0	<4˚C	1	5
TSS	Standard methods 2540D[2]	<4˚C	1	1
Parameter	**Laboratory method**	**Preservation**	**MDL (µg/L)**	**PQL (µg/L)**
Al	EPA method 200.8	HNO_3 (<2 pH), <4˚C	0.96	10
Ca			35.8	250
Cu			0.22	2
Fe			1.76	10
Mg			13.42	250
Mn			0.46	2
Pb			0.174	1
Zn			1.3	10

[1]U.S. EPA 1983
[2]APHA et al. 2012

Data Analysis

The performance of the two permeable pavements for nutrients, metals, chloride, and TSS was determined by comparing EMCs from the impermeable asphalt catchment to the underdrain flow from each of the PICP applications (raw data can be found in Appendix C). Summary statistics for EMCs were determined, including the range, mean ($\overline{x}$), median ($\tilde{x}$),

standard deviation (s), the efficiency ratio (ER), and the median relative efficiency (RE_{median}). The latter two metrics are defined as follows:

$$ER = 1 - \frac{\sum_{i=1}^{n}(Eff\ EMC_i)/n}{\sum_{i=1}^{n}(Asp\ EMC_i)/n} \quad (6\text{-}5)$$

$$RE_{median} = 1 - \frac{Eff\ EMC_{median}}{Asp\ EMC_{median}} \quad (6\text{-}6)$$

where Eff EMC is the effluent EMC from the permeable pavement, Asp EMC is the asphalt EMC, and n is the number of storm events. The efficiency ratio is a commonly used metric for SCM performance, but is influenced by low or "irreducible" influent concentrations (Strecker et al. 2001).

Pollutant loads were calculated because they (1) account for volume reduction and (2) factor into total maximum daily load (TMDL) regulations. Pollutant loads were calculated using:

$$L = \frac{\sum_{i=1}^{n}(EMC_{loc,i} \times V_{loc,i}) \times \frac{RF_{avg\ yearly}}{\sum RF_{sampled}}}{A_{CA}} \times C \quad (6\text{-}7)$$

where L is the pollutant load (kg/ha/yr), n is the total number of sampled storms, EMC_{loc} is the measured EMC at a particular monitoring location (mg/L), V_{loc} is the stormwater volume during the event (m^3), $RF_{avg\ yearly}$ is the average yearly rainfall (mm), and $RF_{sampled}$ is the rainfall depth sampled over the monitoring period (mm), A_{CA} is the area of the catchment (m^2), and C is a conversion factor to convert to kg/ha/yr. Between 15 and 18 wet-weather events were sampled for water quality analysis and thus considered for loading calculations. Storms with no outflow, which only occurred in the Large application, contributed influent but not effluent pollutant load. A substantial volume of surface runoff (24% of the water

balance over the monitoring period), occurred for the Large application due to clogging of the pavement surface (Winston et al. 2015); no pollutant attenuation was assumed for surface runoff in calculations. Influent and effluent loads were compared by calculating a percent load reduction:

$$\%\ Load\ Reduction = \frac{L_{in} - L_{out}}{L_{in}} \quad (6\text{-}8)$$

where L_{in} is the annual loading (kg/ha/yr) from the parking lot and L_{out} is the annual loading (kg/ha/yr) at the outlet of a permeable pavement. Paired statistical analyses were used to compare asphalt runoff and outlet EMCs and loads. If data were normal or log-normal, a paired t-test was utilized to determine significance. Normality was determined using Anderson-Darling and Shapiro-Wilkes tests and through visual analysis of quantile-quantile plots. If data were non-normal, a Wilcoxon rank sum test was applied to determine statistical significance. Differences between effluent EMCs for the Small and Large applications were also investigated to determine if LR affected permeable pavement performance.

Kruskal-Wallis k-sample tests were utilized to determine whether seasonality of rainfall depth and intensity were statistically significant. If this omnibus test was significant, pair-wise comparisons were made using Dunn's test with a Bonferroni adjustment to determine seasons with greater storm depths or intensities. Seasons were demarcated by solstices and equinoxes.

Since seasonality was suspected for portions of the water quality data, summary statistics for TSS, metals, and chloride were tabulated by season. Additionally, these parameters were plotted with time to visualize trends related to season. Spearman's rank correlation was used

to determine significance of relationships between TSS EMCs and rainfall depth, intensity, antecedent dry period, and season.

All data analysis was completed using R version 3.1.2 (R Core Team, 2015). A criterion of 95% confidence (α=0.05) was used for this research. For all pollutants except TAN and OP, all laboratory-reported EMCs for the sampled storms were above the PQL, and were analyzed without transformation. For six storms for OP and one for TAN, a value of one-half the detection limit was substituted for EMCs below the PQL (Antweiler and Taylor 2008).

6.5 Results and Discussion

Sampled Storm Events

Over the 14-month monitoring period, 75 storms exceeding 2.5-mm rainfall depth were observed at Willoughby Hills, Ohio (Table 6-3). Eighteen storms were sampled for water quality for the Small application, while 12 storms were sampled at the Large application (6 storms had no outflow). The rainfall characteristics of all monitored and sampled events are shown in Figure 6-3 and Table 6-3; snowfall occurred during the winter months and was not included in this analysis. Sampled storms tended to be larger and more intense than the overall distribution of storms; however, the four largest storms during the monitoring period were not sampled for water quality analysis. The Kruskal-Wallis k-sample test showed significant difference among seasons for distributions of rainfall depth (p-value=0.01) and rainfall intensity (p-value<0.001). Pairwise comparisons using Dunn's test with a Bonferroni adjustment confirmed spring and summer rainfall depths and intensities were statistically greater than those in the fall (p-values<0.025). Median storm depths were 9 and 18.8 mm,

and 5-minute peak rainfall intensities were 12.2 and 36.6 mm/hr for all and sampled storms, respectively). Since sampled storms were larger and more intense than the overall distribution of storms, data presented herein may provide conservative assessments of water quality. Smaller storms are more likely to be completely captured and have a larger average hydraulic retention time.

Table 6-3. Summary statistics for all monitored storms and sampled storms at Willoughby Hills.

Statistic	All Storms		Sampled Storms	
	Rainfall Depth (mm)	Peak Rainfall Intensity (mm/hr)	Rainfall Depth (mm)	Peak Rainfall Intensity (mm/hr)
Minimum	2.5	3.0	8.6	3.0
Median	9.0	12.2	18.8	36.6
Mean	14.1	25.4	21.3	46.3
Maximum	86.9	167.6	55.1	167.6

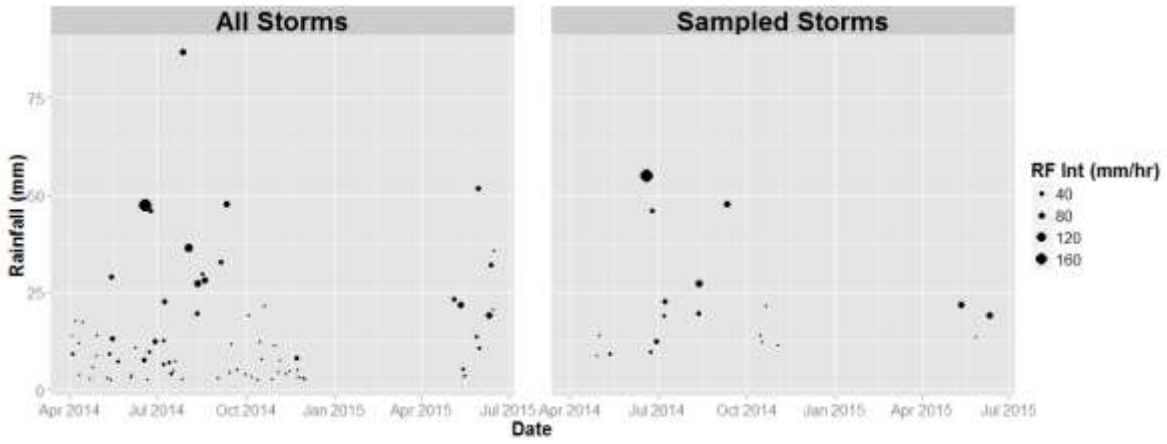

Figure 6-3. Distribution of rainfall depths (mm) for all observed and sampled storms at Willoughby Hills with peak 5-minute rainfall intensity (mm/hr) shown by the diameter of the marker.

Pollutant Concentrations

Nutrients

ER and RE_{median} for nitrogen and phosphorus species for the permeable pavements were near zero (Table 6-4). Paired statistical testing showed most nutrient EMCs were not significantly reduced. Organic nitrogen ERs suggested filtration and sedimentation occurred in the permeable pavement, but no ON and TKN changes were significant for either permeable pavement (Figure 6-4). NO_{2-3} and TN EMCs significantly increased for the Small application (ERs of -1.14 and -0.25, respectively), similar to the findings of Bean et al. (2007) and Drake et al. (2014b). No significant export of NO_{2-3} was observed from the Large application. The effluent EMCs of NO_{2-3} and TN from the Large application were significantly different from those of the Small application, suggesting LR may influence NO_{2-3} export from permeable pavements. This along with surface clogging concerns induced by higher hydraulic loading may be a reason to limit run-on from impermeable surfaces (Lucke and Beecham 2011). Other than NO_{2-3}, TN, and TAN, no significant differences existed between effluent EMCs of nutrients and TSS for the two permeable pavements (Figure 6-4).

Aerobic transformation of TAN and ON to dissolved NO_{2-3} has been cited as a probable cause for this export of NO_{2-3} from permeable pavements (Collins et al. 2010; Tota-Maharaj and Scholz 2010). An anaerobic zone with a carbon source would be needed to encourage denitrification; while the IWS zones *always* had water ponded within them, air entry through the PICP interstitial spaces may have kept the dissolved oxygen levels above 0.5 mg/L, generally accepted to be the value needed for denitrification to occur

(Van Haandel and Van der Lubbe 2012). The IWS zone also lacked a carbon source, such as mulch or other organic matter, needed to drive denitrification (Knowles 1982).

Median and mean TP EMCs from the asphalt catchment at Willoughby Hills were 0.05 mg/L, quite low for an urban parking lot (Table 6-4). Passeport and Hunt (2009) observed mean TP EMCs of 0.19 mg/L for 8 parking lots in North Carolina. Similarly, median TP EMCs were 0.27 mg/L from nearly 4000 samples of urban runoff from across the U.S. compiled in the National Urban Stormwater Quality Database (Pitt et al. 2004). Differences between asphalt runoff and effluent TP EMCs were not statistically different, suggesting influent EMCs were "irreducible" given typical permeable pavement pollutant removal unit processes (Strecker et al. 2001). The Small and Large applications had median effluent TP EMCs of 0.04-0.05 mg/L, which were in the range of those (0.03-0.05 mg/L) observed by Bean et al. (2007), Roseen et al. (2012), and Drake et al. (2014b) for PICP. A similar "irreducible" concentration may also have been observed for orthophosphate, where median effluent EMCs herein (0.017 mg/L) were very similar to those for PICP (0.019 mg/L) in Drake et al. (2014b).

TSS Results

Statistically significant *increases* in TSS EMCs occurred for both the Small and Large applications; this has not been observed by other field or laboratory studies on permeable pavements (Legret et al. 1996; Bean et al. 2007; Roseen et al. 2012; Drake et al. 2014b; Drake et al. 2014c). ERs were -4.1 and -5.1, respectively, for the Small and Large applications; median effluent EMCs were 97 and 154 mg/L, ten-fold greater than other permeable pavements (Bean et al. 2007; Roseen et al. 2011; Drake et al. 2014b;

Drake et al. 2014c). Legret et al. (1996) observed effluent EMCs up to 139 mg/L for a permeable pavement in France; however, the mean effluent EMC was 12 mg/L and no reasoning was given for this elevated EMC.

Increases in TSS EMCs suggested sediment was being entrained by the stormwater as it passed through the cross-section of the permeable pavements. Stormwater passing over the subgrade soil may have collected the clayey subsoil sediment, also helping to export metals (significantly in some cases, discussed later). Since the subgrade soil was 60 cm below grade (i.e., in the B horizon of the Mahoning clay soil, National Cooperative Soil Survey 2014), it should contain very little organic nitrogen. Organic nitrogen EMCs did not significantly increase, suggesting inorganic particulates were lost from both permeable pavements. Eight soil samples obtained at the depth of the subgrade were characterized by 18-21% sand, 47-53% silt, and 28-36% clay.

Table 6-4. Summary statistics for nutrient and sediment EMCs for the Willoughby Hills permeable pavements. Bolded p-values are significant differences. Bolded and underlined p-values are significant increases in pollutant EMC.

Pollutant	Location	Range (mg/L)	$\overline{X}$ [1] (mg/L)	$\tilde{X}$ [2] (mg/L)	s [3] (mg/L)	ER	RE_{median}	Stat. Comp.[4]	p-value
TKN	Asphalt	0.24-5	0.99	0.63	1.07	-	-	SO-LO[5]	0.373
	Sm Out	0.24-2.7	0.86	0.59	0.69	0.13	0.07	I-SO[6]	0.144
	Lg Out	0.14-1.5	0.74	0.81	0.47	0.25	-0.28	I-LO[7]	0.104
NO_{2-3}	Asphalt	0.1-1.7	0.42	0.38	0.33	-	-	SO-LO	**0.006**
	Sm Out	0.2-1.9	0.90	0.63	0.60	-1.14	-0.66	I-SO	**<u>0.001</u>**
	Lg Out	0.11-0.9	0.46	0.46	0.30	-0.1	-0.20	I-LO	0.762
TN	Asphalt	0.43-5.4	1.41	1.01	1.20	-	-	I-SO	**0.018**
	Sm Out	0.64-3.6	1.76	1.22	1.08	-0.25	-0.20	I-LO	**<u>0.028</u>**
	Lg Out	0.36-2.4	1.21	1.00	0.70	0.14	0.02	SO-LO	0.255
TAN	Asphalt	0-1.2	0.23	0.14	0.31	-	-	I-SO	**0.04**
	Sm Out	0.002-0.8	0.19	0.12	0.21	0.19	0.18	I-LO	0.678
	Lg Out	0.01-0.5	0.23	0.28	0.14	-0.01	-0.95	SO-LO	0.700
ON	Asphalt	0.23-3.7	0.76	0.54	0.79	-	-	I-SO	0.070
	Sm Out	0.11-2.3	0.67	0.43	0.55	0.11	0.21	I-LO	0.644
	Lg Out	0.05-1	0.51	0.54	0.37	0.32	0.00	SO-LO	**0.037**
OP	Asphalt	0.002-0.056	0.019	0.017	0.016	-	-	I-SO	0.278
	Sm Out	0.003-0.045	0.013	0.017	0.010	0.29	0.00	I-LO	0.340
	Lg Out	0.004-0.017	0.013	0.017	0.005	0.29	0.00	SO-LO	0.301
PBP	Asphalt	0.007-0.092	0.04	0.05	0.02	-	-	I-SO	0.310
	Sm Out	0.005-0.164	0.04	0.03	0.04	0.10	0.41	I-LO	0.268
	Lg Out	0.019-0.164	0.06	0.04	0.04	-0.29	0.14	SO-LO	0.831
TP	Asphalt	0.02-0.1	0.05	0.05	0.02	-	-	I-SO	0.125
	Sm Out	0.02-0.18	0.05	0.04	0.04	0.03	0.25	I-LO	0.754
	Lg Out	0.02-0.18	0.07	0.05	0.05	-0.21	0.10	SO-LO	0.125
TSS	Asphalt	4-154	26	12	35	-	-	I-SO	0.988
	Sm Out	5-723	131	97	166	-4.06	-6.92	I-LO	**<u>0.002</u>**
	Lg Out	12-360	159	154	89	-5.1	-11.5	SO-LO	**<u><0.0001</u>**

[1] $\overline{X}$ is the mean, [2] $\tilde{X}$ is the median, and [3] s is the standard deviation

[4] Statistical comparison

[5] Small vs. large outlet, [6] inlet vs. small outlet, and [7] inlet vs. large outlet comparisons.

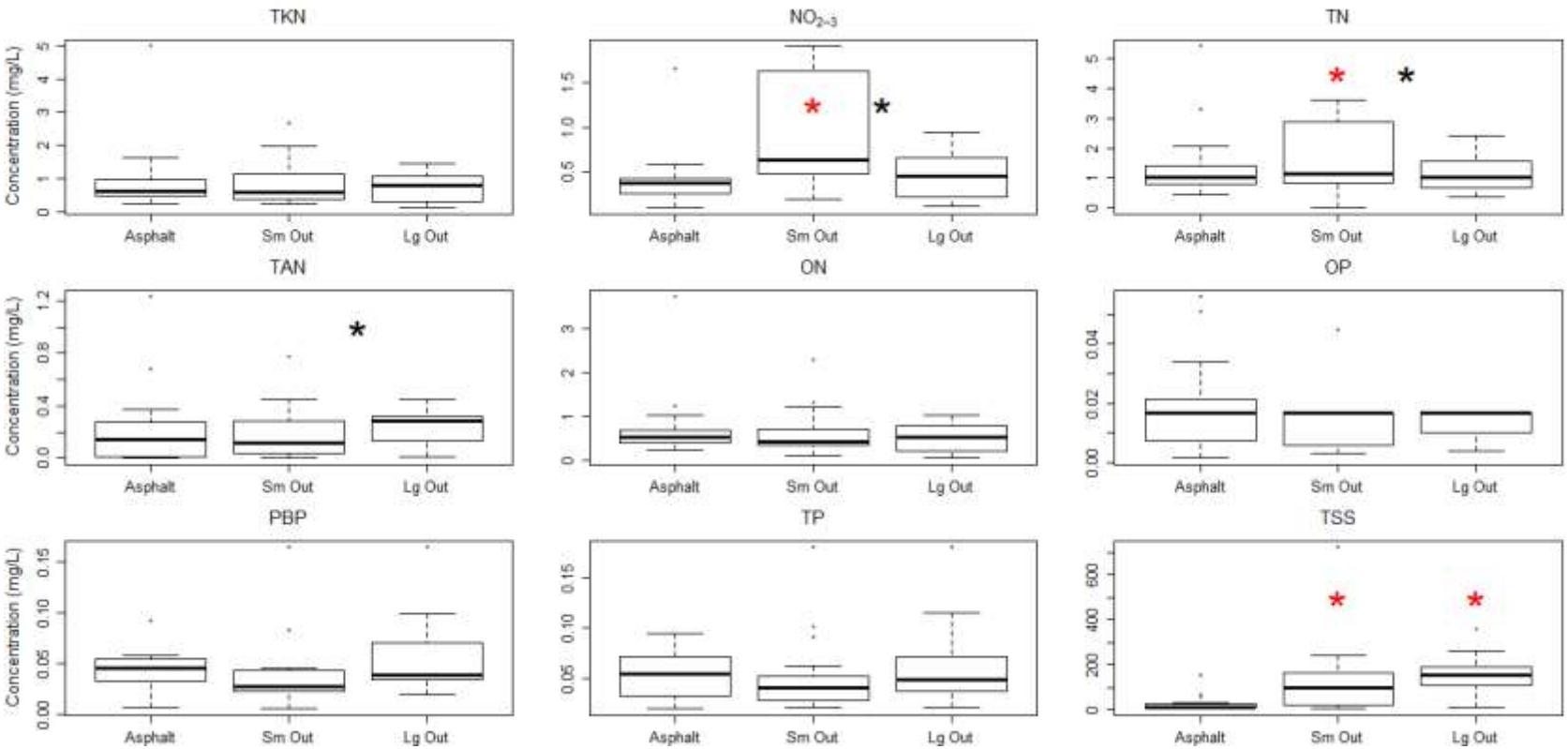

Figure 6-4. Boxplots of nutrient and sediment EMCs showing asphalt, Small application outlet (Sm Out), and Large application outlet (Lg Out) EMCs for Willoughby Hills. Statistically significant differences shown with asterisks, with red asterisks indicating significant increases in pollutant EMC. Asterisks above an outlet boxplot indicate significant differences between the asphalt runoff and outlet EMCs. Asterisks between the two outlet boxplots indicate significant differences between effluent EMCs.

Drake et al. (2014b) found decreasing effluent TSS EMCs over time from permeable pavement mesocosms, presumably due to dust present on the aggregate from quarrying and crushing. The authors suggested "dust release" led to a "maturation period" following construction. Once the dust washed off, consistent drainage water quality was observed. For the first 4 months of monitoring at Willoughby Hills, TSS effluent EMCs were higher than those from the asphalt runoff (Figure 6-5). Asphalt runoff EMCs were quite low (consistently less than 25 mg/L) and less than those in past studies (Bannerman et al. 1993; Drake et al. 2014b). In fall 2014, effluent EMC substantially decreased to less than 25 mg/L. Similar trends were observed for Pb, Cu, and Cl^-, whose effluent EMCs trended downward in a linear fashion over 2015, while asphalt runoff EMCs remained approximately the same (Figure 6-5). Soils were raked during construction with the teeth of the excavator bucket (Figure 6-6) to reduce soil compaction and improve exfiltration; geotextile was not used to separate the aggregate from the underlying soil due to concerns with geotextile clogging (Boving et al. 2004). Therefore, loose sediment could have been entrained in the stormwater; as the finite amount of loose sediment is depleted in the IWS zone, effluent EMCs from these permeable pavements would be expected to decrease with time, which occurred over the course of 2014 (Figure 6-6).

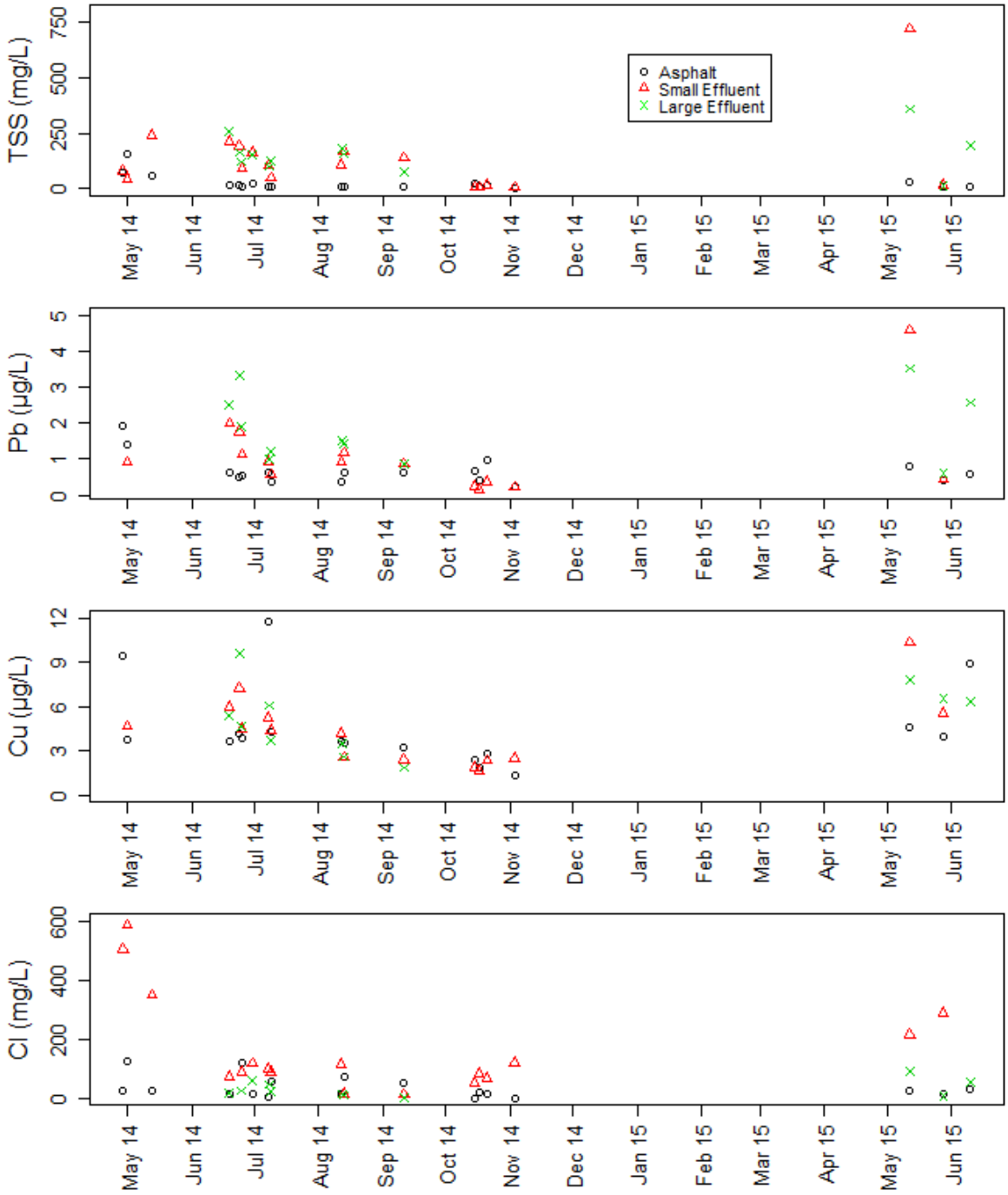

Figure 6-5. TSS, Pb, Cu, and Cl^- EMCs as a function of time for the permeable pavements at Willoughby Hills.

Figure 6-6. Subgrade soil was raked with the teeth of excavator bucket to reduce compaction during construction.

To test whether a "maturation period" existed, additional water quality sampling was undertaken in the spring and early summer of 2015. Had low TSS and metals effluent EMCs continued following winter, then a "maturation period" would be supported. However, the Small and Large applications' effluent TSS, Cu, and Pb EMCs were again markedly higher than those of asphalt runoff during the 2015 sampling campaign (April through June, Figure 6-5). Median effluent TSS EMCs for events sampled in 2015 were 370 mg/L for the Small application and 197 mg/L for the Large application. Spikes in Cu, Pb, and Cl^- EMCs immediately following winter were also observed (Figure 6-5 and Table 6-5). Sediment appeared to again be re-suspended within the cross-section of the pavement, and this trend was more pronounced immediately following winter (Figure 6-5). The Small application, which had a flat subgrade, produced higher effluent EMCs, suggesting the stepped subgrade in the Large application was not the culprit for the sediment loss. Seasonal trends in water

quality were consequently observed for TSS and particulate-bound metals (Cu and Pb). Chloride trends were also seasonal in nature and related to de-icing salt application, which has been observed in other permeable pavement studies in cold climates (Roseen et al. 2014; Drake et al. 2014c; Borst and Brown 2014).

Table 6-5. Median pollutant concentrations by season.

Monitoring location	Season	Number of Sampled Events	TSS (mg/L)	Pb (µg/L)	Cu (µg/L)	Cl^- (mg/L)
Asphalt	Spring 2014	4	62	1.41	3.75	26
	Summer 2014	8	9.0	0.56	3.85	55
	Fall 2014	4	11	0.56	2.13	11
	Spring 2015	3	12	0.56	4.55	28
Small	Spring 2014	4	147	1.45	5.34	428
	Summer 2014	8	123	0.93	4.39	92
	Fall 2014	4	5.8	0.24	2.08	78
	Spring 2015	2	370	2.51	7.97	253
Large	Spring 2014	1	260	2.50	5.40	18
	Summer 2014	8	127	1.41	3.70	24
	Fall 2014	0	No data	No data	No data	No data
	Spring 2015	3	197	2.57	6.56	54

An analysis of potential TSS leaching causes from these permeable pavements was undertaken, including statistical correlation analysis between TSS EMCs and weather parameters (Table 6-6). Asphalt runoff TSS EMCs were significantly negatively correlated to season, meaning the further away the winter, the lower the TSS EMCs were. This is probably due to the statistically smaller precipitation depths and intensities during the fall season, as discussed previously, which should mobilize less TSS. TSS effluent EMCs from

the Small application were significantly correlated to 5-minute peak rainfall intensity, ADP, and season. Thus, significantly higher TSS EMCs occurred in the spring and during more intense (higher flow rate) events. With longer ADP, the IWS zone had more time to drawdown, meaning runoff entered closer to the underlying soil, perhaps providing more momentum to disperse soil and entrain sediment in the effluent. For the large application, no significant correlations were found, perhaps due to the smaller number of sampled storms.

Table 6-6. Spearman's rank correlation coefficients relating weather parameters to TSS EMCs. Bold parameters are statistically significant at the α=0.05 level.

Weather Parameter	Asphalt	Small Outlet	Large Outlet
Rainfall depth	-0.33	0.21	0.09
5-min peak rainfall intensity	-0.14	**0.7**	0.48
Average rainfall intensity	-0.28	0.36	-0.18
Antecedent dry period	0.21	**0.47**	0.29
Season	**-0.51**	**-0.54**	-0.41

De-icing salt (NaCl) was applied liberally at Willoughby Hills during winter months. Sodium-based de-icing salts interact with the clayey subsoils beneath the permeable pavements, causing subsoils to become sodic; this in turn augments both sodium adsorption ratio (SAR) and exchangeable sodium percentage (ESP; Sparks 2003). The SAR and ESP are measures of the amount of Na^+ relative to other cations, such as Ca^{2+}, K^+, and Mg^{2+}. Na^+ preferentially displaces Ca^{2+} from exchange sites, but can also replace fixed K^+ between the layers of 2:1 clay minerals (Norrström and Bergstedt 2001). This causes deflocculation of clay particles and increases soil dispersibility (Keren and Miyamoto 1990;

Norrström and Jacks 1998). Agassi et al. (1981) found that the impacts of rain drops cause greater soil dispersion under sodic soil conditions. Sodic soils are characterized by low infiltration rates due to sealing, which can lead to severe soil erosion (Sumner et al. 1998).

Sodium also impacts leaching of metals from soils. Amrhein et al. (1992) found corresponding increases in metals concentrations in leachate from roadside soils with increasing de-icing salt concentration; the authors contend the dominant mechanism was dispersion of soil caused by high exchangeable Na^+. Norrström and Jacks (1998) found ESP in roadside soils exposed to salting in Sweden was high enough (10-27%) to disperse soil colloids (e.g., clay minerals, hydrous oxides). Colloid-facilitated transport of other pollutants, such as heavy metals, is then quite likely.

PSD Analysis

Particle size distributions of the runoff entering and discharging from the permeable pavements were collected during a storm event on June 10, 2015 (Figure 6-7). A duplicate PSD for each effluent sample (R1 and R2) was performed for repeatability. The runoff from the asphalt parking lot had a median diameter of 108 μm, within the range of median particle diameters (31-144 μm) for eight roadway sites in North Carolina (Winston and Hunt, submitted). Effluent PSDs for the Small and Large applications were very similar, suggesting the dynamics of filtration and sedimentation within the two PICPs were likewise similar, regardless of variation in LR or subgrade design. Particles greater than 100 μm in diameter appear to have been sequestered within the permeable pavement cross-section. This is in spite of the large export of TSS for this storm event (i.e., 12 mg/L asphalt runoff EMC, 197 mg/L Large application effluent EMC). The percentage of clay-sized particles

(defined as <2 μm diameter) increased from less than 2% in the parking lot runoff to 22-28% in the permeable pavement drainage; silt likewise increased from 28% to 68-72%. This suggested silt- and clay-sized particles were being mobilized from the subgrade soils, which were 18-21% sand, 47-53% silt, and 28-36% clay. Given effluent EMCs of TSS were very low (6 mg/L) during the fall season (Table 6-5), and represented a reduction in TSS EMC from asphalt runoff (11 mg/L), these early June PSDs provide greater support to the sodium-induced dispersion of clays and silts in the subgrade causing leaching of both TSS and metals. See Appendix B for photographs of stormwater samples that further support this hypothesis.

It is expected these seasonal trends for TSS and metals export followed by reduction will continue over the lifetime of these permeable pavements, where performance will suffer immediately after winter due to salt application and will improve as time passes from winter. This seasonality in water quality will only impact: (1) sites requiring frequent application of de-icing salts during the winter and (2) sites with substantial fractions of organic matter or 2:1 clay minerals at the subgrade elevation. The percentage of organic matter at the subgrade elevation is expected to be low, since it is often 30-60 cm below the surface.

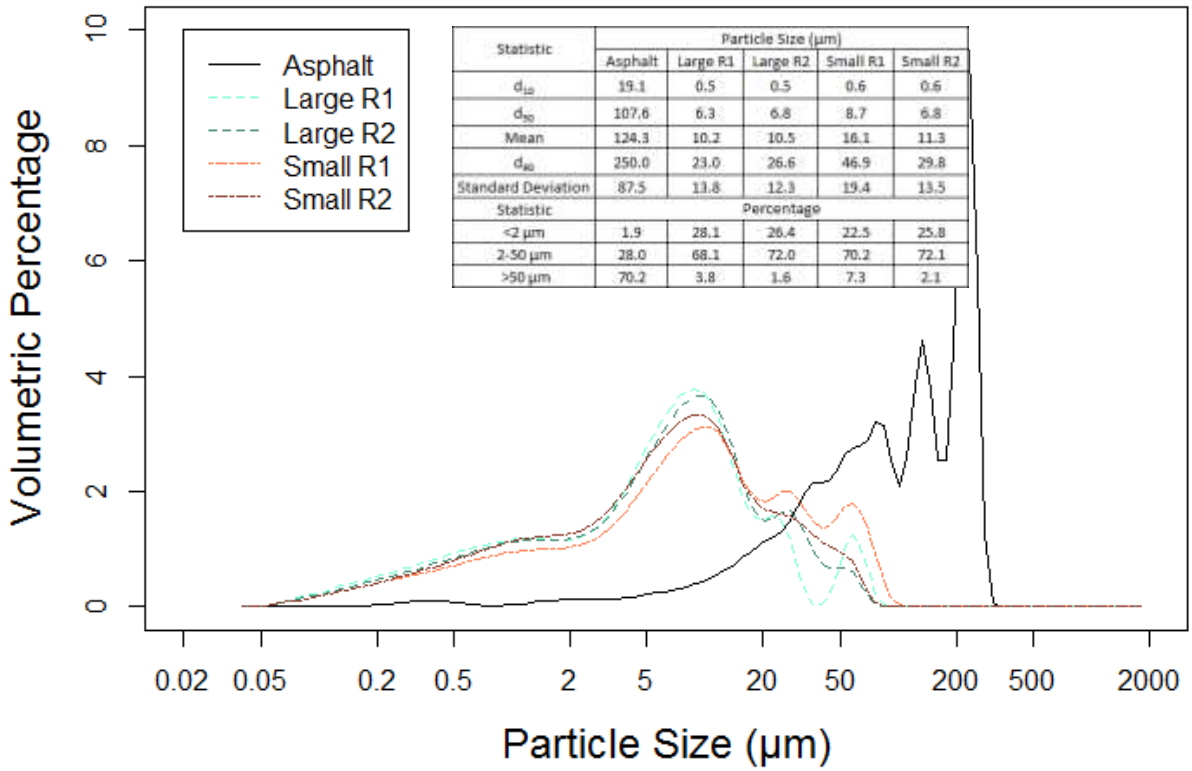

Statistic	Particle Size (µm)				
	Asphalt	Large R1	Large R2	Small R1	Small R2
d_{10}	19.1	0.5	0.5	0.6	0.6
d_{50}	107.6	6.3	6.8	8.7	6.8
Mean	124.3	10.2	10.5	16.1	11.3
d_{90}	250.0	23.0	26.6	46.9	29.8
Standard Deviation	87.5	13.8	12.3	19.4	13.5
Statistic	Percentage				
<2 µm	1.9	28.1	26.4	22.5	25.8
2-50 µm	28.0	68.1	72.0	70.2	72.1
>50 µm	70.2	3.8	1.6	7.3	2.1

Figure 6-7. Particle size distributions for the June 10, 2015, storm event. R1 and R2 are duplicate samples subsampled from the storm event composite samples.

Chloride and Metals

Chloride was significantly exported from the Small application, with an ER of -3.6 (Table 6-7 and Figure 6-8). Similar exports of Cl^- have been observed in Hogland et al. (1987) and Roseen et al. (2012), while Drake et al. (2014c) suggested that permeable pavement provided mechanisms for storage and dilution of Cl^-. Chloride EMCs from the Large application were not statistically different from those of the asphalt runoff. Effluent EMCs of Cl^- from the Large application were significantly less than those from the Small application, perhaps related to greater application of salt in the Small catchment (Figure 6-2).

Drainage from the small application exceeded the U.S. EPA chronic toxicity criterion (230 mg/L) on five occasions, all prior to the end of May (U.S. EPA 2012).

Al, Fe, Ca, and Mg were significantly exported from both the Small and Large applications, with ERs and RE_{median} of at least -2.8 and -3.0, respectively. The SCMs were installed in the subsoil of Mahoning silt loam, and given the TSS export from these SCMs, it is likely that clay-bound Al and Fe were simultaneously lost (Hunt et al. 2008). Mg and Ca could either be leaching from the dolomitic limestone aggregate supporting the permeable pavement or from the subsoil (Kim and Park 2008; National Cooperative Soil Survey 2014). Given the IWS zone constantly held water within both permeable pavement applications, Mg and Ca had adequate time to leach into the stormwater inter-event. Mn and Pb were significantly exported from the Large application. The permeable pavements were a net-zero for Cu treatment. Mean Zn EMC was significantly reduced (by 37%) by the Small application.

In general, metals reduction from the Willoughby Hills permeable pavements was poor compared to published field-scale studies (Brattebo and Booth 2003; Roseen et al. 2012; Drake et al 2014b; Drake et al 2014c). The export of sediment from the two permeable pavements following each winter probably led to substantial sediment-bound metals exports. This assertion is supported by the following: the Large application, which had a 57 mg/L higher median effluent TSS EMC than that of the Small application, had concomitantly higher median metals effluent EMCs (except Mg).

Table 6-7. Summary statistics for chloride and metals EMCs for the Willoughby Hills permeable pavements. Bolded p-values are significant differences. Bolded and underlined p-values are significant increases in pollutant EMC.

Pollutant	Location	Range (µg/L)	$\overline{X}$ [1] (mg/L)	$\tilde{X}$ [2] (mg/L)	s [3] (µg/L)	ER	RE_{median}	Statistical Comparison	p-value
Cl	Asphalt	1.6-128	37	24	37	-	-	SO-LO[4]	**0.002**
	Sm Out	13.8-588	171	101	168	-3.6	-3.2	I-SO[5]	**0.0008**
	Lg Out	3.7-91.8	33	24	27	0.10	0.00	I-LO[6]	0.662
Al	Asphalt	29-363	126	91	98	-	-	SO-LO	0.234
	Sm Out	88-1585	663	701	455	-4.28	-6.7	I-SO	**<0.0001**
	Lg Out	116-1442	976	1080	444	-6.8	-10.9	I-LO	**<0.0001**
Ca	Asphalt	7366-31370	16588	14590	7274	-	-	I-SO	0.118
	Sm Out	21080-231600	63225	52730	51476	-2.8	-2.6	I-LO	**<0.0001**
	Lg Out	14850-122700	66570	54220	34048	-3.0	-2.7	SO-LO	**0.0004**
Cu	Asphalt	1.4-11.8	4.56	3.75	2.80	-	-	I-SO	0.878
	Sm Out	1.7-10.4	4.36	4.39	2.35	0.04	-0.17	I-LO	0.463
	Lg Out	1.9-9.6	5.28	5.40	2.31	-0.16	-0.44	SO-LO	0.821
Fe	Asphalt	91-658	204	164	154	-	-	I-SO	0.203
	Sm Out	116-3210	926	740	847	-3.54	-3.5	I-LO	**0.0002**
	Lg Out	235-2506	1486	1538	721	-6.3	-8.4	SO-LO	**0.0001**
Mg	Asphalt	856-3289	1786	1484	773	-	-	I-SO	0.205
	Sm Out	1951-8318	3635	3396	1536	-1.04	-1.29	I-LO	**0.0002**
	Lg Out	787-5403	2970	2500	1541	-0.66	-0.7	SO-LO	**0.0001**
Mn	Asphalt	6-76	21	9	19	-	-	I-SO	0.160
	Sm Out	2.2-79.8	21	18	19	-0.01	-0.92	I-LO	0.800
	Lg Out	14.2-79.6	35	27	20	-0.68	-1.83	SO-LO	**0.0004**
Pb	Asphalt	0.25-1.9	0.69	0.62	0.42	-	-	I-SO	0.134
	Sm Out	0.15-4.6	1.09	0.91	1.10	-0.57	-0.48	I-LO	0.220
	Lg Out	0.62-3.5	1.86	1.51	0.99	-1.69	-1.44	SO-LO	**0.001**
Zn	Asphalt	12.6-50.3	23	21	10	-	-	I-SO	0.246
	Sm Out	5.8-37.3	15	13	8	0.37	0.36	I-LO	**0.023**
	Lg Out	13.5-34.8	21	16	8	0.10	0.20	SO-LO	0.609

[1] $\overline{X}$ is the mean, [2] $\tilde{X}$ is the median, and [3] s is the standard deviation

[5]Small vs. large outlet, [6]inlet vs. small outlet, and [7]inlet vs. large outlet comparisons.

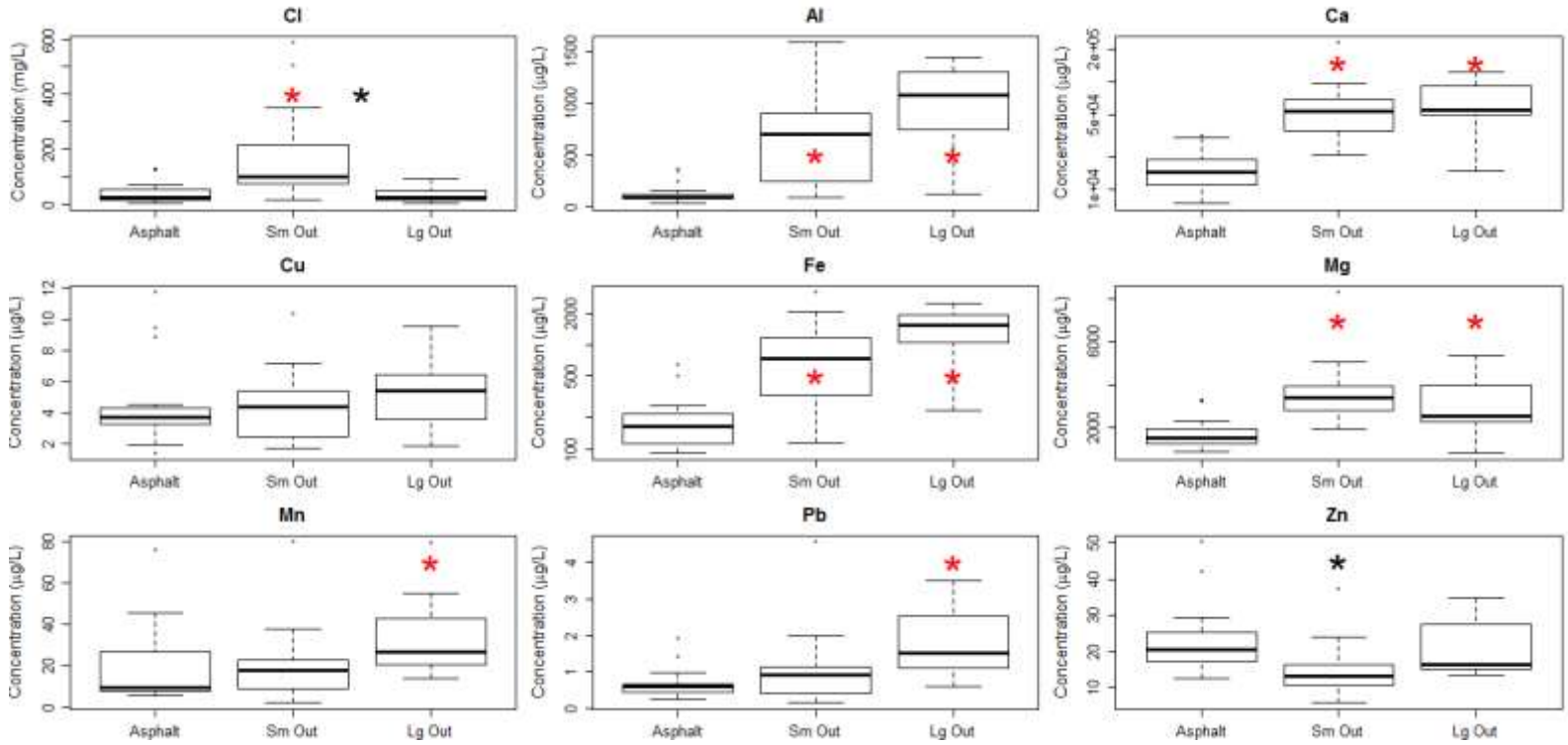

Figure 6-8. Boxplots of chloride and metals EMCs at the asphalt, Small application outlet (Sm Out), and Large application outlet (Lg Out) monitoring locations at Willoughby Hills. Statistically significant differences are shown with asterisks, with red asterisks indicating significant increases in pollutant EMCs. Asterisks above an outlet boxplot indicate significant differences between the asphalt and effluent EMC. Asterisks between the two outlet boxplots indicate significant differences between effluent EMCs.

Pollutant Loads

Of the 75 storms at Willoughby Hills, only 3 were completely captured (i.e., no outflow from the underdrain) by the Small application (maximum depth of 3.3 mm). Nineteen events were completely captured in the Large application (maximum depth of 10.7 mm), illustrating the impact of LR on permeable pavement hydrology. Cumulative volume reductions over the monitoring period for the Small and Large applications were 16 and 32%, respectively (Chapter 4). Nineteen percent of sampled storms were completely captured by the Large application, while the Small application produced drainage for all sampled events. Because of the low permeability underlying soils (measured exfiltration rates less than 0.15 mm/hr) the IWS zones were essential for volume reduction.

TKN and ON loads were significantly reduced in both permeable pavements, with substantially greater load reduction for the Large application versus the Small application (Table 6-8). Particulate nitrogen filtration at the permeable pavement surface is suspected, as suggested by Collins et al. (2010). NO_{2-3} loading was significantly reduced (42%) in the Large application, with no change in the Small application; this was attributed to the proportionally greater volume reduction in the Large application. Mixed results for NO_{2-3} load treatment have been observed in past studies by Collins et al. (2010) and Drake et al. (2014b). TN load was significantly reduced by 52% by the Large application, while the Small application again did not affect loads. Loading ratio is important: exfiltration represents a greater portion of the water balance at lower LR (Chapter 4).

Dissolved, particle-bound, and total P loads were reduced between 19 and 41% by the Large application, which were always superior to load reductions from the Small application

(range of 1-30% reduction for the same pollutants). TSS mass increased significantly by 525% and 337% for the Small and Large applications, respectively, due to the aforementioned loss of sediment from the permeable pavement subgrade. Sediment loss was particularly egregious during five storm events, where ten-fold export of TSS mass occurred for both the Small and Large applications. The lower export of TSS from the Large application could be related to the greater fraction of surface runoff (which could not entrain sediment from the permeable pavement subgrade) and the greater volume reduction due to lower LR.

Chloride load decreased significantly by 53% from the Large application, but no significant change occurred in the small application. This was attributed to exfiltration and the aforementioned differences in winter salting between the two catchments. Chloride is recalcitrant in the environment and probably entered the groundwater through exfiltration, rather than being sequestered within the SCM (Pitt et al. 1999).

Results indicated larger LR generally reduced pollutant mitigation. However, the Large application normalized effluent loads were only significantly smaller for Cl^- and $NO_{2\text{-}3}$; the converse was never true. The Small application, however, often provided greater than half the load reduction of the Large application, even though the LR of the Small application (7.2:1) was more than twice that of the Large (2.2:1). Similar results have been shown for undersized bioretention cells in Luell et al. (2011), where a 50% undersized bioretention cell provided greater than one-half the load reduction of the full sized cell. This was due to the smaller SCM's ability to treat and exfiltrate stormwater for the more frequent, small storms. However, surface clogging of heavily-loaded, high LR permeable pavements must be

considered in design, as this increases the frequency of maintenance (Brown and Borst 2013; Winston et al. 2016).

Table 6-8. Watershed area-normalized pollutant loads for nutrients, sediment, and chloride for the permeable pavements. Bolded relative percent differences are statistically significant at the α=0.05 level.

Parameters	Cl	TKN	NO_{2-3}	TN	TAN	ON	TP	OPO_4	PBP	TSS
Small inlet (kg/ha/yr)	353	6.8	2.9	9.7	1.6	5.2	0.30	0.13	0.26	134
Small outlet (kg/ha/yr)	545	3.9	3.6	7.5	0.9	3.0	0.21	0.13	0.23	836
Large inlet (kg/ha/yr)	453	8.8	3.9	12.7	2.1	6.7	0.41	0.18	0.35	180
Large outlet (kg/ha/yr)	217	3.9	2.3	6.1	1.2	2.6	0.24	0.14	0.23	787
% load reduction small	**-54**	**42**	-23	23	46	**41**	**30**	1	14	**-525**
% load reduction large	**52**	**56**	**42**	**52**	40	**61**	**41**	19	**33**	**-337**
Significantly lower effluent load	Large	N/A	Large	N/A	N/A	N/A	N/A	N/A	N/A	N/A

Loads of Al, Ca, and Fe increased significantly as stormwater moved through both the Small and Large permeable pavements (Table 6-9). Leaching of these pollutants was perhaps related to the limestone aggregate or the aforementioned TSS export (concurrently leaching particulate-bound metals). The Small application had significantly lower normalized effluent loads of Mn, Pb, and Zn, which was due to the lower hydraulic retention time (and therefore less contact time with the subsoil). All other effluent pollutants loads were not statistically different between the two permeable pavements. All load reductions

for heavy metals were less than 40%. Lead load was not significantly reduced, which has not been observed previously (Legret et al. 1996; Gilbert and Clausen 2006; Drake et al. 2014c). Copper load was unaffected, unlike that observed by Drake et al. (2014b). Significant Zn load reduction was observed for both the Small (37%) and Large (36%) applications, but were much lower than those reported by Legret et al. (1996), Bean et al. (2007), Fassman and Blackbourn (2011), and Drake et al. (2014b).

Table 6-9. Watershed area-normalized pollutant loads for metals for the permeable pavements.

Monitoring Location	Al	Ca	Cu	Fe	Mg	Mn	Pb	Zn
Small inlet (kg/ha/yr)	0.89	115	0.03	1.3	14	0.12	0.004	0.14
Small outlet (kg/ha/yr)	4.1	377	0.02	6.1	19	0.13	0.01	0.09
Large inlet (kg/ha/yr)	1.14	150	0.04	1.7	18	0.16	0.01	0.19
Large outlet (kg/ha/yr)	4.4	302	0.03	6.8	15	0.16	0.01	0.12
% load reduction small	**-363**	**-227**	13	**-367**	-33	-16	-55	**37**
% load reduction large	**-288**	**-101**	30	**-288**	**15**	-5	-49	**36**
Significantly Lower Effluent Load	N/A	N/A	N/A	N/A	N/A	Small	Small	Small

6.6 Summary and Conclusions

Two PICP retrofits were installed to treat runoff from an impermeable asphalt parking lot at the Willoughby Hills community center in northeast Ohio. Both permeable pavements were situated over HSG D soils, employed IWS zones, and treated runoff from parking lots

2.2 (Large application) and 7.2 (Small application) times their surface areas. Stormwater samples were obtained from three locations: (1) an impervious asphalt catchment (representative of run-on to the permeable pavement) and from the underdrains of both the (2) Large and (3) Small applications. The following conclusions can be drawn from this study:

1) Total suspended solids EMCs significantly *increased* through the permeable pavements, a finding that has not been reported in the literature to-date. While nearly 100% of particles greater than 100 μm in diameter were trapped by the PICP, loss of sediment from the subgrade far outweighed any filtration by the pavement course. Consequent significant increases in Cu and Pb EMCs suggested loss of particulate-bound metals as stormwater moved through the permeable pavement cross-section and came in contact with the clay subsoil. Initially, loose sediment in the subgrade from construction or attached to the aggregate was thought to be the cause. Rather, further sampling in spring and summer 2015 suggested that the export of TSS, Cu, Pb, and Cl^- were related to the effects of de-icing salts. It is hypothesized that sodium-based de-icing agents would cause changes in the subgrade soil chemistry, leading to deflocculation of clays and silts in the subgrade soils. Particle size distributions showed these particles were then entrained in the infiltrate as it moved through the permeable pavement cross-section to the underdrain. TSS, metals, and chloride release during the autumn was similar to past studies in more temperate climates, suggesting this salt-related effect may last 3-6 months. Permeable pavement performance may be heavily influenced by de-icing salt application.

2) For most nutrient EMCs, the permeable pavements were a net zero, neither improving nor impairing nutrient removal. No significant changes in nutrient EMCs were observed for N and P species (with one exception: $NO_{2\text{-}3}$ EMCs significantly increased from the Small application).

3) For Al, Ca, Fe, Mg, Mn, and Pb, either no significant treatment was provided or EMCs significantly increased as stormwater passed through the permeable pavements. Since many metals are predominantly sediment-bound, this may have been due to the loss of sediment from the subgrade of the permeable pavements. Chloride EMCs increased in the Small application, where salting was more intensive due to proximity to the community center building. The build-up of chloride and subsequent leaching following winter has been observed in other permeable pavement studies. Zinc EMCs were significantly reduced by the small application by 37%.

4) Six storms were completely captured by the Large application, while the Small application had outflow for every sampled storm event. Since exfiltration rates were similar between the two permeable pavements, storm capture was attributed to the lower LR for the Large application. An IWS zone enabled these permeable pavements to provide additional exfiltration, improving SCM performance. Loads of most nutrient forms were reduced significantly (by up to 60%); however, dissolved nitrogen and phosphorus loads were generally unchanged. TSS loads significantly increased by 525% and 329% for the Small and Large applications, respectively. Export of sediment was seasonally significant (related to elapsed time since de-icing salt application). Total suspended solids loss dampened heavy

metal load removal. The mass exported from permeable pavements significantly increased for several metals.

5) Results illustrate the importance of LR for permeable pavements, with generally greater pollutant retention at lower LR. The Small application, however, often provided greater than half the pollutant load reduction of the Large, even though the LR of the Small application (7.2:1) was more than twice that of the Large (2.2:1). Undersized SCMs can be good retrofits given adequate maintenance provision.

6.7 References

American Public Health Association (APHA), American Water Works Association (AWWA), and Water Environment Federation (WEF). (2012). *Standard methods for the examination of water and wastewater*, Ed. Laura Bridgewater. 22nd ed., Washington, DC.

Amrhein, C., Strong, J.E., and Mosher, P.A. (1992). "Effect of deicing salts on metal and organic matter mobilization in roadside soils." *Environ. Sci. Technol.,* 26(4), 703-709.

Antweiler, R.C., and Taylor, H.E. (2008). "Evaluation of statistical treatments of left-censored environmental data using coincident uncensored data sets: 1. Summary statistics." *Environ. Sci. Technol.,* 42(10), 3732‑3738.

Bannerman, R.T., Owens, D.W., Dodds, R.B., and Hornewer, N.J. (1993). "Sources of pollutants in Wisconsin stormwater." *Water Sci. Technol.,* 28(3), 241-259.

Bean, E.Z., Hunt, W.F., and Bidelspach, D.A. (2007). "Evaluation of four permeable pavement sites in eastern North Carolina for runoff reduction and water quality impacts." *J. Irrig. Drain. Eng.,* 133(6), 583-592.

Booth, D.B., Karr, J.R., Schauman, S., Konrad, C.P., Morley, S.A., Larson, M.G., and Burges, S.J. (2004). "Reviving urban streams: Land use, hydrology, biology, and human behavior." *J. Am. Water Resour. Assoc.,* 40(5), 1351-1364.

Borst, M., and Brown, R.A. (2014). "Chloride released from three permeable pavement surfaces after winter salt application." *J. Am. Water Resour. Assoc.,* 50(1), 29-41.

Boving, T., Stolt, M., and Augenstern, J. (2004). "Investigation of the University of Rhode Island, Kingston, RI, porous pavement parking lot and its impact on subsurface water quality." *Proceedings of the 33 Annual Meeting, Int. Association of Hydrologists,* Zacatecas, Mexico.

Brattebo, B.O., and Booth, D.B. (2003). "Long-term stormwater quantity and quality performance of permeable pavement systems." *Water Res.,* 37(18), 4369-4376.

Brown, R.A., and Borst, M. (2013). "Assessment of clogging dynamics in permeable pavement systems with time domain reflectometers." *J. Environ. Eng*., 139(10), 1255-1265.

Collins, K.A., Hunt, W.F., and Hathaway, J.M. (2008). "Hydrologic comparison of four types of permeable pavement and standard asphalt in eastern North Carolina." *J. Hydrol. Eng.,* 13(12), 1146-1157.

Collins, K.A., Hunt, W.F., and Hathaway, J.M. (2010). "Side-by-side comparison of nitrogen species removal for four types of permeable pavement and standard asphalt in eastern North Carolina." *J. Hydrol. Eng.,* 15(6), 512-521.

DeBusk, K.M., Hunt, W.F., and Line, D.E. (2010). "Bioretention outflow: Does it mimic nonurban watershed shallow interflow?" *J. Hydrol. Eng.*, 16(3), 274-279.

Drake, J., Bradford, A., and Van Seters, T. (2014a). "Hydrologic performance of three partial-infiltration permeable pavements in a cold climate over low permeability soil." *J. Hydrol. Eng.*, 19(9), 04014016.

Drake, J., Bradford, A., and Van Seters, T. (2014b). "Stormwater quality of spring–summer-fall effluent from three partial-infiltration permeable pavement systems and conventional asphalt pavement." *J. Environ. Manage.*, 139, 69-79.

Drake, J., Bradford, A., and Van Seters, T. (2014c). "Winter effluent quality from partial-infiltration permeable pavement systems." *J. Environ. Eng*., 140(11), 04014036.

Dunne, T., and Leopold, L.B. (1978). *Water in environmental planning*. W.H. Freeman and Company, San Francisco, California.

Espey Jr, W.H., Morgan, C.W., and Masch, F.D. (1966). *A study of some effects of urbanization on storm runoff from a small watershed*. Technical Report 44D 07-6501 CRWR-2, Center for Water Resources, University of Texas at Austin.

Fassman, E.A., and Blackbourn, S. (2010). "Urban runoff mitigation by a permeable pavement system over impermeable soils." *J. Hydrol. Eng.*, 15(6), 475-485.

Fassman, E.A., and Blackbourn, S.D. (2011). "Road runoff water-quality mitigation by permeable modular concrete pavers." *J. Irrig. Drain. Eng.*, 137(11), 720-729.

Fay, L., and Shi, X. (2012). "Environmental impacts of chemicals for snow and ice control: State of the knowledge." *Water Air Soil Poll.*, 223(5), 2751–2770.

Franks, C.A., Davis, A.P., and Aydilek, A.H. (2014). "Effects of runoff characteristics and filter type on geotextile storm water treatment." *J. Irrig. Drain. Eng.*, 140(2), 04013014.

Gee, G.W., and Bauder, J.W. (1986). Particle size analysis. *Methods of soil analysis. Part 1: Physical and mineraological methods*, A. Klute ed., Soil Science Society of America, Madison, Wis., 383-411.

Grimm, N.B., Sheibley, R.W., Crenshaw, C.L., Dahm, C.N., Roach, W.J., and Zeglin, L.H. (2005). "N retention and transformation in urban streams." *J. North Am. Benthol. Soc.*, 24(3), 626-642.

Hirsch, R. M., Walker, J. F., Day, J. C., and Kallio, R. (1990). The influence of man on hydrologic systems. *Surface Water Hydrology.* Geological Society of America, Boulder, Colorado. 329-359.

Hogland, W., Niemczynowicz, J., and Wajlman, T. (1987). "The unit superstructure during the construction period." *Sci. Total Environ.*, 59, 411–424.

Hunt, W.F., Smith, J.T., Jadlocki, S.J., Hathaway, J.M., and Eubanks, P.R. (2008). "Pollutant removal and peak flow mitigation by a bioretention cell in urban Charlotte, NC." *J. Environ. Eng*., 134(5), 403-408.

Hunt, W.F., Davis, A.P., and Traver, R.G. (2012). "Meeting hydrologic and water quality goals through targeted bioretention design." *J. Environ. Eng*., 138(6), 698-707.

Keren, R., and Miyamoto, S. (1990). "Reclamation of saline, sodic, and boron-affected soils." In *Agricultural salinity assessment and management.* ASCE manuals of practice no. 71, American Society of Civil Engineers. New York, NY.

Kim, H., Seagren, E.A., and Davis, A.P. (2003). "Engineered bioretention for removal of nitrate from stormwater runoff." *Water Environ. Res.*, 75(4), 355-367.

Kim, H.S., and Park, J. (2008). "Effects of limestone on the dissolution of phosphate from sediments under anaerobic condition." *Environ. Technol.,* 29(4), 375-380.

Knowles, R. (1982). "Denitrification." *Microbiol. Rev., 46*(1), 43-70.

Legret, M., Colandini, V., and LeMarc, C. (1996). "Effects of a porous pavement with reservoir structure on the quality of runoff water and soil." *Sci. Total Environ.,* 190, 335–340.

Li, H., Sharkey, L.J., Hunt, W.F., and Davis, A.P. (2009). "Mitigation of impervious surface hydrology using bioretention in North Carolina and Maryland." *J. Hydrol. Eng.*, 14(4), 407-415.

Lucke, T., and Beecham, S. (2011). "Field investigation of clogging in a permeable pavement system." *Build. Res. Inf.,* 39(6), 603-615.

Luell, S.K., Hunt, W.F., and Winston, R.J. (2011). "Evaluation of undersized bioretention stormwater control measures for treatment of highway bridge deck runoff." *Water Sci. Technol.,* 64(4), 974-979.

Morse, C.C., Huryn, A.D., and Cronan, C. (2003). "Impervious surface area as a predictor of the effects of urbanization on stream insect communities in Maine, USA." *Environ. Monit. Assess.,* 89(1), 95-127.

National Cooperative Soil Survey, United States Department of Agriculture. (2014). *Mahoning soil series description.* Rev. AR-DMc-RAR. Available: https://soilseries.sc.egov.usda.gov/OSD_Docs/M/MAHONING.html

National Oceanic and Atmospheric Administration (NOAA). (2015). *National Centers for Environmental Information.* Local climatological data, Cleveland-Hopkins international airport. Accessed October 1, 2015. Available: http://www.ncdc.noaa.gov/qclcd/QCLCD

Neller, R.J. (1989). "Induced channel enlargement in small urban catchments, Armidale, New South Wales." *Environ. Geol. Water Sci.*, 14(3), 167-171.

Norrström, A.C., and Jacks, G. (1998). "Concentration and fractionation of heavy metals in roadside soils receiving de-icing salts." *Sci. Total Environ.*, 218(2), 161-174.

Norrström, A.C., and Bergstedt, E. (2001). "The impact of road de-icing salts (NaCl) on colloid dispersion and base cation pools in roadside soils." *Water Air Soil Poll.*, 127(1-4), 281-299.

Ohio Department of Natural Resources (ODNR), Division of Soil and Water Conservation. (2006). *Rainwater and land development: Ohio's standards for stormwater management, low impact development, and urban stream protection*. 3rd edition. Ed: John Mathews.

Passeport, E., and Hunt, W.F. (2009). "Asphalt parking lot runoff nutrient characterization for eight sites in North Carolina, USA." *J. Hydrol. Eng.*, 14(4), 352-361.

Paul, M.J., and Meyer, J.L. (2001). "Streams in the urban landscape." *Annu. Rev. Ecol. Syst., 32*, 333-365.

Pezzaniti, D., Beecham, S., and Kandasamy, J. (2009). "Influence of clogging on the effective life of permeable pavements." *Proceedings of the ICE-Water Manage.*, 162(3), 211-220.

Pitt, R., Clark, S., and Field, R. (1999). "Groundwater contamination potential from stormwater infiltration practices." *Urban Water J.*, 1(3), 217-236.

Pitt, R., Maestre, A., and Morquecho, R. (2004). *The national stormwater quality database (NSQD) version 1.1 report*. University of Alabama, Department of Civil and Environmental Engineering, Tuscaloosa, AL.

Pratt, C.J., Newman, A.P., and Bond, P.C. (1999). "Mineral oil bio-degradation within a permeable pavement: long term observations." *Water Sci. Technol.*, 39(2), 103-109.

R Core Team. (2015). *A language and environment for statistical computing*. R Foundation for Statistical Computing. Vienna, Austria.

Roesner, L.A., Bledsoe, B.P., and Brashear, R.W. (2001). "Are best-management-practice criteria really environmentally friendly?" *J. Water Resour. Plann. Manage.*, 127(3), 150-154.

Roseen, R.M., Ballestero, T.P., Houle, J.J., Briggs, J.F., and Houle, K.M. (2012). "Water quality and hydrologic performance of a porous asphalt pavement as a storm-water treatment strategy in a cold climate." *J. Environ. Eng.*, 138(1), 81-89.

Roseen, R.M., Ballestero, T.P., Houle, K.M., Heath, D., and Houle, J.J. (2014). "Assessment of winter maintenance of porous asphalt and its function for chloride source control." *J. Transp. Eng.*, 140(2), 04013007.

Roy, A.H., Freeman, M.C., Freeman, B.J., Wenger, S.J., Ensign, W.E., and Meyer, J.L. (2005). "Investigating hydrologic alteration as a mechanism of fish assemblage shifts in urbanizing streams." *J. North Am. Benthol. Soc.*, 24(3), 656-678.

Smith, V.H., Tilman, G.D., and Nekola, J.C. (1999). "Eutrophication: impacts of excess nutrient inputs on freshwater, marine, and terrestrial ecosystems." *Environ. Poll.*, 100(1), 179-196.

Soil Survey Staff, Natural Resources Conservation Service, United States Department of Agriculture. (2015). Web Soil Survey. http://websoilsurvey.nrcs.usda.gov/. Accessed 28 January 2015.

Sparks, D.L. (2003). *Environmental soil chemistry*. Elsevier, San Diego, CA.

Strecker, E.W., Quigley, M.M., Urbonas, B.R., Jones, J.E., and Clary, J.K. (2001). "Determining urban storm water BMP effectiveness." *J. Water Resour. Plann. Manage.*, 127(3), 144-149.

Sumner, M.E., Milles, W.P., Kookana, R.S., and Hazelton, P. (1998). "Sodicity, dispersion, and environmental quality." In *Sodic soils: Distribution, properties, management, and environmental consequences.* Oxford University Press, New York, NY.

Tota-Maharaj, K., and Scholz, M. (2010). "Efficiency of permeable pavement systems for the removal of urban runoff pollutants under varying environmental conditions." *Environ. Prog. Sustainable Energy*, 29, 358-369.

U.S. Environmental Protection Agency (U.S. EPA). (1983). *Methods of chemical analysis of water and waste*. EPA-600/4-79-020, Cincinnati, Ohio.

United States Environmental Protection Agency (U.S. EPA). (1988). *Ambient water quality criteria for chloride-1988*. EPA 440/5-88-001, Office of Water Regulations and Standards, Criteria and Standards Division, Washington, DC.

U.S. EPA. (2002). *Urban storm water BMP performance monitoring: a guidance manual for meeting the national storm water BMP database requirements*. EPA-821-B-02-001. U.S. Environmental Protection Agency, Washington, DC.

U.S. EPA (2012). *National Water Quality Criteria*. U.S. Environmental Protection Agency. http://water.epa.gov/scitech/swguidance/standards/current/index.cfm., accessed October 2015.

Van Haandel, A.C., and Van der Lubbe, J.G.M. (2012). *Handbook of biological wastewater treatment: design and optimisation of activated sludge systems*. 2nd ed. IWA Publishing, London, UK.

Walsh, C.J., Roy, A.H., Feminella, J.W., Cottingham, P.D., Groffman, P.M., and Morgan, R.P. (2005). "The urban stream syndrome: current knowledge and the search for a cure." *J. North Am. Benthol. Soc.*, 24(3), 706-723.

Wardynski, B.J., Winston, R.J., and Hunt, W.F. (2012). "Internal water storage enhances exfiltration and thermal load reduction from permeable pavement in the North Carolina mountains." *J. Environ. Eng*. 139(2), 187-195.

Winston, R.J., Dorsey, J.D. and Hunt, W.F. (2015). *Monitoring the performance of bioretention and permeable pavement stormwater controls in Northern Ohio: Hydrology, water quality, and maintenance needs*. Final Report Submitted to the University of New Hampshire and the Chagrin River Watershed Partners. In Fulfilment of NOAA Award number NA09NOS4190153. Available: http://www.crwp.org/files/OH_StormwaterControls_MonitoringReport2015.pdf

Winston, R.J. and Hunt, W.F. (submitted). "Characterizing runoff from roadways: particle size distributions, nutrients, and gross solids." *J. Environ. Eng*.

Winston, R.J., Al-Rubaei, A.M., Blecken, G.-T., Viklander, M., and Hunt, W.F. (2016). "Maintenance measures for preservation and recovery of permeable pavement surface infiltration rate – the effect of vacuum cleaning, high pressure washing, and milling." *J. Environ. Manage*. 169, 132-144.

CHAPTER 7: **MAINTENANCE MEASURES FOR PRESERVATION AND RECOVERY OF PERMEABLE PAVEMENT SURFACE INFILTATION RATE – THE EFFECTS OF STREET SWEEPING, VACUUM CLEANING, HIGH PRESSURE WASHING, AND MILLING**

(This chapter was printed in a revised format)

Authors: Winston, R.J., Al-Rubaei, A.M., Blecken, G.-T., Viklander, M., and Hunt, W.F.

Published: *Journal of Environmental Management*

Volume 169. March 2016. Pages: 132-144.

7.1 Abstract

The surface infiltration rates (SIR) of permeable pavements decline with time as sediment and debris clog pore spaces. Effective maintenance techniques are needed to ensure the hydraulic functionality and water quality benefits of this stormwater control. Eight different small-scale and full-scale maintenance techniques aimed at recovering pavement permeability were evaluated at ten different permeable pavements in the USA and Sweden. Maintenance techniques included manual removal of the upper 2 cm of filling material, mechanical street sweeping, regenerative-air street sweeping, vacuum street sweeping, hand-held vacuuming, high pressure washing, and milling of porous asphalt. The removal of the upper 2 cm of clogging material did not significantly improve SIR of CGP and PICP due to the inclusion of fines in the joint and bedding stone during construction, suggesting routine maintenance cannot overcome improper construction. For porous asphalt maintenance, industrial hand-held vacuum cleaning, pressure washing, and milling were increasingly successful at recovering SIR. Milling to a depth of 2.5 cm nearly restored SIR for a 21-year old porous asphalt pavement to like-new conditions. For PICP, street sweepers employing

suction were shown to be preferable to mechanical sweepers; additionally, maintenance efforts will become more intensive over time to maintain a threshold SIR, as maintenance was not 100% effective at removing clogging material.

7.2 Review of Literature

Less than half (46%) of the world's population resides in rural areas based on 2014 estimates; the rural to urban population shift is projected to continue and two-thirds of the world's population will reside in urban centers by 2050 (United Nations 2014). Urban development results in the introduction of impervious cover, which has been directly linked to stream health degradation (Wolman 1967; Morse et al. 2003; Schueler et al. 2009). Parking surfaces represent about 10% of the impervious surfaces in residential watersheds, and as much as 50% of imperviousness in commercial developments (Arnold and Gibbons 1996). In the United States, approximately 3500 km^2 of land is utilized for parking lots (Ben-Joseph 2012). Streets and sidewalks constitute 10-20% of commercial and residential land uses (Arnold and Gibbons 1996). Therefore, management of parking lot and roadway runoff through innovative stormwater control measures (SCMs), such as permeable pavement, is critical to watershed health and restoration of pre-development hydrology, the overall goal of Low Impact Development (LID; Dietz 2007).

Permeable interlocking concrete pavers (PICP), pervious concrete, porous asphalt, and concrete grid pavers (CGP) have inherent permeability. In contrast to impermeable pavements, rainfall infiltrates and enters an underground storage reservoir. Depending on project goals and site conditions, the underground reservoir can be designed to provide extended detention, exfiltration into the underlying soil, or both (NCDENR 2012).

Exfiltration systems recharge the groundwater (Brattebo and Booth 2003; Gilbert and Clausen 2006; Collins et al. 2008; Drake et al. 2014) and compared to conventional pavements, permeable pavements reduce runoff volume and peak rate while delaying peak flows (Pratt et al. 1989; Fassman and Blackbourn 2010). Permeable pavements also provide a number of water quality benefits, including filtration and settling of sediment and sediment-bound pollutants (Roseen et al. 2012).

While many permeable pavement demonstration sites have been built and research into their water quality and hydrologic benefits completed, clogging and maintenance frequency and onerousness are commonly cited concerns with this SCM (Drake and Bradford 2013, Blecken et al. in press). Newly-installed permeable pavements provide surface infiltration rates (SIR) well in excess of design rainfall rates, meaning they are capable of capturing and treating even infrequent return interval events (Bean et al. 2007, Al-Rubaei et al. 2013). However, build-up of sediment, organic material, and debris in the pavement and aggregate layers causes a decrease in SIR, hampering hydraulic functionality. Factors such as particle size distribution of the runoff sediment, the pore size distribution of the void spaces, presence of trees, surrounding land use, and winter maintenance (e.g., sand application) have been suggested to influence clogging (Bean et al. 2007; Sansalone et al. 2008; Fassman and Blackbourn 2010).

Clogging can cause 100-fold or greater reductions in SIR of permeable pavements (Illgen et al. 2007). Two porous asphalt sites treating direct rainfall in northern Sweden had SIR of 290 and 470 mm/min immediately after construction (Gyllefjord and Kangas, 1989; Bäckström and Bergström, 2000). After 2 years without maintenance, these rates had

decreased to 19 and 9.5 mm/min, respectively. Without regular maintenance, pavement SIR will continue to decrease. Seven years post-construction with no maintenance, eight PICP test sites in the Netherlands had SIRs between 3 and 37 mm/min (Boogaard et al. 2014a).

Because clogging hydraulically restricts water movement through the pavement, maintenance is needed to maintain pavement SIR. Research has, in most cases, shown clogging occurs near the pavement surface; removal of the upper 2.5 cm (Gerrits and James 2002) or 1.25-2 cm (Bean et al. 2007) of filling material resulted in significant increases in SIR. Street sweeping is one form of recommended maintenance for permeable pavements (Baladès et al. 1995). Various types of street sweepers, including mechanical, regenerative air, and vacuum trucks, may be used to remove the clogging layer. The latter two types apply suction to the pavement, while mechanical sweepers only scarify the pavement surface. Regenerative air street sweepers also apply a downward blast of air to the pavement to dislodge clogging materials. Drake and Bradford (2013) found the SIR of PICP responded more to vacuum-cleaning than did pervious concrete or porous asphalt, suggesting potentially more difficult remediation for the latter two pavement types.

Dougherty et al. (2011) studied a heavily clogged pervious concrete sidewalk, and found pressure washing (85 mm/min post-maintenance SIR) and pressure washing with power blowing (110 mm/min post-maintenance SIR) to be effective in rejuvenating pavement permeability. A porous asphalt in northern Sweden was maintained using truck-mounted vertical pressure washing and vacuum cleaning, with a subsequent increase in mean SIR from 0.5 to 3.5 mm/min (Al-Rubaei et al. 2013). During destructive testing of PICP in Australia, Lucke (2014) showed sediment migrates to the bedding course beneath the PICP;

the authors contended this is the reason efforts to return SIR to newly-installed rates have not succeeded.

A laboratory study on clogging of pervious concrete by clay-laden runoff was conducted by Haselbach (2010). After four wet-dry cycles with clay-laden synthetic runoff, SIR was reduced by minimum and maximum factors of 5 and 90, respectively. The SIR was substantially improved using surface sweeping and subsequent washing, albeit the SIRs never returned to their initial rates. Drake and Bradford (2013) also found various maintenance treatments (pressure washing, hand-held vacuuming, and street sweeping) for porous asphalt, pervious concrete, and PICP only partially restored initial SIR; these results suggest maintenance is not 100% effective at rejuvenating SIR to like-new rates.

The purpose of this work was to test and compare different maintenance techniques for restoration of permeable pavement infiltration rates. While many permeable pavement applications constructed today accept run-on from impermeable pavement (as opposed to treating only direct rainfall), *none* of these have been examined for maintenance needs. All but two sites tested herein received run-on from impermeable pavement. Simulated maintenance was performed on PICPs and CGPs by removing the upper 2 cm of filling material. Full-scale maintenance was also undertaken on clogged PICPs using a mechanical street sweeper, regenerative air street sweeper, and a vacuum truck. Two clogged porous asphalt streets were maintained using pressure washing, vacuuming, and a combination of vacuum cleaning and pressure washing. Additionally, one of these streets was milled to three different depths (0.5 cm, 1.5 cm, and 2.5 cm) to test whether milling (and subsequent

installation of new porous asphalt) could serve to rehabilitate porous asphalt and to determine the milling depth needed to remove the clogging layer.

7.3 Materials and Methods

Site Descriptions

To test the impact of maintenance on permeable pavement SIR, nine permeable pavements up to 28 years old were visited during 2014 and 2015 (Table 7-1). The sites were located in North Carolina, USA (2), Ohio, USA (1), Växjö, southern Sweden (4), Luleå, and Haparanda, northern Sweden (2). At the Ohio site, two permeable pavement applications with different characteristics were located in the same parking lot. The sites in the United States were parking lots serving city or institutional facilities, parks, or community centers, while those in Sweden drained lightly trafficked residential or commercial streets. Sites were between 0.5 and 28 years of age at the time of maintenance and were paved with either porous asphalt, CGP, or PICP. Apart from the two porous asphalt roads in northern Sweden, all sites received run-on from impermeable asphalt. These designs are standard in North Carolina, Ohio, and Sweden where hydrologic loading ratios (HLR; ratio of impermeable to permeable pavement) of 1:1, 3:1, and 5:1, respectively, are typically allowed in engineering design (ODNR 2006; NCDENR 2012). Further details on the sites in the United States, northern Sweden, and southern Sweden may be found in Winston et al. (2015), Al-Rubaei et al. (2013), and Al-Rubaei et al. (2015), respectively. Photographs and plan views of the sites can be found in Appendices D and E.

At each permeable pavement site, SIR was monitored immediately before and after maintenance. During infiltration testing at all sites, the ambient air temperature was between

10 and 25°C. None of the sites received regularly scheduled maintenance other than occasional mechanical sweeping to remove detritus. Winter maintenance at the site in Ohio consisted of road salt application as needed and snow plowing following each winter weather event. In North Carolina, snowfall happened much more infrequently, and neither plowing nor salting was needed. In Växjö, Sweden, the PICP and CGP sites were treated with a mixture of salt and sand (0-8 mm diameter); in Haparanda, Sweden, the porous asphalt received five to 10 treatments with sand mixed with 2% salt to improve road conditions each winter, while in Luleå, fine gravel (2 – 4 mm) was applied two to four times each winter onto the street surface. At all Swedish sites, the sand or gravel was removed with a mechanical sweeper each spring after snow melt. At each site, 3-8 SIR testing locations were established for pre- and post-maintenance testing. For sites with multiple rounds of maintenance (e.g., Willoughby Hills, North Carolina Central University [NCCU]), these initially chosen testing locations were utilized for all SIR tests. Testing locations were chosen to capture a diversity of potential clogging factors described in past research (e.g run-on from impermeable surfaces, landscaped areas draining to permeable pavement, locations beneath trees, locations near intersections, etc; Hunt 2011; Lucke and Beecham 2011). This included the permeable/impermeable interface (PII), or the location where run-on first enters the permeable pavement.

Table 7-1. Characteristics of the nine permeable pavement sites and types of maintenance performed.

Location	Pavement Type	Site Description	Year Built	HLR	Age at Time of Maintenance (Years)	Maintenance Methods	Number of SIR Testing Locations
Kockvägen, Luleå, Sweden	Porous asphalt	Residential street	1994	0	21	Vacuuming, pressure washing, milling	3
Åkergatan, Haparanda, Sweden	Porous asphalt	Residential street	1987	0	28	Vacuuming, pressure washing	3
Välluddevägen, Växjö, Sweden	PICP	Commercial street	2011	5:1	4	Manually remove upper 2 cm	3
Vaxthusgatan, Växjö, Sweden	PICP	Residential street	2006	5:1	9	Manually remove upper 2 cm	3
Kurortsvägen, Växjö, Sweden	CGP	Residential street	2005	5:1	10	Manually remove upper 2 cm	3
Schwerinvägen, Växjö, Sweden	CGP	Residential street	2004	5:1	11	Manually remove upper 2 cm	3
Willoughby Hills, OH, USA	PICP	Community center parking lot	2013	7.2:1, 2.2:1	0.75, 1.5	Vacuum truck	8
Durham, NC USA	PICP	Piney Wood park parking lot	2014	1.8:1	0.5	Regenerative air street sweeper	6
Durham, NC USA	PICP	NCCU law school parking lot	2013	6.5:1	1.25	Mechanical street sweeper, regenerative air street sweeper	5

Description of Maintenance Methods

Varying types of maintenance were performed across the nine sites. At the four Växjö, Sweden, sites, previous attempts at maintenance had included the use of a mechanical street

sweeper (Bucher CityCat 5000) and a regenerative air street sweeper (Johnston Beam 800, Kelemit and Stenbeck 2012). However, the narrow width of the permeable pavement (approximately 1 meter wide) and its proximity to the curb prevented proper suction from being applied to the pavement. Since pre-maintenance testing conducted herein indicated all four sites in Växjö needed maintenance, a flat-head screwdriver was used to simulate maintenance by removing the upper 2 cm of filling material from either the PICP or the CGP (Figure 7-1). Bean et al. (2007) suggested this was the depth that could be removed using a street sweeper. The infiltrometer was then placed over the maintained area and post-maintenance tests were completed (Figure 7-1).

Figure 7-1. Removal of the upper 2 cm of filling material from PICP (left) and installation of the infiltrometer over the maintained area (right).

At the Luleå and Haparanda porous asphalt sites in northern Sweden, three locations were established for triplicate testing of SIR. Following SIR testing, three types of maintenance were randomly applied to each of the testing locations (Figure 7-2). The first was vacuum cleaning using a Dustcontrol DC 50-W industrial wet/dry vacuum. Because the sites were

badly clogged and restorative maintenance was needed, the vacuuming lasted one minute. The second maintenance type was 30 seconds of high pressure washing (using a Nilfisk ALTO Poseidon 2-22 XT high pressure washer) at an approximately 30˚ angle to the asphalt surface. While pressure washing could create a point source of sediment-laden water, in practice it could be combined with vacuuming to protect against the creation a shock load of sediment during maintenance. The final maintenance type was a combination of one minute of vacuuming followed by 30 seconds of pressure washing.

Milling of impermeable asphalt is a common maintenance practice aimed at improving the quality of the surface course of the pavement, extending its overall life (Frigio et al. 2014). Since past research (*inter alia* on the porous asphalt in Luleå and Haparanda) has shown most clogging material is captured near the permeable pavement surface (Lucke and Beecham 2011; Al-Rubaei et al. 2013; Yong et al. 2013), milling could potentially be used to remove the clogging layer, restoring system performance. New porous asphalt could then be overlain. To test this idea, milling of the porous asphalt at Luleå was completed at two locations and three depths: 0.5 cm, 1.5 cm, and 2.5 cm. The milled sections were cleaned with a pressure washer prior to post-maintenance SIR testing to remove fines created by the milling process (Figure 7-2). Post-milling SIR testing was completed on the surface exposed by the milling, rather than on a new porous asphalt overlay.

Figure 7-2. Vacuuming (top left), pressure washing (top right), milling machine (bottom left), and milling test sections (bottom right) at the Luleå, Sweden, porous asphalt site.

At the NCCU site, the PICP was found to be heavily clogged (median SIR of 1 mm/min) during SIR testing on October 6, 2014. Two days later, an Advance RS850 mechanical street sweeper was brought to the site and made 5 passes over the entire parking lot (Figure 7-3). This type of street sweeper applies pressure to the surface of the pavement through rotating bristles, dislodging material accumulated in the interstitial spaces. It did not supply suction to the pavement surface. Infiltration testing was then completed and the SIRs were found to still be unsatisfactory (median SIR of 2.4 mm/min); the following day a TYMCO 600 regenerative air street sweeper performed maintenance by making 3 passes over the entire lot

(Figure 7-3). After the first pass and at the two most heavily clogged testing locations, mechanical agitation was also applied to the interstitial spaces using a pocket knife to dislodge clogging sediment prior to street sweeping. Post-maintenance SIR testing was then completed. At Piney Wood park, a TYMCO 600 regenerative air street sweeper made 5 passes over the permeable pavement, in some cases stopping over heavily clogged areas (Figure 7-3).

Figure 7-3. Mechanical street sweeper at the NCCU site (left) and regenerative air street sweeper maintaining the Piney Wood site (right).

During the first two years following construction, the Willoughby Hills, Ohio, PICP site required maintenance on two occasions, which was performed using an Elgin Megawind vacuum truck (Figure 7-4). The first maintenance effort occurred approximately 10 months after construction after surface runoff was observed and consisted of 1 pass with the vacuum truck over the entire parking lot. The second maintenance effort occurred 11 months later with 3 passes over the entire lot. The operator used the 30-cm diameter vacuum hose to clean constrained areas the truck could not access as well as right-angle corners (Figure 7-4).

Figure 7-4. Elgin Megawind vacuum truck at Willoughby Hills (left) and using the vacuum hose to maintain constrained areas the truck cannot access (right).

Data Collection

The single ring, constant head test described in ASTM C1781 for PICP (ASTM 2013) was utilized to measure SIR. A 30-cm diameter metal infiltrometer was sealed to the pavement surface using plumber's putty to prevent lateral leakage (Figure 7-5). To create an effective seal, plumber's putty was applied to both the inner and outer edges of the infiltrometer. A known volume of water was poured from a nearly-full bucket (typically about 19 liters) into the infiltrometer; water was transferred by pouring as close to the pavement surface as possible to prevent dislodging of the crusted clogging material near the pavement surface. The water level was kept at an approximately constant head of 10 to 15 mm above the pavement surface within the infiltrometer. The total time to infiltrate the known volume of water was recorded, and the SIR calculated as the quotient of the total depth of water applied within the infiltrometer to the time (e.g., mm/min). Duplicate SIR tests were carried out at each testing site both before and after maintenance.

For heavily clogged permeable pavements (<0.1 mm/min), the duration of the ASTM test exceeded 1 hour (Chapter 8). To expedite testing, the ASTM methods were modified slightly: water was poured into the infiltrometer for 15 minutes using the ASTM C1781 procedure. If the entire volume in the bucket could not be infiltrated within that time, no additional water was added; the elapsed time was then recorded at the completion of the test. Then, the remaining volume of water in the bucket was recorded and subtracted from the initial volume to determine a total volume infiltrated. SIR was then calculated as described previously. This testing method resulted in maximum test durations of approximately 1 hour.

Figure 7-5. ASTM surface infiltration rate tests on porous asphalt in Gammelstad, Sweden (left) and PICP in Växjö, Sweden (right).

Data Analysis

Summary statistics pre- and post-maintenance SIR were tabulated and explored using boxplots. All data analysis was completed using R version 3.1.2 (R Core Team 2015). A criterion of 95% confidence (α=0.05) was used for this research unless otherwise stated.

Since pre- and post-maintenance infiltration testing occurred at the same locations on each permeable pavement, paired statistical tests were utilized to determine significance. Duplicate measurements at each testing location were included in the analysis. Normality was determined using quantile-quantile plots and the Shapiro-Wilk test. If data were normal or log-normal, a Student's t-test was used. Otherwise, a non-parametric test (e.g., Wilcoxon signed-rank) was employed. This procedure was utilized for all sites except Luleå and Haparanda.

Pre- and post-maintenance data sets at Luleå and Haparanda were compared using one-way analysis of variance (ANOVA) to determine if differences among maintenance treatments were significant. Treatments included pressure washing, vacuuming, and vacuuming with pressure washing: each was run in triplicate at three separate locations on each porous asphalt roadway. Additionally, ANOVA was used to test for differences in SIR among various depths of milling (0.5 cm, 1.5 cm, and 2.5 cm) at Luleå. If the omnibus test was significant, then post-hoc pairwise comparisons were made using paired t-tests with a Bonferroni adjustment as well as the Tukey's Honest Significant Difference (HSD) test.

7.4 Results and Discussion

Degradation in Permeable Pavement SIR without Regular Maintenance

The Haparanda and Luleå sites were constructed in 1987 and 1994, respectively. Surface infiltration testing was undertaken immediately following construction, approximately 2 years after construction [Gyllefjord and Kangas (1989) and Stenmark (1995)], and at various times in the past 20 years (data collected in Bäckström and Bergström (2000), Al-Rubaei et al. (2013), and herein). Surface infiltration rate data were regressed against age for

21 and 28 year old porous asphalt pavements in Northern Sweden (Luleå and Haparanda; Figure 7-6). In Haparanda, the porous asphalt had never been maintained since construction, while in Luleå, regular vacuuming of the asphalt surface was conducted during the first years of operation; however, no maintenance had been conducted for at least the past ten years. An exponential decay in SIR with time fit the data well (R^2 = 0.89), with infiltration rates declining to less than 0.1 mm/min. In Australia and the Netherlands, research has shown an exponential decay of SIR as a function of age of the permeable pavement, reaching 8.5-17 mm/min within 3-4 years (Boogaard et al. 2014b). Sansalone et al. (2008) also found an exponential model fit the clogging process. These results confirm past research and suggest maintenance is needed to ensure long-term functionality of permeable pavements. Before widespread adoption of permeable pavements can be achieved, reliable maintenance techniques must be developed to restore pavement SIR and prevent hydraulic failure.

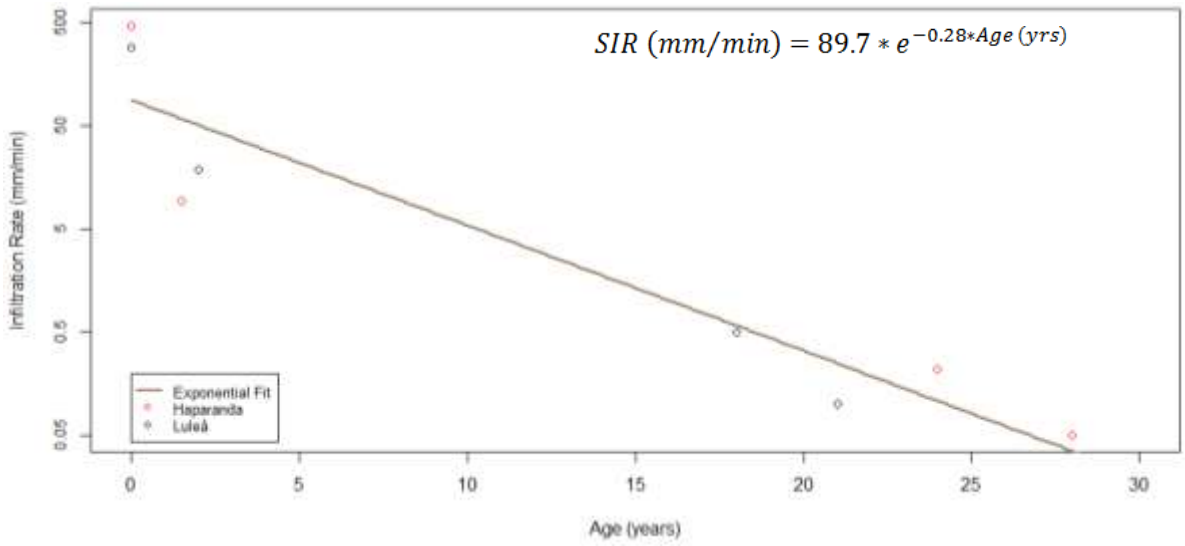

Figure 7-6. Infiltration rate as a function of age for two porous asphalts in northern Sweden. Data from Gyllefjord and Kangas (1989), Stenmark (1995), and Bäckström and Bergström (2000), Al-Rubaei et al. (2013), and herein.

Small-Scale Maintenance Tests on CGP and PICP

Simulated maintenance was performed at four sites in Växjö, Sweden, to see if removal of the upper 2 cm of sediment and aggregate material from the joint space of the CGP and PICP would improve SIR (Figure 7-1). Prior to maintenance, the median SIRs at three of the sites in Växjö (2.6, 3.2, and 6.1 mm/min; Figure 7-7) were similar to those measured three years earlier by Al-Rubaei et al. (2015), suggesting maintenance at these sites was needed. At Växthusgatan, pre-maintenance infiltration rates were ten times higher than those measured three years prior by Al-Rubaei et al. (2015). In general, the variability of the SIR was attributed to improper construction which caused heterogeneity at this site. As described in Al-Rubaei et al. (2015), the PICP and CGP joints in Växjö were erroneously filled with unwashed aggregate (0-8 mm diameter) instead of the 4-8 mm aggregate typical of infiltration system design in this part of Sweden.

Student's t-tests on the paired pre- and post-maintenance data showed no significant improvement in SIR for the PICP and CGP sites in Växjö, Sweden (all p-values>0.625; Figure 7-7). These results are in contrast with similar tests conducted by Bean et al. (2007) and James and Gerrits (2003), which both showed at least partial rehabilitation of permeable pavement SIR through removal of the upper 2-2.5 cm of clogging material. The purported reason for this was the incorrect aggregate material installed over the entire depth of the pavement layer (10 cm for PICP and CGP). So, the removal approximately the upper 20% of the joint material made no appreciable difference in SIR since fines were present throughout the 10-cm cross-section due to installation errors. This highlights the need for construction

supervision during permeable pavement installation, as incorrect installation was not overcome with maintenance.

At Kurortsvägen, one block of CGP was removed and two additional infiltration tests were performed on the 0-8 mm bedding layer (approximately 5 cm thick underlain by a geotextile with a #57 aggregate (4.75-25 mm) base course beneath the geotextile). Mean IR for the bedding layer was 2.4 mm/min, suggesting unwashed aggregate had also been utilized for this layer. The median IR for the #57 aggregate beneath the geotextile was 1770 mm/min. To remediate the performance of this SCM, the pavers, joint stone, geotextile, and bedding course would all need to be removed. Similar IR testing was performed on the aggregate beneath the CGP at Schwerinvägen. Median IR for that aggregate was 164 mm/min, compared with average pre-maintenance SIR of 6.1 mm/min. The Schwerinvägen results suggest restorative maintenance *could be* performed on CGP and PICP (through removal of paving and replacement of aggregate layers) until measured infiltration rates reach desired values, followed by reinstallation of aggregate and paving materials. Because an inappropriate fill aggregate was used in Växjö, no routine maintenance would have restored these CGP installations; thus, results do not imply that the maintenance method itself is inappropriate.

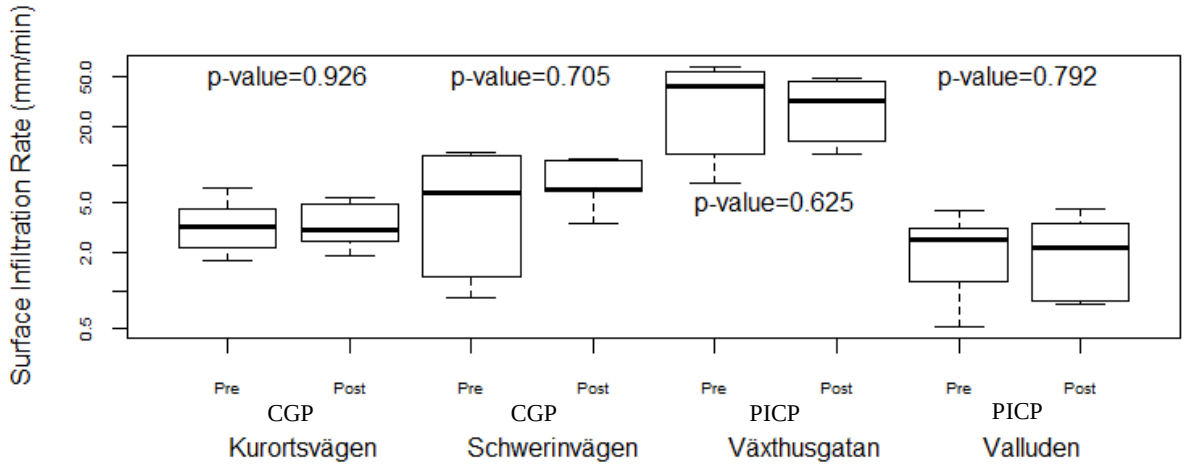

Figure 7-7. Surface infiltration rates (mm/min) of four permeable pavements in Växjö, Sweden pre- and post-simulated maintenance.

Pressure Washing and Vacuuming of Porous Asphalt

Street sweepers with suction have been successfully utilized to dislodge sediment and other clogging materials from permeable pavements (Baladès et al. 1995; Al-Rubaei et al. 2013; Drake and Bradford 2013). However, two 21- and 28-year old porous asphalts in northern Sweden (Luleå and Haparanda) that had been previously maintained with a high-pressure washer/vacuum cleaner truck had post-maintenance SIRs that were either only partially restored (in Luleå) or were unaffected (in Haparanda, see Al-Rubaei et al. [2013] for details). Therefore, three other methods of maintenance were performed at these sites, including an industrial hand vacuum, pressure washing, and a combination of vacuuming followed by pressure washing (Table 7-2). Because these porous asphalts were badly clogged prior to maintenance (median SIRs <0.1 mm/min), these maintenance efforts were an attempt at restoration of system performance.

ANOVA tests for the pre-maintenance data sets at each site showed no significant differences (p-values>0.45) in SIR, suggesting existing conditions were similar where the treatments were to be applied. All maintenance treatments produced significantly greater SIRs than pre-maintenance conditions (Figure 7-8 and Table 7-2). ANOVA tests on the log-transformed post-maintenance data sets showed significant differences between the treatments at both Luleå (p-value = 0.0064) and Haparanda (p-value = 0.0067). Significant differences were observed between the pressure wash vs. vacuum treatments (p-values = 0.0087, 0.0328) and the pressure wash+vacuum vs. vacuum treatments (p-values = 0.0231, 0.0082) at both sites. No significant difference (p-values = 0.76, 1) was observed between the pressure wash vs. pressure wash+vacuum treatment at either site. While the vacuum treatments did improve the SIR substantially and significantly (3.5 and 6-fold increases in SIR at the two sites), pressure washing as part of any treatment provided the 'lion's share' of the benefit to porous asphalt SIR (Figure 7-8). Treatments involving pressure washing increased SIRs by a minimum of 8-fold and a maximum of 467-fold (bracketing the 20-fold increase observed for combined power washing and power blowing utilized in pervious concrete maintenance by Dougherty et al. [2011]). Drake and Bradford (2013) observed 1-fold to 81-fold increases in SIR through pressure washing of porous asphalt, pervious concrete, and PICP. Chopra et al. (2010) also observed substantial increases in pervious concrete SIR through pressure washing.

Following street sweeping with vacuum cleaning and pressure washing, the mean infiltration rate post-maintenance at Luleå was only 3.48 mm/min (Al-Rubaei et al. 2013). Ten-fold greater SIRs were achieved herein by using a hand-held pressure washer, perhaps

due to the lower angle of water application (30˚ herein vs. normal to the pavement surface with the street sweeper) more easily dislodged accumulated sediment. Luleå pavement SIRs were restored to a much greater extent than those of Haparanda. This might be due to the apparent larger pore diameter in cores obtained from the two porous asphalt pavements (Al-Rubaei et al. 2013), allowing the water from the pressure washer to more deeply penetrate the pavement and dislodge sediment.

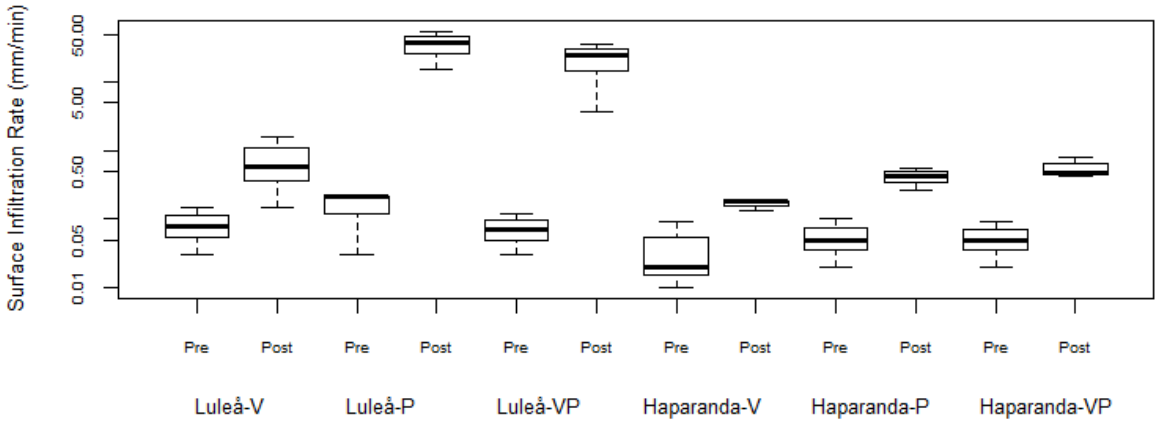

Figure 7-8. Effects of vacuuming (V), pressure washing (P), and vacuuming with pressure washing (VP) on porous asphalt SIR.

Table 7-2. Summary statistics for effects of various maintenance techniques on porous asphalt SIR in Sweden.

Site	Maintenance Type	Number of Tests	Range (mm/min)	Median (mm/min)	Mean (mm/min)	σ (mm/min)
Kockvägen, Luleå	Pre-maintenance	9	0.03-0.22	0.08	0.10	0.07
	Vacuuming	3	0.15-1.6	0.57	0.77	0.75
	Pressure washing	3	15.7-55.0	37.4	36.0	19.7
	Vacuuming + pressure washing	3	3.71-35.0	24.8	21.2	16.0
	0.5 cm milling	6	11.0-140	71.5	73.5	67.3
	1.5 cm milling	6	17.4-153	84.1	84.5	70.6
	2.5 cm milling	6	145.5-351	243	245	104
Åkergatan, Haparanda	Pre-maintenance	9	0.01-0.1	0.05	0.05	0.03
	Vacuuming	3	0.13-0.18	0.18	0.16	0.03
	Pressure washing	3	0.27-0.56	0.43	0.42	0.14
	Vacuuming + pressure washing	3	0.43-0.8	0.48	0.57	0.20

Milling of Porous Asphalt

Commonly, the majority of sediment accumulates near the surface of a permeable pavement (Balades et al. 1995; Bean et al. 2007; Shirke and Shuler 2009; Al-Rubaei et al. 2013). Complete removal of the surface clogging layer might be a viable maintenance option. Standard asphalt is milled as a common maintenance practice to rejuvenate the pavement condition without needing to reconstruct the entire road cross-section (Bausano et al. 2004). Three depths of milling (0.5 cm, 1.5 cm, and 2.5 cm, Figure 7-2) were tested at two test section of the Luleå porous asphalt roadway to see whether milling restored SIR. Following milling, pressure washing removed debris created by the milling process.

Pre-milling SIR did not vary among the testing locations (ANOVA test, p-value = 0.939), and little variability existed in pre-maintenance pavement SIR (Figure 7-9 and Table 7-2).

Differences in milling depth treatments were statistically significant (ANOVA p-value = 0.0244). No significant difference existed between the 0.5 cm and 1.5 cm (p-value = 0.87) or the 1.5 cm and 2.5 cm milling treatments (p-value = 0.07). However, the 2.5 cm treatment produced significantly better SIR (p-value = 0.027) than the 0.5 cm treatment. All post-milling SIRs were significantly better than those of pre-milling, and post-milling rates were at least 3 times greater than pre-milling SIRs. Post-milling SIRs also were at least twice those from pressure washing maintenance treatments at the same site.

Milling to a 2.5 cm depth appeared to be the best treatment, producing SIRs roughly three times those of the 0.5 and 1.5 cm depths. In fact, the median infiltration rates of 243 mm/min for the 2.5 cm milling depth was essentially the same for that porous asphalt immediately after construction (290 mm/min, Stenmark 1995), 21 years prior to the milling. The marginal increase in SIR from 0.5 to 1.5 cm milling depth suggested little sediment was present between 0.5-1.5 cm below the pavement surface. However, clearly additional clogging factors were eliminated when milling to a 2.5 cm depth. Three possible explanations for this exist: (1) sediment accumulated at 1.5-2.5 cm depth (not likely based on core samples presented in Al-Rubaei et al. (2013); (2) asphalt binder draindown restricted flow at 1.5-2.5 cm depth (Mansour and Putman 2013), or (3) removing 2.5 cm of asphalt allowed the pressure washer to penetrate more deeply into the bedding course, since the pre-milled pavement thickness was 4.5 cm. Considering all factors, milling (regardless of depth) appeared to be the best method tested for restoration of (even completely) clogged porous asphalt SIRs.

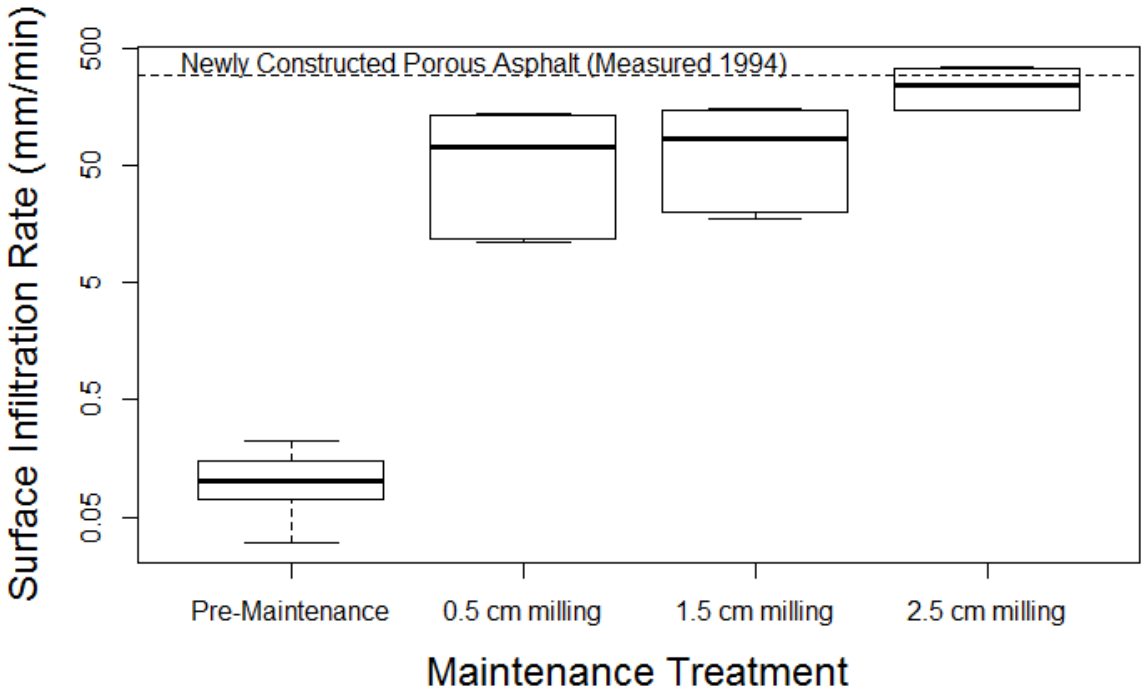

Figure 7-9. Effects of milling on porous asphalt SIR at Luleå.

Street Sweeping

Since street sweeping is an oft-suggested maintenance practice for maintenance of permeable pavements (Drake et al. 2013), a variety of methods of street sweeping were tested at NCCU, Piney Wood, and Willoughby Hills to determine their impact on SIR.

Two street sweeper types were applied over a two-day period at the NCCU site: mechanical street sweeping followed by regenerative air street sweeping (Figure 7-3). While mechanical sweepers are not recommended for PICP maintenance due to their lack of suction, this most-prevalent type of sweeper was initially used to maintain the badly clogged site (median pre-maintenance SIR 1.0 mm/min; Figure 7-10 and Table 7-3). Five passes were made over the entire parking lot with the mechanical sweeper, which produced a

significant (350%) increase in SIR (p-value 0.0293) to a median value of 2.40 mm/min. Observations showed mechanical sweeping dislodged only the uppermost 6-13 mm of clogging material. SIR did not improve at the most heavily clogged measurement location. Using a hose, water was applied to the PICP surface, and surface runoff still occurred; therefore, further maintenance was scheduled the following day using a regenerative air street sweeper (Figure 7-3).

The regenerative air street sweeper removed, on average, the upper 5 cm of clogging material and aggregate with only 3 passes over the parking lot. However, similar to Drake and Bradford's (2013) results, removal of aggregate and sediment did not occur to a consistent depth and was highly spatially variable. SIR testing was performed immediately following this second round of maintenance, and significant improvement of SIR was measured (p-value = 0.0035). Median SIR increased to 14.1 mm/min, a 14-fold increase over the pre-maintenance rates and a 5-fold increase over the post-mechanical street sweeper maintenance rates. Median SIRs pre- and post-maintenance suggested the greater improvement in pavement hydraulics was provided by the regenerative air street sweeper, which was able to dislodge the clogging material at deeper depths than the mechanical street sweeper. However, the median post-maintenance SIR of 14.1 mm/min was much less than those of newly-installed PICP, which can range from 310-680 mm/min (Bean et al. 2007). None of these maintenance techniques was able to fully restore pavement hydraulics. Results suggest permeable pavements receiving run-on from impermeable pavements should be maintained with street sweepers providing suction, similar to results of past studies (Baladès et al. 1995; Bean et al. 2007; Shirke and Shuler 2009).

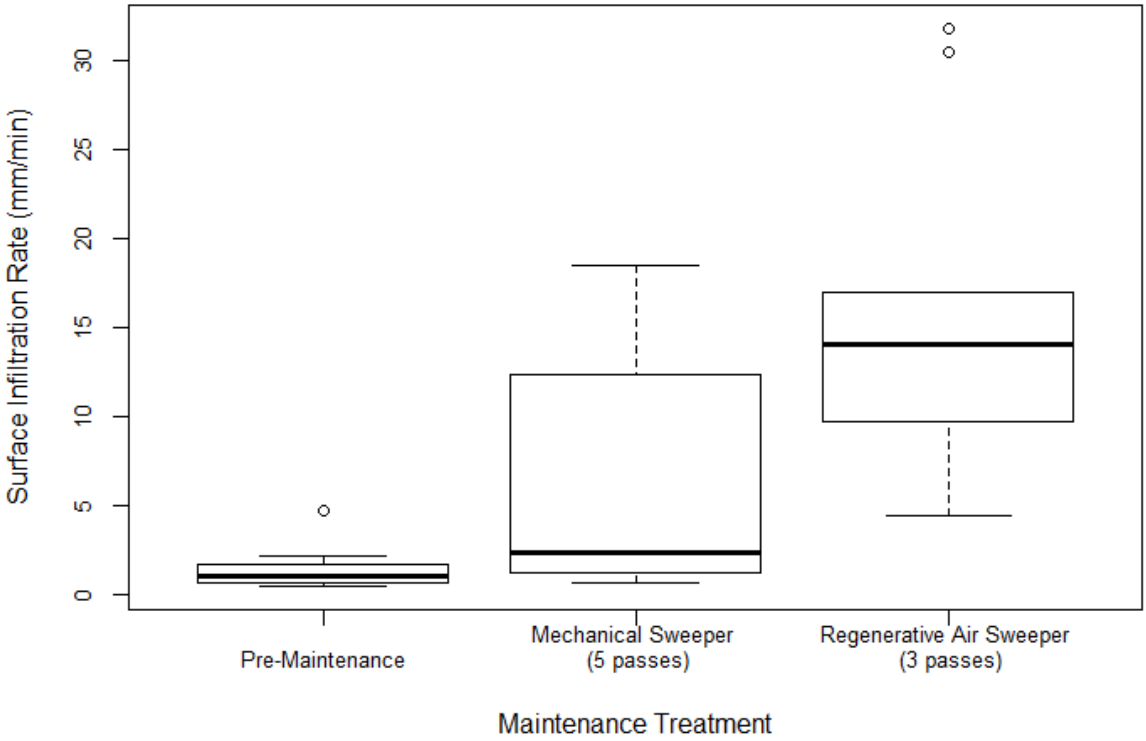

Figure 7-10. Effects of standard mechanical and regenerative air street sweepers on SIR of PICP at NCCU in Durham, NC.

Table 7-3. Summary statistics pre- and post-maintenance SIR using various types of street sweepers on PICP.

Site	Maintenance Type	Number of Tests	Range (mm/min)	Median (mm/min)	Mean (mm/min)	σ (mm/min)	p-value	Statistical Test
NCCU	Pre-maintenance	10	0.44-4.71	1.00	1.41	1.28	-	-
	5 passes mechanical sweeper	10	0.65-18.5	2.40	6.38	6.71	0.0293	Student's t-test
	3 passes regenerative air sweeper	10	4.45-31.9	14.1	15.7	9.07	0.0035	Student's t-test
Piney Wood	Pre-maintenance	12	1.3-10.8	1.76	3.43	3.69	-	-
	5 passes regenerative air sweeper	12	9.4-165	154	111	75.4	0.0167	Student's t-test
	Pre-maintenance	12	135-315	231	229	77.7	-	-
	1 pass regenerative air sweeper	12	103-193	143	146	36.7	0.0975	Student's t-test
Willoughby Hills	Pre-maintenance	16	1.54-361	64.4	100	108	-	-
	1 pass vacuum Truck	16	33.9-381	173	173	114	0.0148	Student's t-test
	Pre-maintenance	16	0.81-190	4.39	36.4	63.7	-	-
	3 passes vacuum truck	16	8.52-699	148	202	192	0.0020	Student's t-test

At Piney Wood, maintenance was performed using a regenerative air street sweeper (Figure 7-3) in the fall of 2014. The three testing locations within 2 meters of the PII had pre-maintenance median SIRs of 6, 2, and 3 mm/min (Figure 7-11 and Table 7-3). These three locations were swept 5 times by the street sweeper, with the sweeper moving slowly and stopping over heavily clogged areas. Personnel observed the pavement surface under the moving street sweeper to determine the depth to which the clogging material was removed.

Following maintenance, median SIR significantly increased from 1.76 to 154 mm/min, an 86-fold increase. However, this SIR is still below rates for newly installed PICP, estimated to be 310-680 mm/min (Bean et al. 2007). Additionally, one of the three locations nearest the PII had a post-maintenance SIR of 10 mm/min, which is still less than the desirable range for sites treating run-on (based on observed surface runoff from the PICP during rainfall and simulated rainfall using a garden hose for locations with SIR less than 20 mm/min). These results reaffirmed what Drake and Bradford (2013) suggested: regenerative air street sweepers are not capable of restoring heavily clogged permeable pavements to like-new SIRs. They surmised frequent maintenance will be needed to maintain acceptable SIRs at sites receiving high particulate loading.

The other three SIR monitoring locations at Piney Wood were at minimum 5 meters from where run-on entered the PICP and were therefore less susceptible to clogging (Brown and Borst 2013; Al-Rubaei et al. 2015). Pre-maintenance, their median SIR was 231 mm/min and visually little clogging material was present in the interstitial spaces. Due to high SIR, only one pass was made over these locations with the regenerative air street sweeper. This pass made no significant difference in SIR; thus, the number of passes and speed at which passes are made affect maintenance success. Multiple passes over heavily clogged areas, even stopping the truck to allow the suction to have maximum effect, may be desirable as a single pass made no discernable difference in SIR. The spatial variability in clogging at Piney Wood (mostly related to the PII) suggests simple, quick, and reliable infiltration tests are needed to determine areas of a permeable pavement lot needing maintenance (Lucke et al. 2015; Chapter 8).

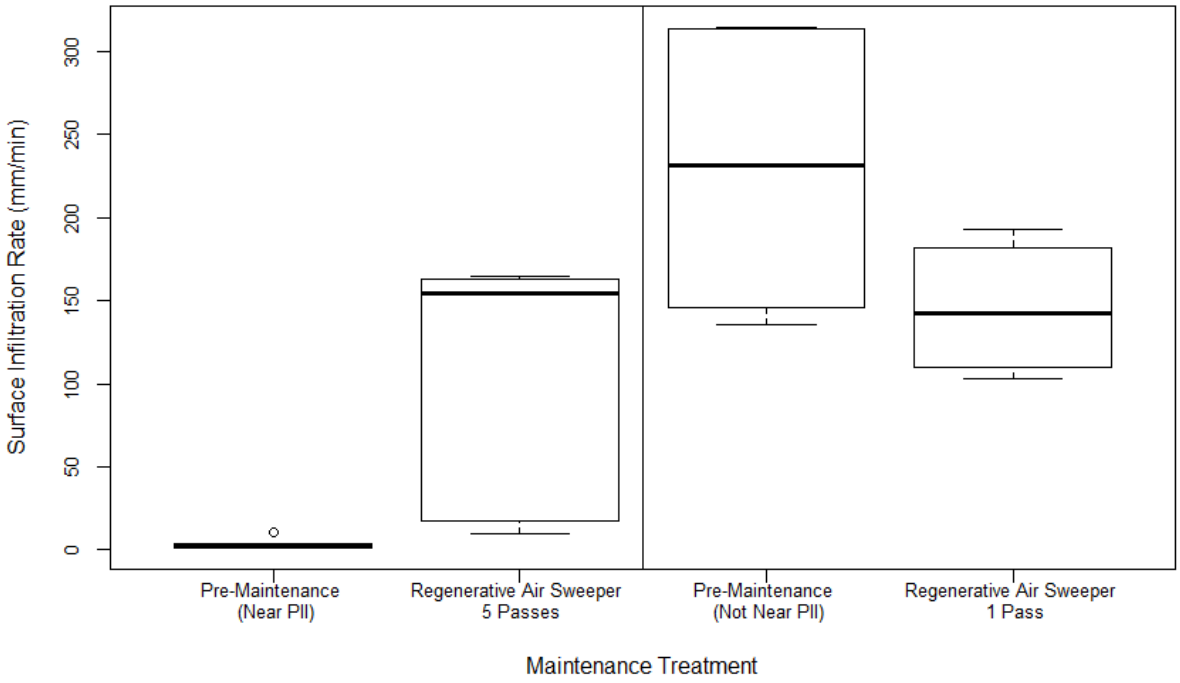

Figure 7-11. The spatial extent of clogging at Piney Wood, Durham, NC and the effects of a regenerative air street sweeper on SIR.

Similar pre- and post-maintenance infiltration testing was undertaken at Willoughby Hills using an Elgin Megawind vacuum truck (Figure 7-4) during July 2014 and again in July 2015 (Figure 7-12 and Table 7-3). This type of sweeper provides greater suction with dual suction hoses (86 kW provided by the engine at 2400 RPM) than the regenerative air street sweeper (one suction and one blower hose; 74 kW at 2400 RPM) used to maintain NCCU and Piney Wood. Maintenance in July 2014 consisted of one pass over the entire parking lot, with replacement of stone in the interstitial spaces following maintenance. Median pre-maintenance SIR was 64.4 mm/min, but the three locations receiving run-on from impermeable asphalt (located <1 meter from the PII) had SIRs <20 mm/min; surface runoff was observed during a small, minimally intense rainfall event at these SIRs (5 mm depth,

0.15 mm/min peak intensity). Post-maintenance, the median SIR increased significantly by 168% to 173 mm/min. While five of the eight monitoring locations had substantial increases in SIR post-maintenance (up to 8-fold), three did not. One of these sites was not clogged prior to maintenance (median SIR 352 mm/min), because it received no run-on. The other two locations were located less than 1 meter from the PII, suggesting more than one pass with a vacuum truck may be needed to dislodge clogging material from heavily clogged locations. Given the large hydraulic loading to these locations (impervious flow path lengths of 21 and 42 meters), frequent and intensive maintenance (perhaps the removal of the pavers and some of the bedding course, where clogging material also accumulates [Lucke and Beecham 2011]) will be needed to keep sites alongside the PII from failing hydraulically. This also suggests designers should be conservative when directing run-on to permeable pavement; higher run-on ratios will lead to quicker clogging and higher maintenance burden.

Following another year of rainfall, the SIRs at Willoughby Hills had degraded substantially to a median value of 4.39 mm/min; SIRs at 5 of the 8 sites were below 6 mm/min. Maintenance was completed using the same vacuum truck, but this time making 3 passes over the parking lot. In the most-clogged areas, this method was unable to uniformly remove 5 cm of clogging material; although, a sufficient number of clogged gaps would be rejuvenated to allow water to pass at higher rates. Following maintenance, median SIR for the site significantly improved to 148 mm/min, a 33-fold increase. However, these rates were still significantly (at the $\alpha = 0.10$ level) below the median SIRs (173 mm/min) measured the prior year post-maintenance. In this case, more intensive maintenance produced lower infiltration rates, suggesting each maintenance effort is not 100% effective.

Thus, in order to realize a similar post-maintenance SIR, maintenance intervals may become shorter as the pavement ages. At some point, major restorative maintenance, including removal of the pavers, interstitial stone, and portions of the bedding course may be needed to prevent surface runoff.

For locations most susceptible to clogging (i.e., nearest the PII), the vacuum truck and regenerative air street sweepers similarly restored SIRs. The caveat is that the vacuum truck required one or three passes to restore median SIR to 150-175 mm/min at Willoughby Hills. At Piney Wood, 5 passes with the regenerative air street sweeper were needed to achieve similar median SIR (150 mm/min). This suggested the vacuum truck was more efficient for maintenance due to its greater suction.

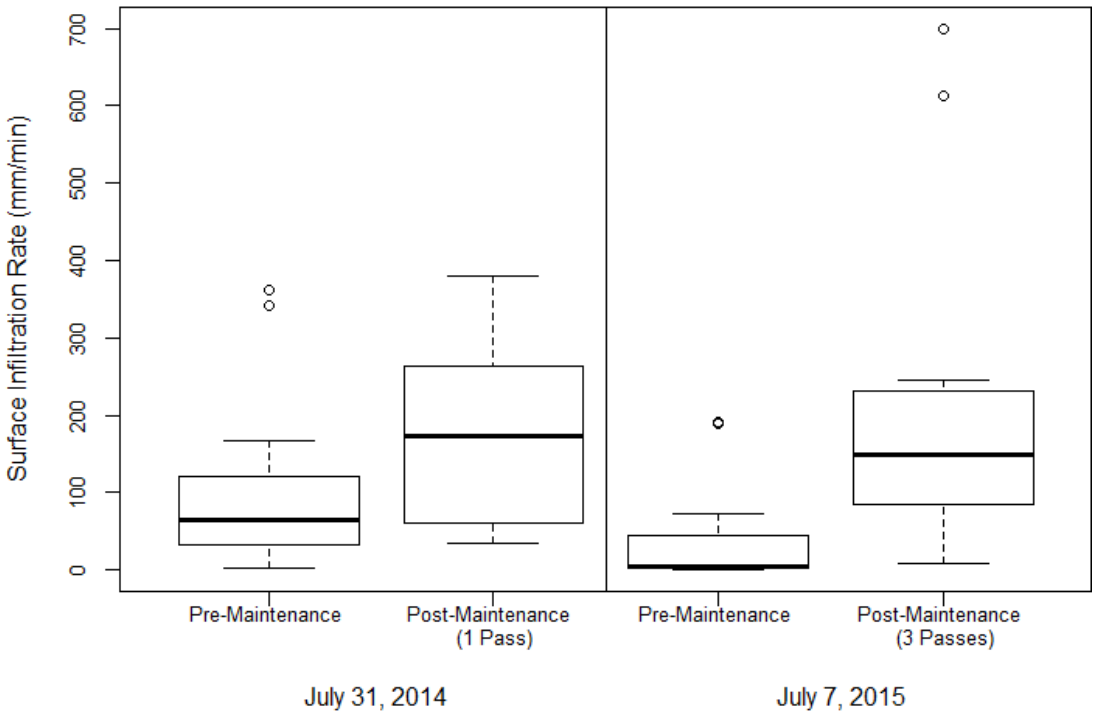

Figure 7-12. Improvement in SIR through the use of a vacuum truck at Willoughby Hills, Ohio.

Effects of Maintenance on Retention of Design Rainfall Intensities

One of the purported benefits of permeable pavements is the potential for peak flow mitigation during design storm events, since the aggregate reservoir can be designed to detain and slowly release stormwater through the underdrain (Drake et al. 2014; ASCE 2015). However, this benefit is lost if stormwater cannot infiltrate the pavement during extreme rainfall intensities. Design rainfall intensities were obtained for small, parking lot watersheds (i.e., time of concentration of 5 minutes) for annual recurrence intervals (ARI) between 1-year and 100-years (SWWA 2011; NOAA 2014) for all locations tested herein. These rainfall intensities were utilized to calculate the peak flow rate of runoff draining or falling onto each permeable pavement installation using the Rational Method (McCuen 1998). The calculated peak flow rate was compared against the measured SIR at each testing location both pre- and post-maintenance. While this comparison assumed even flow distribution, in reality preferential flow onto permeable pavement occurs due to site slopes and concentration of flow along curbs and parking lot islands.

The fraction of SIR monitoring locations able to completely infiltrate rainfall intensities with ARIs between 1-yr and 100-yr, which are typically used for flood control (Nehrke and Roesner 2004), are presented in Table 7-4. For each monitoring location (e.g., 12 monitoring locations at Piney Wood pre-maintenance), the percentage of the 100-yr design rainfall intensity which could be infiltrated was calculated as the quotient of the infiltration rate and the aforementioned rainfall intensity.

$$\%(100-yr\ storm\ infiltrated) = \frac{SIR_{Meas,i}}{Q_{p,100}} * 100 \qquad (7\text{-}1)$$

where $SIR_{Meas,i}$ is the measured SIR at the i^{th} measurement location at a permeable pavement site and $Q_{p,100}$ is the peak flow rate from the 100-yr ARI storm event. This yielded a range of values for each site/monitoring period combination, since pavement SIR was highly spatially variable (Table 7-4). While none of the monitored permeable pavements had enough void space in the aggregate to detain the 100-yr event, this method is still valuable to observe predicted infiltration performance under potential engineering designs for peak flow mitigation.

At three of the four sites in Växjö, Sweden, more intense design rainfall events were able to be completely infiltrated following maintenance. However, Växthusgatan was the only site where the fraction of the 100-yr storm that could be infiltrated changed substantially, where at minimum 61% of this storm could be infiltrated post-maintenance as opposed to 36% pre-maintenance.

While results from Luleå and Haparanda showed vacuuming with a hand-held industrial vacuum had a modestly positive effect on runoff capture, but vacuuming was not as effective as high pressure washing (Table 7-4). While improvements in SIR at Haparanda were significant and substantial when pressure washed, the pre-maintenance infiltration rates were so low that the site remained unable to infiltrate the 1-yr design rainfall intensity post-maintenance. Any depth of milling allowed the porous asphalt at Luleå to completely infiltrate the 100-yr design rainfall intensity.

Street sweeping increased the fraction of monitoring locations able to completely infiltrate design rainfall intensities, albeit the standard mechanical sweeper did so modestly (Table 7-4). The vacuum truck appeared to be able to best restore pavement infiltration rate

at locations with heavy clogging, such as near the PII. In general, well-maintained permeable pavements are capable of reducing peak runoff rate through storage in the subgrade aggregate; without maintenance, clogged permeable pavement will provide little to no peak flow mitigation.

Table 7-4. Fraction of SIR monitoring locations theoretically able to infiltrate design rainfall intensities and the range of the fraction of the 100-yr storm theoretically able to be infiltrated at all monitoring locations.

Location	Monitoring Period	1-yr[1]	2-yr	5-yr	10-yr	25-yr	50-yr	100-yr	% 100-yr ARI captured
Kurortsvägen, Växjö, Sweden	Pre-maintenance	2/6	1/6	0/6	0/6	0/6	0/6	0/6	9-33%
	Post-maintenance	2/6	1/6	0/6	0/6	0/6	0/6	0/6	9-27%
Schwerinvägen, Växjö, Sweden	Pre-maintenance	3/6	3/6	2/6	2/6	2/6	0/6	0/6	4-62%
	Post-maintenance	5/6	5/6	2/6	2/6	0/6	0/6	0/6	17-55%
Växthusgatan, Växjö, Sweden	Pre-maintenance	6/6	6/6	5/6	5/6	5/6	4/6	4/6	36-100%
	Post-maintenance	6/6	6/6	6/6	6/6	6/6	4/6	4/6	61-100%
Valluden, Växjö, Sweden	Pre-maintenance	0/6	0/6	0/6	0/6	0/6	0/6	0/6	3-21%
	Post-maintenance	1/6	0/6	0/6	0/6	0/6	0/6	0/6	4-22%
Gammelstad, Luleå, Sweden	Pre-maintenance	0/9	0/9	0/9	0/9	0/9	0/9	0/9	1-5%
	Hand vacuuming	1/3	1/3	1/3	0/3	0/3	0/3	0/3	4-40%
	Pressure washing	3/3	3/3	3/3	3/3	3/3	3/3	3/3	100%
	Vacuuming + pressure washing	3/3	3/3	3/3	3/3	3/3	3/3	2/3	92-100%
	0.5 cm milling	6/6	6/6	6/6	6/6	6/6	6/6	6/6	100%
	1.5 cm milling	6/6	6/6	6/6	6/6	6/6	6/6	6/6	100%
	2.5 cm milling	6/6	6/6	6/6	6/6	6/6	6/6	6/6	100%
Åkergatan, Haparanda, Sweden	Pre-maintenance	0/9	0/9	0/9	0/9	0/9	0/9	0/9	0.3-4%
	Hand vacuuming	0/3	0/3	0/3	0/3	0/3	0/3	0/3	3-5%
	Pressure washing	0/3	0/3	0/3	0/3	0/3	0/3	0/3	7-14%
	Vacuuming + pressure washing	0/3	0/3	0/3	0/3	0/3	0/3	0/3	11-20%
Piney Wood, Durham, NC, USA	Pre-maintenance	7/12	7/12	7/12	7/12	7/12	7/12	7/12	13-100%
	Post-maintenance	12/12	12/12	12/12	12/12	12/12	11/12	11/12	91-100%
NCCU, Durham, NC, USA	Pre-maintenance	0/10	0/10	0/10	0/10	0/10	0/10	0/10	2-17%
	Post-maintenance (mechanical sweeper)	2/10	1/10	0/10	0/10	0/10	0/10	0/10	2-68%
	Post-maintenance (Regenerative Air)	4/10	2/10	2/10	2/10	2/10	2/10	2/10	16-100%
Willoughby Hills, OH, USA	Pre-maintenance	15/16	14/16	14/16	14/16	14/16	14/16	13/16	5-100%
	Post-maintenance (vacuum truck 1 pass)	16/16	16/16	16/16	16/16	16/16	16/16	16/16	100%
	Pre-maintenance	8/16	6/16	6/16	5/16	4/16	4/16	4/16	4-100%
	Post-maintenance (vacuum truck 3 passes)	16/16	16/16	16/16	16/16	15/16	15/16	15/16	76-100%

[1]all events have 5-minute duration.

7.5 Summary and Conclusions

Nine permeable pavement sites in four climatic regions and two countries were utilized for testing of various maintenance treatment technologies. Between 3-8 monitoring locations were established at each site for pre- and post-maintenance SIR testing to evaluate (1) locations expected to clog quickly and (2) reference locations without clogging stimuli. Maintenance treatments included manual removal of the upper 2 cm of clogging material, hand-held vacuum cleaning, pressure washing, a combination of vacuum cleaning and pressure washing, milling of porous asphalt, and three different types of street sweeping. Maintenance was performed on CGP, PICP, and porous asphalt pavements. The following conclusions are gleaned from this work:

1) Manual removal of the upper 2 cm of clogging material at the Växjö, Sweden, CGP and PICP sites did not provide significant improvement in pavement SIR. This was due to errors in construction, where fines were present in entirety of the joint stone and the bedding course, vastly diminishing pavement SIRs. Routine maintenance cannot overcome poor construction practices and lack of construction supervision.

2) Hand-held industrial vacuum cleaning, pressure washing, and a combination of vacuum cleaning and pressure washing all significantly improved the SIR of two clogged porous asphalt sites in northern Sweden. Treatments with pressure washing were significantly different from vacuuming alone. At Luleå, post-maintenance SIRs were 0.6 mm/min for the vacuuming treatment, and 21-36 mm/min for treatments involving pressure washing. Treatments with pressure washing were able to infiltrate larger design rainfall intensities than those with vacuuming only. This suggested appropriately applied

pressure washing was capable of restoring porous asphalt permeability, especially if applied at a low angle to the pavement surface.

3) Milling of the porous asphalt at Luleå was tested to restore SIR at three different depths: 0.5 cm, 1.5 cm, and 2.5 cm. All depths of milling were successful in restoring pavement SIR to a median rate of at least 70 mm/min. The 2.5 cm milling depth yielded a median SIR of 245 mm/min, near the 290 mm/min infiltration rate measured immediately after construction (21 years earlier). This was the only maintenance technology tested capable of rejuvenating pavement SIR to nearly-newly installed rates. These results suggest milling and subsequent reinstallation of a porous asphalt is a viable option to restore porous asphalt permeability. Further, these results confirmed the clogging layer in this porous asphalt occurred within the uppermost 2.5 cm of the pavement surface.

4) Three types of street sweepers (mechanical, regenerative air, and a vacuum truck) were utilized to maintain PICP in North Carolina and Ohio, USA. All methods of maintenance produced significantly higher post-maintenance SIRs. However, maintenance of the NCCU site on successive days with a mechanical sweeper followed by a regenerative air sweeper showed that suction provided by the latter more deeply penetrates clogging layers and therefore SIR benefits. For monitoring locations with high debris loading (i.e., near the PII, beneath trees, etc.), maintenance needs are more intensive than locations with few clogging stimuli. Multiple passes with a regenerative air street sweeper or vacuum truck, and even stopping over heavily clogged locations, were needed to create acceptable post-maintenance SIRs. At Willoughby Hills, maintenance regimens were performed with a vacuum truck and were separated by one year. To reach similar post-maintenance SIRs (median

150-175 mm/min), one pass with the vacuum truck was needed during the first maintenance effort; 3 were needed one year later. To maintain a desired threshold SIR, the frequency of permeable pavement maintenance will likely increase with time.

5) To mitigate peak flows from flood-inducing events, permeable pavements must have surface infiltration rates exceeding expected peak flow rates from the catchment. In nearly every case estimated herein, maintenance with vacuuming, pressure washing, milling, or street sweeping increased the frequency with which a permeable pavement could completely infiltrate a design rainfall intensity. Additionally, all maintenance treatments except the simulated maintenance performed in Växjö allowed a greater fraction of the 100-yr storm to infiltrate the pavement surface than during pre-maintenance conditions.

6) Since the Luleå and Haparanda sites treated only direct rainfall (while the other locations had hydraulic loading ratios $\geq$ 1.8:1), the loading of sediment onto these pavements was much less, resulting in less frequent maintenance needs. Diminishing the hydraulic loading ratio will result in a reduced maintenance burden. Concentrated flow to a permeable pavement should be avoided in engineering design because maintenance will be onerous and frequent to ensure pavement hydraulic performance.

7.6 References

Al-Rubaei, A.M., Stenglein, A.L., Viklander, M., and Blecken, G.T. (2013). "Long-term hydraulic performance of porous asphalt pavements in northern Sweden." *J. Irrig. Drain. Eng*., 139(6), 499-505.

Al-Rubaei, A.M., Viklander, M., and Blecken, G.-T. (2015). "Long-term hydraulic performance of stormwater infiltration systems." *Urban Water J*., 12(8), 660-671.

American Society of Civil Engineers. (2015). *Permeable pavements*. Permeable pavement task committee. Eds. B. Eisenberg, K.C. Lindow, and D.R. Smith. Reston, VA.

Arnold Jr, C.L., and Gibbons, C.J. (1996). "Impervious surface coverage: the emergence of a key environmental indicator." *J. Am. Plann. Assoc*., 62(2), 243-258.

American Society for Testing and Materials (ASTM). (2013). Standard test method for surface infiltration rate of permeable unit pavement systems. C1781/C1781M-13.

Bäckström, M., and Bergström, A. (2000). "Draining function of porous asphalt during snowmelt and temporary freezing." *Can. J. Civ. Eng*., 27(3), 594-598.

Baladès, J.D., Legret, M., and Madiec, H. (1995). "Permeable pavements: pollution management tools." *Water Sci. Technol*., 32(1), 49–56.

Bausano, J., Chatti, K., and Williams, R. (2004). "Determining life expectancy of preventive maintenance fixes for asphalt-surfaced pavements." *Transp. Res. Rec*., 1866, 1-8.

Bean, E.Z., Hunt, W.F., and Bidelspach, D.A. (2007). "Field survey of permeable pavement surface infiltration rates." *J. Irrig. Drain. Eng*., 133(3). 249-255.

Ben-Joseph, E., (2012). *ReThinking a Lot: the Design and Culture of Parking*. MIT Press, Cambridge, Massachusetts, USA.

Blecken, G.-T., Hunt, W.F., Al-Rubaei, A.M., Viklander, M., and Lord, W. In press. "Stormwater Control Measure (SCM) Maintenance Considerations to Ensure Designed Functionality." *Urban Water J.*

Boogaard, F., Lucke, T., van de Giesen, N., and van de Ven, F. (2014a). "Evaluating the infiltration performance of eight Dutch permeable pavements using a new full-scale infiltration testing method. *Water*. 6(7), 2070-2083.

Boogaard, F., Lucke, T., and Beecham, S. (2014b). "Effect of age of permeable pavements on their infiltration function." *CLEAN–Soil, Air, Water*. 42(2), 146-152.

Brattebo, B. O., and Booth, D. B. (2003). "Long-term stormwater quantity and quality performance of permeable pavement systems." *Water Res.*, 37(18), 4369-4376.

Brown, R.A., and Borst, M. (2013). "Assessment of clogging dynamics in permeable pavement systems with time domain reflectometers." *J. Environ. Eng.*, 139(10), 1255-1265.

Chopra, M., Kakuturu, S., Ballock, C., Spence, J., and Wanielista, M. (2009). "Effect of rejuvenation methods on the infiltration rates of pervious concrete pavements." *J. Hydrol. Eng.*, 15(6), 426-433.

Collins, K.A., Hunt, W.F., and Hathaway, J.M. (2008). "Hydrologic comparison of four types of permeable pavement and standard asphalt in eastern North Carolina." *J. Hydrol. Eng.*, 13(12), 1146-1157.

Dietz, M.E. (2007). "Low impact development practices: A review of current research and recommendations for future directions." *Water Air Soil Poll.*, 186(1-4), 351-363.

Dougherty, M., Hein, M., Martina, B.A., and Ferguson, B.K. (2011). "Quick surface infiltration test to assess maintenance needs on small pervious concrete sites." *J. Irrig. Drain. Eng.*, 137(8), 553-563.

Drake, J., and Bradford, A. (2013). "Assessing the potential for restoration of surface permeability for permeable pavements through maintenance." *Water Sci. Technol.*, 68(8), 1950-1958.

Drake, J.A., Bradford, A., and Marsalek, J. (2013). "Review of environmental performance of permeable pavement systems: state of the knowledge." *Water Qual. Res. J. Can.*, 48(3), 203-222.

Drake, J., Bradford, A., and Van Seters, T. (2014). "Hydrologic performance of three partial-infiltration permeable pavements in a cold climate over low permeability soil." *J. Hydrol. Eng.*, 19(9), 04014016.

Fassman, E.A., and Blackbourn, S. (2010). "Urban runoff mitigation by a permeable pavement system over impermeable soils." *J. Hydrol. Eng.*, 15(6), 475-485.

Frigio, F., Pasquini, E., Partl, M.N., and Canestrari, F. (2014). "Use of reclaimed asphalt in porous asphalt mixtures: Laboratory and field evaluations." *J. Mater. Civ. Eng.*, 27(7), 04014211.

Gerrits, C., and James, W. (2002). "Restoration of infiltration capacity of permeable pavers." *Proceedings of the 9th International Conference on Urban Drainage*. ASCE, Portland, Ore.

Gilbert, J.K., and Clausen, J.C. (2006). "Stormwater runoff quality and quantity from asphalt, paver, and crushed stone driveways in Connecticut." *Water Res.*, 40(4), 826-832.

Gyllefjord, A., and Kangas, J. (1989). *Infiltration measurements of permeable asphalt in the laboratory*. (In Swedish: Infiltrationsmätning på permeabel asfalt i labmiljö). MSc thesis, Luleå University of technology, Luleå, Sweden.

Haselbach, L.M. (2010). "Potential for clay clogging of pervious concrete under extreme conditions." *J. Hydrol. Eng.*, 15(1), 67-69.

Hunt, W.F. (2011). *Maintaining permeable pavements*. North Carolina Cooperative Extension Urban Waterways fact sheet series. AG-588-23 W.

Illgen, M., Harting, K., Schmitt, T.G., and Welker, A. (2007). "Runoff and infiltration characteristics of permeable pavements – Review of an intensive monitoring program." *Water Sci. Technol*., 56(10), 133-40.

James, W., and Gerrits, C. (2003). "Maintenance of infiltration in modular interlocking concrete pavers with external drainage cells." In: *Practical Modeling of Urban Stormwater Systems*, Vol. 11 (W. James, ed.). Computational Hydraulics International, Guelph, Canada. pp. 417–435.

Kelemit, D. and Stenbeck, P. (2012). Investigation of existing infiltration strips in Växjö. Translated from Swedish: Utredning av funktion hos befintliga infiltrationsstråk i Växjö. Master's Thesis, Linné University, Växjö, Sweden.

Lucke, T., and Beecham, S. (2011). "Field investigation of clogging in a permeable pavement system." *Build. Res. Inf*., 39(6), 603-615.

Lucke, T. (2014). "Using drainage slots in permeable paving blocks to delay the effects of clogging: Proof of concept study." *Water*. 6(9), 2660-2670.

Lucke, T., White, R., Nichols, P., and Borgwardt, S. (2015). "A simple field test to evaluate the maintenance requirements of permeable interlocking concrete pavements. *Water, 7*(6), 2542-2554.

Mansour, T.N., and Putman, B.J. (2012). "Influence of aggregate gradation on the performance properties of porous asphalt mixtures." *J. Mater. Civ. Eng*., 25(2), 281-288.

McCuen, Richard H. 1998. *Hydrology analysis and design*. Prentice-Hall. 2ed.

Morse, C.C., Huryn, A.D., and Cronan, C. (2003). "Impervious surface area as a predictor of the effects of urbanization on stream insect communities in Maine, USA." *Environ. Monit. Assess*., 89(1), 95-127.

National Oceanic and Atmospheric Administration (NOAA). (2014). NOAA Atlas 14 Precipitation Frequency Estimates: Ohio and North Carolina. Available: http://hdsc.nws.noaa.gov/hdsc/pfds/index.html

Nehrke, S.M., and Roesner, L.A. (2004). "Effects of design practice for flood control and best management practices on the flow-frequency curve." *J. Water Resour. Plann. Manage*., 130(2), 131-139.

North Carolina Department of Environment and Natural Resources (NCDENR). (2012). *NCDENR stormwater BMP manual*. Chapter 18: Permeable Pavement. Revised 10/16/2012.

Ohio Department of Natural Resources (ODNR), Division of Soil and Water Conservation. (2006). *Rainwater and land development: Ohio's standards for stormwater management, low impact development, and urban stream protection*. 3rd edition. Ed: John Mathews.

Page, J.L., Winston, R.J., Mayes, D.B., Perrin, C., and Hunt, W.F. (2015). "Hydrologic mitigation of impervious cover in the municipal right-of-way through innovative stormwater control measures." *J. Hydrol.,* 527, 923-932.

Pratt, C.J., Mantle, J.D.G., and Schofield, P.A. (1989). "Urban stormwater reduction and quality improvement through the use of permeable pavements." *Water Sci. Technol*., 21(8), 769–778.

R Core Team. (2015). *A language and environment for statistical computing*. R Foundation for Statistical Computing. Vienna, Austria.

Roseen, R.M., Ballestero, T.P., Houle, J.J., Briggs, J.F., and Houle, K.M. (2012). "Water quality and hydrologic performance of a porous asphalt pavement as a storm-water treatment strategy in a cold climate." *J. Environ. Eng*., 138(1), 81-89.

Sansalone, J., Kuang, X., and Ranieri, V. (2008). "Permeable pavement as a hydraulic filtration interface for urban drainage." *J. Irrig. Drain. Eng*., 134(5), 666–674.

Schueler, T.R., Fraley-McNeal, L., and Cappiella, K. (2009). "Is impervious cover still important? Review of recent research." *J. Hydrol. Eng.,* 14(4), 309-315.

Shirke, N.A., and Shuler, S. (2009). "Cleaning porous pavements using a reverse flush process." *J. Transp. Eng*., 135(11), 832–838.

Stenmark, C. (1995). "An alternative road construction for stormwater management in cold climates." *Water Sci. Technol*., 32(1), 79-84.

The Swedish Water and Wastewater Association (SWWA). (2011). Precipitation data for dimensioning and analysis of waste water systems [in Swedish: Nederbördsdata vid dimensionering och analys av avloppssystem]. Publication P104. Stockholm, Sweden: Svenskt Vatten.

United Nations, Department of Economic and Social Affairs, Population Division. (2014). *World Urbanization Prospects: The 2014 revision, highlights*. ST/ESA/SER.A/352.

Winston, R.J., Dorsey, J.D. and Hunt, W.F. (2015). Monitoring the performance of bioretention and permeable pavement stormwater controls in Northern Ohio: Hydrology, water quality, and maintenance needs. Final Report Submitted to the University of New Hampshire and the Chagrin River Watershed Partners. In Fulfilment of NOAA Award number NA09NOS4190153. Available: http://www.crwp.org/files/OH_StormwaterControls_MonitoringReport2015.pdf

Wolman, M.G. (1967). "A cycle of sedimentation and erosion in urban river channels." *Geografiska Annaler. Series A. Physical Geography*. 385-395.

Yong, C.F., McCarthy, D.T., and Deletic, A. (2013). "Predicting physical clogging of porous and permeable pavements." *J. Hydrol.,* 481, 48-55.

CHAPTER 8: **A SIMPLE INFILTRATION TEST FOR DETERMINATION OF PERMEABALE PAVEMENT MAINTENANCE NEEDS**

8.1 Abstract

Permeable pavements allow stormwater to pass through the pavement surface, filtering out sediment and debris; over time, regular preventative maintenance will be needed to maintain the pavement surface infiltration rate (SIR). SIR testing is commonly used to determine maintenance needs and frequencies. American Society for Testing and Materials (ASTM) standard methods (C1781 or C1701) may be used to measure permeable pavement SIR; however, these tests can take hours to complete and require infiltrometers not readily available to maintenance contractors. A simple infiltration test (SIT) has been devised which (1) is conducted using easily acquired materials, (2) has a larger surface area (i.e., more representative of average pavement conditions), and (3) requires, on average, 72% less time to conduct than the ASTM test. ASTM and SIT methods were compared by conducting a total of 873 SIR tests at the same locations on twelve permeable pavements in North Carolina, Ohio, and Sweden. Results showed: (1) a segmented linear relationship related SIT and ASTM-measured SIRs; (2) the SIT and ASTM tests predicted approximately the same SIR up to 250 mm/min; (3) the larger surface area of the SIT reduced measurement variability (average 40% less) compared to the ASTM method. The SIT took one-quarter the time to run, on average, making this newly-devised tool more efficient when assessing SIR than ASTM methods, potentially saving maintenance personnel time and money.

8.2 Review of Literature

Urbanization often detrimentally affects surface waters through increases in the rate and volume of stormwater conveyed through storm sewer systems (Leopold et al. 1964). Impervious cover, such as rooftops, roadways, and parking lots, reduces the potential for infiltration and evapotranspiration within a watershed. Source-control stormwater management, where small distributed stormwater control measures are placed throughout the watershed, has gained popularity in recent years (Dietz and Clausen 2008; Page et al. 2015). One method of reducing impervious cover is to use permeable pavement, an alternative to traditional asphalt or concrete surfaces (Collins et al. 2008; ASCE 2015).

Permeable pavements have been shown to reduce runoff volume, peak flow rate, and runoff temperature, while providing substantial pollutant load reductions (Wardynski et al. 2012; Drake et al. 2014a; Drake et al. 2014b). Widespread adoption of permeable pavements has been hampered by concerns about cost, winter performance, and the frequency and effort of maintenance (Roseen et al. 2012). Newly installed pervious concrete (PC) and permeable interlocking concrete pavers (PICP) exhibited surface infiltration rates (SIR) in the range of 340-1100 and 310-680 mm/min, respectively (Bean et al. 2007; Al-Rubaei et al. 2015). Over time, the pore spaces in permeable pavements begin to clog with organic debris, sediment, and grit, causing a decrease in SIR. As larger particles clog the void spaces, small particles begin to be trapped, resulting in further reduction of SIR (Pratt et al. 1995), and clogging can be modeled using an exponential decay (Sansalone et al. 2008). Maintenance of permeable pavements is needed to sustain their infiltration capacity, preventing surface runoff and ensuring treatment functionality (Bean et al. 2007; Blecken et al. in press).

Maintenance of permeable pavements is often prescribed using a particular method (usually street sweeping with vacuuming) at a given frequency (e.g., once quarterly, NCDENR 2012; 2-4 times per year, NHDES 2008). However, these blanket prescriptions of maintenance intensity and frequency do not account for the spatial variability in clogging within a particular permeable pavement due to: run-on from impervious catchments, overhanging trees, soil or mulch from pervious areas, or other sources. A variety of SIR measurement techniques for permeable pavements have been tested, including double-ring infiltrometers (Bean et al. 2007; Fassman and Blackbourn 2010; Al-Rubaei et al. 2013; Drake and Bradford 2013), single-ring infiltrometers (Welker et al. 2012; Brown and Borst 2014), large-scale inundation methods (Lucke et al. 2014), other simplified estimation methods (Lucke et al. 2015), or purpose-built infiltrometers (Lucke and Beecham 2011; Li et al. 2013) using either constant or falling-head methods. Recently, American Society for Testing and Materials (ASTM) methodologies have been developed for PC (C1701; ASTM 2009) and PICP (C1781; ASTM 2013) consisting of constant-head tests conducted using a 30-cm diameter metal, single-ring infiltrometer. These tests take multiple hours to perform if a permeable pavement is severely clogged. Additionally, the infiltration testing methods described above require infiltrometers which are somewhat costly and/or labor intensive to construct. A simple infiltration test (SIT) method has been developed to allow maintenance personnel to easily and rapidly measure permeable pavement SIR. All materials for the infiltrometer can be furnished from a hardware store. The purpose of this work was to compare the SIT to the ASTM methods for SIR measurement and to validate the use of the SIT for determination of permeable pavement maintenance needs in the field.

8.3 Materials and Methods

Site Descriptions

Twelve permeable pavement installations located in North Carolina and Ohio, USA and Växjö, Sweden were utilized in this study (Table 8-1). PICP, PC, and concrete grid pavement (CGP) applications were tested. The test sites varied with respect to loading ratio (i.e., the ratio of surface area of impermeable pavement contributing runoff to a permeable pavement) and age at the time of testing (Table 8-1). For PICP, loading ratio varied from 0-7.2:1 and age from 1 month to 9 years. The PC site had low loading ratios (0.6:1 and 0.75:1) and was 17-32 months when tested. The two CGP sites were 10 and 11 years old and had loading ratios of 5:1.

One to seven visits were made per site to test SIR (Table 8-1); each set of tests was separated by a minimum of three months or maintenance of the permeable pavement. At each site, 3-8 testing locations were established, and during each round of SIR tests, three SIT and two ASTM replicates were completed at each testing location. Greater replication was needed for the SIT, as the test would often last less than 30 seconds under optimal pavement conditions, magnifying any errors in timing. Assuming an average stopwatch timing error of 0.15 seconds (Hetzler et al. 2015), percent error due to timing was less than 2% for the SIT and less than 1% for the ASTM method. SIR testing was performed on the same day at each location, with the order of testing (SIT and ASTM) randomized. Testing was conducted on permeable pavements in various climates, winter maintenance regimens, loading ratio, age, pavement type, and other predictors of clogging to determine the relationship between the SIT and ASTM tests across a range of factors.

Table 8-1. Characteristics of the permeable pavement applications subjected to SIR testing.

Site Name and Location	Pavement Type	Loading Ratio	Age at Time of SIR Tests	Number of Testing Locations	Number of Times Tested
Piney Wood, Durham, NC, USA	PICP	1.8	1-10 months	6	5
NC Central University, Durham, NC, USA	PICP	6.5	10-19 months	5	5
Willoughby Hills, OH, USA	PICP	7.2, 2.2	6-21 months	8	7
Perkins Township, OH, USA	PC	0.6, 0.75	17-32 months	7	5
Orange Village, OH, USA	PICP	0	6-21 months	5	5
Kurortsvägen, Växjö, Sweden	CGP	5	10 years	3	1
Schwerinvägen, Växjö, Sweden	CGP	5	11 years	3	1
Växthusgatan, Växjö, Sweden	PICP	5	9 years	3	1
Valluden, Växjö, Sweden	PICP	5	4 years	3	1
Lillavallen, Växjö, Sweden	PICP	5	3 years	3	1

Infiltration Testing Methods and Data Collection

The single ring, constant head test described in ASTM C1781 for PICP (ASTM 2013) and ASTM C1701 for PC (ASTM 2009) was utilized as a baseline for SIR measurement. A 30-cm diameter infiltrometer (surface area 0.07 m^2) was sealed to the pavement surface using plumber's putty (Figure 8-1). Twenty liters of water were poured from a bucket into the infiltrometer (as close to the pavement surface as possible to prevent dislodging of any clogging material), maintaining an approximate head between 10-15 mm above the pavement surface (which is nearly impossible under optimal pavement conditions with high SIR). On sloped testing locations, the elapsed time to completely infiltrate water over the entire testing surface was recorded. The SIR was calculated as the quotient of depth of water applied in the infiltrometer to time (e.g., mm/min). Two modifications were made to the ASTM

methods: (1) to prevent leaks, plumber's putty was applied to both the inner and outer edges where the infiltrometer met the permeable pavement surface, and (2) for heavily clogged test locations, no additional water was added to the infiltrometer after 15 minutes had elapsed. The total time was taken at the end of the test and the volume infiltrated recorded as the difference between the initial and final volume in the bucket. In this way, more tests could be conducted in a day; otherwise, a single test would take more than 3 hours at heavily clogged sites (<0.1 mm/min).

Figure 8-1. ASTM SIR test (left) on PICP in Willoughby Hills, Ohio and (center) on CGP in Växjö, Sweden. SIT test (right) on PICP in Durham, North Carolina.

The SIT infiltrometer was constructed with materials purchased from a home improvement store; a standard wall stud – a 2.44-m long, 38 mm by 89 mm piece of pressure treated lumber - was cut into four equal lengths, and screwed together to make a square (inner side length: 0.56 m, inner surface area: 0.32 m^2; Figure 8-1). A wall stud was utilized since they are commercially available in most parts of the world. All other testing methodologies were similar to those for the ASTM method, except the SIT was conducted as

a falling head test. The entire initial volume (approximately 20 L of water) was poured into the infiltrometer at once.

Data Analysis

Descriptive statistics and boxplots were used to analyze differences in SIR measured using the ASTM and SIT methods. A segmented linear regression analysis related the SIRs from the two methods, with the breakpoint determined through an iterative process. Graphical analysis and paired statistical testing of the coefficient of variation [(CV), the quotient of the standard deviation to the mean] provided a quantification of the repeatability of each test method. For paired statistical testing, all data sets were not normal or log-normal, so Wilcoxon signed rank tests were employed. All data analysis was completed in R statistical software (R Core Team 2015).

8.4 Results and Discussion

A total of 505 and 368 SIR tests were performed using the SIT and ASTM methods, respectively. Summary statistics for these tests are presented in Table 8-2.

Measures of central tendency suggested the ASTM test predicted higher SIR than the SIT. Median and mean SIR measured with the ASTM test were 26% and 32.5% greater than those for the SIT, respectively. Infiltration rates measured with the ASTM and SIT were significantly different ($p<0.001$). It is surmised this may be due to the proportionally greater infiltrometer perimeter (normalized by surface area) for the ASTM test. The ratio of perimeter to surface area of each infiltrometer was computed for the ASTM (13 m-1) and SIT methods (7.6 m-1). In the center of each infiltrometer, infiltration is limited to the vertical direction. However, below the infiltrometers, infiltration can occur vertically and

laterally (for single-ring infiltrometers). Because of the higher perimeter to area ratio for the ASTM test, lateral water movement could have elevated the SIRs measured herein, since infiltrometers with smaller surface areas are more vulnerable to these effects (Nimmo et al. 2009).

At SIRs representing newly installed permeable pavements (i.e., 90th percentile and maximum values), the SIT test further diverged from the SIRs predicted by the ASTM. This is most likely due to the extremely short duration (<10 seconds) of the SIT at these elevated SIRs. The 20 L of water could not be applied in the SIT infiltrometer fast enough to induce ponding, and the maximum measured SIR was limited by the rate of pouring from the bucket, not the pavement. Conversely, at the most clogged testing locations, the smaller surface area of the ASTM method meant it more likely represented a completely clogged pavement. The 335% larger SIT surface area increased the likelihood that a small portion of better draining pavement (i.e not fully clogged) was tested, resulting in slightly higher SIR for the SIT method at the most-clogged locations. Practically, the larger surface area of the SIT method better represented the average conditions of the pavement.

Table 8-2. Summary statistics for surface infiltration rate for the SIT and ASTM methods.

Statistic	SIT (mm/min)	ASTM (mm/min)
Minimum	0.5	0.2
10th percentile	6.0	1.7
Median	67.8	85.5
Mean	136	180
90th percentile	427	592
Maximum	575	892

Segmented linear regression was utilized to establish a relationship between SIR measured using the ASTM and SIT methods to predict ASTM-equivalent SIR when using the SIT test (Figure 8-2). For each set of SIT and ASTM data at a particular monitoring location on a given day, the median SIR was calculated for the SIT and ASTM tests. These data were then paired and used in the segmented linear regression, resulting in a total of 184 paired data sets from the 12 permeable pavements. The segmented linear model fit the data well, with SIT-measured SIR explaining 93.2% of the variability in the ASTM-measured SIR. The t statistic was highly significant (p-value <2E-16), suggesting the SIRs from the two tests were highly correlated.

The break point between the segmented linear relationships occurred at a SIT-measured SIR of 247.5 mm/min. The slope of the linear regression below this value (i.e., 1.12) suggests that a nearly 1:1 relationship existed between the two measurement methods up to 247.5 mm/min. Given measurement error inherent in infiltration testing (Li et al. 2013), it appears the SIT can be used to obtain comparable results to the ASTM test up to approximately 250 mm/min. Up to this break point, the linear regression explained 73% of the variability in the data. At SIRs above this value, the conversion of SIT to ASTM method SIR is not of great concern, as these pavements are essentially not clogged (i.e., capable of infiltrating nearly all storm events). The deviation in slope when SIR is greater than 247.5 mm/min may be due to measurement errors, as previously discussed.

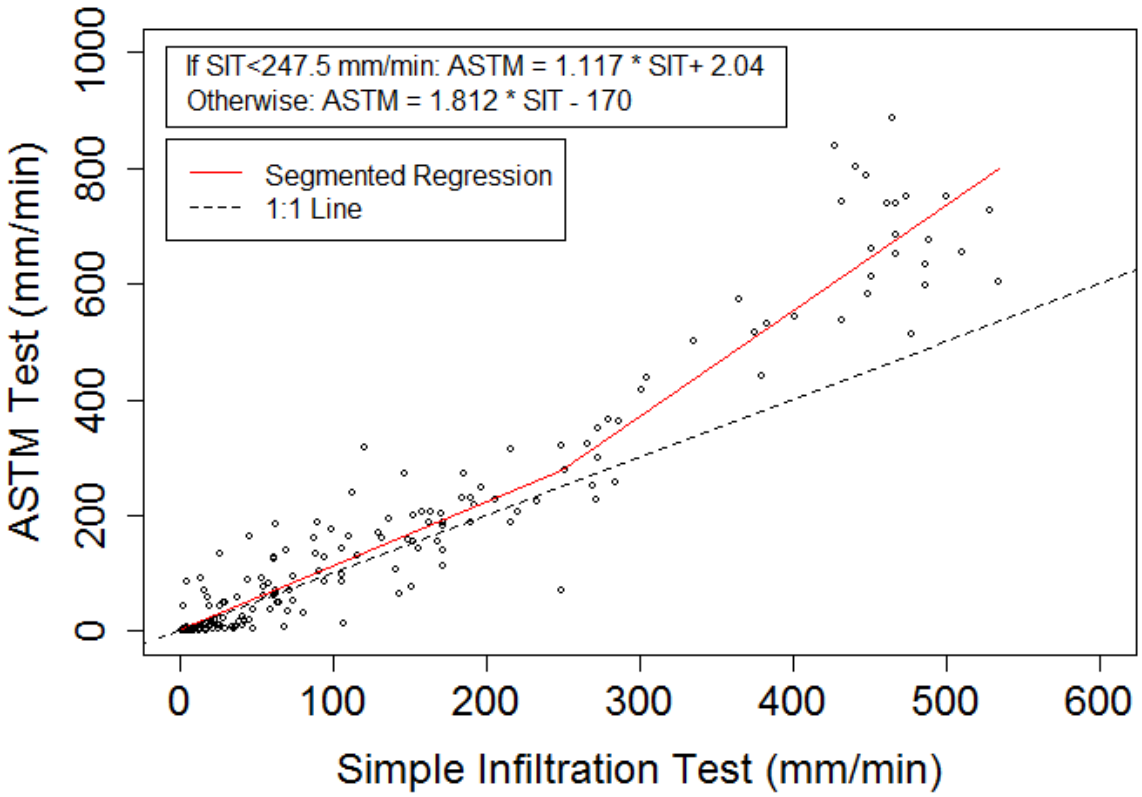

Figure 8-2. Relationship (derived using segmented linear regression) between surface infiltration rates measured using ASTM and SIT methods. The 1:1 line is also shown for reference.

To determine the repeatability of both tests, the CV was calculated for each test date and measurement location. The relationship between the CV and the mean SIR is shown in Figure 8-3, with higher variability exhibited at lower SIR. For sites with SIR less than 10 mm/min, the organic material and accumulated sediment in the pore spaces caused a decrease in SIR as its water content increased. This meant for each successive infiltration test, SIR would often decrease as the water content of the clogged pore spaces approached saturation. At very high SIR (>100 mm/min), little variability existed in the measurements, and CV approached zero asymptotically. Paired CV values for ASTM and SIT methods

were compared using a Wilcoxon signed rank test and were significantly different (p-value 0.036). The average CV for the SIT was 12.2%, while that for the ASTM was 16.9% [substantially lower than the 30% CV value reported for the ASTM test in Li et al (2013)]. However, the average standard deviations for the SIT (8.0) and ASTM (7.5) methods were similar. Taken together, these results suggested the larger surface area of the SIT reduced the variability in the measured SIR.

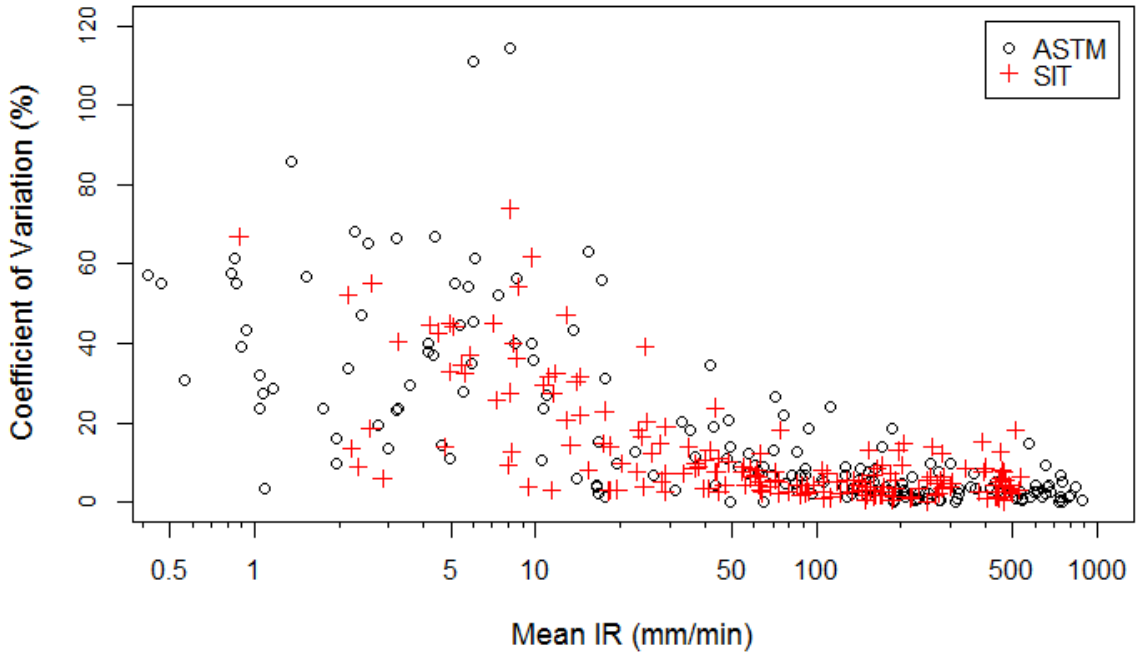

Figure 8-3. Coefficient of variation for all SIT and ASTM surface infiltration rate measurements.

Because the surface area of the SIT is 335% greater than that for the ASTM test and approximately the same volume of water was applied using either test, the ASTM test took longer to complete ($\bar{x}$ = 11.4 ± 18.7 minutes, range 0.3 - 176 minutes) than the SIT

($\bar{x}$ = 3.2 ± 6.1 minutes, range 0.1 - 47.6 minutes). SIR test duration was compared using a Wilcoxon signed rank test, and ASTM test duration was significantly greater than that for the SIT test ($p<0.001$). On average, 72% less time was required for the SIT than for the ASTM test. SIR test duration for the most clogged locations, represented by the 90^{th} percentile duration of testing, was 9.6 minutes for the SIT and 31.8 minutes for the ASTM test. In addition, the ASTM test was modified herein (described previously) to shorten the test duration; otherwise, this difference would have been greater. Practically, this meant maintenance personnel could determine maintenance needs for a permeable pavement 3-4 times more quickly using the SIT. Given the advantages of the SIT (shorter time to complete, cheaper and simpler to build the infiltrometer, and reduced measurement variability), it may be a preferable method to measure SIR for determination of permeable pavement maintenance needs.

8.5 Conclusions

Two different types of infiltrometers were utilized to measure surface SIR of twelve different permeable pavements of three types: PICP, PC, and CGP. A single ring, constant head method (ASTM standard) and a simple infiltration test employing falling head techniques were compared under varying conditions to determine their relative performance. The following conclusions can be drawn from this study:

1) Measures of central tendency suggested the ASTM test produced 30% higher SIR than the SIT method. It was surmised this may be due to greater lateral water movement below the ASTM infiltrometer, which has a higher perimeter to area ratio. The larger surface area

of the SIT meant it had proportionately less lateral flow, resulting in a more representative SIR for the permeable pavement. For newly constructed pavements not exhibiting clogging, the SIT appeared less accurate than the ASTM test, since the SIR for the SIT was limited mainly by the rate water was poured onto the pavement surface, and not by the pavement itself. For heavily clogged pavements, the ASTM test yielded lower SIRs than the SIT, perhaps because the larger surface area of the SIT meant it was more likely to test an area of the pavement with a slightly higher SIR where water would preferentially infiltrate.

2) A segmented linear relationship between SIRs measured using the SIT and the ASTM methods and explained 93% of the variability in the data; using this relationship at SIRs less than 250 mm/min, an approximately 1:1 relationship existed between the SIRs measured using the SIT and ASTM methods (i.e., the two infiltrometers produced very comparable results). Maintenance of permeable pavement is generally not needed when SIR is greater than 250 mm/min, so the conversion of SIT to ASTM method SIR is inconsequential above this SIR. The SIT took on average 72% less time to complete than the ASTM method, reducing the time needed to determine permeable pavement maintenance needs, concomitantly reducing maintenance cost.

3) To determine the variability in SIR inherent in each test method, the CV was calculated for each set of ASTM and SIT methods. The mean CV for the ASTM was 40% greater than that for the SIT. The CVs for the two tests were significantly different, suggesting the larger surface area of the SIT provides a more repeatable estimate of the SIR of a permeable pavement. The 335% larger surface area of the SIT also better represents

average pavement conditions and reduces variability of the results resulting from heterogeneity of pavement surface clogging.

4) Taken together, the reduced variability and duration of results acquired using the SIT as well as the ease of infiltrometer construction potentially make it a preferred method to the ASTM standard.

8.6 References

Al-Rubaei, A.M., Stenglein, A.L., Viklander, M., and Blecken, G.-T. (2013). "Long-term hydraulic performance of porous asphalt pavements in northern Sweden." *J. Irrig. Drain. Eng*., 139(6), 499-505.

Al-Rubaei, A.M., Viklander, M., and Blecken, G.-T. (2015). "Long-term hydraulic performance of stormwater infiltration systems." *Urban Water J*., 12(8), 660-671.

American Society of Civil Engineers (ASCE). (2015). *Permeable pavements*. Written by the permeable pavements task committee. Eds Eisenberg, B., Lindow, K.C., and Smith, D.R. ASCE, Reston, VA, USA.

American Society for Testing and Materials (ASTM). (2009). *Standard test method for infiltration rate of in place pervious concrete.* ASTM standard C1701.

American Society for Testing and Materials (ASTM). (2013). Standard test method for surface infiltration rate of permeable unit pavement systems. ASTM standard C1781.

Bean, E.Z., Hunt, W.F., and Bidelspach, D.A. (2007). "Field survey of permeable pavement surface infiltration rates." *J. Irrig. Drain. Eng*., 133(3), 249-255.

Blecken, G.-T., Hunt, W.F., Al-Rubaei, A.M., Viklander, M., and Lord, W. In press. "Stormwater Control Measure (SCM) Maintenance Considerations to Ensure Designed Functionality." *Urban Water J*.

Brown, R.A., and Borst, M. (2014). "Evaluation of surface infiltration testing procedures in permeable pavement systems." *J. Environ. Eng*., 140(3), 04014001.

Collins, K.A., Hunt, W.F., and Hathaway, J.M. (2008). "Hydrologic comparison of four types of permeable pavement and standard asphalt in eastern North Carolina." *J. Hydrol. Eng*., 13(12), 1146-1157.

Dietz, M.E., and Clausen, J.C. (2008). "Stormwater runoff and export changes with development in a traditional and low impact subdivision." *J. Environ. Manage*., 87(4), 560-566.

Drake, J., and Bradford, A. (2013). "Assessing the potential for restoration of surface permeability for permeable pavements through maintenance." *Water Sci. Tech*., 68(8), 1950-1958.

Drake, J., Bradford, A., and Van Seters, T. (2014a). "Stormwater quality of spring–summer-fall effluent from three partial-infiltration permeable pavement systems and conventional asphalt pavement." *J. Environ. Manage*., 139 69-79.

Drake, J., Bradford, A., and Van Seters, T. (2014b). "Winter effluent quality from partial-infiltration permeable pavement systems." *J. Environ. Eng*., 140(11), 04014036.

Fassman, E.A., and Blackbourn, S. (2010). "Urban runoff mitigation by a permeable pavement system over impermeable soils." *J. Hydrol. Eng.,* 15(6), 475-485.

Hetzler, R.K., Stickley, C.D., Lundquist, K.M., and Kimura, I.F. (2008). "Reliability and accuracy of handheld stopwatches compared with electronic timing in measuring sprint performance." *J. Strength Cond. Res*., 22(6), 1969-1976.

Leopold, L.B., Wolman, M.G., and Miller, J.P. (1964). *Fluvial processes in geomorphology*. W.H. Freeman and Company, San Francisco, USA.

Li, H., Kayhanian, M., and Harvey, J.T. (2013). "Comparative field permeability measurement of permeable pavements using ASTM C1701 and NCAT permeameter methods." *J. Environ. Manage*., 118, 144-152.

Lucke, T., and Beecham, S. (2011). "Field investigation of clogging in a permeable pavement system." *Build. Res. Inf*., 39(6), 603-615.

Lucke, T., Boogaard, F., and van de Ven, F. (2014). "Evaluation of a new experimental test procedure to more accurately determine the surface infiltration rate of permeable pavement systems." *Urban Plann. Transp. Res*., 2(1), 22-35.

Lucke, T., White, R., Nichols, P., and Borgwardt, S. (2015). "A Simple Field Test to Evaluate the Maintenance Requirements of Permeable Interlocking Concrete Pavements." *Water*, 7(6), 2542-2554.

New Hampshire Department of Environmental Services (NHDES). (2008). *New Hampshire stormwater manual.* Volume 2: Post-construction Best Management Practices selection and design. Revision 1.0.

Nimmo, J.R., Schmidt, K.M., Perkins, K.S., and Stock, J.D. (2009). "Rapid measurement of field-saturated hydraulic conductivity for areal characterization." *Vadose Zone J*., 8(1), 142-149.

North Carolina Department of Environment and Natural Resources (NCDENR). (2012). *NCDENR stormwater BMP manual*. Chapter 18: Permeable Pavement. Revised 10/16/2012.

Page, J.L., Winston, R.J., Mayes, D.B., Perrin, C., and Hunt, W.F. (2015). "Hydrologic mitigation of impervious cover in the municipal right-of-way through innovative stormwater control measures." *J. Hydrol.*, 527, 923-932.

Pratt, C.J., Mantle, J.D.G., and Schofield, P.A. (1995). "UK research into the performance of permeable pavement, reservoir structures in controlling stormwater discharge quantity and quality." *Water Sci. Tech*., 32(1), 63–69.

R Core Team. (2015). *A language and environment for statistical computing*. R Foundation for Statistical Computing. Vienna, Austria.

Roseen, R.M., Ballestero, T.P., Houle, J.J., Briggs, J.F., and Houle, K.M. (2012). "Water quality and hydrologic performance of a porous asphalt pavement as a storm-water treatment strategy in a cold climate." *J. Environ. Eng*., 138(1), 81-89.

Sansalone, J., Kuang, X., and Ranieri, V. (2008). "Permeable pavement as a hydraulic filtration interface for urban drainage." *J. Irrig. Drain. Eng*., 134(5), 666–674.

Wardynski, B.J., Winston, R.J., and Hunt, W.F. (2012). "Internal water storage enhances exfiltration and thermal load reduction from permeable pavement in the North Carolina mountains." *J. Environ. Eng*., 139(2), 187-195.

Welker, A.L., Barbis, J.D., and Jeffers, P.A. (2012). "A side-by-side comparison of pervious concrete and porous asphalt." *J. Am. Water Resour. Assoc*., 48(4), 809-819.

CHAPTER 9: **CONCLUSIONS AND RECOMMENDATIONS FOR FUTURE WORK**

9.1 Conclusions

In order to function over their intended design life (which might be 20-30 years), SCMs must be resilient to anthropogenic and natural (e.g., climate, sediment which might clog an infiltration-based practice, etc.) stressors. The response of bioretention cells and permeable pavements to various stimuli, including low permeability underlying soils, surface clogging of permeable pavements, application of de-icing salt during winter weather, climate change, and various design alternatives (such as undersizing a bioretention cell) was studied herein.

Both bioretention cells and permeable pavements are resilient to being installed over low permeability underlying soils. While volume reduction is reduced vis-à-vis similarly-designed SCMs situated over high permeability soils, they still ameliorate urban hydrology. When located in poor soils, SCMs should be designed to optimize lateral exfiltration through the incorporation of an IWS zone and by reducing the perimeter to surface area ratio (generally resulting in smaller, distributed controls).

Bioretention modeling in Chapter 3 showed that their hydrologic performance varies substantially depending on design. Undersized bioretention cells, which might be useful in retrofit situations where land is not available for a full-sized practice, were modeled under loading ratios of 35:1 and 50:1. Loading ratios up to 35:1 provided resilient hydrologic performance (defined here as less than 10% overflow) in HSG B underlying soils (>0.51 cm/hr K_{sat}). In less permeable soils, overflow was up to 20% of the overall water balance. Undersized bioretention cells resilience is therefore dependent on the underlying soil conductivity. In HSG A underlying soils, bioretention may be resilient at a 35:1 loading

ratio, whereas in an HSG D soil, a 20:1 loading ratio is more appropriate. In no case did a 50:1 loading ratio provide resilient bioretention hydrology. Consideration should also be given to the fact that undersized bioretention cells will require more frequent maintenance of pretreatment devices to prevent clogging.

Because bioretention cells employ plant- and soil-based processes, they tend to be more resilient SCMs than permeable pavement. Plant roots provide soil macropores to rejuvenate media K_{sat} and prevent sediment load from the catchment from clogging a bioretention cell. With permeable pavement, pretreatment is often difficult or impossible to provide, and the practice itself acts as a sediment trap; this is especially true when run-on from a catchment is directed to the permeable pavement surface. As discussed in Chapter 8, without routine and, if necessary, restorative maintenance, a permeable pavement treating only direct rainfall will clog to the point of failure over a period of approximately 20 years. When run-on is directed to the pavement surface, the frequency and onerousness of maintenance increases substantially. To provide the greatest resilience to clogging, permeable pavements should be designed to minimize run-on from impervious surfaces and, to the extent practicable, eliminate run-on from pervious surfaces.

The application of de-icing salts during winter weather appears to substantially affect the water quality performance of permeable pavements, especially when constructed over clay soil. Sodium could also potentially disperse clays in bioretention media, reducing the pollutant sorption capacity and modifying the K_{sat} of the media. To improve resilience of SCMs to sodium, options include reducing the amount of de-icing salt used or applying alternative de-icers.

The final stressor studied was climate change, with two different dynamically downscaled data sets used to project bioretention hydrologic performance under mid-21st century precipitation and temperature. Each portion of the water balance (drainage, overflow, and exfiltration/ET) was predicted to change by less than 10%, suggesting bioretention cells in this region will be resilient to climate change (at least under these climate projections). In some cases, volume reduction actually increased under future climate due to lower annual rainfall depth and longer dry periods. Proper design, construction, and long-term maintenance of bioretention cells appeared to be more important to resilience than potential changes in climate.

9.2 Recommendations for Future Work

This research focused on the resilience of bioretention cells and permeable pavement systems to various natural and anthropogenic stimuli. While it has helped to answer certain questions, further research is needed:

During design of infiltration-based SCMs, better methods are needed to predict post-construction drawdown rate, since it is one of the most critical factors to their hydrologic performance. Single or double-ring field saturated hydraulic conductivity tests can be used to determine an average vertical conductivity. This should serve as a minimum drawdown rate, as long as soil compaction during construction is avoided. However, for SCMs with relatively small surface areas where lateral conductivity through the side-walls may play a large role, better field methods are needed to estimate these processes. Also, improved estimation of ET is needed to include it in pre-construction, modeled performance of an SCM, which would further refine crediting of volume reduction.

While DRAINMOD modeling using Thornthwaite method and separate spreadsheet-based estimations using the Penman-Monteith equation (coupled with field-collected weather data) suggested that it was not a major factor (i.e., less than 7% of the overall water balance), improved data on ET from bioretention cells and evaporation from permeable pavement systems are needed. Many studies use ET as their error term in the water balance (i.e., measure inflow and outflow, estimate or measure exfiltration, with ET being the remainder). However, this does not account for monitoring error. Weighing lysimeters or other models could be used to better define ET.

The performance of these and other SCMs needs to be studied over their lifespan to determine system resilience and performance beyond the first few years. Due to sediment and debris, filters such as bioretention and permeable pavement tend to clog over time. How does this impact the K_{sat} of the media or the surface infiltration rate of a permeable pavement over a period of many years? As plants grow and mature in a bioretention cell, do they provide statistically greater volume reduction? How does the vegetation type (i.e., trees and shrubs vs. turfgrass vs. deep rooted native grasses) impact volume reduction in bioretention over the long-term?

Both bioretention and permeable pavement often employ an underdrain. Because hydraulic residence time is very important to water quality treatment (i.e., additional time for settling and biological treatment to occur), various restrictions to drainage should be explored. This could include valves, weirs, or orifices. These discharge-limiting devices (similar to controlled drainage in agriculture) may also be paired with real-time control, which would allow the drain to be completely open during periods of high-flow, but restrict

flow during inter-event periods to improve exfiltration and mitigate pollutants. Hydraulic modeling could be performed to optimize their design, maximizing hydraulic retention time while allowing enough storage for subsequent storm events.

The hydrologic function of permeable pavements, even when constructed in low permeability soils, is vastly improved through the incorporation of an internal water storage (IWS) zone. However, ponded water in the subgrade of a pavement is anathema to structural design. Research needs to be undertaken to determine the environmental factor in the structural number calculation for flexible pavement design under continuous ponding. This will allow for factors-of-safety to be applied to design, and allow the structural design to account for an improved design methodology for hydrology.

This and other studies have shown DRAINMOD to be an excellent model for long-term bioretention hydrology. However, for its use in urban SCM to flourish, it needs to be further developed to ameliorate some of its shortcomings. The following would help to improve its utility: (1) DRAINMOD needs to include routines to model runoff from a highly impervious watershed, similar to those in USEPA SWMM, (2) DRAINMOD does not output hydrographs, so analysis of peak flow rates or flow durations is not possible, (3) it needs to accept weather files with time steps much less than 1-hour, and (4) the model could allow modification of soil K_{sat} or infiltration rate over time to allow it to model clogging or seasonal processes.

Water quality performance of bioretention and permeable pavement systems needs to be improved to meet numerical effluent limits. There are certain critical points to ensure pollutant mitigation – low organic matter content in bioretention media to prevent nutrient

leaching, clay and silt fractions in bioretention media to promote phosphorus, bacteria, and metals adsorption, and washed gravel to prevent flushing of TSS. However, additional amendments to bioretention media and aggregate layers need to be the focus of future research. Amendments targeted at heavy metals, dissolved nutrients, and indicator bacteria are of particular interest to surface water quality.

With regard to water quality, the effects of cold-climate issues need to be pursued further. The apparent loss of clay and silt-sized particles (due to de-icing salt application) from the permeable pavements in Chapter 6 was a surprise. Stormwater controls are installed frequently in cold climates, where de-icers may interact with clay soils and cause poor performance during a portion of the year. Further analysis of these interactions is needed so improved design recommendations can be given. Evaluations of economical substitutes to NaCl de-icers are desired due to their effects on surface and ground waters.

While this dissertation improves the understanding of permeable pavement maintenance, additional work is necessary to determine best methods, frequency, and intensity of maintenance. Loading ratio is a critical factor in establishing the frequency and onerousness of maintenance. Modeling clogging of infiltration-based SCMs, such as bioretention and permeable pavement, is needed to quantify expected maintenance intervals and therefore costs of maintenance.

APPENDICES

Appendix A:Additional Analysis of Site Climate and Bioretention and Permeable Pavement Hydrology

Summary Statistics for Rainfall

To supplement rainfall data presented in Chapter 2 (bioretention sites) and Chapter 5 (permeable pavement sites), additional analysis of rainfall data is presented herein. A frequency analysis of rainfall events was conducted for each site (Tables A-1 through A-5). Summary statistics are presented for rainfall depth, rainfall intensity, peak rainfall intensity, rainfall duration, and antecedent dry period. Additionally, these characteristics were summarized in 10 mm bins of rainfall depth to better represent the distribution of rainfall by site. The number of events and fraction of the total rainfall depth in each bin of rainfall depth were also determined.

Table A-1. Frequency analysis of rainfall events at UC.

Site	Statistic	Number of events	Rainfall depth* (mm)	Fraction of total rainfall depth	Rainfall intensity* (mm/hr)	Peak 5-minute rainfall intensity* (mm/hr)	Rainfall duration* (hr)	Antecedent dry period[1] (days)
UC	0-10 mm events	28	5.1	0.20	1.5	15.4	6.4	4.1
	>10-20 mm events	10	12.5	0.16	2.4	23.8	9.2	3.7
	>20-30 mm events	5	24.1	0.16	2.4	41.5	14.8	2.0
	>30-40 mm events	1	32.0	0.04	2.2	48.8	14.5	0.6
	>40-50 mm events	4	44.6	0.23	7.9	92.2	8.6	2.2
	>50 mm events	2	79.6	0.21	4.4	115.8	18.3	0.7
	Maximum		89.2		12.9	152.4	30.4	20.0
	Overall Mean		14.4		2.3	29.2	8.5	3.5
	Overall Median		8.1		1.4	16.8	6.4	2.2
	Minimum		2.5		0.3	3.0	0.4	0.3
	Standard Deviation		17.6		2.7	31.8	6.3	3.9

*The average value was calculated for each bin of rainfall depth

[1]Average length of the antecedent dry period for the given bin of storm depth

Table A-2. Frequency analysis of rainfall events at HA.

Site	Statistic	Number of events	Rainfall depth* (mm)	Fraction of total rainfall depth	Rainfall intensity* (mm/hr)	Peak 5-minute rainfall intensity* (mm/hr)	Rainfall duration* (hr)	Antecedent dry period[1] (days)
HA	0-10 mm events	53	5.4	0.24	3.2	14.0	5.7	3.4
	>10-20 mm events	20	13.4	0.23	2.2	19.4	12.9	3.9
	>20-30 mm events	6	25.7	0.13	1.9	36.6	16.3	4.2
	>30-40 mm events	4	32.8	0.11	2.6	76.2	13.9	1.2
	>40-50 mm events	5	43.8	0.18	4.2	67.7	17.1	3.4
	>50 mm events	2	64	0.11	7.1	89.9	11.8	1.7
	Maximum		70.9		49.5	103.6	39.2	19.7
	Overall Mean		12.7		2.8	22.6	9.1	4.0
	Overall Median		7.1		1.2	9.1	7.3	2.6
	Minimum		2.5		0.3	3.0	0.1	0.3
	Standard Deviation		13.5		6.1	27.7	7.6	3.3

*The average value was calculated for each bin of rainfall depth

[1]Average length of the antecedent dry period for the given bin of storm depth

Table A-3. Frequency analysis of rainfall events at PT.

Site	Statistic	Number of events	Rainfall depth (mm)	Fraction of total rainfall depth	Rainfall intensity* (mm/hr)	Peak 5-minute rainfall intensity* (mm/hr)	Rainfall duration* (hr)	Antecedent dry period[1] (days)
PT	0-10 mm events	48	5.4	0.21	2.4	16.4	7.0	6.5
	>10-20 mm events	23	13.9	0.26	4.3	46.1	6.7	4.4
	>20-30 mm events	7	24.6	0.15	3.6	47.9	10.1	4.8
	>30-40 mm events	4	32.9	0.11	3.1	84.6	16.1	4.7
	>40-50 mm events	0	-	0.00	-	-	-	-
	>50 mm events	5	59.8	0.26	5.2	78.0	25.4	5.4
	Maximum		66.0		22.1	128.0	52.0	24.8
	Overall Mean		13.5		3.0	33.8	8.7	5.7
	Overall Median		8.9		1.4	25.9	6.6	4.2
	Minimum		2.5		0.3	3.0	0.3	0.3
	Standard Deviation		66.0		22.1	128.0	52.0	24.8

*The average value was calculated for each bin of rainfall depth

[1]Average length of the antecedent dry period for the given bin of storm depth

Table A-4. Frequency analysis of rainfall events at WH.

Site	Statistic	Number of events	Rainfall depth (mm)	Fraction of total rainfall depth	Rainfall intensity* (mm/hr)	Peak 5-minute rainfall intensity* (mm/hr)	Rainfall duration* (hr)	Antecedent dry period[1] (days)
WH	0-10 mm events	43	5.4	0.21	2.3	14.7	6.2	4.0
	>10-20 mm events	18	13.9	0.23	3.2	24.9	11.9	2.8
	>20-30 mm events	8	26.4	0.20	2.7	55.2	12.8	2.6
	>30-40 mm events	3	34.8	0.10	4.0	61.0	9.6	3.2
	>40-50 mm events	3	47.1	0.13	3.3	98.6	14.4	1.8
	>50 mm events	2	70.9	0.13	3.3	42.7	29.5	0.5
	Maximum		86.9		21.8	167.6	42.8	18.6
	Overall Mean		13.5		2.5	25.4	9.3	3.5
	Overall Median		8.9		1.0	12.2	7.9	2.6
	Minimum		2.5		0.3	3.0	0.1	0.3
	Standard Deviation		14.8		4.1	29.7	195.2	73.0

*The average value was calculated for each bin of rainfall depth

[1]Average length of the antecedent dry period for the given bin of storm depth

Table A-5. Frequency analysis of rainfall events at OV.

Site	Statistic	Number of events	Rainfall depth (mm)	Fraction of total rainfall depth	Rainfall intensity* (mm/hr)	Peak 5-minute rainfall intensity* (mm/hr)	Rainfall duration* (hr)	Antecedent dry period[1] (days)
OV	0-10 mm events	47	5.7	0.29	2.3	15.8	6.7	4.9
	>10-20 mm events	16	14.3	0.24	1.6	24.8	12.6	3.9
	>20-30 mm events	9	23.7	0.21	2.2	33.5	11.9	2.4
	>30-40 mm events	2	30.9	0.07	5.4	47.2	8.4	2.5
	>40-50 mm events	2	45.3	0.10	6.2	96.0	8.7	2.1
	>50 mm events	1	89.2	0.10	4.3	152.4	20.9	0.7
	Maximum		89.2		30.5	152.4	29.6	24.4
	Overall Mean		12.3		2.4	24.4	8.7	4.2
	Overall Median		8.5		1.2	18.3	6.9	2.9
	Minimum		2.5		0.2	3.0	0.3	0.3
	Standard Deviation		13.0		4.0	26.1	6.6	4.6

*The average value was calculated for each bin of rainfall depth

[1]Average length of the antecedent dry period for the given bin of storm depth

Summary of Hydrologic Performance of Bioretention Cells under Varying Rainfall Depth

Bioretention hydrology, including volume and peak flow, was analyzed under a range of rainfall depths (Tables A-6 and A-7). For each rainfall depth bin, the median volume and peak flow are presented for the inlet (runoff) and outlet of each bioretention cell. Volume reduction and peak flow mitigation are greatest for storms less than 20 mm in depth. Generally, as rainfall depth increases, pore space within the IWS zone of the bioretention cells is filled, and therefore runoff reduction (as a percentage) decreases with increasing rainfall depth. This is similar to results in past studies by Hunt et al. (2008), Davis (2008), and Li and Lam (2015). While peak flow rate is more directly related to rainfall intensity (Collins et al. 2008), better peak flow mitigation occurred with smaller rainfall depths. At smaller rainfall depths, the bowl will not be full, and the peak flow throttled by the media K_{sat} and/or by the hydraulics of the underdrain. At greater rainfall depths, there is a heightened probability of overflow, during which little peak flow mitigation is expected.

Table A-6. Median hydrologic characteristics by event depth for UC.

Storm Depth (mm)	HA North				HA South			
	Volume (mm)		Peak Flow (mm/hr)		Volume (mm)		Peak Flow (mm/hr)	
	Runoff	Outflow	Runoff	Outflow	Runoff	Outflow	Runoff	Outflow
0-10 mm events	1.5	0.2	6.1	0.0	1.4	0.0	5.5	0.0
>10-20 mm events	5.0	2.8	11.2	0.6	5.1	1.8	10.0	0.5
>20-30 mm events	14.0	11.0	17.3	1.2	14.3	11.0	15.5	1.4
>30-40 mm events	22.4	16.6	63.1	2.8	22.8	16.1	56.6	5.5
>40-50 mm events	28.4	20.0	63.1	7.1	28.9	23.0	56.6	7.3
>50 mm events	48.8	45.0	60.0	36.6	49.7	46.0	53.8	29.6
Overall Mean	6.7	4.9	15.8	2.0	6.9	4.4	14.2	1.8
Overall Median	2.6	1.4	8.1	0.2	2.6	0.5	7.3	0.1
Overall Maximum	59.9	58.5	69.2	51.8	61.0	55.1	62.0	44.2
Overall Standard Deviation	10.2	8.9	18.5	7.0	10.4	9.1	16.6	5.5

Table A-7. Median hydrologic characteristics by event depth for UC.

Storm Depth (mm)	UC			
	Volume (mm)		Peak Flow (mm/hr)	
	Runoff	Outflow	Runoff	Outflow
0-10 mm events	2.4	0.0	6.3	0.0
>10-20 mm events	7.8	0.0	16.8	0.0
>20-30 mm events	20.2	6.0	25.2	2.5
>30-40 mm events	27.8	13.9	33.6	5.7
>40-50 mm events	39.9	19.9	67.2	12.9
>50 mm events	77.2	55.7	79.8	38.5
Overall Mean	11.4	4.8	19.9	3.2
Overall Median	4.1	0.0	10.5	0.0
Overall Maximum	87.2	68.6	105.0	49.9
Overall Standard Deviation	17.6	12.7	22.0	9.3

Summary of Hydrologic Performance of Permeable Pavements under Varying Rainfall Depth

Permeable pavement hydrology, including volume and peak flow rate, was analyzed under a range of rainfall depths (Tables A-6 and A-7). For each rainfall depth bin, the median volume and peak flow rate are presented for the runoff entering and outflow leaving each permeable pavement. A dichotomy in hydrologic response existed: for sites without surface runoff (PT and OV), volume reduction and peak flow mitigation are greater than 60% up to 30-mm rainfall depth. For sites experiencing surface runoff due to clogging, the permeable pavements generate substantial outflow in storms as small as 10-mm rainfall depth. WH Small, the site with the largest loading ratio, produced outflow more quickly and to a greater extent than any other site. Since a finite amount of pore space is available at the onset of inflow, runoff reduction (as a percentage) decreases with increasing rainfall depth. This is similar to results in past studies of permeable pavements by Collins et al. (2008) and Fassman and Blackbourn (2010). While peak flow may be more directly related to rainfall intensity (Collins et al. 2008), the general trend is more peak flow mitigation at smaller rainfall depth. At smaller rainfall depths, the pore space in the IWS zone may not completely fill, eliminating outflow. At greater rainfall depths, the IWS zone fills, resulting in drainage. However, this flow rate is still throttled by the hydraulic capacity of the drain. Peak flow mitigation is severely reduced when clogging occurs (causing surface runoff), as observed at WH Large and WH Small.

Table A-8. Median hydrologic characteristics by event depth for PT and OV.

Storm Depth (mm)	PT				OV			
	Volume (mm)		Peak Flow (mm/hr)		Volume (mm)		Peak Flow (mm/hr)	
	Runoff	Outflow	Runoff	Outflow	Runoff	Outflow	Runoff	Outflow
0-10 mm events	1.6	0.0	10.9	0.0	5.3	0.0	8.2	0.0
>10-20 mm events	9.0	2.7	44.9	1.3	13.3	0.0	21.8	0.0
>20-30 mm events	18.9	6.1	27.2	1.6	24.3	0.0	24.5	0.0
>30-40 mm events	26.5	17.2	69.4	10.6	30.9	0.3	42.2	0.1
>40-50 mm events	-	-	-	-	45.3	0.5	85.7	0.8
>50 mm events	57.2	39.0	73.5	17.9	89.2	3.8	136.0	11.1
Overall Mean	10.0	4.7	30.3	2.8	12.1	0.1	21.3	0.2
Overall Median	4.7	0.2	24.5	0.3	8.1	0.0	16.3	0.0
Overall Maximum	59.7	58.4	114.3	27.3	89.2	3.8	136.0	11.1
Overall Standard Deviation	13.2	10.0	26.9	5.7	12.8	0.5	23.0	1.3

Table A-9. Median hydrologic characteristics by event depth WH Large and WH Small.

Storm Depth (mm)	WH Large				WH Small			
	Volume (mm)		Peak Flow (mm/hr)		Volume (mm)		Peak Flow (mm/hr)	
	Runoff	Outflow	Runoff	Outflow	Runoff	Outflow	Runoff	Outflow
0-10 mm events	1.4	0.0	8.1	0.8	1.3	1.0	8.2	1.2
>10-20 mm events	7.8	0.3	13.5	3.3	7.7	6.5	15.0	6.8
>20-30 mm events	22.1	14.1	55.3	46.4	21.8	15.2	54.4	21.5
>30-40 mm events	28.9	22.0	70.1	66.6	29.1	24.2	70.7	38.7
>40-50 mm events	41.4	33.5	70.1	66.8	41.8	13.7	70.7	56.4
>50 mm events	67.7	41.4	45.8	42.9	68.3	56.3	46.2	34.1
Overall Mean	8.9	4.6	22.9	15.2	1.3	1.0	8.2	1.2
Overall Median	3.6	0.0	10.8	2.4	7.7	6.5	15.0	6.8
Overall Maximum	80.2	75.4	148.3	139.1	21.8	15.2	54.4	21.5
Overall Standard Deviation	13.8	11.6	26.1	25.7	29.1	24.2	70.7	38.7

Determination of Peak Ratio

The determination of peak ratio and watershed curve numbers accompanies the results presented in Chapters 2 and 5 for bioretention and permeable pavement, respectively.

Peak ratio, defined as the ratio of the outlet peak to the inlet peak, is a suggested performance metric for bioretention cells (Davis 2008). The author suggested a 0.33 peak ratio for LID SCMs, as this is the ratio of pre-development (0.3) and impervious surface (0.9) rational runoff coefficients (Chin 2006). Mean peak ratios were 5% at UC and 8% at HA; median peak ratios were zero at UC, 1% at HA South, and 3% at HA North (Figure A-1). This suggested for most events, peak flow mitigation was excellent. Mean peak ratios for un-lined bioretention cells in New Hampshire (UNHSC 2006) and Charlotte, NC (Hunt et al. 2008) with connectivity to the underlying soil were 15% and 1%, respectively, similar to results herein. The bioretention cells met the target peak ratio of 0.33 during 92%, 94%, and 94% of the monitored events at UC, HA North, and HA South, respectively. This compared favorably to the two lined cells in Maryland, which met this target for 25 and 43% of the storms (Davis 2008). When designing for peak flow mitigation, oversized bioretention cells employing IWS zones provide improved peak flow mitigation.

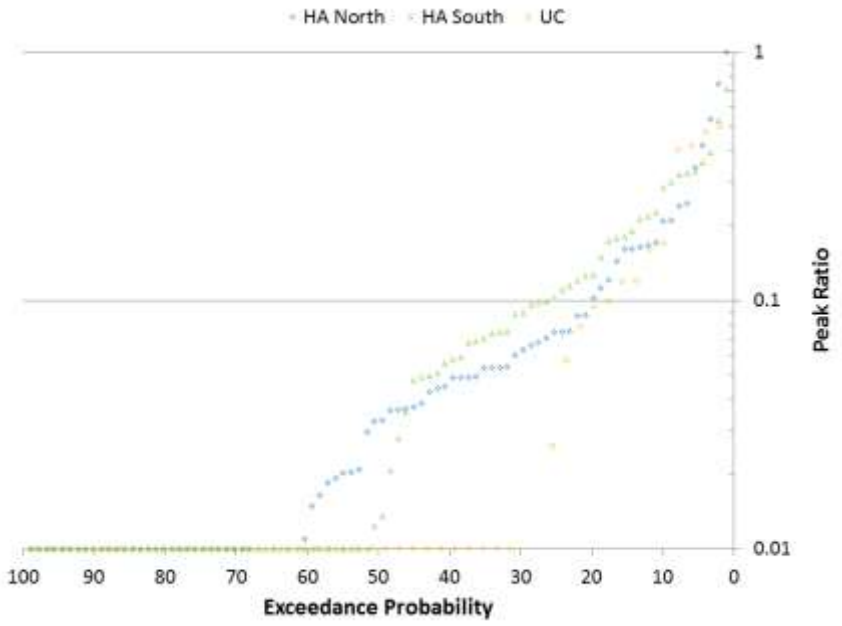

Figure A-1. Analysis of peak ratio for monitored storm events at UC and HA.

Mean and median peak ratios were less than 0.33 for PT and OV, which had no surface runoff (Figure A-2). WH Small approached this value with mean and median peak ratios of 0.31 and 0.28, respectively, while WH Large had mean and median peak ratios of 0.38 and 0.30. The percentage of events meeting the 0.33 target was 100% for OV, 98% for PT, 58% for WH large, 55% for WH Small. This shows if stormwater is able to infiltrate the pavement surface, peak flow mitigation should be 67% or greater in all but the largest events.

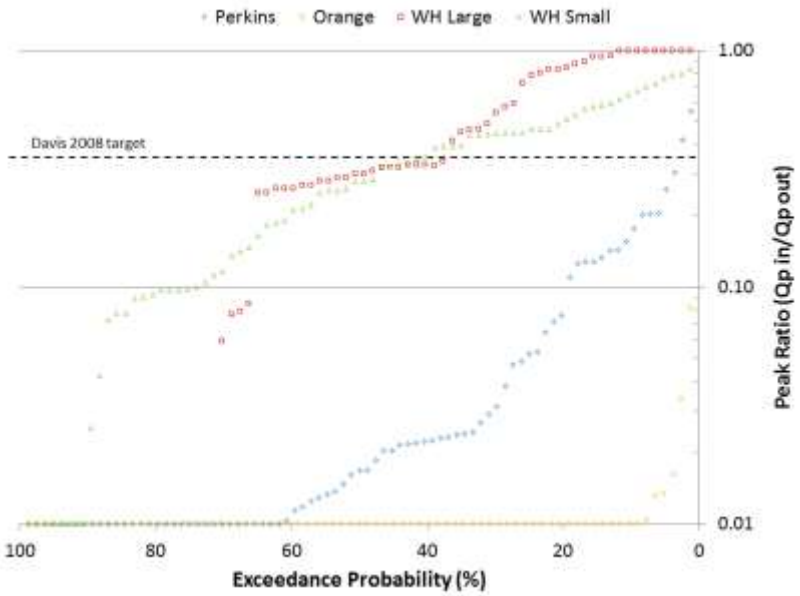

Figure A-2. Analysis of peak ratio for monitored storm events at PT, WH, and OV.

Watershed Curve Numbers pre and post-SCM Implementation

Defining metrics for predevelopment hydrology and "no net impact" to surface waters is challenging. One such method is uses the Natural Resources Conservation Service (NRCS) Curve Number (CN) method, which relates runoff to rainfall depth based upon land use (USDA-NRCS 1986). It is the most commonly-used runoff estimation method in the United States, and thus an effective way to evaluate the hydrologic impacts of bioretention facilities on their catchments. By comparing runoff generated from a catchment treated by bioretention to that expected from a forested condition (representative of the predevelopment condition in Ohio), one can determine whether this SCM is successful in mimicking predevelopment runoff volume.

Outflow plotted against rainfall depth for each bioretention cell was overlain with the respective CN model that best fit the field data (Figure A-3). The runoff volume from each

catchment is also shown for comparison. Based on the field collected data, effective CNs for the catchments were 93.1 for HA and 98.5 for UC (Figure A-3). All three bioretention cells reduced their catchment's volumetric impact, with CNs ranging from 87 to 90, a decrease of 4-8 due to exfiltration and ET within each bioretention cell. Because these cells were oversized with respect to storage of the water quality volume, bioretention cells sized for the water quality event would have less impact on the catchment CN. These data were compared against a CN of 77, representative of a surrogate pre-development condition for each site (i.e., forest in good condition over HSG D soil, USDA-NRCS 1986). While the bioretention cells did not return the catchments to a pre-development state, they did reduce the catchment CNs. Perhaps a treatment train of SCMs is needed to provide greater volume reduction and meet this particular pre-development hydrology metric (Wilson et al. 2015).

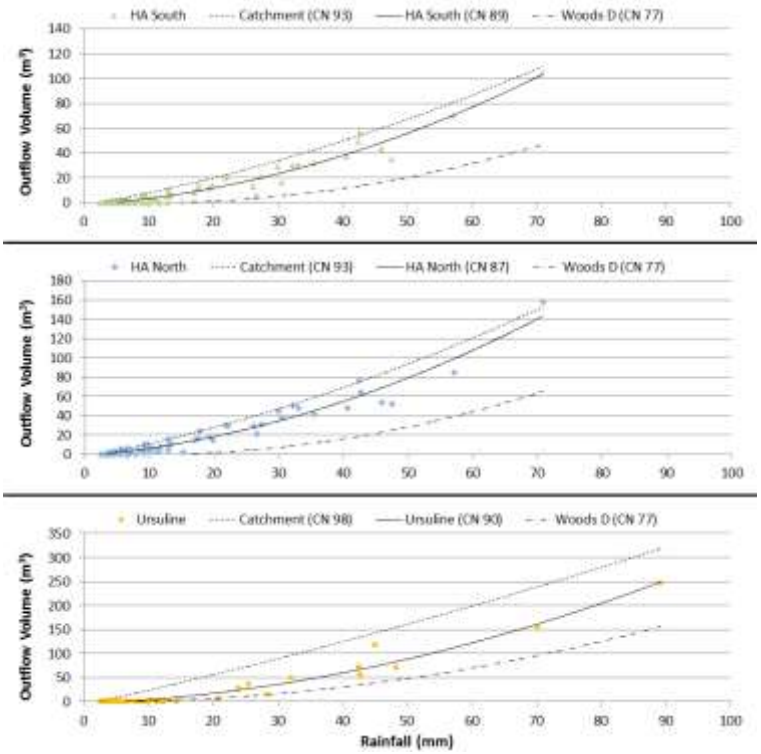

Figure A-3. Comparison of pre- and post-bioretention implementation curve numbers for the catchments.

Engineers typically use CNs to determine expected runoff volume from a development project (NRCS 1986). While data exist for CNs as a function of land use and HSG, little data are available on the effect of permeable pavements on CN, especially as a function of LR. For instance, Bean et al. (2007) calculated median CNs of 45-89 for permeable pavements treating direct rainfall and located over sandy soils in North Carolina. Schwartz (2010) suggested a CN of 87 for permeable pavements over poorly drained soils, but this was for permeable pavements with a LR of 1.0.

Curve numbers for each catchment treated by permeable pavement were back-calculated (Table A-1) using methods in Hawkins (1993). The storage parameter, S, was calculated using a quadratic formula originally proposed by Hawkins (1973):

$$S = 5 * [P + 2Q - (4Q^2 + 5PQ)^{1/2}] \quad \text{(A-1)}$$

where P and Q are paired rainfall and runoff (inches) for a given storm event. Curve numbers were calculated for events with rainfall depths greater than 50 mm. Median watershed CNs post-permeable pavement implementation ranged from 93 to 94 for permeable pavements with run-on, a decrease of 1-4 points from pre-SCM implementation. Mean CNs varied from 88-92. These values were in the range of open space in poor condition over an HSG D soil (Fangmeier et al. 2006). For OV, the site with no run-on, the median and mean CNs were 59, similar to open space in good condition over an HSG B soil and findings from Bean et al. (2007). The curtain drain probably impacted the performance of this site.

These post-SCM installation CNs were compared against a surrogate CN for pre-development hydrology in Ohio, such as a forest in good condition over an HSG D soil (i.e., CN of 77, NRCS 1986). The permeable pavements accepting run-on do not meet this criterion, and would need to be paired with another runoff reduction SCM in a treatment train to approach pre-development runoff volumes (Wilson et al. 2015). However, the site treating only direct rainfall was easily able to meet this metric.

Table A-10. Comparing pre- and post-permeable pavement implementation curve numbers for the catchments.

Site	Number of Storm Events	Catchment	Median with permeable pavement	Mean with permeable pavement
PT	5	94.6	93.6	88.5
WH small	8	98.0	94	91.5
WH large	8	98.0	93.3	90.2
OV	4	N/A	59	58.6

Rating Curve for Drainage Estimation at Ursuline College

As described in Chapter 2, a rating curve was developed to relate driving head above the invert of the underdrain to drainage flow rate. Because an IWS zone was employed at Ursuline College, this relationship is valid only when the IWS zone is full and drainage is actively occurring (Figure A-4). The rating curve was developed a pipe flow relationship inherent in EPA SWMM software with driving head from stormwater within the bioretention cell.

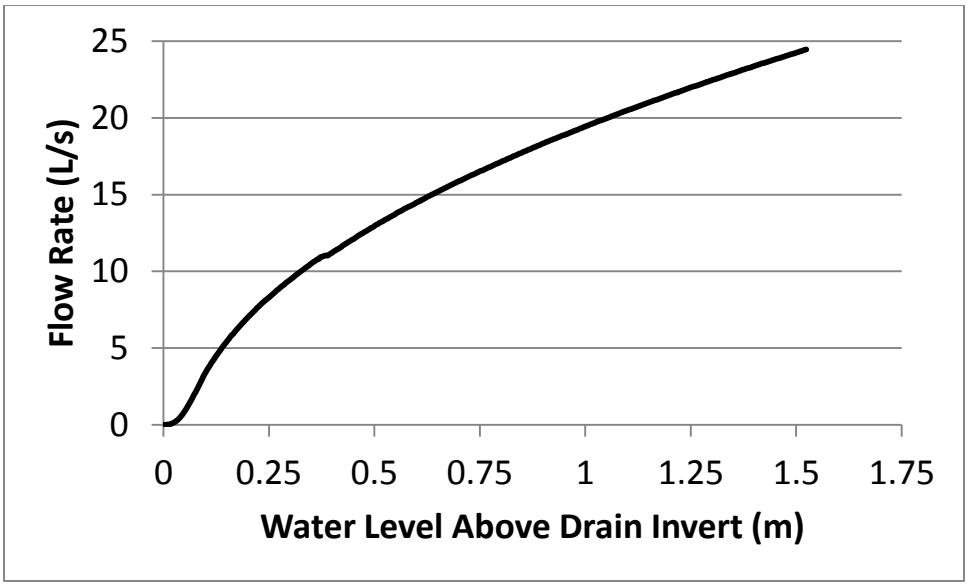

Figure A-4. Rating curve relating drainage flow rate to water level above the drain invert for Ursuline College.

References:

Bean, E.Z., Hunt, W.F., and Bidelspach, D.A. (2007). "Evaluation of four permeable pavement sites in eastern North Carolina for runoff reduction and water quality impacts.*" J. Irrig. Drain. Eng.*, 133(6), 583-592.

Chin, D.A. (2006). *Water resources engineering*. 2nd edition. Pearson Prentice Hall, Upper Saddle River, NJ.

Collins, K.A., Hunt, W.F., and Hathaway, J.M. (2008). "Hydrologic comparison of four types of permeable pavement and standard asphalt in eastern North Carolina." *J. Hydrol. Eng*., 13(12), 1146-1157.

Davis, A.P. (2008). "Field performance of bioretention: hydrology impacts." *Journal of Hydrologic Engineering*. 13(2), 90-95.

Fangmeier, D.D., Elliot, W.J., Workman, S.R., Huffman, R.L., and Schwab, G.O. (2006). *Soil and water conservation engineering*. 5th edition. Thomson Delmar learning, Clifton Park, NY.

Fassman, E.A., and Blackbourn, S. (2010). "Urban runoff mitigation by a permeable pavement system over impermeable soils." *J. Hydrol. Eng.,* 15(6), 475-485.

Hawkins, R.H. (1973). "Improved prediction of storm runoff in mountain watersheds." *J. Irrig. Drain. Div.*, 99(4), 519-523.

Hawkins, R.H. (1993). "Asymptotic determination of runoff curve numbers from data." *J. Irrig. Drain. Eng.,* 119(2), 334-345.

Hunt, W.F., Smith, J.T., Jadlocki, S.J., Hathaway, J.M., and Eubanks, P.R. (2008). "Pollutant removal and peak flow mitigation by a bioretention cell in urban Charlotte, NC." *J. Environ. Eng.*, 134(5), 403-408.

Li, Z. Y., and K. M. Lam. "Statistical evaluation of bioretention system for hydrologic performance." (2015). *Water Science and Technology.* 71(11), 1742-1749.

Schwartz, S.S. (2010). "Effective curve number and hydrologic design of pervious concrete storm-water systems." *J. Hydrol. Eng.,* 15(6), 465-474.

University of New Hampshire Stormwater Center (UNHSC). (2006). *2005 Data Report,* CICEET, Durham, N.H.

United States Department of Agriculture, Natural Resources Conservation Service (USDA-NRCS). (1986). *Urban hydrology for small watersheds*. Technical Release 55 (TR-55). 2nd

edition. United States Department of Agriculture (USDA), Natural Resources Conservation Service, Conservation Engineering Division.

Wilson, C.E., Hunt, W.F., Winston, R.J., and Smith, P. (2015). “Comparison of runoff quality and quantity from a commercial low-impact and conventional development in Raleigh, North Carolina.” *J. Environ. Eng.*,141(2), 05014005.

Appendix B: Photos of Water Quality Samples at Willoughby Hills

These photos were taken during sample collection for the storm event on 7/8/2014. Note the presence of large organic matter and sediment particles in the control sample. Also note the cloudiness of the two effluent samples, signifying the silt and clay that were mobilized from the subgrade.

Figure B-1. Control asphalt catchment runoff sample from the 7-8-2014 storm event.

Figure B-2. WH Large runoff sample from the 7-8-2014 storm event.

Figure B-3. WH Small runoff sample from the 7-8-2014 storm event.

Appendix C: Water Quality Data for Willoughby Hills Permeable Pavements

Table C-1. Nutrient and sediment concentrations for WH Small.

Collection Date & Time	TKN EPA 351.2 mg/L	Nitrate-Nitrite EPA 353.2 mg/L	TN (TKN + NO2-3)	Ammonia EPA 350.1 mg/L	ON (TKN-TAN)	Ortho-Phosphate EPA 300.0 mg/L	PBP (TP-OP)	Total Phosphorus EPA 365.1 mg/L	TSS SM25 40D mg/L
4/29/2014 2:15 PM	1.995	1.627	3.622	0.776	1.22	0.045	0.007	0.052	80.0
5/1/2014 8:00 AM	1.141	1.865	3.006	0.454	0.69	0.007	0.029	0.036	42.7
5/13/14 12:45 PM	1.432	1.908	3.34	0.118	1.31	0.008	0.083	0.091	240
6/19/14 1:30 PM	0.714	0.679	1.393	0.282	0.43	0.0167	0.045	0.062	214.7
6/24/14 11:30 AM	0.884	1.147	2.031	0.212	0.67	NS	NS	0.024	192
6/25/14 4:10 PM	0.337	0.697	1.034	0.05	0.29	0.0167	0.025	0.042	89.5
6/30/14 12:50 PM	NS	NS	NS	NS	NS	0.0167	NS	NS	164.4
7/8/14 8:30 AM	0.587	0.633	1.22	0.161	0.43	0.01667	0.022	0.039	105.3
7/9/14 12:30 PM	0.253	0.524	0.777	0.0015	0.25	0.006	0.020	0.026	46.8
8/12/14 2:40 PM	0.437	0.382	0.819	0.04	0.40	0.004	0.036	0.04	108.8
8/13/14 9:00 AM	2.66	0.199	2.859	0.372	2.29	0.005	0.043	0.048	166
9/11/14 2:30 PM	0.242	0.396	0.638	0.131	0.11	0.0167	0.025	0.042	138
10/15/14 1:15 PM	0.374	0.325	0.699	0.004	0.37	0.0167	0.005	0.022	4.9
10/17/14 9:15 AM	0.278	0.574	0.852	0.012	0.27	NS	NS	0.02	5.5
10/21/14 4:30 PM	0.508	0.475	0.983	0.089	0.42	0.003	0.024	0.027	18.6
11/3/14 2:30 PM	0.375	0.545	0.92	0.018	0.36	NS	NS	0.102	6
5/12/15 9:25 AM	1.54	1.66	3.192	0.35	1.18	0.0167	0.164	0.18	723.0
5/28/15 12:08 PM	0.80	1.68	2.479	0.09	0.71	0.0060	0.030	0.04	17.3

Table C-2. Nutrient and sediment concentrations for WH Large.

Collection Date & Time	TKN EPA 351.2 mg/L	Nitrate-Nitrite EPA 353.2 mg/L	TN (TKN + NO2-3)	Ammonia EPA 350.1 mg/L	ON (TKN-TAN)	Ortho-Phosphate EPA 300.0 mg/L	PBP (TP-OP)	Total Phosphorus EPA 365.1 mg/L	TSS SM25 40D mg/L
6/19/14 1:50 PM	0.54	0.459	0.999	0.338	0.20	0.0167	0.164	0.18	260
6/24/14 11:45 AM	1.357	0.926	2.283	0.322	1.04	NS	NS	0.02	164
6/25/14 4:30 PM	0.137	0.301	0.438	0.082	0.06	0.0167	0.039	0.056	121.2
6/30/14 1:00 PM	NS	NS	NS	NS	NS	0.0167	NS	NS	151.5
7/8/14 8:45 AM	0.863	0.631	1.494	0.322	0.54	0.0167	0.039	0.056	100
7/9/14 12:45 PM	0.289	0.473	0.762	0.043	0.25	0.011	0.025	0.036	126.5
8/12/14 2:50 PM	0.329	0.233	0.562	0.01	0.32	0.004	0.034	0.038	180.5
8/13/14 9:10 AM	1.246	0.202	1.448	0.281	0.97	0.006	0.039	0.045	156
9/11/14 2:45 PM	0.243	0.114	0.357	0.197	0.05	0.0167	0.019	0.036	78
5/12/15 9:30 AM	1.467	0.944	2.411	0.45	1.02	0.0167	0.099	0.116	360
5/28/15 12:20 PM	0.808	0.144	0.952	0.22	0.59	0.009	0.039	0.048	11.6
6/10/15 5:00 PM	0.904	0.685	1.589	0.288	0.62	0.0167	0.070	0.087	196.7

Table C-3. Nutrient and sediment concentrations for WH Control.

Collection Date & Time	TKN EPA 351.2 mg/L	Nitrate-Nitrite EPA 353.2 mg/L	TN (TKN + NO2-3)	Ammonia EPA 350.1 mg/L	ON (TKN-TAN)	Ortho-Phosphate EPA 300.0 mg/L	PBP (TP-OP)	Total Phosphorus EPA 365.1 mg/L	TSS SM25 40D mg/L
4/29/2014 3:15:00 PM	0.880	0.240	1.12	0.271	0.61	0.0167	0.054	0.071	69.0
5/1/2014 8:30:00 AM	0.846	0.205	1.051	0.153	0.69	0.003	0.056	0.059	154.0
5/13/14 1:30 PM	1.575	0.502	2.077	0.341	1.23	0.003	0.092	0.095	55
6/19/14 2:05 PM	0.544	0.434	0.978	0.135	0.41	0.0167	0.007	0.024	14.6
6/24/14 12:00 PM	0.587	0.36	0.947	0.015	0.57	NS	NS	0.031	17
6/25/14 4:50 PM	0.243	0.19	0.433	0.017	0.23	0.0167	0.015	0.032	9
6/30/14 1:15 PM	NS	NS	NS	NS	NS	0.056	NS	NS	22.6
7/8/14 9:05 AM	0.734	0.365	1.099	0.183	0.55	0.0167	0.058	0.075	9
7/9/14 1:00 PM	0.47	0.303	0.773	0.111	0.36	0.006	NS	0.03	7.3
8/12/14 2:20 PM	0.539	0.423	0.962	0.01	0.53	0.01	0.033	0.043	12.3
8/13/14 9:20 AM	4.972	0.438	5.41	1.231	3.74	0.026	0.045	0.071	7.8
9/11/14 3:00 PM	0.485	0.29	0.775	0.0015	0.48	0.0167	0.050	0.067	8.4
10/15/14 12:45 PM	0.488	0.101	0.589	0.005	0.48	0.034	0.045	0.079	26.7
10/17/14 9:30 AM	0.378	0.262	0.64	0.036	0.34	NS	NS	0.037	6.1
10/21/14 4:50 PM	0.68	0.4	1.08	0.25	0.43	0.0015	0.047	0.048	16.8
11/3/14 2:45 PM	0.408	0.398	0.806	0.065	0.34	NS	NS	0.019	4
5/12/15 9:35 AM	1.6	1.7	3.3	0.685	0.96	0.017	0.053	0.070	31.6
5/28/15 12:40 PM	1.0	0.4	1.409	0.369	0.62	0.009	0.037	0.046	10.0
6/10/15 5:00 PM	1.3	0.6	1.876	0.276	1.02	0.051	0.026	0.077	12.0

Table C-4. Chloride and heavy metals concentrations for WH Small.

Collection Date & Time	Chloride EPA 300.0 mg/L	Aluminum EPA 200.8 ug/L	Calcium EPA 200.8 ug/L	Copper EPA 200.8 ug/L	Iron EPA 200.8 ug/L	Magnesium EPA 200.8 ug/L	Manganese EPA 200.8 ug/L	Lead EPA 200.8 ug/L	Zinc EPA 200.8 ug/L
4/29/2014 2:15 PM	506.2	NS	NS	NS	NS	NS	NS	NS	NS
5/1/2014 8:00 AM	588	1108	46,600	4.679	740.0	4261	15.01	0.912	11.12
5/13/14 12:45 PM	350	NS	NS	NS	NS	NS	NS	NS	NS
6/19/14 1:30 PM	73.84	1298	85660	5.995	2103	3695	37.7	1.988	24
6/24/14 11:30 AM	NS	827.2	96860	7.227	1563	5079	33.77	1.756	17.58
6/25/14 4:10 PM	90.6	791.2	54270	4.519	1370	3396	22.5	1.123	13.62
6/30/14 12:50 PM	119.4	NS	NS	NS	NS	NS	NS	NS	NS
7/8/14 8:30 AM	100.9	565.8	64080	5.232	798.3	3181	19.86	0.929	20.5
7/9/14 12:30 PM	91.53	701.4	40620	4.391	651.4	2586	10.46	0.566	9.964
8/12/14 2:40 PM	116	731.8	54280	4.162	774.9	3626	18.95	0.922	15.39
8/13/14 9:00 AM	17.27	974.1	71030	2.564	994.7	2744	23.76	1.18	12.98
9/11/14 2:30 PM	13.84	332.6	52730	2.383	575.3	1951	18.03	0.88	13.07
10/15/14 1:15 PM	53.86	155	21080	1.843	157	2144	4.913	0.249	6.704
10/17/14 9:15 AM	86	88	23800	1.687	115.8	2828	2.241	0.153	5.767
10/21/14 4:30 PM	69.9	122.7	26900	2.321	191.6	2886	7.258	0.385	11.46
11/3/14 2:30 PM	120.8	123.6	29170	2.497	180.3	3809	6.717	0.238	13.95
5/12/15 9:25 AM	215.5	1585.0	231600	10.360	3210.0	8318	79.770	4.567	37.260
5/28/15 12:08 PM	290.5	541.6	49700	5.571	458.5	4025	11.500	0.443	7.192

Table C-5. Chloride and heavy metals concentrations for WH Large.

Collection Date & Time	Chloride EPA 300.0 mg/L	Aluminum EPA 200.8 ug/L	Calcium EPA 200.8 ug/L	Copper EPA 200.8 ug/L	Iron EPA 200.8 ug/L	Magnesium EPA 200.8 ug/L	Manganese EPA 200.8 ug/L	Lead EPA 200.8 ug/L	Zinc EPA 200.8 ug/L
6/19/14 1:50 PM	17.56	1442	90350	5.404	2506	3068	40.05	2.498	24.35
6/24/14 11:45 AM	NS	1184	113800	9.58	2183	5403	79.58	3.323	32.23
6/25/14 4:30 PM	27.5	1059	46880	4.689	1723	2428	33.8	1.891	18.16
6/30/14 1:00 PM	60.8	NS	NS	NS	NS	NS	NS	NS	NS
7/8/14 8:45 AM	47.4	631.8	51070	6.087	873	2500	19.89	1.005	15.87
7/9/14 12:45 PM	23.96	1410	51770	3.704	1429	2262	21.42	1.202	15.16
8/12/14 2:50 PM	16.71	1418	59670	3.456	1538	2663	26.62	1.509	16.32
8/13/14 9:10 AM	11.02	1080	54220	2.595	1223	2260	24.6	1.414	14.38
9/11/14 2:45 PM	3.65	351.4	32620	1.873	592.3	1254	14.15	0.86	13.49
5/12/15 9:30 AM	91.84	1194	122700	7.803	2356	5204	55.12	3.52	30.47
5/28/15 12:20 PM	9.066	115.9	14850	6.561	235.4	786.8	18.93	0.619	15.2
6/10/15 5:00 PM	54.04	849.4	94340	6.31	1691	4839	45.8	2.568	34.78

Table C-6. Chloride and heavy metals concentrations for WH Control.

Collection Date & Time	Chloride EPA 300.0 mg/L	Aluminum EPA 200.8 ug/L	Calcium EPA 200.8 ug/L	Copper EPA 200.8 ug/L	Iron EPA 200.8 ug/L	Magnesium EPA 200.8 ug/L	Manganese EPA 200.8 ug/L	Lead EPA 200.8 ug/L	Zinc EPA 200.8 ug/L
4/29/2014 3:15 PM	26.16	362.5	27,530	9.474	658.0	3223	45.59	1.921	50.25
5/1/2014 8:30 AM	128	346.3	31,370	3.747	508.9	3289	34.19	1.411	27.78
5/13/14 1:30 PM	25	NS	NS	NS	NS	NS	NS	NS	NS
6/19/14 2:05 PM	16.77	100.7	14650	3.68	164.4	1363	8.779	0.618	19.69
6/24/14 12:00 PM	NS	79.1	13540	4.222	117.7	1357	9.234	0.512	21
6/25/14 4:50 PM	122.6	119.8	18920	3.849	164.8	3208	7.04	0.555	16.83
6/30/14 1:15 PM	14.2	NS	NS	NS	NS	NS	NS	NS	NS
7/8/14 9:05 AM	8.103	54.02	12500	11.78	90.79	1191	26.62	0.626	20.52
7/9/14 1:00 PM	60.52	87.15	16590	4.278	113.8	1744	5.739	0.37	17.21
8/12/14 2:20 PM	13.77	62.9	9315	3.658	100.4	1321	6.444	0.36	24.62
8/13/14 9:20 AM	71.77	238.8	14590	3.588	257	1954	7.81	0.649	16.89
9/11/14 3:00 PM	54.67	156.1	12540	3.274	218.9	2314	9.123	0.649	17.61
10/15/14 12:45 PM	1.565	99.22	7366	2.367	167.8	855.5	21.8	0.673	29.52
10/17/14 9:30 AM	22.92	73.93	10610	1.902	113	1230	9.415	0.438	13.12
10/21/14 4:50 PM	18.32	74.34	11000	2.851	145.1	1484	75.95	0.994	23.3
11/3/14 2:45 PM	2.82	29.04	10910	1.387	108.8	1162	20.5	0.253	12.62
5/12/15 9:35 AM	27.6	110.6	30240	4.548	245.5	1619	36.6	0.8	25.2
5/28/15 12:40 PM	15.7	50.2	18790	3.977	107.5	1250	6.8	0.4	19.3
6/10/15 5:00 PM	31.9	91.1	21530	8.882	184.4	1790	18.8	0.6	42.0

Table C-7. Influent pollutant loads for WH Small application.

Pollutant Loads (mg)								Pollutant Loads (g)									
Al	Ca	Cu	Fe	Mg	Mn	Pb	Zn	Cl	TKN	Nox	TN	TAN	ON	TP	OPO4	PBP	TSS
NS	NS	NS	NS	NS	NS	NS	NS	38	1.29	0.35	1.64	0.40	0.89	0.10	0.02	0.08	100.92
1035	93768	11	1521	9831	102	4	83	383	2.53	0.61	3.14	0.46	2.07	0.18	0.01	0.17	460.32
NS	NS	NS	NS	NS	NS	NS	NS	40	2.52	0.80	3.33	0.55	1.98	0.15	0.00	0.15	88.06
1363	198244	50	2225	18444	119	8	266	227	7.36	5.87	13.23	1.83	5.53	0.32	0.23	0.10	197.57
138	23579	7	205	2363	16	1	37	NS	1.02	0.63	1.65	0.03	1.00	0.05	NS	NS	29.60
1563	246787	50	2150	41844	92	7	220	1599	3.17	2.48	5.65	0.22	2.95	0.42	0.22	0.20	117.39
NS	NS	NS	NS	NS	NS	NS	NS	35	NS	NS	NS	NS	NS	NS	0.14	0.14	55.73
137	31748	30	231	3025	68	2	52	21	1.86	0.93	2.79	0.46	1.40	0.19	0.04	0.15	22.86
491	93401	24	641	9819	32	2	97	341	2.65	1.71	4.35	0.62	2.02	0.17	0.03	0.14	41.10
295	43641	17	470	6189	30	2	115	65	2.53	1.98	4.51	0.05	2.48	0.20	0.05	0.15	57.63
1687	103045	25	1815	13801	55	5	119	507	35.12	3.09	38.21	8.69	26.42	0.50	0.18	0.32	55.09
2125	170712	45	2980	31501	124	9	240	744	6.60	3.95	10.55	0.02	6.58	0.91	0.23	0.68	114.35
11	806	0	18	94	2	0	3	0	0.05	0.01	0.06	0.00	0.05	0.01	0.00	0.00	2.92
182	26161	5	279	3033	23	1	32	57	0.93	0.65	1.58	0.09	0.84	0.09	NS	NS	15.04
395	58453	15	771	7886	404	5	124	97	3.61	2.13	5.74	1.33	2.28	0.26	0.01	0.25	89.27
65	24494	3	244	2609	46	1	28	6	0.92	0.89	1.81	0.15	0.77	0.04	NS	NS	8.98
589	161003	24	1307	8620	195	4	134	147	8.75	8.82	17.57	3.65	5.10	0.09	0.28	0.37	168.24
142	53213	11	304	3540	19	1	55	44	2.80	1.19	3.99	1.05	1.75	0.03	0.10	0.13	28.32

Table C-8. Effluent pollutant loads for WH Small application.

Pollutant Loads (mg)								Pollutant Loads (g)									
Al	Ca	Cu	Fe	Mg	Mn	Pb	Zn	Cl	TKN	Nox	TN	TAN	ON	TP	OPO4	PBP	TSS
NS	NS	NS	NS	NS	NS	NS	NS	275	1.08	0.88	1.96	0.42	0.66	0.03	0.02	0.00	43.39
1312	55180	6	876	5046	18	1	13	696	1.35	2.21	3.56	0.54	0.81	0.04	0.01	0.03	50.56
NS	NS	NS	NS	NS	NS	NS	NS	251	1.03	1.37	2.40	0.08	0.94	0.07	0.01	0.06	172.35
11945	788327	55	19354	34005	347	18	221	680	6.57	6.25	12.82	2.60	3.98	0.57	0.15	0.42	1975.88
154	18031	1	291	945	6	0	3	NS	0.16	0.21	0.38	0.04	0.13	0.00	NS	NS	35.74
6945	476394	40	12026	29811	198	10	120	795	2.96	6.12	9.08	0.44	2.52	0.37	0.15	0.22	785.65
NS	NS	NS	NS	NS	NS	NS	NS	199	NS	NS	NS	NS	NS	NS	0.03	NS	274.66
1791	202882	17	2527	10071	63	3	65	319	1.86	2.00	3.86	0.51	1.35	0.12	0.05	0.07	333.39
3462	200523	22	3216	12766	52	3	49	452	1.25	2.59	3.84	0.01	1.24	0.13	0.03	0.10	231.03
2769	205383	16	2932	13720	72	3	58	439	1.65	1.45	3.10	0.15	1.50	0.15	0.02	0.14	411.67
5554	405015	15	5672	15646	135	7	74	98	15.17	1.13	16.30	2.12	13.05	0.27	0.03	0.25	946.54
3562	564765	26	6162	20896	193	9	140	148	2.59	4.24	6.83	1.40	1.19	0.45	0.18	0.27	1478.05
18	2388	0	18	243	1	0	1	6	0.04	0.04	0.08	0.00	0.04	0.00	0.00	0.00	0.56
154	41784	3	203	4965	4	0	10	151	0.49	1.01	1.50	0.02	0.47	0.04	NS	NS	9.66
504	110450	10	787	11850	30	2	47	287	2.09	1.95	4.04	0.37	1.72	0.11	0.01	0.10	76.37
196	46256	4	286	6040	11	0	22	192	0.59	0.86	1.46	0.03	0.57	0.16	NS	NS	9.51
7595	1109768	50	15381	39858	382	22	179	1033	7.36	7.94	15.30	1.70	5.66	0.08	0.79	0.87	3464.43
1304	119638	13	1104	9689	28	1	17	699	1.91	4.05	5.97	0.21	1.71	0.01	0.07	0.09	41.64

Table C-9. Influent pollutant loads for WH Large application.

Pollutant Loads (mg)								Pollutant Loads (g)									
Al	Ca	Cu	Fe	Mg	Mn	Pb	Zn	Cl	TKN	Nox	TN	TAN	ON	TP	OPO4	PBP	TSS
2074	157489	54	3764	18438	261	11	287	150	5.0	1.4	6.4	1.6	3.5	0.4	0.1	0.3	394.7
4041	366020	44	5938	38376	399	16	324	1493	9.9	2.4	12.3	1.8	8.1	0.7	0.0	0.7	1796.8
NS	NS	NS	NS	NS	NS	NS	NS	156	9.9	3.1	13.0	2.1	7.7	0.6	0.0	0.6	344.2
5795	843052	212	9461	78436	505	36	1133	965	31.3	25.0	56.3	7.8	23.5	1.4	1.0	0.4	840.2
538	92029	29	800	9223	63	3	143	NS	4.0	2.4	6.4	0.1	3.9	0.2	NS	NS	115.5
6107	964466	196	8401	163531	359	28	858	6250	12.4	9.7	22.1	0.9	11.5	1.6	0.9	0.8	458.8
NS	NS	NS	NS	NS	NS	NS	NS	137	NS	NS	NS	NS	NS	NS	0.5	0.5	217.6
719	166380	157	1208	15853	354	8	273	108	9.8	4.9	14.6	2.4	7.3	1.0	0.2	0.8	119.8
1918	365057	94	2504	38376	126	8	379	1332	10.3	6.7	17.0	2.4	7.9	0.7	0.1	0.5	160.6
451	66742	26	719	9465	46	3	176	99	3.9	3.0	6.9	0.1	3.8	0.3	0.1	0.2	88.1
5728	349971	86	6165	46871	187	16	405	1722	119.3	10.5	129.8	29.5	89.7	1.7	0.6	1.1	187.1
8302	666939	174	11642	123070	485	35	937	2908	25.8	15.4	41.2	0.1	25.7	3.6	0.9	2.7	446.8
955	70926	23	1616	8237	210	6	284	15	4.7	1.0	5.7	0.0	4.7	0.8	0.3	0.4	257.1
364	52283	9	557	6061	46	2	65	113	1.9	1.3	3.2	0.2	1.7	0.2	NS	NS	30.1
1543	228344	59	3012	30806	1577	21	484	380	14.1	8.3	22.4	5.2	8.9	1.0	0.0	1.0	348.7
255	95781	12	955	10201	180	2	111	25	3.6	3.5	7.1	0.6	3.0	0.2	NS	NS	35.1
2296	627739	94	5096	33608	760	16	523	574	34.1	34.4	68.5	14.2	19.9	0.3	1.1	1.5	656.0
557	208596	44	1193	13877	76	4	214	174	11.0	4.7	15.6	4.1	6.9	0.1	0.4	0.5	111.0
1426	337116	139	2887	28028	294	9	657	499	20.3	9.1	29.4	4.3	16.0	0.8	0.4	1.2	187.9

Table C-10. Effluent pollutant loads for WH Large application.

Pollutant Loads (mg)								Pollutant Loads (g)									
Al	Ca	Cu	Fe	Mg	Mn	Pb	Zn	Cl	TKN	Nox	TN	TAN	ON	TP	OPO4	PBP	TSS
626	47542	16	1136	5566	79	3	87	45	1.5	0.4	1.9	0.47	1.05	0.12	0.03	0.09	119
1225	111011	13	1801	11639	121	5	98	453	3.0	0.7	3.7	0.54	2.45	0.21	0.01	0.20	545
NS	NS	NS	NS	NS	NS	NS	NS	40	2.5	0.8	3.4	0.55	1.99	0.15	0.00	0.15	89
45814	3013352	228	79436	117148	1375	87	1082	824	25.8	21.47	47.29	12.65	13.18	1.76	0.80	0.96	8200
1705	176179	21	3086	9841	123	5	85	NS	3.0	1.95	4.93	0.45	2.53	0.09	NS	NS	249
17918	1003280	131	28688	86339	622	37	535	2309	5.8	7.50	13.33	1.51	4.32	1.34	0.51	0.83	1978
NS	NS	NS	NS	NS	NS	NS	NS	401	NS	NS	NS	NS	NS	NS	0.26	NS	962
4367	385674	87	6099	21208	238	9	187	344	8.6	5.61	14.23	2.85	5.77	0.67	0.18	0.49	693
18662	774292	76	19083	40611	313	18	309	710	6.8	8.08	14.91	1.29	5.54	0.66	0.18	0.48	1671
10156	427382	25	11016	19074	191	11	117	120	2.4	1.67	4.03	0.07	2.28	0.27	0.03	0.24	1293
25897	1300118	62	29326	54192	590	34	345	264	29.9	4.84	34.72	6.74	23.14	1.08	0.14	0.94	3741
12646	1158198	87	20959	59253	532	33	579	558	11.8	6.03	17.80	6.40	5.38	1.71	0.68	1.03	2596
289	21479	7	489	2495	64	2	86	5	1.4	0.3	1.7	0.01	1.41	0.23	0.10	0.13	78
111	15920	3	170	1846	14	1	20	34	0.6	0.4	1.0	0.05	0.51	0.06	NS	NS	9
467	69133	18	912	9327	477	6	146	115	4.3	2.5	6.8	1.57	2.70	0.30	0.01	0.29	106
77	29033	4	290	3092	55	1	34	8	1.1	1.1	2.1	0.17	0.91	0.05	NS	NS	11
17350	1782953	113	34235	75619	801	51	443	1335	21.3	13.7	35.0	6.5	14.8	0.2	1.4	1.7	5231.2
965	123642	55	1960	6551	158	5	127	75	6.7	1.2	7.9	1.8	4.9	0.1	0.3	0.4	96.6
8645	960163	64	17210	49250	466	26	354	550	9.2	7.0	16.2	2.9	6.3	0.2	0.7	0.9	2002.0

Appendix D: Surface Infiltration Testing Locations in North Carolina and Ohio

Figure D-1. Locations of surface infiltration rate tests conducted at the North Carolina Central University (Durham, NC) permeable pavement parking lot. The permeable interlocking concrete pavement lot is hatched in blue. The speed bump is shown in red. The watershed is outlined with hashed yellow lines.

Figure D-2. Locations of surface infiltration rate testing at Piney Wood park in Durham, NC. The permeable interlocking concrete pavement parking lot is hatched in blue, with the watershed outlined using a yellow dashed line.

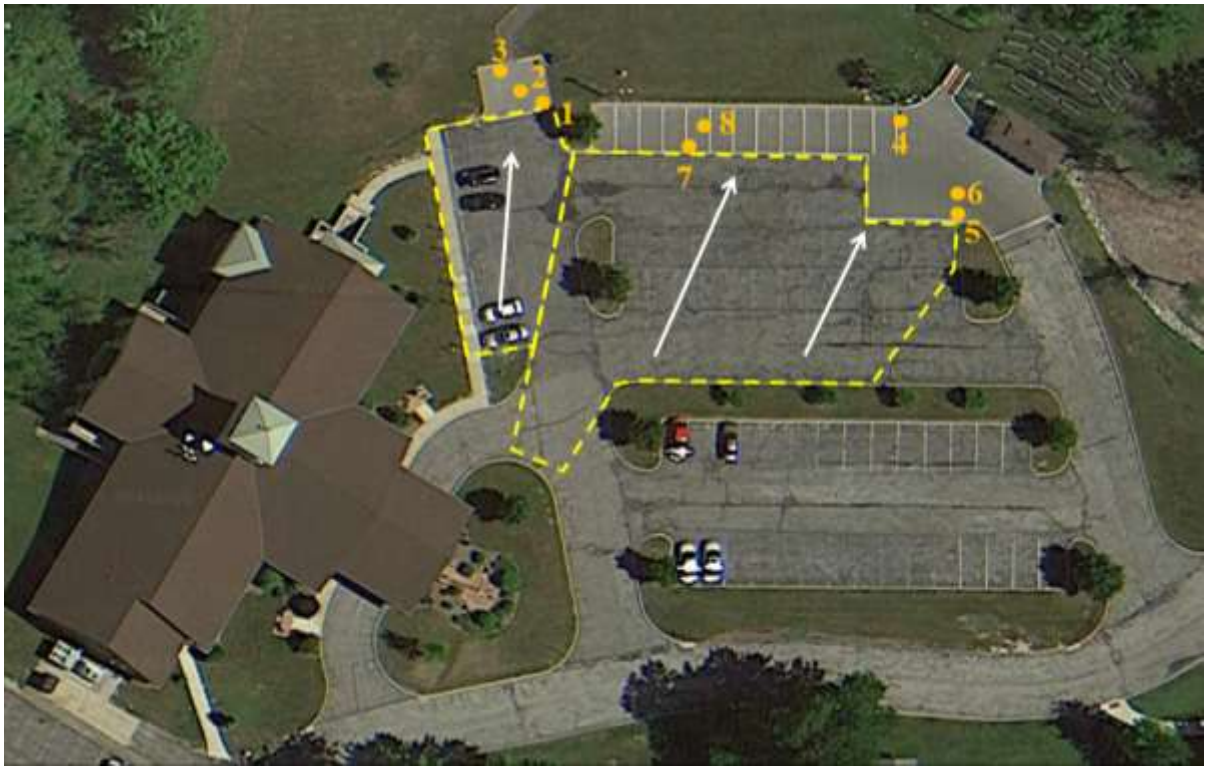

Figure D-3. Plan view showing surface infiltration testing locations for Willoughby Hills, Ohio. Catchments are outlined in yellow and flow direction is marked with white arrows.

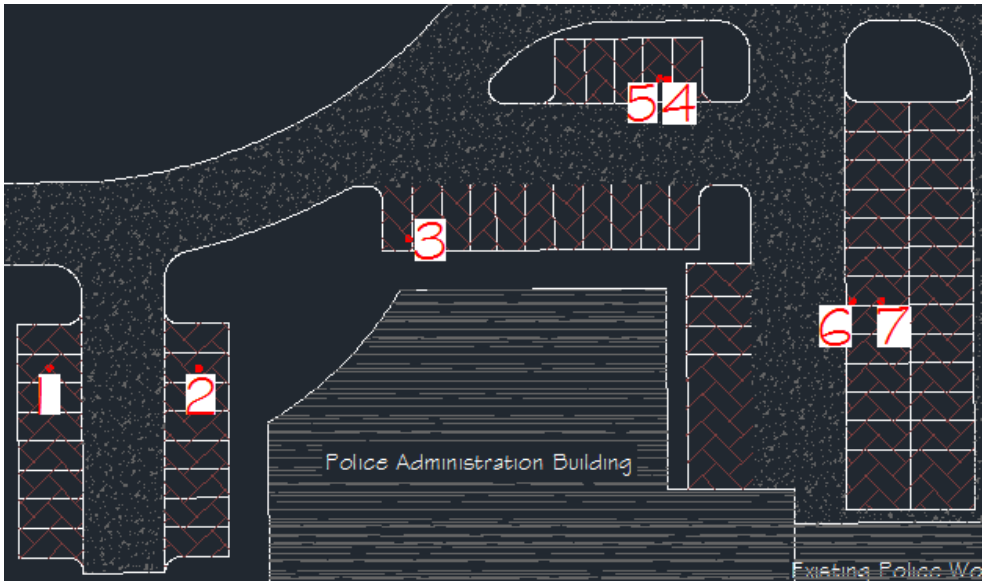

Figure D-4. Locations of surface infiltration rate tests conducted at the Perkins Township, Ohio site. Pervious Concrete is shown in brown hatching. Concrete drive aisles were crowned in the center and drained to the pervious concrete.

Figure D-5. Plan view showing surface infiltration testing locations for the Orange Village, Ohio permeable interlocking concrete pavement.

Appendix E:Permeable Pavement Surface Infiltration and Maintenance Testing Sites in Sweden

Figure E-1. Photos of the Kockvägen, Luleå, Sweden porous asphalt site.

Figure E-2. Photos of the Åkergatan, Haparanda, Sweden porous asphalt site.


Figure E-3. Photos of the Välluddevägen, Växjö, Sweden permeable interlocking concrete pavement site.


Figure E-4. Photos of the Vaxthusgatan, Växjö, Sweden permeable interlocking concrete pavement site.


Figure E-5. Photos of the Lillavallen, Växjö, Sweden permeable interlocking concrete pavement site.


Figure E-6. Photos of the Kurortsvägen, Växjö, Sweden concrete grid paver site.


Figure E-7. Photos of the Schwerinvägen, Växjö, Sweden concrete grid paver site.